N° d'ordre NNT : 2016LYSE1285

THÈSE DE DOCTORAT DE L'UNIVERSITÉ DE LYON
opérée au sein de
l'Université Claude Bernard Lyon 1

École Doctorale ED206 Chimie, Procédés, Environnement

Spécialité de doctorat : Chimie

Soutenue à huis clos le 15/12/2016, par :
Thomas Galeandro-Diamant

Metal nanoparticles as catalysts for alkene hydrosilylation

Devant le jury composé de :

M. Stéphane Daniele, Professeur des universités, Université Claude Bernard Lyon 1	Président
M. Christophe Darcel, Professeur des universités, Université de Rennes 1	Rapporteur
M. Nicolas Mézailles, Directeur de recherche, CNRS	Rapporteur
M. Philippe Marion, Responsable R&D, Solvay	Examinateur
Mme Valérie Meille, Chargée de recherche, CNRS	Directrice de thèse
Mme Chloé Thieuleux, Chargée de recherche, CNRS	Co-directrice de thèse
Mme Magali Bousquié, Ingénieure R&D, Bluestar Silicones	Invitée

UNIVERSITE CLAUDE BERNARD - LYON 1

Président de l'Université	**M. le Professeur Frédéric FLEURY**
Président du Conseil Académique	M. le Professeur Hamda BEN HADID
Vice-président du Conseil d'Administration	M. le Professeur Didier REVEL
Vice-président du Conseil Formation et Vie Universitaire	M. le Professeur Philippe CHEVALIER
Vice-président de la Commission Recherche	M. Fabrice VALLÉE
Directrice Générale des Services	Mme Dominique MARCHAND

COMPOSANTES SANTE

Faculté de Médecine Lyon Est – Claude Bernard	Directeur : M. le Professeur G.RODE
Faculté de Médecine et de Maïeutique Lyon Sud – Charles Mérieux	Directeur : Mme la Professeure C. BURILLON
Faculté d'Odontologie	Directeur : M. le Professeur D. BOURGEOIS
Institut des Sciences Pharmaceutiques et Biologiques	Directeur : Mme la Professeure C. VINCIGUERRA
Institut des Sciences et Techniques de la Réadaptation	Directeur : M. X. PERROT
Département de formation et Centre de Recherche en Biologie Humaine	Directeur : Mme la Professeure A-M. SCHOTT

COMPOSANTES ET DEPARTEMENTS DE SCIENCES ET TECHNOLOGIE

Faculté des Sciences et Technologies	Directeur : M. F. DE MARCHI
Département Biologie	Directeur : M. le Professeur F. THEVENARD
Département Chimie Biochimie	Directeur : Mme C. FELIX
Département GEP	Directeur : M. Hassan HAMMOURI
Département Informatique	Directeur : M. le Professeur S. AKKOUCHE
Département Mathématiques	Directeur : M. le Professeur G. TOMANOV
Département Mécanique	Directeur : M. le Professeur H. BEN HADID
Département Physique	Directeur : M. le Professeur J-C PLENET
UFR Sciences et Techniques des Activités Physiques et Sportives	Directeur : M. Y.VANPOULLE
Observatoire des Sciences de l'Univers de Lyon	Directeur : M. B. GUIDERDONI
Polytech Lyon	Directeur : M. le Professeur E.PERRIN
Ecole Supérieure de Chimie Physique Electronique	Directeur : M. G. PIGNAULT
Institut Universitaire de Technologie de Lyon 1	Directeur : M. le Professeur C. VITON
Ecole Supérieure du Professorat et de l'Education	Directeur : M. le Professeur A. MOUGNIOTTE
Institut de Science Financière et d'Assurances	Directeur : M. N. LEBOISNE

Remerciements

Cette thèse est l'aboutissement d'un projet auquel de nombreuses personnes ont pris part. Même si ils ne reflèteront pas à leur juste valeur la contribution de chacun, des remerciements s'imposent.

Merci à MM. Stéphane Daniele, Nicolas Mézailles, Christophe Darcel, Philippe Marion et Mme. Magali Bousquié pour avoir accepté de faire partie de mon jury de thèse.

Merci à Valérie Meille et Chloé Thieuleux pour leur encadrement pendant ces trois ans. J'ai énormément appris lors de cette thèse, et c'est en grande partie grâce à vous.

Merci aux stagiaires qui ont participé au projet : Briony Munslow et Alice Relave pour les travaux sur les nanotubes de carbone ainsi qu'Antoine Degenne pour les travaux sur les colloïdes de platine.

Merci aux membres des laboratoires LGPC et C2P2 qui m'ont aidés à de multiples occasion avec compétence et bienveillance : Laurent Veyre, Marie-Line Zanota, Claude de Bellefon, Pascal Fongarland, Stéphanie Pallier, Frédéric Bornette, Fabrice Campoli, Laurent Vanoye, Régis Philippe, Cyrille Nalet, Nesrine Oueslati, Kai Chung Szeto, François Bayard, Emmanuelle Fouilhé, Anne-Lise Cœur, Lynda Cherguy, Virginie Messina, David Baudouin, Reine Sayah, Giuliana Rubulotta, Frédéric Le Quéméner, Thibault Alphazan et ceux que j'oublie certainement.

Merci à Sébastien Marrot, Magali Bousquié, Christelle Lenoir, Delphine Blanc, Jean-Marc Francès et Céline Fustier pour leur participation au projet du côté Bluestar Silicones.

Merci à Vincent Meille pour son assistance informatique à distance.

Merci à Xavier Jaurand (CTμ, Lyon) pour son assistance avec les analyses TEM et STEM, à Bernard Fenet, Anne Baudouin et Christophe Gilbert (CCRMN, Lyon) pour leur assistance avec les analyses RMN et à Moulay-Tahar Sougrati (ICG, Montpellier) pour sa collaboration pour les analyses Mössbauer.

Merci à tous mes collègues pour les très bons moments que j'ai passés avec vous et les discussions très enrichissantes que nous avons eues ensemble. Je pense notamment, en plus des collègues cités plus haut, à Jihène, Mohamed, Marion, Matthieu, Marc, Alain, Dominique, Clément, Yousef, Amara et Édouard.

Merci aux membres de l'ATEC, avec qui j'ai aussi passé d'excellents moments.

Merci au CNRS pour avoir financé une formation à la microscopie électronique en transmission, une école d'été sur la préparation de catalyseurs hétérogènes et une école d'été sur le génie de la réaction catalytique. Merci également à l'école doctorale de chimie de Lyon pour avoir subventionné ma participation à l'International Symposium on Relations between Homogeneous and Heterogeneous Catalysis à Utrecht (Pays-Bas) en 2015.

Merci aux développeurs de logiciels libres que j'ai utilisés lors de ces trois ans (Linux, LaTeX, GNUplot, etc.), qui font souvent ce travail de manière bénévole.

Merci enfin à ma famille, pour m'avoir toujours soutenu.

Si quelqu'un a été oublié dans cette liste de remerciements, qu'il ou elle me le fasse savoir, et je réparerai volontiers cet oubli !

À ma famille

Abstract

Alkene hydrosilylation is a crucial method of forming carbon-silicon bonds. It is used industrially for the production of functional silicone fluids and silicone elastomers. The current industrial alkene hydrosilylation processes use platinum complexes as catalysts. Although these complexes are extremely efficient, they are usually not recovered at the end of the synthesis, making their use expensive and unsustainable, given the scarcity of platinum. In this work, we have synthesized and evaluated several kinds of metal nanoparticles as catalysts for alkene hydrosilylation, in a quest towards sustainable catalyts. First, we have synthesized platinum nanoparticles of 2 nm diameter and compared them with Karstedt's complex, the benchmark catalyst in alkene hydrosilylation. It was shown that platinum nanoparticles were as efficient as Karstedt's complex in industrially relevant hydrosilylation conditions, despite their lower metal dispersion. These findings reactivated the debate on whether's Karstedt's complex was truly homogeneous or colloidal during catalysis. Then, a leaching-resistant heterogeneous platinum catalyst was developed, based on the embedding of platinum nanoparticles in the matrix of a mesostructured silica, SBA-15. Finally, other alternative catalytic systems were developed, based on other metals.

Résumé

L'hydrosilylation des alcènes est une méthode cruciale de formation de liaisons carbone-silicium. Elle est utilisée industriellement pour la production de fluides silicones fonctionnels et d'élastomères silicones. Les procédés actuels d'hydrosilylation des alcènes utilisent des complexes de platine comme catalyseurs. Bien que ces complexes soient extrêmement efficients, ils ne sont d'habitude pas récupérés en fin de réaction, ce qui rend leur utilisation coûteuse et peu durable, étant donnée la rareté du platine. Dans ce projet, nous avons synthétisé et testé plusieurs types de nanoparticules métalliques comme catalyseurs pour l'hydrosilylation des alcènes, dans un effort vers des catalyseurs durables. D'abord, nous avons synthétisé des nanoparticules de platine de 2 nm de diamètre et les avons comparées avec le complexe de Karstedt, le catalyseur de référence en hydrosilylation des alcènes. Nous avons montré que les nanoparticules de platine étaient aussi efficientes que le complexe de Karstedt dans des conditions proches des conditions industrielles, malgré leur dispersion métallique plus faible. Ces observations ont réactivé le débat sur la nature réellement homogène ou colloïdale du complexe de Karstedt pendant la catalyse. Ensuite, un catalyseur hétérogène à base de platine, résistant à la lixiviation, a été développé, basé sur l'encapsulation de nanoparticules de platine dans la matrice d'une silice mésostructurée, la SBA-15. Enfin, d'autres catalyseurs alternatifs ont été développés, basés sur d'autres métaux.

Résumé substantiel

L'hydrosilylation des alcènes est une méthode importante de formation de liaisons carbone-silicium (Figure 1). Elle est utilisée industriellement pour la production de fluides silicones fonctionnels et d'élastomères silicones. Les procédés actuels d'hydrosilylation des alcènes utilisent des complexes de platine comme catalyseurs. Bien que ces complexes soient extrêmement efficients, ils ne sont d'habitude pas récupérés en fin de réaction, ce qui rend leur utilisation coûteuse et peu durable, étant donnée la rareté du platine.



Figure 1: L'hydrosilylation des alcènes.

Dans la littérature, on trouve principalement deux types de catalyseurs comme alternatives aux complexes de platine développés dans un souci de durabilité. Les premiers sont des catalyseurs hétérogènes à base de platine, développés dans l'optique de faciliter la séparation des produits de réaction et du platine, afin de réutiliser ou recycler ce dernier. Malheureusement, la lixiviation du platine dans la phase liquide est un problème rencontré très fréquemment pour ces catalyseurs, et qui limite leur intérêt à l'échelle industrielle. Ensuite, des catalyseurs à base de métaux non-nobles comme le fer, le cobalt et le nickel ont été développés, dans l'optique de complètement remplacer le platine. Ces catalyseurs se présentent principalement sous la forme de complexes. L'utilisation de ces métaux non-nobles a longtemps conduit à des catalyseurs peu sélectifs, mais le développement récent de complexes utilisant des ligands non-innocents a permis d'atteindre des activités et sélectivités rivalisant avec les complexes de platine.

Dans ce projet, nous avons synthétisé et testé plusieurs types de nanoparticules métalliques comme catalyseurs pour l'hydrosilylation des alcènes, dans un effort vers des catalyseurs durables.

D'abord, nous avons synthétisé des nanoparticules de platine de 2 nm de diamètre par décomposition de complexes de Pt(0). Nous avons ensuite testé ces nanoparticules ainsi que le complexe de Karstedt, le catalyseur de référence en hydrosilylation des alcènes, sur la réaction entre un polyméthylhydrosiloxane et le 1-octène, une réaction d'intérêt industriel. Nous avons montré que les nanoparticules de platine étaient aussi efficientes (même activité et même sélectivité à quantité de Pt total identique) que le complexe de Karstedt dans des conditions proches des conditions industrielles, malgré leur dispersion métallique plus faible. Ces observations ont réactivé le débat sur la nature réellement homogène ou colloïdale du complexe de Karstedt pendant la catalyse.

Ensuite, nous avons développé deux types de catalyseurs hétérogènes pour la réaction. Tout d'abord, nous avons étudié un catalyseur hétérogène (appelé Pt@{walls}SBA-15) basé sur l'encapsulation de nanoparticules de platine dans la matrice d'une silice mésostructurée (Figure 3). Nous avons démontré que ce catalyseur était capable d'atteindre des turnover numbers (TONs) de 10^5 mol(SiH)/mol(Pt) sans lixiviation du platine dans le milieu réactionnel, un phénomène récurrent et problématique pour l'industrie. Cette absence de lixiviation a été attribuée au piégeage des nanoparticules de platine dans la matrice de silice, tout en restant accessibles aux réactifs *via* la microporosité.

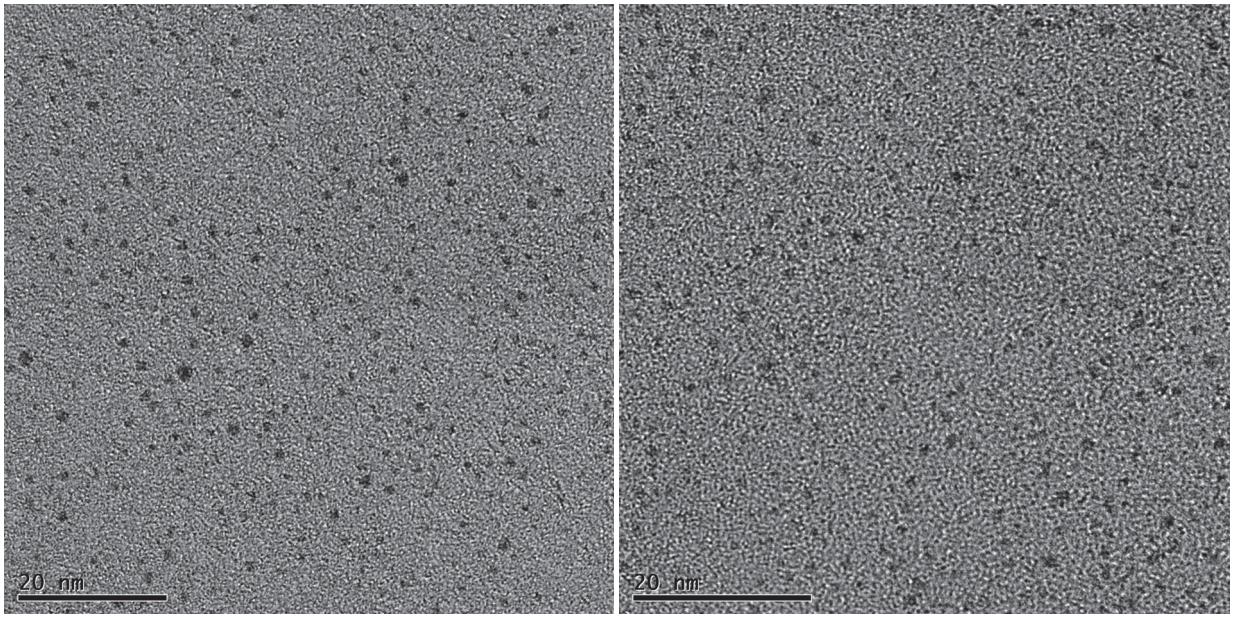


Figure 2: Images TEM de nanoparticules de platine.

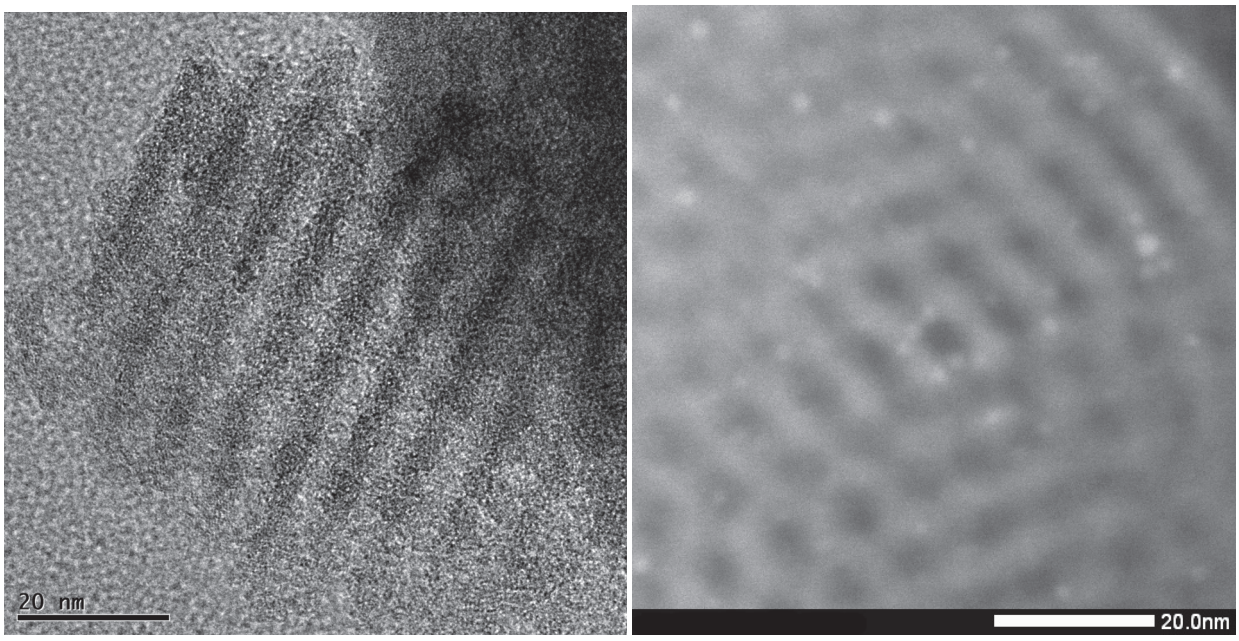


Figure 3: Gauche : image TEM du solide Pt@{walls}SBA-15, droite : image STEM du solide Pt@{walls}SBA-15.

Ensuite, des catalyseurs hétérogènes à base de supports carbonés (charbon actif et nanotubes de carbone) ont été préparés par imprégnation avec de l'acide hexachloroplatinique (H_2PtCl_6) puis réduction par de l'hydrogène. Une caractérisation par microscopie électronique en transmission à balayage (Figure 4) a mis en évidence la présence de nanoparticules de platine de 2 à 3 nm de diamètre pour la plupart des solides, sauf pour le solide Pt/charbon actif réduit à 450 °C, où des particules de platine de 5 à 20 nm de diamètre ont été observées, certainement formées par frittage lors de la réduction.

Lors des tests catalytiques sur la réaction entre l'heptaméthyltrisiloxane et le 1-octène, nous avons mis en évidence un phénomène de dissolution-

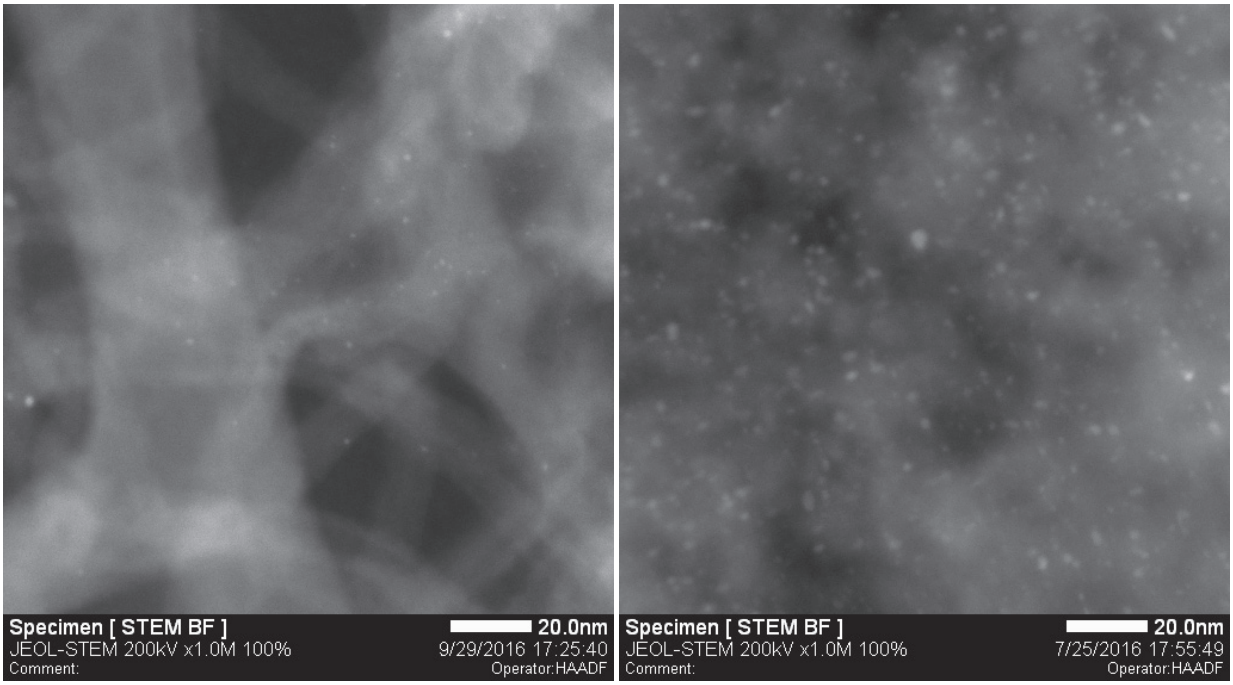


Figure 4: Gauche : image STEM du solide Pt/nanotubes de carbone, droite : image STEM du solide Pt/charbon actif.

redéposition du platine. Ce phénomène avait déjà été observé pour d'autres réactions comme les réactions de Heck et de Suzuki, catalysées par le palladium, mais jamais pour l'hydrosilylation des alcènes. Nous avons également observé une forte influence de la réduction des catalyseurs sur leurs performances: les solides non-réduits étaient très actifs, mais peu réutilisables, tandis que les catalyseurs réduits à 320 °C ou 450 °C étaient réutilisables plusieurs fois sans perte d'activité. Les catalyseurs réduits à 320 °C étaient cependant plus actifs que ceux réduits à 450 °C, et ils présentaient une période d'induction négligeable. Ces catalyseurs hétérogènes ont atteint des turnover numbers de plus de 4×10^5, rivalisant ainsi avec les catalyseurs industriels tels que le complexe de Karstedt.

Nous nous sommes ensuite intéressés à l'étude de plusieurs types de nanoparticules de nickel : des nanoparticules de siliciure de nickel Ni_3Si_2, des nanoparticules d'oxyde de nickel NiO et des nanoparticules de nickel métallique déposées sur silice Ni/SiO_2. Ces trois types de nanoparticules ont été caractérisés par microscopie électronique en transmission (Figure 5), et avaient des diamètres proches, entre 1 et 3 nm.

Des tests catalytiques ont été réalisés sur la réaction du triéthoxysilane avec le triéthoxyvinylsilane, une réaction qui comporte un enjeu de sélectivité. Les nanoparticules de Ni_3Si_2 ont donné majoritairement le produit de silylation déshydrogénante et le produit d'hydrogénation, tandis que le solide Ni/SiO_2 a donné majoritairement le produit d'hydrosilylation. Cette différence de sélectivité montre que l'environnement des atomes de nickel influe fortement sur la séléctivité de la réaction. Les nanoparticules de NiO n'ont pas montré d'activité catalytique, ce qui montre que la présence de Ni(0) est nécessaire pour que la catalyse ait lieu. Des tests catalytiques du solide Ni/SiO_2 et des nanoparticules de Ni_3Si_2 sur la réaction entre l'heptaméthyltrisiloxane et le 1-octène ont montré que la réaction d'hydrosilylation n'avait pas lieu, mais que le 1-octène s'isomérisait en 2-octène, 3-octène et 4-octène. Le même test en

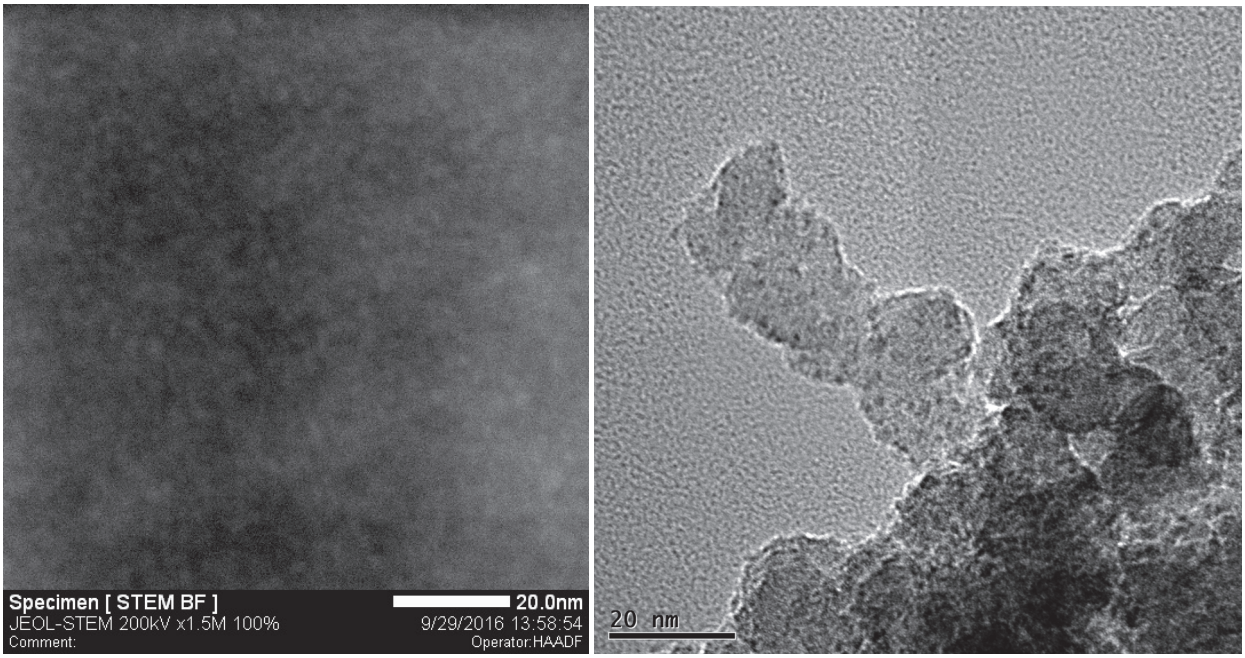


Figure 5: Gauche : image STEM du colloïde Ni_3Si_2, droite : image TEM du solide $Ni(0)/SiO_2$.

absence d'heptaméthyltrisiloxane n'a pas conduit à l'isomérisation du 1-octène, indiquant que la formation d'un hydrure de nickel par réaction du Ni(0) avec l'heptaméthyltrisiloxane était nécessaire à l'isomérisation.

Enfin, nous avons développé une nouvelle synthèse de nanoparticules de fer à partir d'un précurseur de Fe(0), le $Fe_3(CO)_{12}$. Une caractérisation par microscopie électronique en transmission à montré que ces nanoparticules avaient un diamètre inférieur à 2 nm (Figure 6, gauche). À partir de ces nanoparticules de fer, plusieurs autres formes de nanoparticules de fer ont été préparées. Par imprégnation sur silice puis oxydation à l'air à température ambiante, un premier solide a été obtenu. Par calcination de ce solide sous air à 500 °C, un second solide a été obtenu. Par réduction de ce solide sous hydrogène à 500 °C, un autre solide a été obtenu (Figure 6, droite).

Des analyses préliminaires par spectroscopie Mössbauer ont mis en évidence une différence d'environnement chimique entre les nanoparticules de Fe(0) obtenues par la synthèse colloïdale et celles obtenues par imprégnation-calcination-réduction. Nous émettons l'hypothèse que les nanoparticules obtenues par la synthèse colloïdale sont formées de siliciure de fer (Fe_xSi_y), que l'oxydation provoque une ségrégation des atomes de fer et de silicium et que la réduction sous hydrogène forme des particules de fer métallique, par analogie avec ce qui a été publié par notre groupe avec des nanoparticules de siliciure de nickel (*J. Am. Chem. Soc.* **2012**, 134, 20624). Une caractérisation de ces nanoparticules par EXAFS est prévue, et permettra de confirmer ou infirmer cette hypothèse.

Nous avons testé ces nanoparticules de fer sur la réaction de l'heptaméthyltrisiloxane avec le 1-octene. Les nanoparticules issues de la synthèse colloïdale ont donné un mélange de produit d'hydrosilylation (26% de rendement après 24 h), de silylation déshydrogénante sous forme de plusieurs isomères (8% de rendement) et d'isomérisation du 1-octène (69% de rendement). Ceci est le pre-

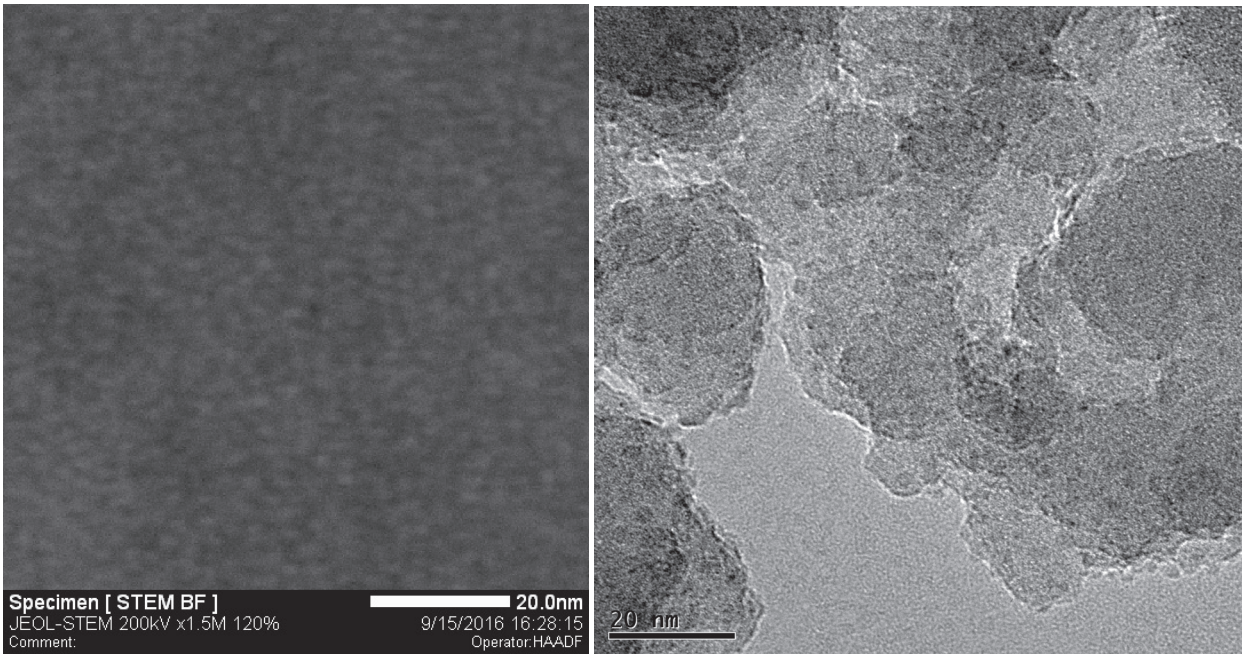


Figure 6: Gauche: image STEM des nanoparticules de fer, droite: image TEM du solide Fe/SiO_2 réduit.

mier exemple de nanoparticules de fer catalysant une réaction d'hydrosilylation d'un alcène, à notre connaissance. Les silices imprégnées de nanoparticules de fer oxydées n'ont pas donné d'activité, et le solide obtenu par imprégnation-calcination-réduction n'a catalysé que l'isomérisation du 1-octène (17% de rendement).

L'amélioration des performances (activité et sélectivité) des catalyseurs à base de nickel et de fer que nous avons étudiés lors de ce projet nécessitera d'étudier le mécanisme suivi par ces catalyseurs. La détermination des facteurs influant sur les performances des catalyseurs permettra une conception rationnelle de catalyseurs plus performants. Il apparaît clairement qu'un des paramètres importants est l'environnement du fer et du nickel dans les nanoparticules. Le test d'autres formes de nanoparticules contenant ces deux métaux permettra peut-être d'établir des relations structure-activité.

Contents

Remerciements 5
Abstract 9
Résumé 9
Résumé substantiel 11
Abbreviations 19
Siloxanes nomenclature 20

1 Introduction 21
1.1 The formation of C – Si bonds 21
1.2 Hydrosilylation 22
1.3 Applications of alkene hydrosilylation 22
1.4 Generalities about the reaction 27
1.5 Alkene hydrosilylation catalysts: state of the art 32
1.6 The research project 55

2 Platinum nanoparticles in suspension 63
2.1 Introduction 63
2.2 Results 64
2.3 Conclusion 68
2.4 Experimental 69
2.5 Appendices 72

3 Heterogeneous Pt catalysts: two strategies to improve platinum recovery 75
3.1 Introduction on heterogeneous Pt catalysts 75
3.2 Pt nanoparticles in SBA-15 mesostructured silica matrices 76
3.3 Pt nanoparticles on carbon nanotubes 81
3.4 Conclusion 97
3.5 Experimental 97

4 *Nickel nanoparticles* 101
- *4.1 Introduction* 101
- *4.2 Results* 102
- *4.3 Conclusion* 114
- *4.4 Experimental* 115
- *4.5 Appendices* 116

5 *Iron nanoparticles* 119
- *5.1 Introduction* 119
- *5.2 Results* 119
- *5.3 Conclusion* 131
- *5.4 Experimental* 132
- *5.5 Appendices* 133

6 *Conclusion* 135

A *Bibliography analysis* 137
- *A.1 Platinum* 138
- *A.2 Cobalt* 146
- *A.3 Iron* 149
- *A.4 Nickel* 152
- *A.5 Ruthenium* 157
- *A.6 Rhodium* 160
- *A.7 Iridium* 160

B *Chemicals* 161

C *Analytical methods* 163
- *C.1 Elemental analyses* 163
- *C.2 N_2 and H_2 adsorption* 163
- *C.3 Gazometry* 163
- *C.4 Gas chromatography* 163

Abbreviations

AC Active carbon

Ad Adamantyl

CNT Carbon nanotube

COD Cyclooctadiene

COE Cyclooctene

Cy Cyclohexyl

dba dibenzylideneacetone

DFT Density functional theory

DHSI Dehydrogenative silylation

DNP Dynamic nuclear polarization

d.r. Diastereoisomeric ratio

HRTEM High resolution transmission electron microscopy

HSI Hydrosilylation

Mes Mesityl

NHC *N*-heterocyclic carbene

NP Nanoparticle

SEM Scanning electron microscopy

STEM Scanning transmission electron microscopy

THF Tetrahydrofuran

TEM Transmission electron microscopy

TOF Turnover frequency

TON Turnover number

Vi Vinyl

Siloxanes nomenclature

Siloxanes are often designated using their abbreviated form, using letters to indicate the number of oxygen atoms linked to the silicon atom (Table 1) and modifiers (Table 2) to indicate the substitution of these units.

Table 1: Siloxane base units.

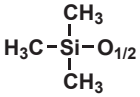
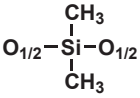
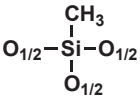
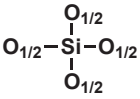
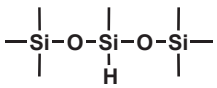
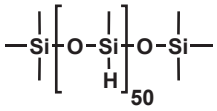
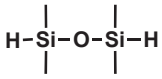
Abbreviation	Formula
M	
D	
T	
Q	

Table 2: Examples of siloxane modifiers.

Abbreviation	Formula
H or ’	Hydrogen atom
Vi	Vinyl (– CH = CH_2)
oct	Octyl (– $(CH_2)_7CH_3$)

Three examples of siloxanes and their abbreviations are given in Table 3.

Table 3: Examples of siloxanes.

Abbreviation	Formula
MD′M	
$MD^{oct}{}_{50}M$	
M'_2	

1

Introduction

1.1 The formation of C – Si bonds

When one wants to form a C – Si bond, several reactions can be used,[1] of which the most important are shown in Figure 1.1.

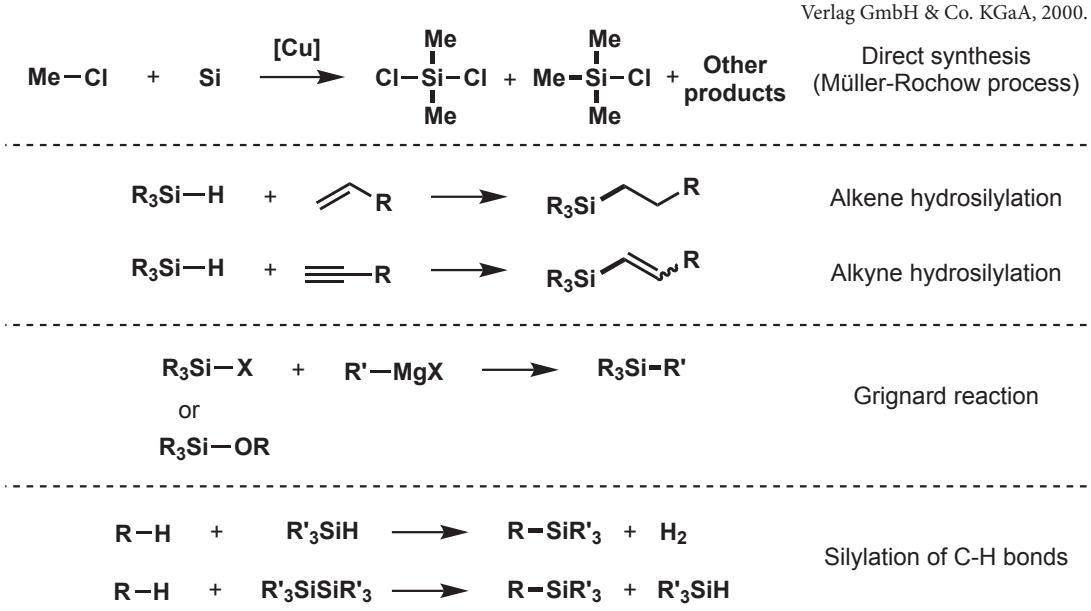


Figure 1.1: Important methods of forming C – Si bonds.

The direct synthesis is the reaction of methyl chloride with metallic silicon in presence of a copper catalyst. If forms a mixture of chloromethylsilanes, of which dimethyldichlorosilane is the major product, which is isolated by fractionnal distillation. This synthesis is carried out to produce more than one million ton of methylchlorosilanes per year. The same synthesis is used for the synthesis of phenylchlorosilanes.

Alkene hydrosilylation, the subject of this PhD project, is the addition of a hydrosilane (molecule comprising a Si – H bond) on an alkene, to give an alkylsilane. This reaction does not form byproducts *per se*, and is thus perfectly atom-economical. Alkyne hydrosilylation is a very similar reaction and produces a vinylsilane from a hydrosilane and an alkyne.

The Grignard reaction of an alkylmagnesium halide (or arylmagnesium halide) on a chlorosilane produces the corresponding alkylsilane (or arylsilane).

[1] L. Rösch, P. John and R. Reitmeier. "Silicon Compounds, Organic" in: *Ullmann's Encyclopedia of Industrial Chemistry*. Wiley-VCH Verlag GmbH & Co. KGaA, 2000.

Since it also produces one equivalent of magnesium dihalide or magnesium alkoxyhalide, it is not atom-economical.

The direct silylation of C – H bonds is a rather new method,[2] allowing to access alkyl- or arylsilanes. When using a hydrosilane as coupling partner, the reaction produces one equivalent of hydrogen, while when a disilane is used, one equivalent of hydrosilane is produced.

[2] C. Cheng and J. F. Hartwig, *Chem. Rev.* **2015**, 115, 8946–8975.

1.2 Hydrosilylation

The hydrosilylation reaction is not limited to alkene substrates and is very general. It is defined as the addition of a hydrosilane onto a multiple bond, which can be for example C = O (carbonyls or carbon dioxide), C = N (imine), C ≡ N (nitrile) C = C (alkene) or C ≡ C (alkyne) (Figure 1.2).

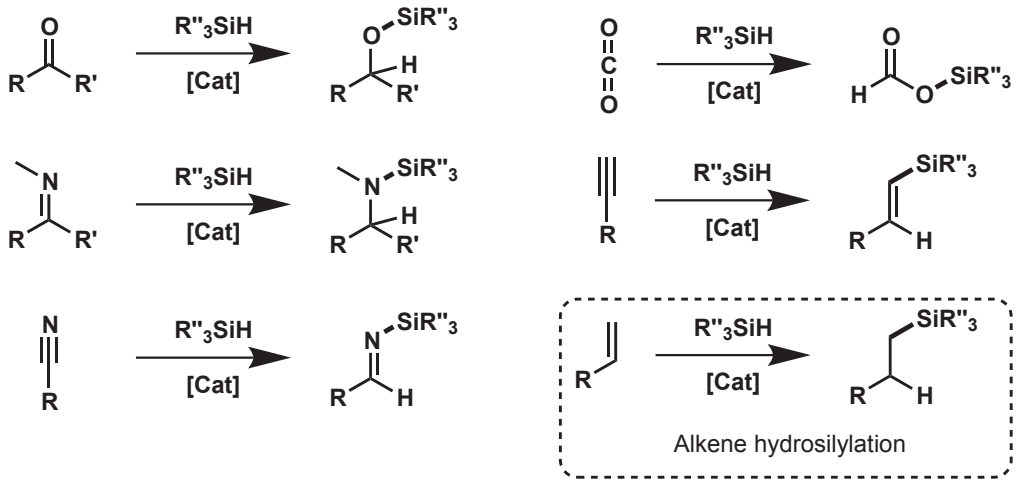


Figure 1.2: Examples of hydrosilylation reactions.

The current research project is exclusively focused on alkene hydrosilylation, a reaction discovered in 1947,[3] which has become of great industrial importance. It has been the object of multiple reviews[4–7] and books,[8–13] and is today still the subject of an extensive academic and industrial research.

[3] L. H. Sommer, E. W. Pietrusza and F. C. Whitmore, *J. Am. Chem. Soc.* **1947**, 69, 188–188.

1.3 Applications of alkene hydrosilylation

1.3.1 Functionalization of silicone fluids

Alkene hydrosilylation is used in the silicone industry to produce functional silicone fluids.[14]

Silicone fluids can either be functionalized on their D' units[a] (Figure 1.3, top and middle), or at the extremities of the siloxane chain (Figure 1.3, bottom), depending on the position of the Si – H bonds on the starting silicone.

The functionalization of silicone fluids by various alkenes (Figure 1.4) gives fluids with very different properties and applications.

For example, aminosilanes are useful for their chemical reactivity (ability to bond with polyimides, polyureas or polyurethanes), their ability to form hydrogen bonds and to chelate species (for diamines). Silicones with piperidine-containing side-chains are used in textile softeners, while perfluoroalkyl chains

[14] Gelest, Inc. *Reactive Silicones: Forging New Polymer Links* 2015

[a] See the "Siloxane nomenclature" section located before this chapter.

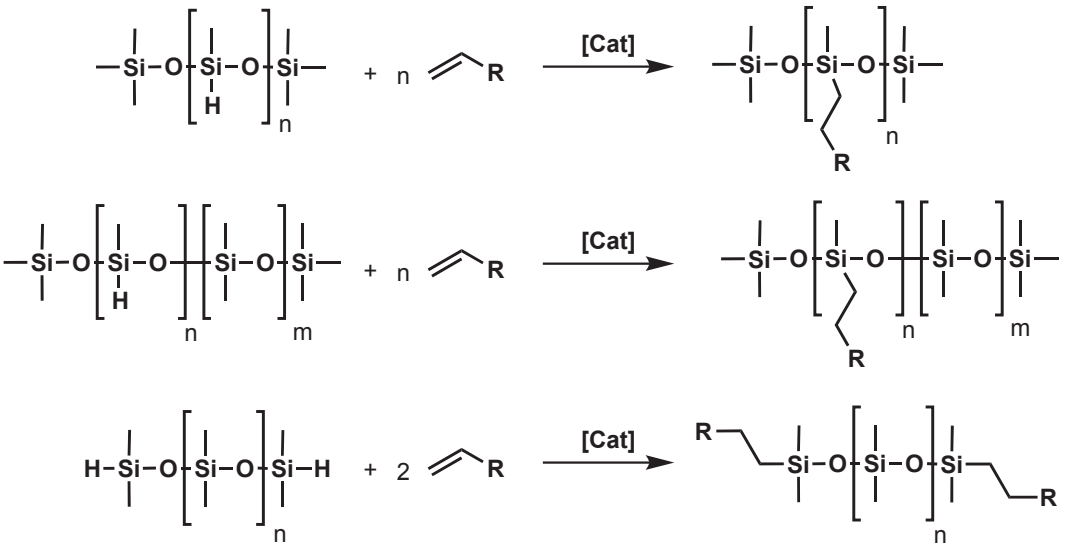


Figure 1.3: Functionalization of silicone fluids. Top: functionalization of D' units of a homopolymer. Middle: functionalization of D' units of a block copolymer. Bottom: functionalization of terminal M' units.

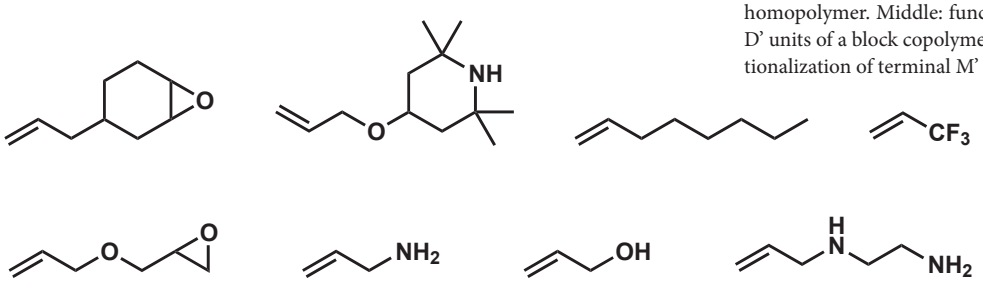


Figure 1.4: Examples of alkenes that can be used to functionalize silicone fluids.

are used to give silicones lipophobic properties. Epoxy-functionalized silicones can be cross-linked by reaction with different nucleophiles or reacted with epoxy resins. Alkyl- (with alkyl chain lengths typically from 2 to 32 carbon atoms) or alkylaryl-functionalized silicones are often used as lubricants. Acrylate-functionalized silicones can used to modify polyacrylates. Polyethers side-chains are used to manufacture surfactants.

1.3.2 Silicones cross-linking

Alkene hydrosilylation is also used to cross-link silicone fluids.[15] In the example given in Figure 1.5, the reaction between a polydimethylsiloxane-*block*-polymethylhydrosiloxane ($MD_{15}D^{H}_{30}M$) and a vinyl-terminated polydimethylsiloxane $M^{vi}D_{120}M^{vi}$ in presence of a Fe complex gives an elastomer.[16] It is important to note that in cross-linking reactions, since the reaction products are solid, it is impossible to recover the catalyst once the reaction is finished.

[15] H. Moretto, M. Schulze and G. Wagner. "Silicones" in: *Ullmann's Encyclopedia of Industrial Chemistry*. Wiley-VCH Verlag GmbH & Co. KGaA, 2000.

[16] A. M. Tondreau et al., *Science* **2012**, 335, 567–570.

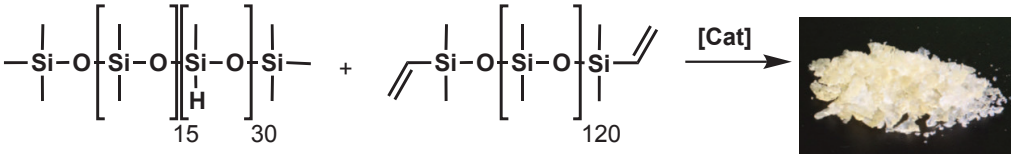


Figure 1.5: Cross-linking of silicone fluids.[16]

Silicone elastomers are often high performance materials and show high stability, high durability, little variation of mechanical properties over wide

temperature ranges, little flamability and are electrically insulating. They find applications as insulating rubbers for high voltage applications, cookware, sealants, gaskets, adhesives, etc.

1.3.3 Synthesis of functional silanes

Applications

Functional silanes, i.e. silanes bearing at least one organic chain, are produced and used at an industrial scale for various applications (Table 1.1).[17]

[17] Gelest, Inc. *Silane Coupling Agents: Connecting Across Boundaries* 2014

Type	Role
Coupling agent	Improve compatibility of organic polymers with inorganic materials
Adhesion promoter	Improve adhesion of a paint, ink, adhesive, coating or sealant
Hydrophobing and dispersing agent	Make surfaces hydrophobic
Crosslinking agent	Give polymers the ability to cross-link when exposed to moisture
Moisture scavenger	React with water (in water-sensitive formulations)
Polypropylene catalyst donor	Control stereochemistry (tacticity) of polypropylene
Silicate stabilizer	Prevent agglomeration and precipitation of silicates

Table 1.1: Role of functional silanes in different applications.[18]

Their main application is as coupling agents, to improve the compatibility of organic materials and inorganic materials such as silicates, aluminates or borates.[17,19] The functional part of the silane (Figure 1.6) binds with the organic material, while the hydrolyzable groups are either hydrolyzed to Si – OH groups which then condense on OH groups of the inorganic material (Figure 1.7), or directly condense on these OH groups.

[19] U. Deschler, P. Kleinschmit and P. Panster, *Angew. Chem. Int. Ed.* **1986**, 25, 236–252.

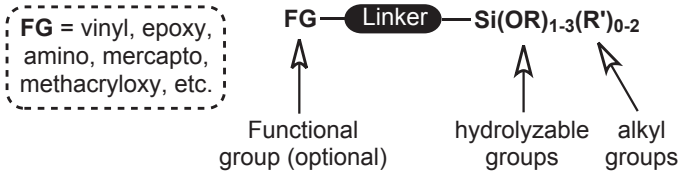


Figure 1.6: Usual structure of functional silanes.

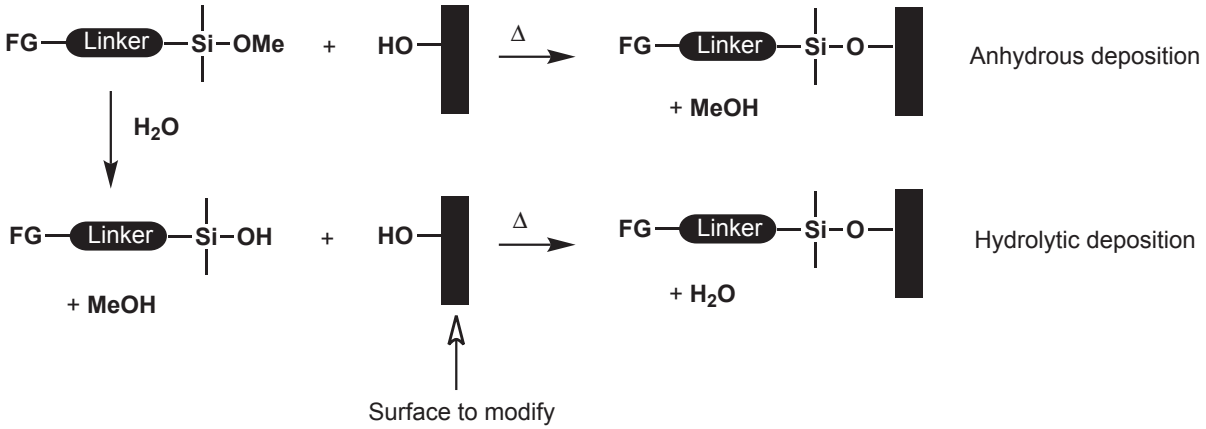


Figure 1.7: Surface modifications with functional silanes.

Common organic-inorganic composite materials produced with the aid

of these silane coupling agents include glass-fiber-containing resins, mineral-filled rubbers (eg. for the manufacture of tires). Their surface-modificating ability is also used as adhesion promoters (for example in paint formulations) and hydrophobing agents (used a lot in constructions).

Less common roles for functional silanes include moisture scavengers in water-sensitive formulations (by reacting with water) and crosslinking agents, where the alkoxysilane groups' purpose is to condense with each other in the presence of moisture. They can also be used for the preparation of stationary phases for chromatography.[20]

[20] H. Engelhardt and P. Orth, *J. Liq. Chrom.* **1987**, 10, 1999–2022.

Synthesis

The synthesis of these functional silanes often comprises a hydrosilylation step. In the top example of Figure 1.8, trichlorosilane is reacted with allyl chloride, to give chloropropyltrichlorosilane, which can then react with an alcohol to give a chloropropyltrialkoxysilane. These chloropropyl-functionalized silanes can be further functionalized, for example by nucleophilic substitution on the Cl atom of the chloropropyl chain, to obtain a great diversity of functional silanes. Nucleophile such as ammonia, ethylenediamine, disodium tetrasulfide or hydrogen sulfide can be used.[19] In the bottom example of Figure 1.8, an alternative route is presented, where a trialkoxysilane is directly functionalized with a functional alkene by hydrosilylation.

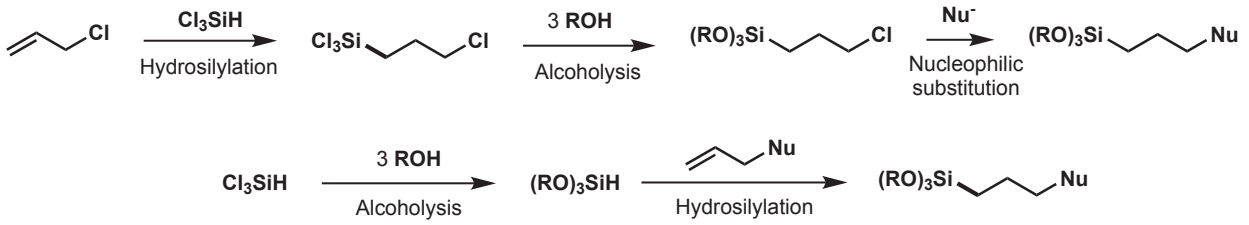


Figure 1.8: Two routes to functional silanes using an alkene hydrosilylation step.

1.3.4 Multi-step synthesis of complex molecules

A less well-known utilization of alkene hydrosilylation is in the multi-step synthesis of complex molecules.[13] This is a rather academic use of the reaction, but some commercial products are manufactured thanks to it. For example, Drometrizole trisiloxane (Figure 1.9) is used by L'Oréal in sunscreens as UV absorber. Its Si – CH_2 bond is made by alkene hydrosilylation.[21]

[21] R. Farkas et al., *Molecules* **2010**, 15, 6205–6216.

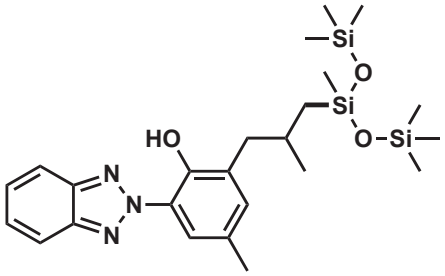


Figure 1.9: Drometrizole trisiloxane, a molecule used in sunscreens to absorb UV radiations. The C – Si bond in bold is formed by alkene hydrosilylation.[21]

In a perspective from 2013, Franz and Wilson state that "the incorporation of silicon and synthesis of organosilicon small molecules provide unique opportu-

nities for medicinal applications".[22] Potential benefits of incorporating silicon atoms in active molecules include: an enhanced lipophilicity compared to their carbon analogs (enhancing cell penetration), the possibility to access different geometric structures (bond lengths or angles), the electropositive nature of silicon (which can lead to original physicochemical properties) and an absence of intrinsic toxicity associated with silicon atoms. They also commented several studies in which alkene hydrosilylation was used in the synthesis of bioactive molecules.

Alkene hydrosilylation is also a valuable reaction for the multi-step synthesis of silicon-containing heterocycles, as reported in a review by Cheng and Hartwig.[2]

Furthermore, alkene hydrosilylation can be used to install a transient Si – C bond in a molecule, which can then be oxidized to an alcohol using the Tamao-Fleming conditions.[23,24] This reaction proceeds with stereoretention and is diastereoselective. For example, it allows the obtention of 1,3-diols from homoallylic alcohols, and the same strategy can be used starting from allylamines to obtain *syn*-β-aminoalcohols. Starting from prochiral alkenes and using asymetric hydrosilylation catalysts, it can be an interesting strategy to access chiral alcohols.[25] For instance, in 1991 Uozumi and Hayashi used a chiral palladium complex to catalyze the hydrosilylation of 1-hexene by trichlorosilane (Figure 1.10).[26] Oxidation of the C – Si bond with Tamao-Fleming conditions afforded (*R*)-hexan-2-ol with 94% enantiomeric excess.

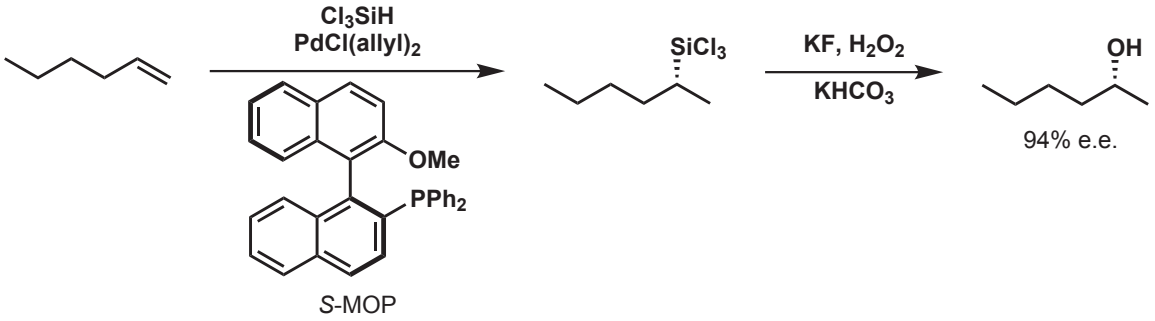


Figure 1.10: Asymetric hydrosilylation followed by Tamao-Fleming oxidation to give a chiral alcohol.[26]

In 2014, Gevorgyan *et al.* presented a new multi-step method for the conversion of terminal alkenes into 1,4-diols.[27] The synthesis (Figure 1.11, top) comprises the hydrosilylation of the alkene by dichlorosilane, installation of a newly-developed directing group on the silicon atom (including a picolyl group and a tert-butyl group), intramolecular dehydrogenative silylation of a δ-C – H bond, and finally oxidation of the C – Si bond. This method was applied to substrates such as a steroid (Figure 1.11, bottom left) or camphene (Figure 1.11, bottom right).

In a very recent article, Hartwig *et al.* published a hydrosilyl-directed borylation of alkyl C – H bonds.[28] Starting from a 1,1-disubstituted alkene, hydrosilylation with diethylsilane yielded a hydrosilyl-functionalized molecule (Figure 1.12, top), which C – H bond located in the γ position to the hydrosilyl group was selectively borylated using $Et_3SiBpin$ and an iridium catalyst. The reaction was diastereoselective. An example of obtained molecule was derivatized to the products of oxidation, amination and arylation (Figure 1.12,

[22] A. K. Franz and S. O. Wilson, *J. Med. Chem.* **2013**, 56, 388–405.

[23] K. Tamao et al., *Organometallics* **1983**, 2, 1694–1696.
[24] I. Fleming, R. Henning and H. Plaut, *J. Chem. Soc., Chem. Comm.* **1984**, 29–31.

[25] I. Fleming, A. Barbero and D. Walter, *Chem. Rev.* **1997**, 97, 2063–2192.

[26] Y. Uozumi and T. Hayashi, *J. Am. Chem. Soc.* **1991**, 113, 9887–9888.

[27] N. Ghavtadze et al., *Nat. Chem.* **2014**, 6, 122–125.

[28] M. A. Larsen, S. H. Cho and J. Hartwig, *J. Am. Chem. Soc.* **2016**, 138, 762–765.

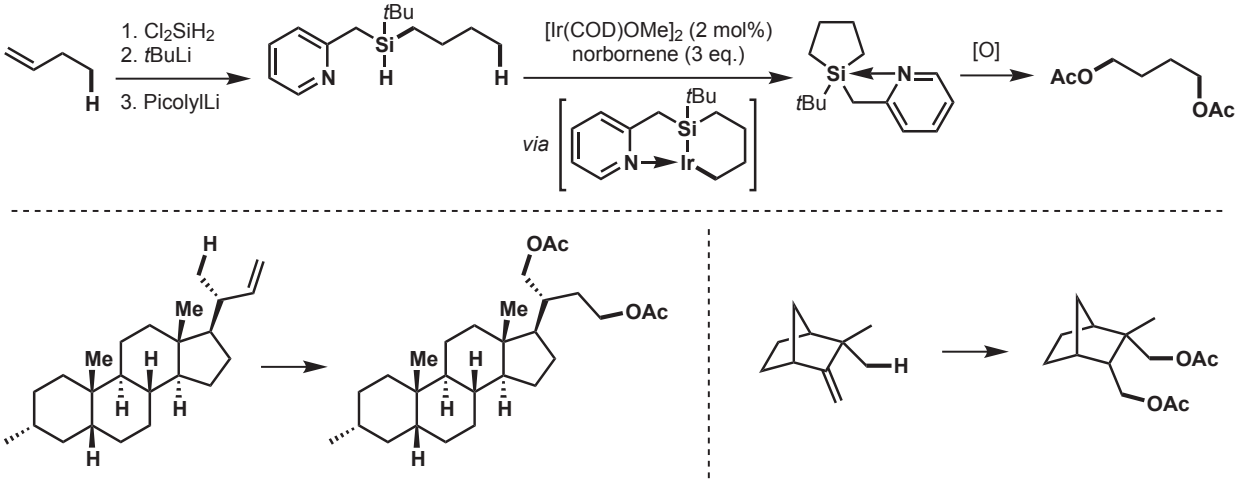


Figure 1.11: Top: general method for obatining 1,4-diols from terminal alkenes.[27] Bottom left: application to the derivatization of a steroid. Bottom right: application to the derivatization of camphene.

bottom).

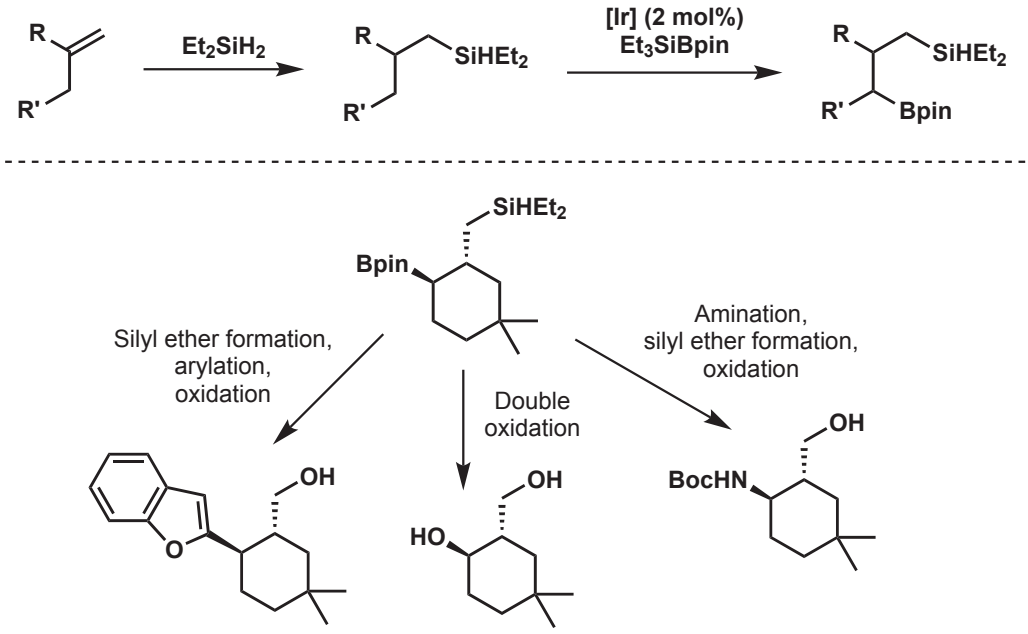


Figure 1.12: Top: hydrosilane-directed borylation of C – H bonds. Bottom: possible derivatizations of the obtained products.[28]

1.4 Generalities about the reaction

1.4.1 Brief history and challenges

Alkene hydrosilylation was first reported in 1947,[3] for the reaction of trichlorosilane with 1-octene catalyzed by peroxides (Figure 1.13). The reaction was a remarkable improvement over the previous method (reaction of *n*-octylmagnesium bromide with silicon tetrachloride), from a point of view of yield and atom economy.

In 1953, Wagner, working at Union Carbide & Carbon Corporation, patented the utilization of Pt/charcoal as catalyst for alkene hydrosilylation.[29] In the patent, he disclosed that Pt/C (commercial or prepared by impregnation with

[29] G. H. Wagner *Reaction of silanes with aliphatic unsaturated compounds* US2637738 Patent 1953

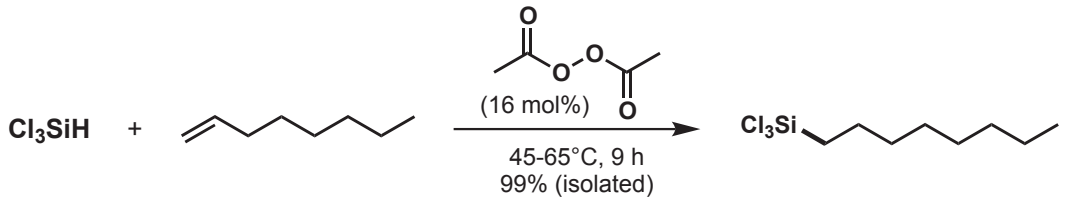


Figure 1.13: The first example of alkene hydrosilylation.[3]

chloroplatinic acid followed by reduction with hydrogen) was a very efficient catalyst for the hydrosilylation of various olefins (or acetylene) with alkoxysilanes or chlorosilanes, without solvent. High temperatures were needed (130 °C to 160 °C), leading to selectivity issues with some substrates, but high TONs (up to 2×10^6) were reached (Figure 1.14).

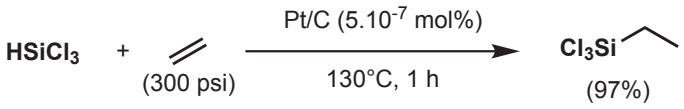


Figure 1.14: The first platinum catalyst for alkene hydrosilylation.[29]

In 1957, Speier, from Dow Corning, reported that $H_2PtCl_6 \cdot 6\,H_2O$ in isopropanol was a very active catalyst.[30–32] With 1-pentene and methyldichlorosilane in an autoclave, he obtained TONs as high as 1.6×10^7 using a heating bath at 100 °C, even if he recorded temperatures as high as 210 °C inside the reactor because of the exothermicity of the reaction. Speier's discovery of $H_2PtCl_6 \cdot 6\,H_2O$ as a very active catalyst enabled the wide adoption of alkene hydrosilylation to prepare organosilanes and organosiloxanes.

[30] J. L. Speier, J. A. Webster and G. H. Barnes, *J. Am. Chem. Soc.* **1957**, 79, 974–979.
[31] J. C. Saam and J. L. Speier, *J. Am. Chem. Soc.* **1958**, 80, 4104–4106.
[32] J. L. Speier and D. E. Hook *Process for the production of organo-silicon compounds* 1958

In 1973, Karstedt, working at General Electric, patented a Pt(0) complex featuring divinyltetramethylsiloxane (DVTMS) ligands (Figure 1.15), prepared from Pt(II) halogen species and the DVTMS ligand, and also demonstrated in the patent its application to the cross-linking of functional silicone fluids.[33] As written in the patent, "although [Pt/C and Speier's catalyst]-catalyzed hydrosilylation methods provide for valuable results, the parts by weight of platinum metal values, per million parts of hydrosilylation mixture, required for effective results, often render these methods economically unattractive. In many instances, for example, substantial amounts of platinum metal values are rendered catalytically inactive and beyond recovery." Indeed, Karstedt's complex is more stable than Speier's catalyst and has the added benefit of having a much shorter induction period than Speier's catalyst (that needs to be reduced from Pt(IV) to Pt(0).) Because of these superior performances, Karstedt's complex is now the most used catalyst in the silicone industry.

[33] B. D. Karstedt *Platinum complexes of unsaturated siloxanes and platinum containing organopolysiloxanes* U.S. Patent 3,775,452 1973

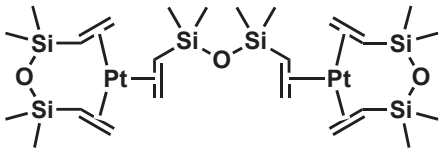


Figure 1.15: Karstedt's complex.[34]

However, because platinum is a very rare metal in Earth's crust, its use is unsustainable (Figure 1.16),[35] and also very expensive.[36] Moreover, its price is subject to important fluctuations due to speculation.[37] Platinum is also said to

[35] *The Periodic Table's Endangered Elements* [Online; accessed 23-August-2016] 2015
[36] H. Renner et al. "Platinum Group Metals and Compounds" in: *Ullmann's Encyclopedia of Industrial Chemistry*. Wiley-VCH Verlag GmbH & Co. KGaA, 2000.
[37] C. Yang, *Energy Policy* **2009**, 37, 1805–1808.

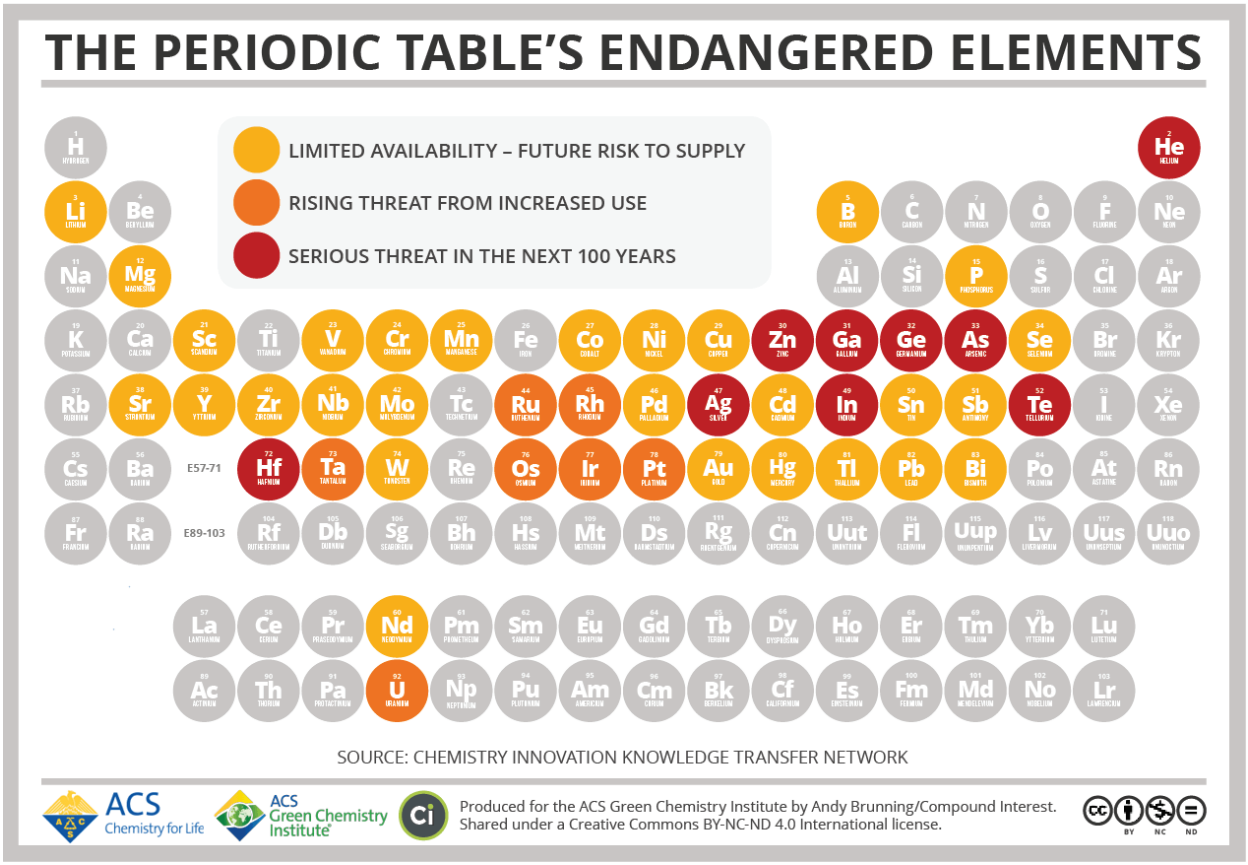


Figure 1.16: The periodic table of endangered elements.[35]

be toxic, especially in the form of water-soluble salts, even if the amount of toxicity studies available is limited. Because of all these reasons, alternative catalysts to the Pt complexes are highly desired. A lot of attention has been devoted to the development of efficient heterogeneous Pt catalysts (that could decrease the quantity of Pt used) and catalysts based on non-noble metals (that could completely replace Pt catalysts). Up to now, however, very few of these catalysts are industrially relevant alternatives to Karstedt's catalyst.

1.4.2 Selectivity

Regioselectivity

For platinum catalysts, alkene hydrosilylation usually favours anti-Markovnikov addition (silicon atom added on the least substituted carbon atom of the C = C bond) and gives the linear addition product (Figure 1.17). In some cases, for example with styrenes, the branched Markovnikov product (silicon atom on the most substituted carbon atom) can be obtained to some extent, too. For other metals, the regioselectivity can be completely different, as discussed later in this chapter.

Side reactions

Several side reactions are commonly observed when performing alkene hydrosilylation (Figure 1.18).[13]

Alkene isomerization, the migration of the C = C bond along the carbon

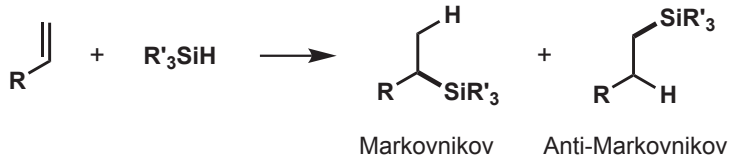


Figure 1.17: Markovnikov and Anti-Markovnikov selectivities.

chain, can happen when there is a hydrogen atom in α position to the C = C bond. It is especially thermodynamically favourable when going from a terminal C = C bond to an internal one.

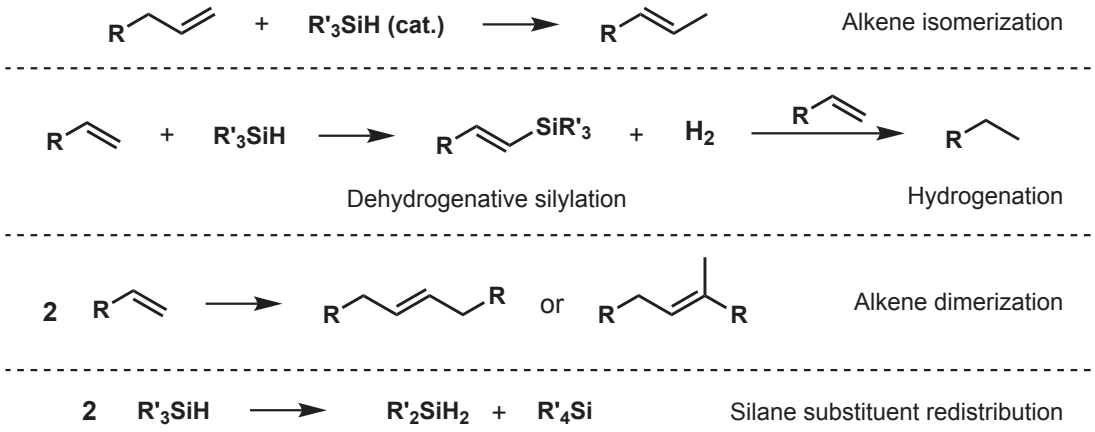


Figure 1.18: Side reactions of alkene hydrosilylation.

Dehydrogenative silylation is similar to hydrosilylation, except that a vinylsilane is obtained instead of an alkylsilane. The reaction is accompanied by the formation of molecular hydrogen or by hydrogenation of the alkene.

Alkene dimerization has also been observed with some catalysts, but is a rarer side reaction.

The silane substituent redistribution reaction, which is a disproportionation reaction when it happens between identical silanes, is an exchange of substituents. Although quite rarely observed, it sometimes happens with alkoxysilanes or phenylsilanes.

1.4.3 Substrate reactivity trends

Some reactivity trends have been observed for the alkenes and hydrosilanes used in hydrosilylation and are presented here. However, one must keep in mind that they may depend on the catalyst used.

On the SiH side

The reactivity of primary silanes is usually higher than the reactivity of secondary silanes, and tertiary silanes are usually less reactive. However, there are examples where this order is not respected,[38] and primary silanes have been reported to inhibit catalysis with certain metallic complexes by coordinating strongly with the metal.

In general, the more electron-withdrawing the substituents on the SiH molecule, the faster the reaction.[39]

In the particular case of polymethylhydrosiloxanes, Si – H bonds located next to both M groups are less reactive than Si – H bonds that are farther from

[38] I. Buslov et al., *Angew. Chem. Int. Ed.* **2015**, 54, 14523–14526.

[39] L. N. Lewis, *J. Am. Chem. Soc.* **1990**, 112, 5998–6004.

the chain extremities, due to steric hinderance of the M groups. Additionally, a Si – H bond located next to another Si – H bond is statistically hydrosilylated faster than an Si – H bond isolated on the chain, as demonstrated by Cancouët *et al.*, due to a possible simultaneous activation of two vicinal Si – H bonds by a binuclear Pt complex.[40]

[40] P. Cancouët et al., *J. Polym. Sci. A: Polym. Chem.* **2000**, 38, 837–845.

On the alkene side

Alkene hydrosilylation is most of the time performed with terminal alkenes, because internal alkenes are usually not reactive for hydrosilylation. However, if there is in the reaction medium some species which are able to catalyze alkene isomerization, an isomerization-hydrosilylation tandem reaction can happen, where internal alkene isomers are in equilibrium with the terminal alkene, the terminal alkene is consumed by the hydrosilylation reaction and displaces the equilibrium towards formation of more terminal alkene (see subsections 1.5.4 and 1.5.5). For some mechanisms such as the Glaser-Tilley mechanism (see subsection 1.5.6), or for Lewis acid catalysts, internal alkenes (and even trisubstituted alkenes) are sometimes reactive.

Lewis reported that there was a direct correlation between the electron density at alkenes and their reactivity, for aliphatic and aromatic alkenes.[39]

1.4.4 Safety first!

The alkene hydrosilylation reaction presents three main risks that must be taken into account while attempting to perform experiments described in the present thesis.

The first risk is linked to the hydrosilanes, which react with protic reagents (such as water, alcohols or carboxylic acids) to give H_2 (Figure 1.19, top). This reaction is catalyzed by acids, bases, and transition metals. An essential safety rule when working on alkene hydrosilylation is to keep SiH starting materials, reaction products (which may contain unreacted SiH) and waste isolated from incompatible substances.

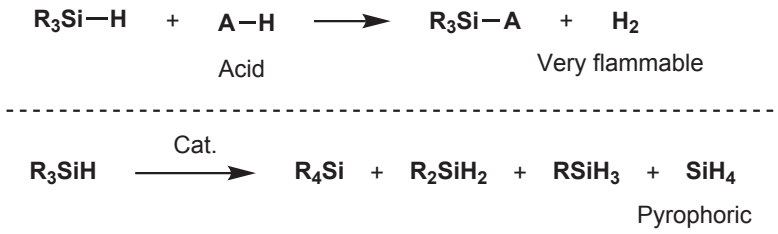


Figure 1.19: Top: formation of H_2 by reaction between a hydrosilane and an acid. Bottom: dismutation of a hydrosilane forming pyrophoric silanes such as SiH_4.

Silane dismutation, as evoked in paragraph 1.4.2, is also a risk, because it can lead to the formation of pyrophoric silanes such as SiH_4 (Figure 1.19, bottom).[41,42] The reaction is particularly easy when labile groups are present on the silicon atom, such as alkoxy or phenyl groups, and is catalyzed by Lewis acids or alkali bases. Thus, when performing reactions at large scale, it is preferrable to set up a stream of inert gas in the headspace of the reactor, to avoid inflammation or build-up of flammable gases in the reactor.

[41] J. W. Ryan, *J. Am. Chem. Soc.* **1962**, 84, 4730–4734.
[42] S. C. Berk and S. L. Buchwald, *J. Org. Chem.* **1992**, 57, 3751–3753.

The third risk is the high exothermicity of the reaction,[b] which can lead to a runaway if the reaction heat is not dissipated enough. This is especially true when the reaction is performed without using a solvent, as it is in indus-

[b] The enthalpy of reaction is typically of -100 kJ mol^{-1} to -160 kJ mol^{-1} of SiH.

trial processes. To prevent such runaway, the temperature inside the reactor must be carefully monitored and the reactor must be equipped with an appropriately sized cooling system. Additionnaly, a catalyst poison (such as triphenylphosphite for platinum catalyst) can be introduced in the reactor when an unexpected heat buildup happens.

1.5 Alkene hydrosilylation catalysts: state of the art

A history and state of the art of alkene hydrosilylation catalysts is presented here, with an emphasis on platinum catalysts, because they are widely used in the industry, and non-noble metals, because they represent potential sustainable alternatives to current platinum catalysts.

1.5.1 Platinum

The early history of Pt catalysis, including the first Pt/C catalyst, Speier's catalyst (H_2PtCl_6 in isopropanol) and Karstedt's complex, has already been written in subsection 1.4.1. Karstedt's catalyst is still today the most widely used Pt catalyst and a reference for other studies, but other developments have been carried out since its discovery.

A significant advance in homogeneous Pt catalysis was reported in 2002 by Markó's group,[43] completed by further studies[44–47] and summarized in two book chapters.[48,49] They used Pt(0) complexes with N-heterocyclic carbenes ligands (NHCs) as catalysts (Figure 1.20, top), and were able to almost suppress the undesirable alkene isomerization reaction and the formation of Pt colloids which usually arises from decomposition of Pt(0) complexes under hydrosilylation conditions. They correlated the low alkene isomerization to the slow activation of the precatalyst, and they explained absence of complex decomposition to Pt colloid to the high strength and stability of the Pt – NHC bond. Interestingly, a higher chemoselectivity was observed with alkenes bearing reactive functionalities such as epoxides. In this case, epoxide opening was not observed (Figure 1.20, bottom), contrary to what is observed with Karstedt's complex. One drawback of this catalyst family is that they have slightly lower activities than Karstedt's complex.

[43] I. E. Markó et al., *Science* **2002**, 298, 204–206.
[44] I. E. Markó et al., *Adv. Synth. Catal.* **2004**, 346, 1429–1434.
[45] O. Buisine et al., *Chem. Comm.* **2005**, 3856–3858.
[46] G. Berthon-Gelloz et al., *J. Organomet. Chem.* **2005**, 690, 6156–6168.
[47] G. Berthon-Gelloz et al., *Organometallics* **2007**, 26, 5731–5734.

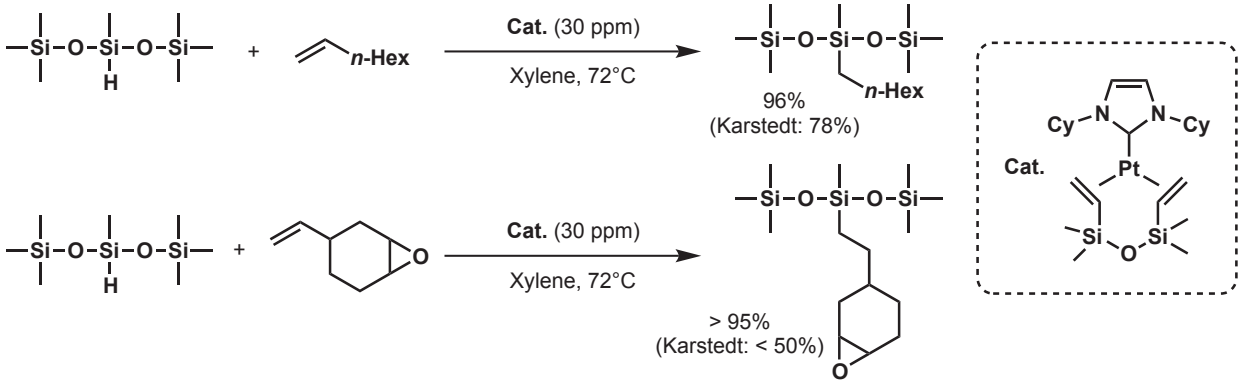


Figure 1.20: Hydrosilylation of 1-octene or vinylcyclohexene epoxide by MD'M catalyzed by Pt-NHC complexes.[43]

Another development in homogeneous Pt catalysis is especially relevant

for the cross-linking of silicones: the need for catalysts that are activable on demand, also called "switchable catalysts".[5] They allow to prepare formulations that contain a vinyl-functionalized silicone, a Si – H-functionalized silicone and the switchable catalyst, and to activate the cross-linking when desired, by applying a stimulus (generally heat or light).

For example, inhibitors such as malonates, fumarates or alkynols (Figure 1.21) are thermally switchable.[5] Their mechanism of action is often attributed to a chelation of the Pt centers by these polyfunctional molecules. It has also been attributed to the creation of a second phase where the Pt is located (and thus separated from the silicones), which disappears when the mixture is heated above the vaporization point of the inhibitor, allowing the catalyst to be mixed with the reactive silicones.

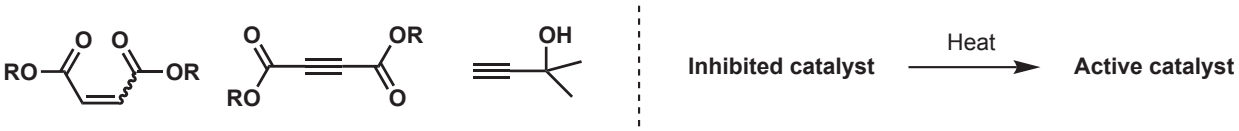


Figure 1.21: Left: examples of Pt catalysts inhibitors that are thermally activable.[5] Right: activation of thermally switchable Pt catalysts.

Photoswitchable catalysts have also been developed,[5] in which excitation of a catalytically inactive species from its ground state to an excited and active state is achieved by applying radiations, typically in the UV domain. It is more difficult to perform and control than thermal activation, but has the advantage of being feasible at room temperature.

A seemingly promising area of innovation is the development of heterogeneous Pt catalysts, that would combine the high activity and selectivity that are typical of Pt catalysts with an ease of separation from the reaction products and a possibility of reuse or recycle.[6] However, the development of such heterogeneous catalysts has been hampered by the recurring leaching of Pt species in the reaction medium and by catalyst fouling caused by the reaction products.[50]

Supported Pt complexes, prepared by impregnation of a solid comprising coordinating functional groups with Pt salts or complexes, have been studied a lot, but suffered from poor performances. In the rare cases where Pt leaching has been assessed, it was found to be high, presumably because of the weak bonding of the Pt centers to the support. In a recent review titled "Why Does Industry Not Use Immobilized Transition Metal Complexes as Catalysts?",[51] Hübner *et al.* state that the absence of supported metallic complexes in industrial processes, in particular in the pharmaceutical and fine chemistry industries, comes from the low stability of these complexes, a higher catalyst development cost, slower kinetics and sometimes metal leaching. All these problems do not confer supported complexes a significant advantage over homogeneous complexes.

Supported Pt nanoparticles offered in some cases better performances than supported complexes, including higher TONs and lower Pt leaching.[50,52,53] However, the articles/patents often lack detailed catalysts preparation prodedures and characterizations.

What is often missing from studies on heterogeneous catalysts is quantitative data allowing the comparison of new catalysts with catalysts of the literature.

[50] R. Ciriminna et al., *ACS Sustain. Chem. Eng.* **2013**, 1, 249–253.

[51] S. Hübner, J. G. de Vries and V. Farina, *Adv. Synth. Catal.* **2016**, 358, 3–25.

[52] S. J. Thomas and W. H. Retsch *Heterogeneous Hydrosilylation Catalysts, Polymers Formed Therewith, and Related Coating Compositions* Patent application WO 2007106427 A3 2007

[53] H. Bai, *Ind. Eng. Chem. Res.* **2014**, 53, 1588–1597.

For example, TONs allow to know the quantity of Si – H transformable per mole of precious metal. Pt concentration measurements in the products indicate how much Pt has leached, and how stable is the catalyst. Finally, reusability tests in batch[c] and tests in continuous reactors allow to study deactivation that can be due to platinum leaching, fouling or chemical poisoning.

[c] To provide valuable information, these recyclability tests must be done by comparison of kinetics over several runs, and not only by comparing conversions after a certain time, especially at very high conversions.

Up to now, it appears that none of the published heterogeneous Pt catalysts offer a significant global advantage over Karstedt's catalyst.

1.5.2 Reaction mechanism with platinum catalysts

Studies on the active species

A fundamental part of a mechanistic study is the elucidation of the nature of the active species.[54] For alkene hydrosilylation with Pt catalysts, this has been very difficult and controversial. Larry N. Lewis and colleagues, from General Electric, have made some major contributions to this question.

[54] S. J. Meek, C. L. Pitman and A. J. M. Miller, *J. Chem. Ed.* **2016**, 93, 275–286.

In 1986, they affirmed that the formation of Pt colloids from molecular Pt precatalysts was the key step in the reaction.[55] They compared various characteristics of (COD)$PtCl_2$, a Pt colloid formed from (COD)$PtCl_2$ and Speier's catalyst. They observed that the induction was greatly reduced when using a Pt colloid, compared to (COD)$PtCl_2$, and that the Pt colloid was more active than (COD)$PtCl_2$. A poisoning test with Hg (that is known to selectively poison metallic particles but not molecular complexes) revealed that all three precatalysts were inactive in presence of Hg. From all these observations, they concluded that the active species was colloidal, and that when starting from a Pt complex, its decomposition (preceded by its reduction to Pt(0) if starting from a higher oxidation state) was a necessary step for the catalysis to start. However, they acknowledged that some cases of truly homogeneous Pt species existed, and that their findings only apply to Pt complexes where ligands (such as alkenes or vinylsilanes) can be reduced in hydrosilylation conditions or are labile.

[55] L. N. Lewis and N. Lewis, *J. Am. Chem. Soc.* **1986**, 108, 7228–7231.

In 1990, they studied the beneficial effects of molecular oxygen on Pt colloidal catalysts.[39] They observed that the presence of molecular oxygen prevented irreversible colloid aggregation, thus leading to the increase of activity. Another hypothesis explaining the higher activities was that coordination of oxygen made the Pt complex more reactive. They also noted that no O – O bond was broken during catalysis.

Nine years later, they repeated the mercury poisoning tests that they had performed in 1986,[55], except that they did not pre-incubate the Pt complex during 7 h, contrary to what they had done previously.[56] This time, they did not observe inhibition of the catalyst. They concluded that pre-incubation of the Pt complex caused its decomposition, and that it probably stayed homogeneous during catalysis, contrary to what they had written. They also conducted *in situ* EXAFS experiments and observed no Pt – Pt bonds, indicating that the active species were not colloidal in these conditions. However, their EXAFS experiments were performed with very low SiH/Pt ratios, typically 1000 to 3000, which didn't allow observations of what happens at high TONs (up to 10^6) which are routinely attained in alkene hydrosilylation catalysis.

[56] J. Stein et al., *J. Am. Chem. Soc.* **1999**, 121, 3693–3703.

Efforts to identify active Pt species are made difficult by several factors. The first is the difficulty to work at very low Pt concentrations, which are

relevant for alkene hydrosilylation. This difficulty is acknowledged by Roy and Taylor in a mechanistic study, who write: "A deliberate effort was made to use a relatively high platinum concentration in solution (0.05-0.3 M) for faster analysis and easier observation with NMR spectroscopy".[57] This limitation comes from the relatively low sensitivity of the analytical techniques used (EXAFS, NMR, etc.). This means that even if the observation of Pt species at high Pt concentrations is useful in order to understand better the reaction and its mechanism, it is not necessarily representative of what happens at low Pt concentrations. The second difficulty is that interconversion between homogeneous and heterogeneous Pt species is possible: it is well-known that leaching from initially heterogeneous Pt species happens frequently, and the formation of Pt colloids from molecular complexes is also well-known. Then, an active species is not necessary under the same form (homogeneous or heterogeneous) than the precatalyst.

[57] A. K. Roy and R. B. Taylor, *J. Am. Chem. Soc.* **2002**, 124, 9510–9524.

Experimental studies on the mechanism

Chalk and Harrod, from General Electric, were the first to propose a catalytic mechanism for platinum and rhodium complexes.[58] They wrote that they "expected olefin coordination and Si-H bond cleavage to be probable functions of the metal catalyst in the hydrosilation reaction". They proposed a mechanism to account for both hydrosilylation and the frequently observed alkene isomerization (Figure 1.22), in which oxidative addition of the SiH on the Pt followed by insertion of the alkene in the Pt – H bond, followed by either reductive elimination (leading to the hydrosilylation product) or β-H elimination (leading to alkene isomerization).

[58] A. J. Chalk and J. F. Harrod, *J. Am. Chem. Soc.* **1965**, 87, 16–21.

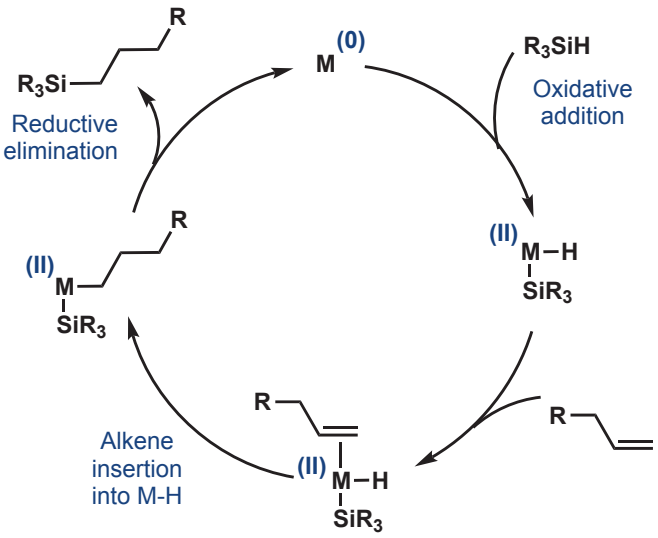


Figure 1.22: The Chalk-Harrod mechanism.[58]

In a kinetic study published in 1988, Caseri and Pregosin studied *trans*-$PtCl_2(styrene)_2$ and $Pt(styrene)_3$ in the hydrosilylation of styrene with triethylsilane.[59] They concluded that the alkene insertion in the Pt – H bond was the rate limiting step of the mechanism, followed by an irreversible reductive elimination. However, they note that in the literature there are several examples of catalytic systems which rate depend on the silane used, which indicates that their conclusions may not be general.

[59] W. Caseri and P. S. Pregosin, *J. Organomet. Chem.* **1988**, 356, 259–269.

In 2002, Roy and Taylor, also from General Electric, took advantage of

the fact that cyclooctene and cyclooctadiene are very resistant to hydrosilylation to use them to stabilize Pt species in order to ease their observation *in situ*.[57] Starting from $Pt(COD)Cl_2$, they were able to synthesize several Pt dimers containing simultaneously alkene (η^2-bonded COD) and silyl groups (Figure 1.23) and to show that these complexes were catalytically active. Their observations supported the fact that alkene insertion in the Pt – H bond is facile, supporting the Chalk-Harrod mechanism for Pt catalysts. They also stated that the well-known difficulty to hydrosilylate internal alkenes such as COD does not come from a slow alkene insertion into the Pt – H bond, but from a slow reductive elimination from the Pt(alkyl)(silyl) complex, because of steric factors.

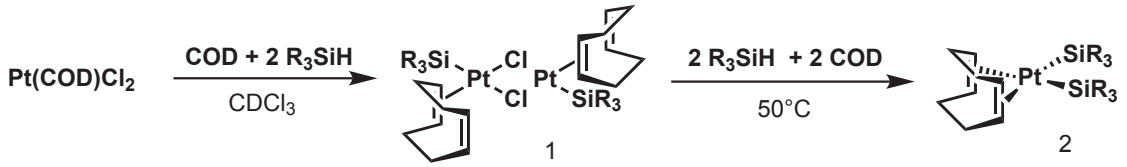


Figure 1.23: Metastable Pt(alkenyl)(silyl) complexes synthesized by Roy and Taylor.[57] Complex 1 is a precatalytic intermediate, whereas complex 2 is a catalytic intermediate.

Markó *et al.* have studied several aspects of the mechanism of their Pt-NHC catalysts.[49] Interestingly, they observed that the slower the initiation step (involving decoordination of the divinyltetramethylsiloxane ligand), the lower the alkene isomerization proportion. Thus, activity and selectivity toward the hydrosilylation product seem to be inversely related. They also used quantitative kinetic modeling to select a mechanism between several proposals, based on experimental kinetic curves. The selected mechanism (Figure 1.24) involves decoordination of the dvtms ligand as initiation step, coordination of an alkene and a silane, a concerted oxidative addition of the SiH and insertion of the alkene in the Pt – H bond, followed by a reductive elimination of the hydrosilylation product. Additionally, alkene isomerization is taken into account, and their mechanim accounts for an inhibition of the catalyst in presence of an excess of alkene and an irreversible deactivation pathway by formation of a dimer.

In a recent study, Kühn *et al.* brought new insights to the reaction mechanism with Karstedt's complex.[60] By studying the product distribution of reactions with Cl_3SiD, they concluded that alkene 1,2-insertion in the Pt – D bond was irreversible and followed by reductive elimination (leading to the hydrosilylation product) and that 2,1-insertion was also irreversible, and followed by β-H elimination (leading to the isomerization product). The relative rate of these two reactions would determinate the proportion of alkene isomerization relative to alkene hydrosilylation. Kinetic isotope measurements supported the conclusions of Caseri and Pregosin[59] that the rate-determining step was the alkene insertion in the Pt – H bond. In agreement with this hypothesis, which implies that a significant amount of Pt hydride should be present in solutions, they observed a Pt – D species in solution by deuterium NMR when they used a deuterated silane. Finally, they noted that "the nature of the active catalyst species as well as the rate law for the hydrosilylation reaction appear to be linked to the coordination strength of the olefin substrate".

Overall, kinetic data that were reported for Pt catalysts were highly depen-

[60] T. K. Meister et al., *ACS Catal.* **2016**, 1274–1284.

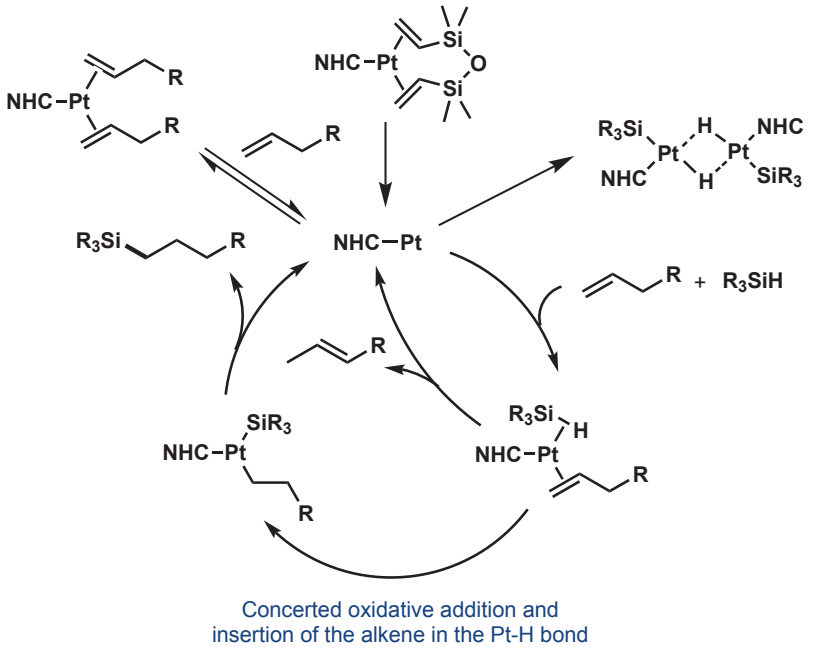


Figure 1.24: Mechanism proposed by Markó *et al.* for their Pt(NHC)(dvtms) catalysts.[49] Top left: inhibition by an excess of alkene, top right: irreversible deactivation by dimerization.

dent on the reagents, catalysts and reaction conditions. For example Caseri and Pregosin reported first order in Pt and a zeroth order in both reagents.[59] Marciniec *et al.* who studied heterogeneous Pt catalyst reported a first order in both alkene and silane, and a change in Pt order from 1 to 0 when increasing Pt concentration, suggesting a mass transport limitation.[61] Kühn *et al.*, while studying the effect of the coordinating strength of the alkenes on the reaction, found with norbornene a first order in silane and platinum and a zeroth order in norbornene (which is strongly coordinating).[60] When working 1-octene (weakly coordinating), they found a second order in silane, first order in Pt and an order of –1 in 1-octene.

[61] B. Marciniec et al., *Appl. Organomet. Chem.* **2003**, 17, 127–134.

Theoretical studies

Several theoretical studies have been performed on hydrosilylation reactions. They were summarized in a book chapter by Wu *et al.* in 2008.[62] Some studies about Pt complexes are commented here.

In 1998 and 1999, Sakaki *et al.* used computational chemistry to determine which of the Chalk-Harrod or the modified Chalk-Harrod mechanism (Figure 1.25) was more plausible for the hydrosilylation of ethylene by simple silanes (SiH_4, Me_3SiH and Cl_3SiH) using a $Pt(PH_3)_2$ catalyst.[63,64] For the Chalk-Harrod mechanism, they calculated that the rate-determining step was the isomerization from *cis* to *trans* of the intermediate formed by ethylene insertion in the Pt – H bond, with an activation barrier around 22 kcal/mol. For the modified Chalk-Harrod mechanism, the rate-determining step was calculated to be ethylene insertion in the Pt – Si bond, with an activation barrier around 44 kcal/mol for SiH_4 and Me_3SiH and 60 kcal/mol for Cl_3SiH. This was the confirmation that for this catalytic system, the Chalk-Harrod mechanism was favoured.

[62] Y. Wu, L. W. Chung and X. Zhang. "Hydrosilylation Reactions Discovered in the Last Decade: Combined Experimental and Computational Studies on the New Mechanisms" in: *Computational Modeling for Homogeneous and Enzymatic Catalysis* ed. by K. Morokuma and D. G. Musaev. Wiley-VCH Verlag GmbH & Co. KGaA, 2008. 285–316

[63] S. Sakaki, N. Mizoe and M. Sugimoto, *Organometallics* **1998**, 17, 2510–2523.

[64] S. Sakaki et al., *Coord. Chem. Rev.* **1999**, 190–192, 933–960.

In 2002, Faglioni *et al.* investigated the Karstedt's complex-catalyzed reaction between simplified vinylsilanes and hydrosilanes.[67] They found that

[67] F. Faglioni et al., *J. Phys. Chem. B* **2002**, 106, 1714–1721.

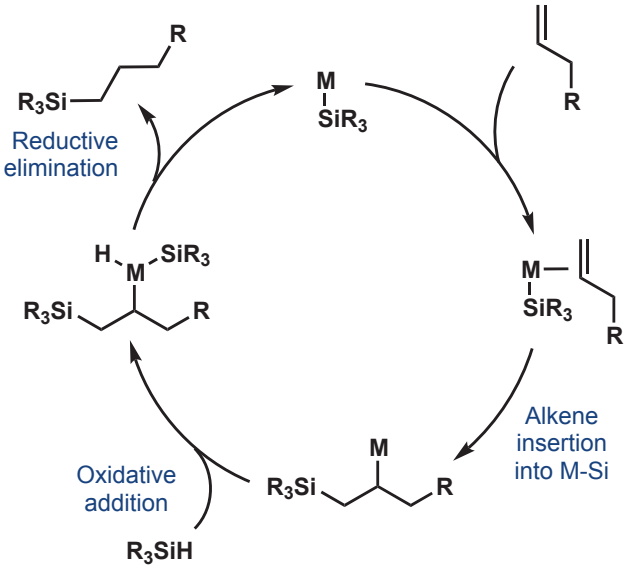


Figure 1.25: Modified Chalk-Harrod mechanism.[65,66]

"possible rate-determining steps are the olefin insertion and reductive elimination" and calculated a total energy barrier on the catalytic cycle of 18 kcal/mol.

In 2003 Giorgi *et al.* continued the work of Sakaki *et al.* on the hydrosilylation of ethylene by SiH_4 with $Pt(PH_3)_2$ as catalyst, but with a DFT approach.[68] They found the Chalk-Harrod mechanism kinetically favoured over its modified version, confirming the conclusion of Sakaki *et al.*, but with slightly lower energy barrier for the ethylene insertion and isomerization steps.

Tsipis *et al.* explored hydrido-bridged diplatinum complexes,[69] and found two steps with high energy barriers: ethylene insertion in the Pt – H bond with an energy barrier of 14 kcal/mol to 20 kcal/mol and reductive elimination, with an energy barrier of 20 kcal/mol to 31 kcal/mol. Here, the reductive elimination was thus found to be rate-determining, contrary to the findings presented above.

In conclusion, it seems that the nature of the rate-determining steps is not the same for all catalytic systems, and can depend on the active species and the substrates. However, for Pt catalysts, the Chalk-Harrod mechanism is apparently favoured most of the time.

1.5.3 Iron

The first example of Fe-catalyzed hydrosilylation was published in 1962 by Nesmeyanov *et al.*[70] Using $Fe(CO)_5$ or colloidal iron, prepared by decomposition of $Fe(CO)_5$ in naphtalene, they were able to catalyze the addition of $MeCl_2SiH$ on propylene. They reached up to 100 turnovers, and obtained mixtures of the hydrosilylation and dehydrogenative silylation products.

Several other examples of iron carbonyl-catalyzed reactions (sometimes under UV irradiation to decoordinate a CO molecule and generate a vacant site on the Fe center) were subsequently published.[71–74] Hydrosilylation was also often in competition with dehydrogenative silylation, and was frequently a minor reaction.

A breakthrough came in 2004 when Chirik *et al.* reported that an iron complex bearing a bisiminopyridine ligand was able to catalyze hydrosilyla-

[68] G. Giorgi et al., *J. Mol. Struct.: THEOCHEM* **2003**, 623, 277–288.

[69] C. A. Tsipis, A. C. Tsipis and C. E. Kefalidis. "Exploring the Catalytic Cycle of the Hydrosilylation of Alkenes Catalyzed by Hydrido-Bridged Diplatinum Complexes Using Electronic Structure Calculation Methods" in: *Fundamental World of Quantum Chemistry* ed. by E. J. Brändas and E. S. Kryachko. Dordrecht: Springer Netherlands, 2004. 619–643

[70] A. Nesmeyanov et al., *Tetrahedron* **1962**, 17, 61–68.

[71] M. A. Schroeder and M. S. Wrighton, *J. Organomet. Chem.* **1977**, 128, 345–358.

[72] J. C. Mitchener and M. S. Wrighton, *J. Am. Chem. Soc.* **1981**, 103, 975–977.

[73] F. Kakiuchi et al., *J. Organomet. Chem.* **1993**, 456, 45–47.

[74] B. Marciniec and M. Majchrzak, *Inorg. Chem. Comm.* **2000**, 3, 371–375.

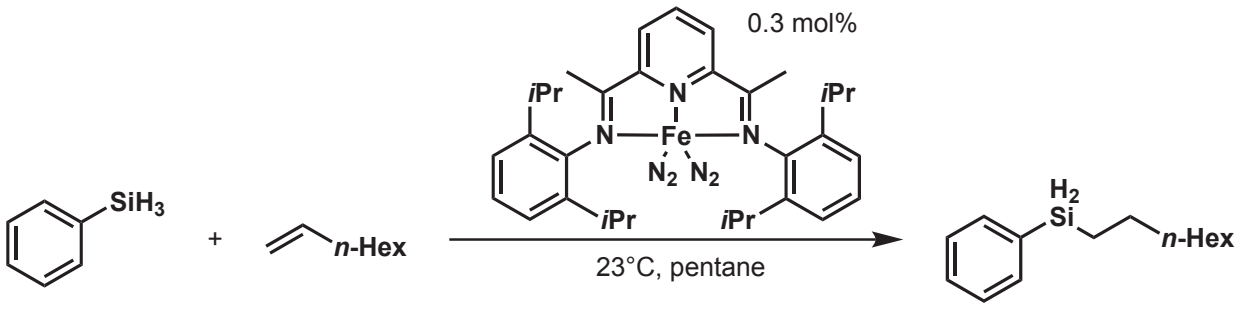


Figure 1.26: Hydrosilylation of 1-octene by phenylsilane catalyzed by Chirik's catalyst (first generation).[75]

[75] S. C. Bart, E. Lobkovsky and P. J. Chirik, *J. Am. Chem. Soc.* **2004**, 126, 13794–13807.

tion of various alkenes with primary and secondary silanes (Figure 1.26).[75] The catalyst reached 300 turnovers, was exclusively anti-Markovnikov selective, and active at room temperature. The key factor explaining this selectivity was the non-innocent (ie. redox-active) character of the ligand. The Fe(bisiminopyridine)$(N_2)_2$ was thoroughly characterized, and several potential catalytic intermediates were synthesized, including a Fe(bisiminopyridine)-$(silane)_2$ species. The complex could catalyze alkene isomerization, but in hydrosilylation conditions, the hydrosilylation reaction was much faster than isomerization, so that no alkene isomer was detected.

In 2012, Chirik published a second generation of his catalyst where the isopropyl groups of the aryl rings beared by the imine groups were replaced by methyl groups (Figure 1.27).[16] By decreasing steric hinderance, the catalyst was active with primary silanes such as Et_3SiH, $(EtO)_3SiH$ and MD'M. The hydrosilylation of these tertiary silanes is of industrial interest, contrary to primary and secondary silanes. Furthermore, this catalyst reached TONs of 5000 to 25000, which is remarkable for iron catalysts. This catalyst was also able to functionalize industrially relevant alkenes such as allyl polyethers, *N,N*-dimethylallylamine and to cross-link silicones in order to produce silicone elastomers.

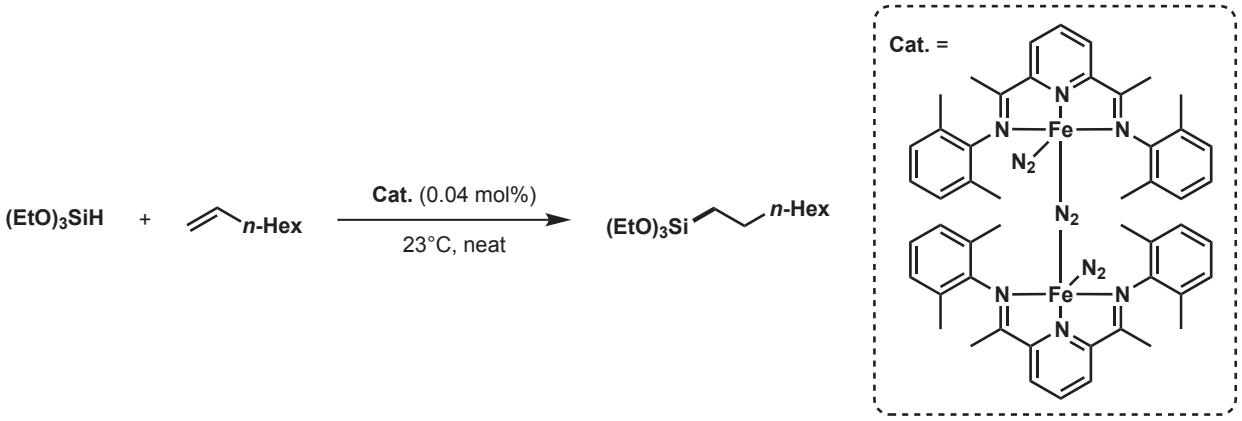


Figure 1.27: Hydrosilylation of triethoxysilane by 1-octene catalyzed by Chirik's catalyst (second generation).[16]

The same year, they reported that a slightly modified version of their first-generation catalyst (Figure 1.28) was able to selectively functionalize different isomers of 1,2,4-trivinylcyclohexane (TVCH) at the 4- position (95% selectivity respective to the 1- and 2- positions), with 80% selectivity for the monohy-

drosilylation.[76] For comparison, in industrially optimized conditions, Speier's catalyst gives a 45% selectivity for 4-functionalization (hardly higher than for a statistical mixture), and needs a substoichiometric amount of silane to reach 80% selectivity in monohydrosilylation. Furthermore, the iron complex was able to reach full conversion of silane in less than 5 min, while the Pt catalysts needed several hours. The products of monohydrosilylation of isomers of TVCH by triethoxysilane are used industrially as "coupling agents in silica-filled automotive tires with low rolling resistance and improved wear."

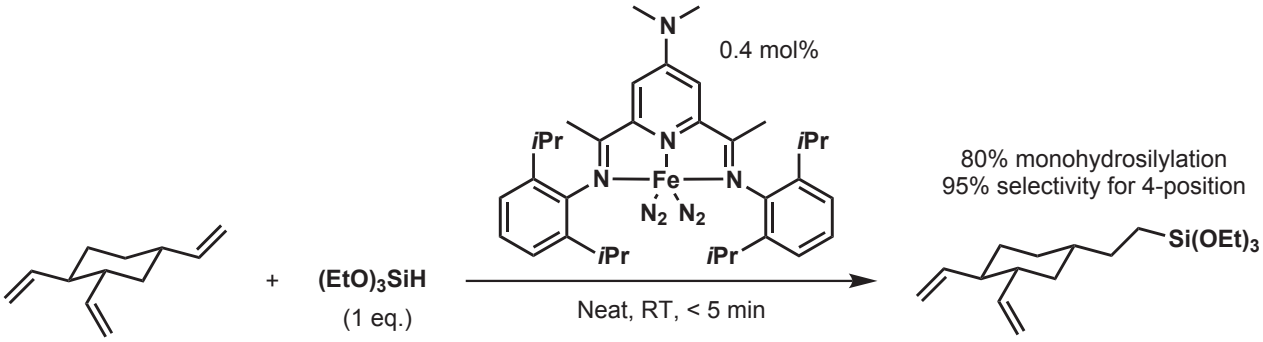


Figure 1.28: Selective hydrosilylation of 1,2,4-trivinylcyclohexane with triethoxysilane at the 4-position with a Fe-bisiminopyridine complex.[76]

Recently, a press release from Princeton University stated that Chirkik's catalyst "[had] been prepared at large scale and [had] undergone pilot manufacturing plant evaluation" at Momentive Performance Materials, and that "this new process [would] likely impact at least five major product lines ranging from agricultural adjuvants to tires to health care products to fiberglass".[77]

Several variants of these bisiminopyridine complexes have subsequently been developed. For example, a phosphinite-iminopyridine ligand developed by Peng *et al.* yielded an iron catalyst more chemoselective than Chirik's catalyst towards *C*-hydrosilylation with substrates bearing carbonyl functional groups (Figure 1.29, left).[78] An asymetric variant of Chirik's complex has also been developed for the enantioselective reaction of 1,1-disubstituted alkenes with diphenylsilane (Figure 1.29, right).[79]

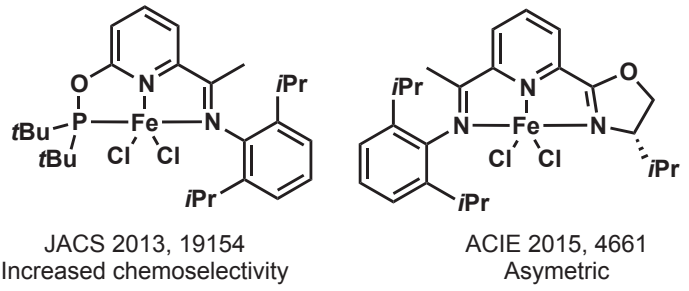


Figure 1.29: Variants of Chirik's catalyst.[78,79]

Recently, Nagashima *et al.* used iron and cobalt carboxylates in combination with alkyl isocyanides for the hydrosilylation of industrially relevant hydrosiloxanes (Figure 1.30),[80] and reached TONs of 100 to 10 000. They didn't study the reaction mechanism yet, but hypothesized that the isocyanide ligands could easily stabilize Fe(0) species given their π-acceptor character and that carboxylate salts were easily reduced by hydrosilanes given the high affinity of

[76] C. C. Hojilla Atienza et al., *ACS Catal.* **2012**, 2, 2169–2172.

[77] *Sustainability Research: Silicone Production | Sustainability at Princeton* [Online; accessed 21-June-2016] 2016

[78] D. Peng et al., *J. Am. Chem. Soc.* **2013**, 135, 19154–19166.

[79] J. Chen et al., *Angew. Chem. Int. Ed.* **2015**, 54, 4661–4664.

[80] D. Noda et al., *J. Am. Chem. Soc.* **2016**, 138, 2480–2483.

silicon for oxygen.

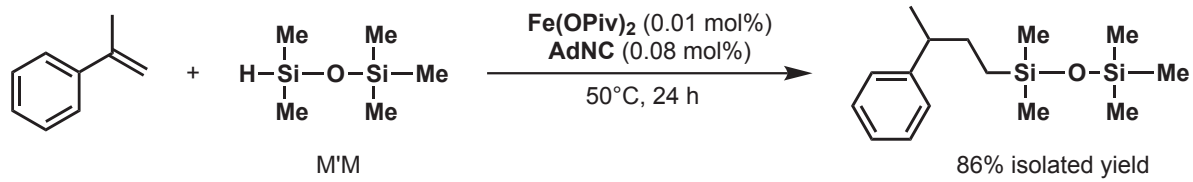


Figure 1.30: Hydrosilylation of α-methylstyrene by MM' catalyzed by Nagashima's catalytic system.[80]

To summarize, even if simple iron complexes are usually neither very active nor selective for hydrosilylation, by using finely tuned ligands (in particular non-innocent ligands), it was possible to achieve excellent catalytic performances with a wide range of substrates, including industrially relevant tertiary silanes.

1.5.4 Cobalt

Cobalt catalysis for hydrosilylation, which has recently been reviewed,[81] has started to gain much importance only some years ago.

It started in 1967 with the discovery by Chalk and Harrod that $Co_2(CO)_8$ was able to catalyze the hydrosilylation of terminal alkenes with several tertiary silanes.[82] Unfortunately, alkene isomerization was the major reaction, but it was noted that hydrosilylation continued even when all the terminal alkene had been isomerized. They proposed a Chalk-Harrod mechanism, with a cobalt hydride resting state.

Wrighton *et al.* proposed an alternative mechanism, often called the "modified Chalk-Harrod mechanism", where alkene insertion occurs in the Co – Si bond, and is followed by a C-H reductive elimination (Figure 1.25).[65,66]

Other studies about cobalt carbonyls soon followed, also giving important amounts of isomerized alkenes.[65,83,84]

In 1993, Brookhart and Grant studied the $[Cp^*Co(P(OMe)_3)(CH_2CH_3)][B(3,5\text{-ditrifluoromethylphenyl})_4]$ complex as catalyst for the reaction of triethylsilane with 1-hexene.[85] They proposed an unusual mechanism, comprising an alkene insertion in the Co – Si bond, followed by a sequence of β-H eliminations/insertions provoking the migration if the Co – C bond along the carbon chain, until the Co is bound with the terminal carbon (Figure 1.31), at which point the complex reacts with triethylsilane to form the product.

In 2013, Mo *et al.* disclosed a Co(II) complex comprising a silyl-functionalized NHC ligand (Figure 1.32) as an efficient catalyst for the reaction of phenylsilane with 1-octene, that could reach a TON of 15 000 with very low amounts of Markovnikov addition, hydrogenation and alkene isomerization.[86]

In 2014, Chirik *et al.* disclosed that a cobalt complex bearing a bisiminopyridine ligand selectively catalyzed dehydrogenative silylation of terminal alkenes to allylsilanes with tertiary silanes (Figure 1.33),[87] using a second equivalent of alkene as hydrogen acceptor. Surprisingly, the complex was also able to give the same allylsilane products starting from internal alkenes, indicating that the cobalt complex also catalyzed alkene isomerization. This ability was utilized to catalyze the cross-linking of polymethylhydrosiloxanes by simple alkenes, with a first dehydrogenative silylation of the alkene followed by an isomerization and a second dehydrogenative silylation of the obtained allyl-

[81] J. Sun and L. Deng, *ACS Catal.* **2016**, 6, 290–300.

[82] A. J. Chalk and J. F. Harrod, *J. Am. Chem. Soc.* **1967**, 89, 1640–1647.

[65] C. L. Reichel and M. S. Wrighton, *Inorg. Chem.* **1980**, 19, 3858–3860.

[66] F. Seitz and M. S. Wrighton, *Angew. Chem. Int. Ed. Eng.* **1988**, 27, 289–291.

[83] A. J. Chalk, *J. Organomet. Chem.* **1970**, 21, 207–213.

[84] L. Wilczek *Hydrosilation of fluorinated olefins with cobalt catalysts* Patent US 5233071 A 1993

[85] M. Brookhart and B. E. Grant, *J. Am. Chem. Soc.* **1993**, 115, 2151–2156.

[86] Z. Mo, Y. Liu and L. Deng, *Angew. Chem. Int. Ed.* **2013**, 52, 10845–10849.

[87] C. C. H. Atienza et al., *J. Am. Chem. Soc.* **2014**, 136, 12108–12118.

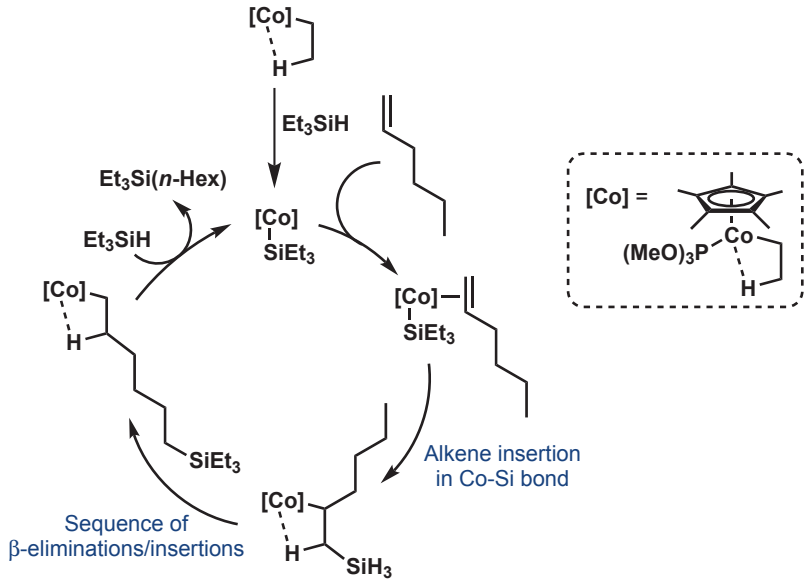


Figure 1.31: Mechanism proposed by Brookhart and Grant.[85]

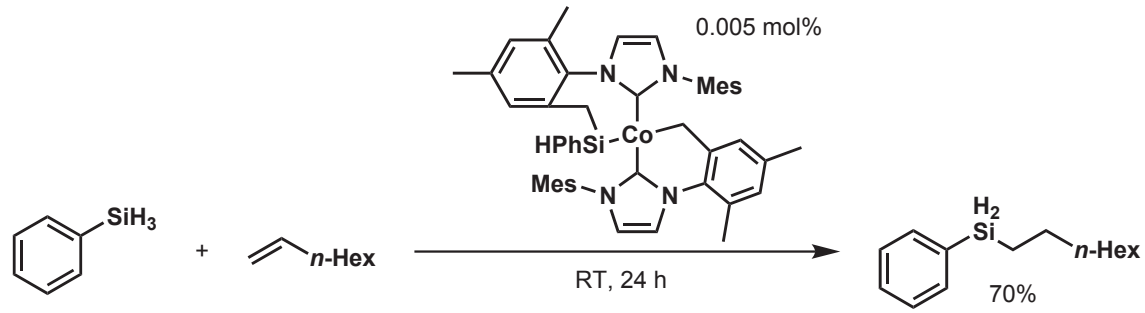


Figure 1.32: Hydrosilylation of 1-octene by phenylsilane catalyzed by the complex developed by Mo *et al.*[86]

silane. Surprisingly, in two cases (diphenylsilane + 1-octene and MD'M + cyclohexene), significant quantities of hydrosilylation products were obtained.

They proposed a mechanism (Figure 1.34) involving a cobalt silyl resting state, 2,1-insertion of the alkene in the Co – Si bond (resembling Brookhart's mechanism[85]), β-H elimination yielding the allylsilane product. Then, insertion of a second alkene molecule in the newly formed Co – H bond occurs, and the obtained cobalt alkyl complex reacts with a silane molecule (this step appears to be turnover-limiting), yielding the alkane and regenerating the cobalt silyl complex.

In 2015, Chen *et al.* published a β-diketiminate Co(I) complex (Figure 1.35, top) able to functionalize terminal olefins with primary and tertiary silanes.[88] They were also able to perform an isomerization/hydrosilylation tandem reaction starting from an internal alkene, by using a combination of two Co(I) complexes bearing slightly different ligands, one efficiently catalyzing isomerization and the other catalyzing hydrosilylation (Figure 1.35, bottom).

In 2016, Chirik *et al.* modified the cobalt complex published in 2014[87] to favor hydrosilylation over dehydrogenative silylation (Figure 1.36).[89] Starting from a mechanistic study that revealed that β-H elimination (leading to the allylsilane product) happened before reductive elimination could occur,

[88] C. Chen et al., *J. Am. Chem. Soc.* **2015**, 137, 13244–13247.

[89] C. H. Schuster et al., *ACS Catal.* **2016**, 6, 2632–2636.

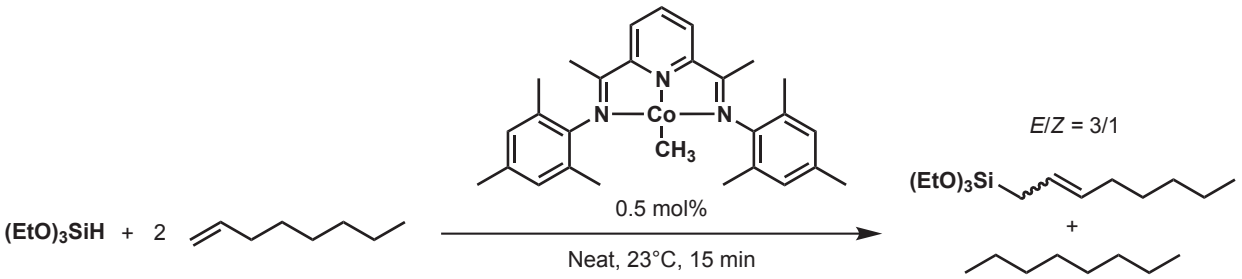


Figure 1.33: Selective formation of an allylsilane arising from the dehydrogenative silylation of 1-octene by triethoxysilane catalyzed by the complex developed by Chirik *et al.*[87]

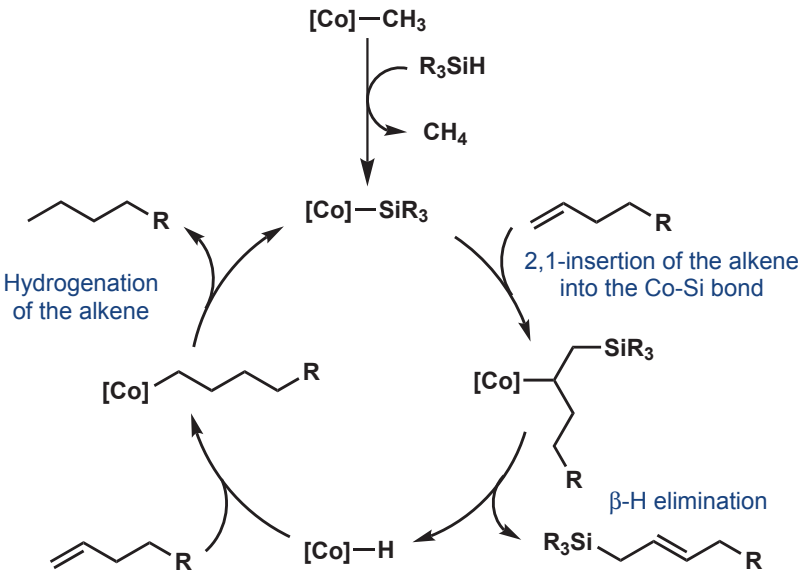


Figure 1.34: Mechanism proposed by Chirik *et al.*[87]

they modified the bisiminopyridine ligand. The rationale was that smaller substituents on the bisiminopyridine would favor the bimolecular reaction of the alkyl complex with the silane over the monomolecular β-H elimination (which is favored when the Co environment is too hindered). Indeed, with the modified ligand, they completely reversed the selectivity to hydrosilylation. Their complex was reactive with tertiary silanes and remarkably selective with a variety of alkenes, including bifunctional alkenes containing epoxide, ketone, ester and tertiary amine functional groups. Finally, with only ppm levels of their Co complex, they were able to perform a gram-scale reaction of ally glycidyl ether and triethoxysilane and to cross-link silicones.

An interesting ligand was published in 2016 by Du *et al.* (Figure 1.37).[90] Its iron complex catalyzed anti-Markovnikov hydrosilylation, while the cobalt complex produced the Markovnikov regioisomer. Only phenylsilane was used in the paper, limiting the industrial interest of this complex. However, the possibility to produce selectively the Markovnikov isomer enables the production of secondary alcohols by using the Tamao-Fleming reaction.[23,24]

A cobalt complex bearing a bis-NHC ligand was synthesized by Ibrahim *et al.* (Figure 1.38),[91] and displayed high chemoselectivity with tertiary silanes and a variety of alkenes bearing oxygen- or nitrogen-containing substituents. Preliminary experiments aimed at elucidating the mechanism were in support of a Chalk-Harrod mechanism.

[90] X. Du et al., *Angew. Chem. Int. Ed.* **2016**, 55, 6671–6675.

[91] A. D. Ibrahim et al., *ACS Catal.* **2016**, 6, 3589–3593.

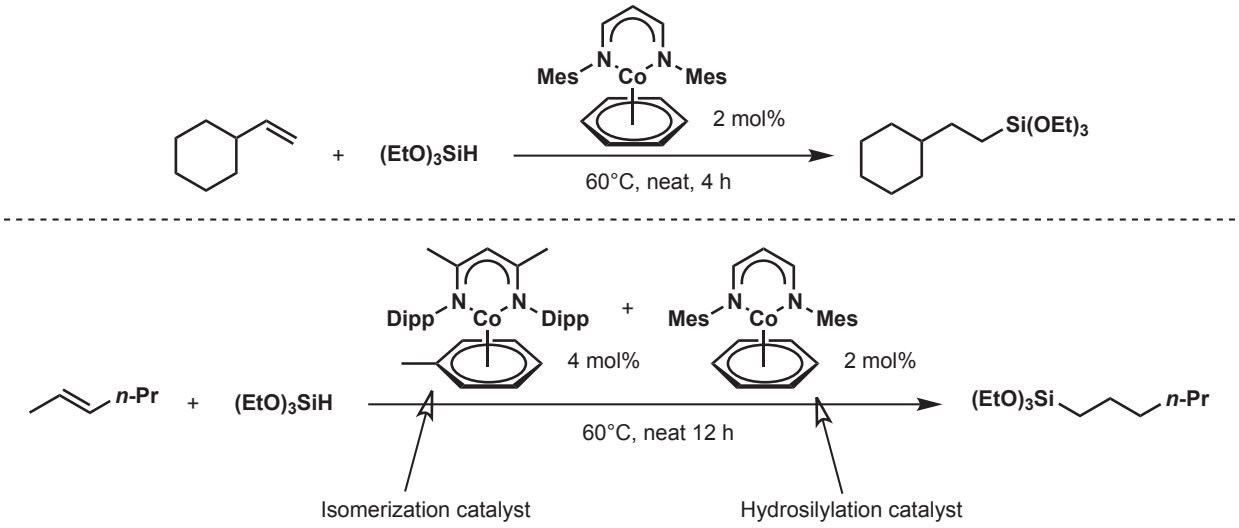


Figure 1.35: Top: selective anti-Markovnikov hydrosilylation with Chen's complex.[88] Bottom: tandem isomerization-hydrosilylation reaction starting from *cis*-2-hexene.

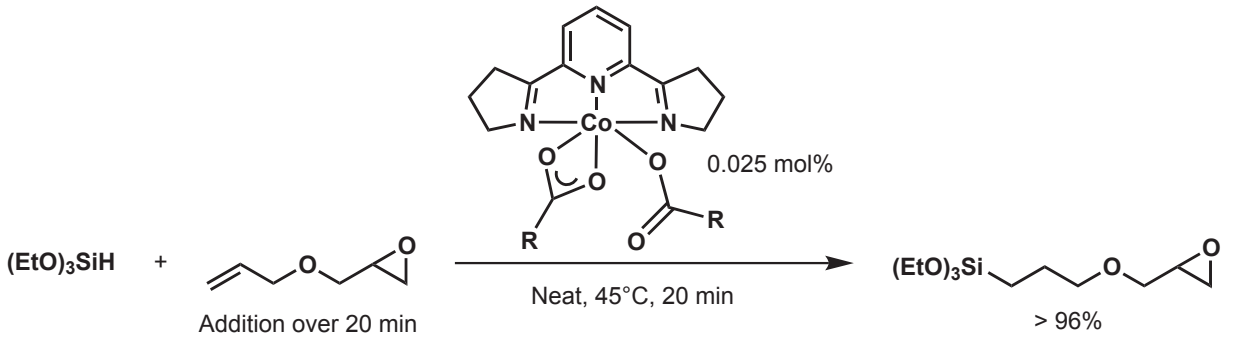


Figure 1.36: Selective anti-Markovnikov hydrosilylation of allyl glycidyl ether by triethoxsilane catalyzed by the second generation of Chirik's cobalt complex.[89]

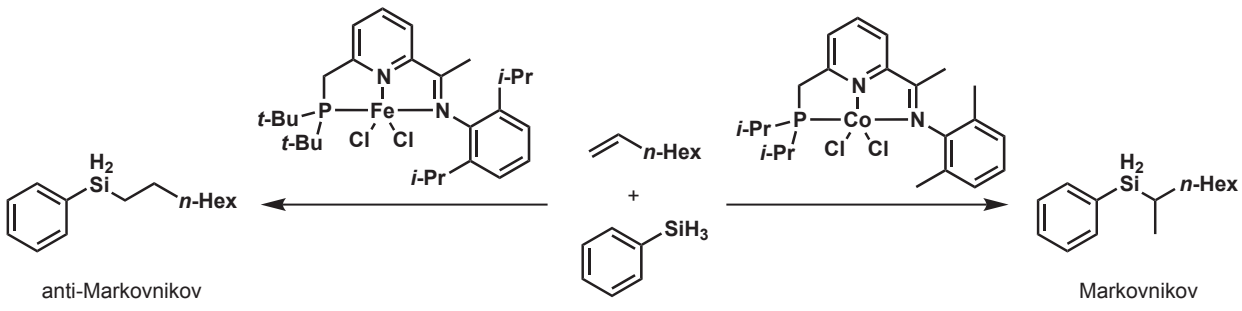


Figure 1.37: Selective anti-Markovnikov or Markovnikov hydrosilylation of 1-octene by phenylsilane depending on the metal used.[90]

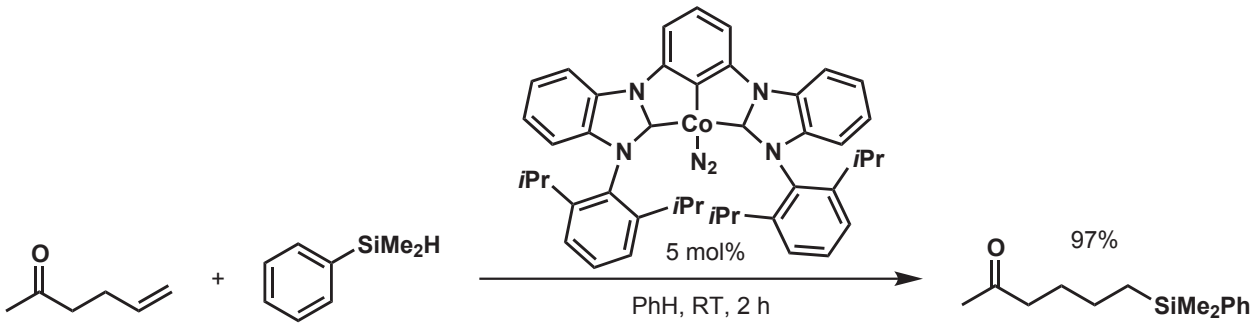


Figure 1.38: Chemoselective hydrosilylation of an alkene containing a ketone functional group by dimethylphenylsilane catalyzed by a cobalt bis-NHC complex.[91]

To summarize, high selectivity for hydrosilylation with tertiary silanes has been obtained only very recently. As for iron, the rational use of non-innocent ligands was crucial for this achievement.

1.5.5 Nickel

Petrov *et al.* opened the way for nickel catalysis as early as 1956,[92] when they used Raney nickel to react trichlorosilane with acrylonitrile. The reaction, conducted at 160 °C, yielded only 12% of hydrosilylation product, the rest being polymers (probably because of the high reaction temperature). The same year, Nozakura *et al.* got 22% yield for the same reaction with $NiCl_2 \cdot C_5H_5N \cdot HCl$ as catalyst.[93] The low yield also probably suffered from the reaction temperature of 160 °C.

During the following decades, several studies used simple nickel salts or complexes (with ligands such as phosphines or COD).[94–102] The reaction temperature was often around 120 °C, with TONs reaching usually between 100 and 1000. Quite often, hydrosilylation was a minor product, among products of dehydrogenative silylation, hydrogenation and silane substituent redistribution.

In 2003, Zargarian *et al.* synthesized a cationic Ni(II) indenyl complex generated by *in situ* activation with methylaluminoxane or $NaBPh_4$ (Figure 1.39) and used it to catalyze the reaction of phenylsilane and styrene, with almost exclusive Markovnikov selectivity.[103] Diphenylsilane was also reactive, but tertiary silanes were not. They proposed a Chalk-Harrod mechanism, with a nickel hydride resting state. Interestingly, when this nickel complex is mixed with phenylsilane alone, it catalyzes its dehydrogenative polymerization, but when styrene is present, this reaction is not observed at all. In a following publication, Zargarian *et al.* showed that by introducing bulky substituents on the indenyl ligand, it was unnecessary to activate the complex with MAO to get catalytic activity.[104]

[92] A. D. Petrov et al., *Izvestiya Akademii Nauk SSSR, Seriya Khimicheskaya* **1956**, 256–257.

[93] S. Nozakura and S. Konotsune, *Bull. Chem. Soc. Jpn.* **1956**, 29, 326–331.

[103] F. Fontaine, R. Nguyen and D. Zargarian, *Can. J. Chem.* **2003**, 81, 1299–1306.

[104] Y. Chen et al., *Organometallics* **2005**, 24, 149–155.

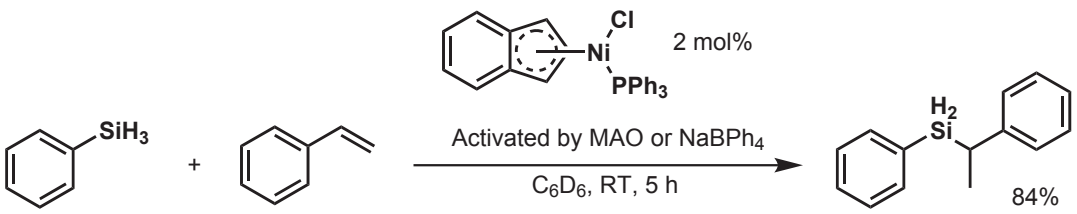


Figure 1.39: Markovnikov hydrosilyation of styrene by phenylsilane catalyzed by a cationic Ni(II) indenyl complex developed by Zargarian *et al.*[103]

In 2015, Srinivas *et al.* used a salicylaldiminato-Ni(II) complex (Figure 1.40) to catalyze the reaction between diethylsilane or diphenylsilane and a variety of alkenes, and reached high yields and selectivities within hours at room temperature.[105] Unfortunately, tertiary silanes were not reactive. Based on preliminary experiments aiming at elucidating the mechanism, they proposed a modified Chalk-Harrod mechanism with a Ni – silyl resting state of the complex.

[105] V. Srinivas et al., *Catal. Sci. Tech.* **2015**, 5, 2081–2084.

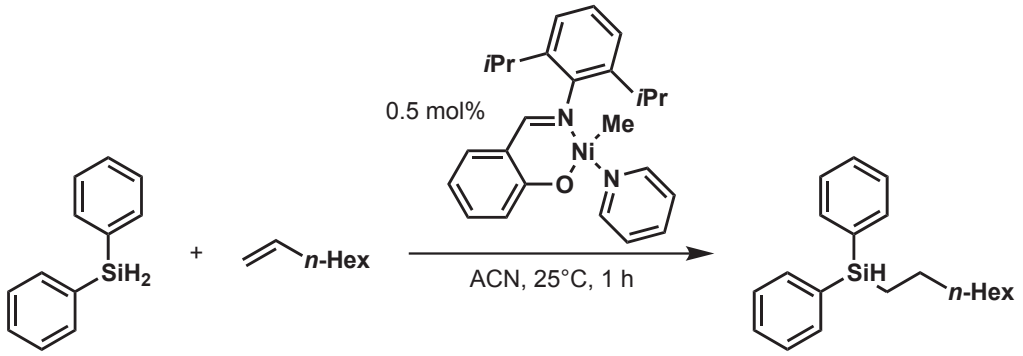


Figure 1.40: Selective anti-Markovnikov hydrosilylation of 1-octene by diphenylsilane catalyzed by a salicylaldiminato-Ni(II) complex.[105]

The same year, Steiman and Uyeda showed that a Ni(I) – Ni(I) bond supported by a redox-active naphtyridine-diimine ligand (Figure 1.41) catalyzed hydrosilylation of 1-octene, styrene and other unsaturated molecules (such as alkynes or carbonyl-containing molecules) with diphenylsilane.[106] The very interesting feature of this complex is that the Ni(I) – Ni(I) bond remained intact during catalysis, something that had never been observed before with a bimetallic complex. Adducts between the complex and disilanes were described as falling "on the continuum between a σ-complex and a product of double Si – H oxidative addition".

[106] T. J. Steiman and C. Uyeda, *J. Am. Chem. Soc.* **2015**, 137, 6104–6110.

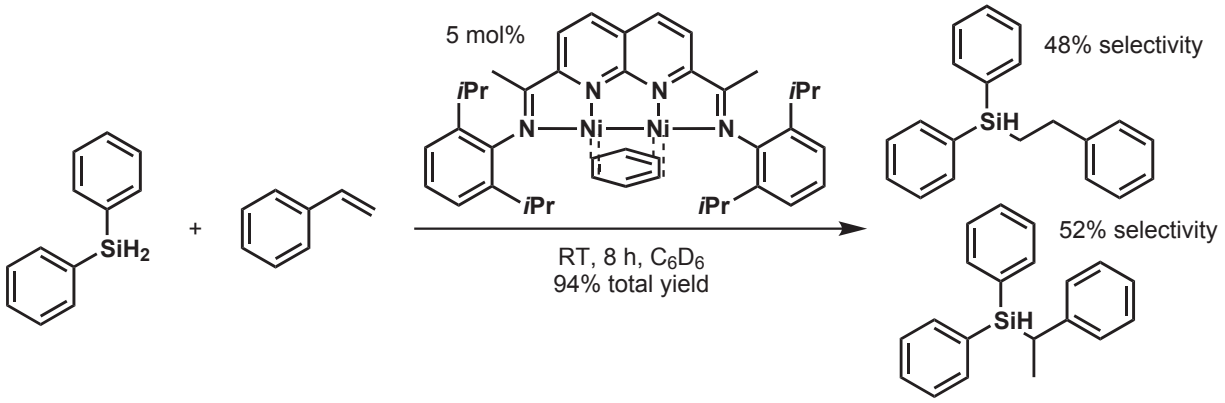


Figure 1.41: Hydrosilylation of styrene by diphenylsilane catalyzed by a Ni(I) – Ni(I) complex featuring a naphtyridine-diimine ligand. The Ni(I) – Ni(I) bond stays intact during catalysis.[106]

In 2015 also, Hu *et al.* published a nickel pincer complex (Figure 1.42) that was able to catalyze the reaction of diphenylsilane with a great variety of terminal and internal alkenes.[38] TONs didn't reach more that 100, but the reaction was completed within hours at room temperature, giving only anti-Markovnikov products and being chemoselective. They specified that even if the catalyst was more active with secondary silanes, primary and tertiary

silanes were still reactive. They also demonstrated that with a tandem isomerization/hydrosilylation reaction with 10 mol% catalyst it was possible to functionalize internal alkenes and to obtain the linear products.

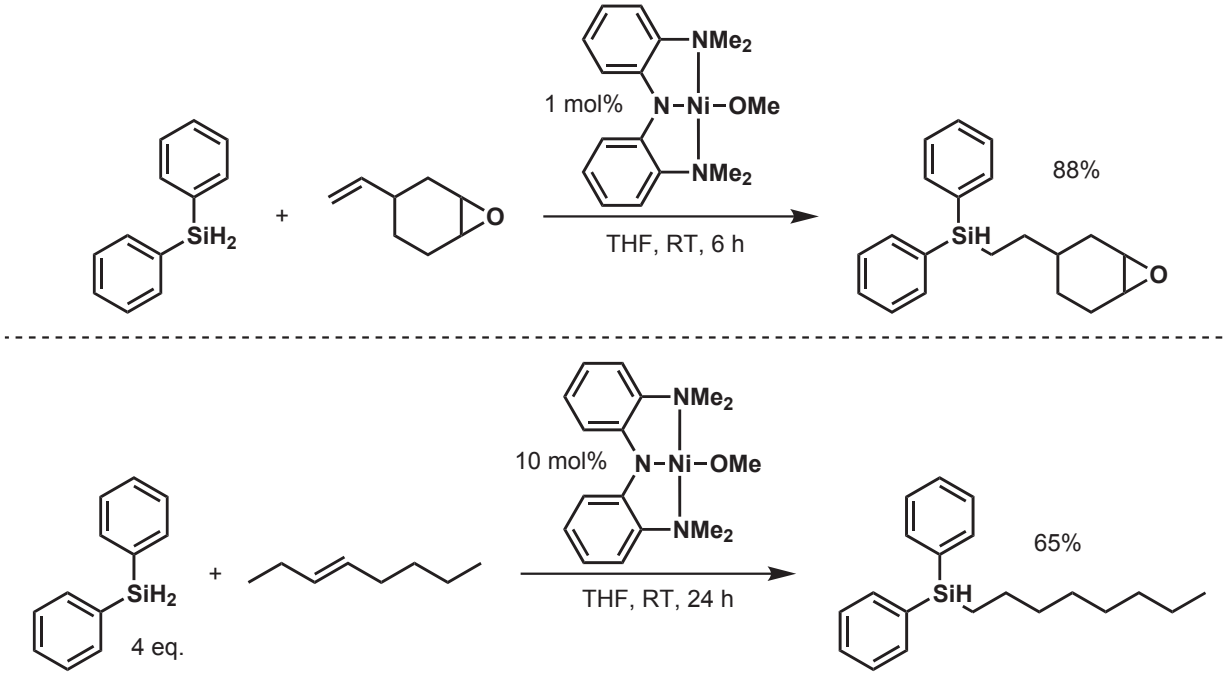


Figure 1.42: Top: chemoselective hydrosilylation of vinylcyclohexene epoxide. Bottom: isomerization-hydrosilylation tandem with internal alkenes.[38]

[107] I. Pappas, S. Treacy and P. J. Chirik, *ACS Catal.* **2016**, 4105–4109.

In 2016, Chirik *et al.* disclosed an α-diimine nickel catalyst (Figure 1.43) catalyzing the reaction of industrially relevant tertiary silanes or siloxanes with 1-octene or a vinylsiloxane.[107] The reaction proceeded at room temperature, with significant isomerization of 1-octene, but gave only the anti-Markovnikov hydrosilylation product. The performances of the catalyst were demonstrated on a 10 g scale for the reaction of 1-octene and triethoxysilane, and for the cross-linking of a vinylsiloxane with a poly(dimethylsiloxane-*co*-methylhydrosiloxane). Interestingly, the cross-linking product was colorless, a desirable feature for commercial applications.

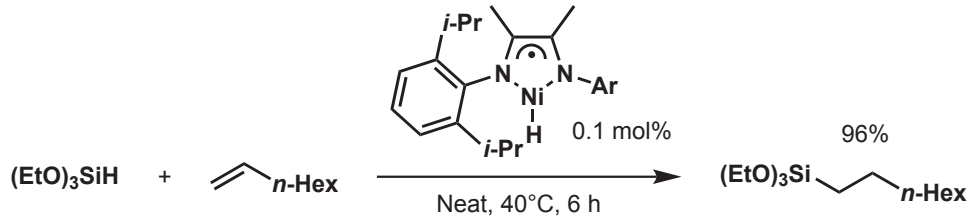


Figure 1.43: Hydrosilylation of 1-octene by triethoxysilane catalyzed by an α-diimine nickel catalyst developed by Chirik *et al.*[107]

A short mechanistic study established that the catalyst resting state was a nickel hydride dimer (Figure 1.44) and that the rate law for the reaction of triethoxysilane and 1-octene in hexane was

$$r = k[\mathrm{Ni}]^{1/2}[\text{1-octene}][(\mathrm{EtO})_3\mathrm{SiH}]$$

They also showed that interaction of the nickel alkyl intermediate with the silane was rate-limiting and that the complex was "best described as Ni(II) with a one electron reduced α-diimine ligand" (this was shown by DFT calculations).

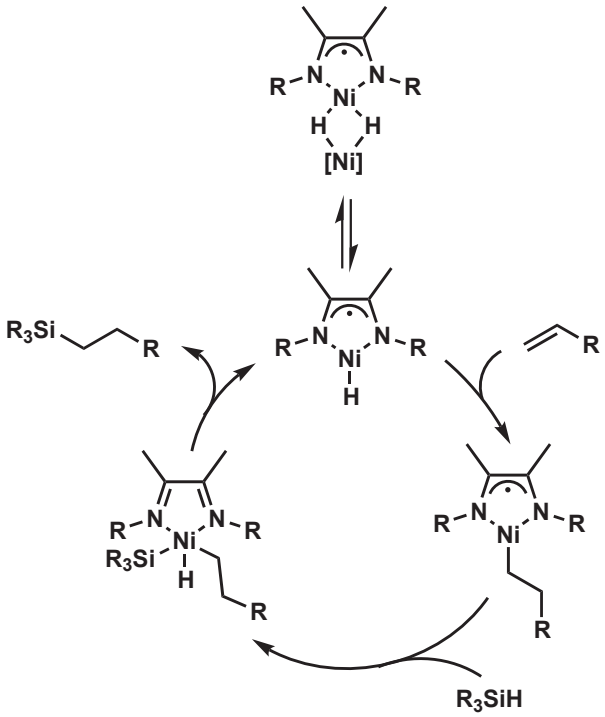


Figure 1.44: Mechanism proposed by Chirik *et al.*[107]

This year also, Mathew *et al.* studied a cationic Ni(II) allyl complex (Figure 1.45) as catalyst.[108] Even if it was limited to primary and secondary silanes, they provided evidence for a new mechanism using DFT. In this mechanism, the allyl ligand is non-innocent "for both the Si – H bond cleavage and the Si – C bond forming steps". Note that this mechanism is not supported by any experimental study.

[108] J. Mathew et al., *Chem. Comm.* **2016**, 52, 6723–6726.

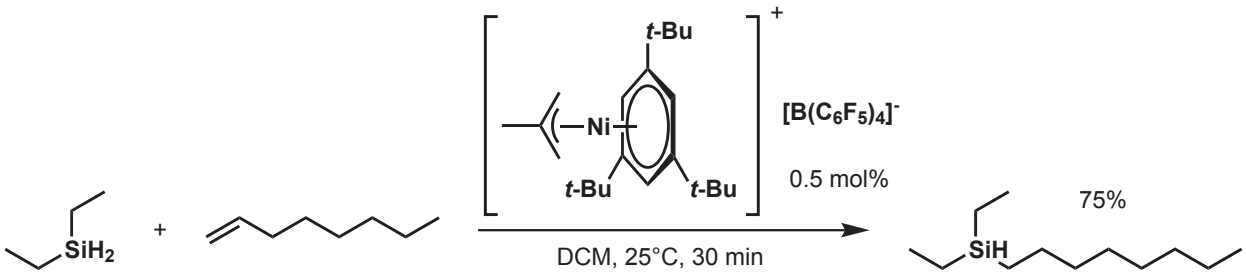


Figure 1.45: Hydrosilylation of 1-octene by diethylsilane catalyzed by a cationic Ni(II) complex featuring a non-innocent allyl ligand.[108]

To summarize, it was only recently that nickel complexes (featuring non-innocent ligands) able to functionalize alkenes with tertiary silanes were reported, even if nickel complexes that were reactive with primary and secondary silanes were already known.

During the redaction of this manuscript, Hu *et al.* reported the use nickel alcoholate salts such as $Ni(OtBu)_2 \cdot xKCl$ as catalysts for the reaction of tertiary silanes with various alkenes (Figure 1.46).[109] The authors claimed that nickel NPs, formed *in situ* from the alcoholate salt, were the active species. Even if NPs of 2 nm to 5 nm diameter were effectively observed in the reaction mixture by TEM and were proven to be metallic Ni(0) by electron diffraction, more

[109] I. Buslov, F. Song and X. Hu, *Angew. Chem. Int. Ed.* **2016**, 55, 12295–12299.

experiments are needed to determine if the active species are the nickel NPs, as claimed by the authors. They hypothesized that the role of the KCl salt, which is reported to be essential for catalysis, may be to prevent the Ni NPs from sintering, by electrostatic stabilization. This study is an important first step for the development of efficient catalysts based on Ni NPs, even this catalytic system must be studied more in-depth.

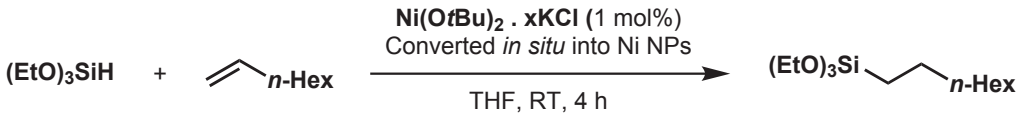


Figure 1.46: Use of an alcoholate Ni salt converted *in situ* into Ni NPs to catalyze the reaction of 1-octene and triethoxysilane.[109]

1.5.6 Ruthenium

The ruthenium literature contains mostly simple ruthenium salts such as $RuCl_3$ and complexes such as $Ru_3(CO)_{12}$, $RuCl_2$(*p*-cymene) or $RuCl_2(PPh_3)_2$.[110–116] Dehydrogenative silylation is often a side reaction, sometimes the main reaction.

In 2003, Glaser and Tilley published a ruthenium silylene complex able to catalyze hydrosilylation of unfunctionalized alkenes with phenylsilane or *n*-hexylsilane (Figure 1.47).[117] Interestingly, internal alkenes and tetrasubstituted alkenes such as 1-methylcyclohexene, which are usually unreactive towards hydrosilylation, were converted. Moreover, the silylene ligand was necessary for the catalysis to happen, since related silyl complexes were unreactive.

[117] P. B. Glaser and T. D. Tilley, *J. Am. Chem. Soc.* **2003**, 125, 13640–13641.

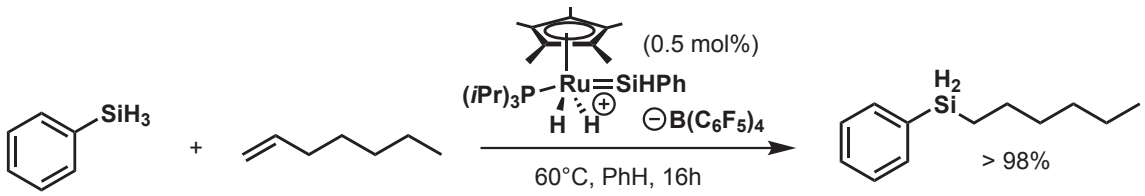


Figure 1.47: Hydrosilylation of 1-hexene by phenylsilane catalyzed by a ruthenium silylene complex.[117]

These observations allowed Glaser and Tilley to propose a new mechanism (Figure 1.48), very different from the Chalk-Harrod mechanism, where a Si – H bond of a silylene complex, located remotely from the Ru center, is directly added to an alkene in a concerted way.

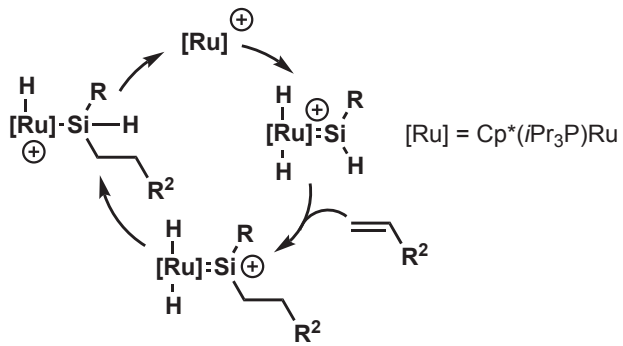


Figure 1.48: Mechanism proposed by Glaser and Tilley.[117]

This new mechanism recieved support from Beddie and Hall the next year,[118] who performed DFT calculations for the addition of ethylene on a

[118] C. Beddie and M. B. Hall, *J. Am. Chem. Soc.* **2004**, 126, 13564–13565.

simplified complex: $[Cp(PH_3)Ru(H)_2(SiH_2)\cdot OMe_2]^+$. Calculations for Chalk-Harrod or modified Chalk-Harrod pathways revealed that they were energetically disfavoured compared to the Glaser-Tilley mechanism. Indeed, the highest energy transition state of the Glaser-Tilley mechanism is lower than the highest transition state of the other mechanisms by at least 8 kcal/mol.

In 2007, Rankin *et al.* provided experimental evidence that the formation of a ruthenium silylene complex happened by double activation of two geminal Si – H bonds of a silane,[119] further confirming the plausibility of the Glaser-Tilley mechanism.

[119] M. A. Rankin et al., *J. Am. Chem. Soc.* **2007**, 129, 15855–15864.

In 2013, Tilley *et al.* provided interesting additional data to confirm the Glaser-Tilley mechanism.[120] They started by synthesizing complexes with a weakly coordinating $[CB_{11}H_6Br_6]^-$ carborane anion instead of the previously used $[B(C_6H_5)_4]^-$ anion, to facilitate crystallization. Crystallized compounds provided valuable structural information on these complexes, in particular a short Ru – H···Si distance, indicating that the silicon center was very electrophilic, a probable reason for its reactivity in hydrosilylation. A kinetic study established a first-order in ruthenium complex, a competition of silane with alkene at high alkene concentrations (associated with an inverse order in alkene), and a saturation in silane at high silane concentrations. It was established that the rate-determining step was not the Si – H addition on the alkene but rather the exchange of the secondary silane product with the primary silane (reagent). From the determination of activation parameters, in particular the activation entropy, it was determined that this exchange process was dissociative (elimination of the product followed by addition of the reagent) and not associative. This is in agreement with the fact that at low substrate concentrations, the rate depends only on the catalyst concentration. The mechanism they proposed is depicted in Figure 1.49.

[120] M. E. Fasulo, M. C. Lipke and T. D. Tilley, *Chem. Sci.* **2013**, 4, 3882–3887.

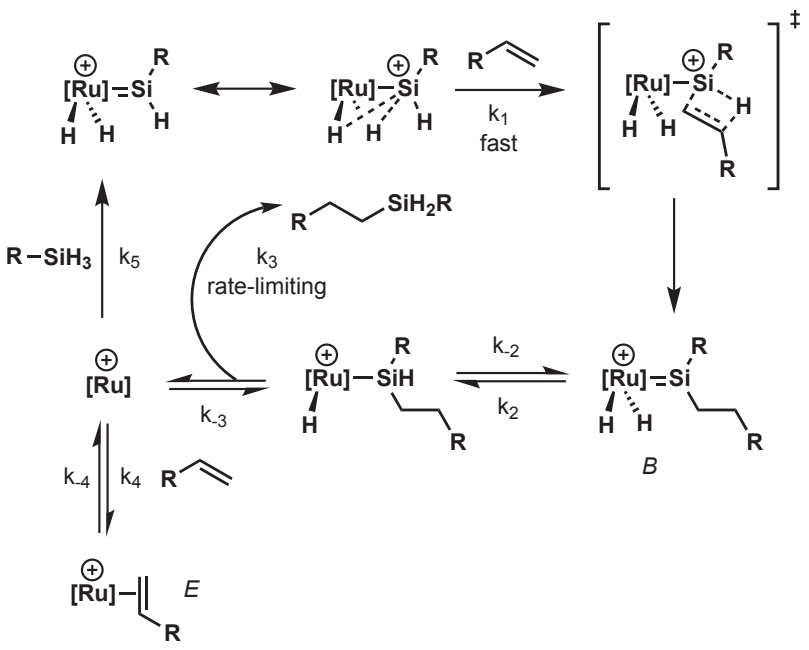


Figure 1.49: Mechanism determined by Tilley *et al.*[120]

A rate law taking into account these observations has also been determined in this study:

$$\frac{d[\text{silane}]}{dt} = \frac{-k_5[\text{silane}](k_3K_2[B] + k_{-4}[E])}{k_{-3}[\text{product}] + k_4[\text{alkene}] + k_5[\text{silane}]}$$

To conclude, ruthenium silylene complexes have enabled the discovery of a new mechanism (Glaser-Tilley mechanism), in which the alkene directly adds onto a silylene complex. Even if this mechanism allows the functionalization of internal alkenes, which is not common for other catalysts (except when isomerization to terminal alkenes occurs), these ruthenium complexes are only reactive with tertiary silanes, thus limiting their practical usability. Likewise, the other ruthenium complexes have not reached performances that are comparable with platinum complexes.

1.5.7 Rhodium

Rhodium, despite being a noble metal, has not been turned into catalysts as performant as platinum ones.

However, it has led to some interesting results for the multi-step synthesis of small molecules. For example, Hua *et al.* published a catalytic system which allows to obtain 1,3-*anti*-diols or 1,4-diols starting from homoallylic silyl ethers, depending on the ligand used (Figure 1.50).[121]

[121] Y. Hua et al., *Org. Lett.* **2013**, 15, 3412–3415.

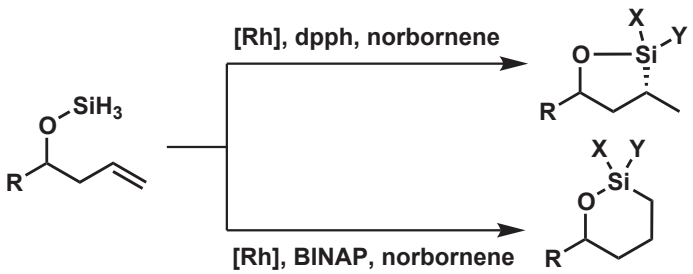


Figure 1.50: Ligand-controlled selectivity of intramolecular hydrosilylation selectivity of homoallylic silyl ethers.[121]

In 1991, Lewis *et al.* studied rhodium nanoparticles as catalysts,[122] in their quest of determining whether active species in hydrosilylation were homogeneous or heterogeneous. In this study, they used the mercury poisoning test and observed a strong inhibition of the catalyst, showing that the active species was probably heterogeneous.

[122] L. N. Lewis, R. J. Uriarte and N. Lewis, *J. Mol. Catal.* **1991**, 66, 105–113.

1.5.8 Iridium

As for rhodium, iridium has never topped the performance of platinum in alkene hydrosilylation catalysis, but has been used to develop complexes with interesting selectivities. For example, in 2014,[123] Muchnij *et al.* disclosed that $[IrCl(COD)]_2$ in presence of 4 equivalents of COD was able to selectively functionalize terminal alkenes with alkylnylhydrosilanes instead of catalyzing the usually easier reaction of the alkynylhydrosilane with itself (Figure 1.51).

[123] J. A. Muchnij, F. B. Kwaramba and R. J. Rahaim, *Org. Lett.* **2014**, 16, 1330–1333.

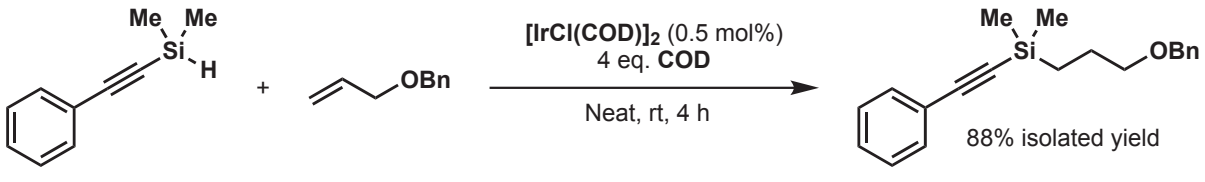


Figure 1.51: Selective functionalization of terminal alkenes with alkynylsilanes instead of the usual self-reaction of the alkynylsilane.[123]

1.5.9 Palladium

Examples of palladium catalysts for alkene hydrosilylation are rare, because palladium complexes readily decompose to metallic palladium in hydrosilylation conditions, leading to fast catalyst deactivation.[13]

However, there are some interesting palladium catalysts, mostly in the area of asymetric hydrosilylation,[124] such as the complex published by Uozumi and Hayashi in 1991,[26] that we commented in subsection 1.3.4.

[124] S. E. Gibson and M. Rudd, *Adv. Synth. Catal.* **2007**, 349, 781–795.

1.5.10 Other catalysts

Complexes of early transition metals such as titanium and zirconium have been proven to go through different mechanistic pathways than late transition metals.

In 1991, Takahashi *et al* showed that a Cp_2ZrCl_2 activated by EtMgBr catalyzed hydrosilylation of 1-octene by diphenylsilane with perfect anti-Markovnikov selectivity (Figure 1.52), and avoided alkene polymerization in these conditions.[125]

[125] T. Takahashi et al., *J. Am. Chem. Soc.* **1991**, 113, 8564–8566.

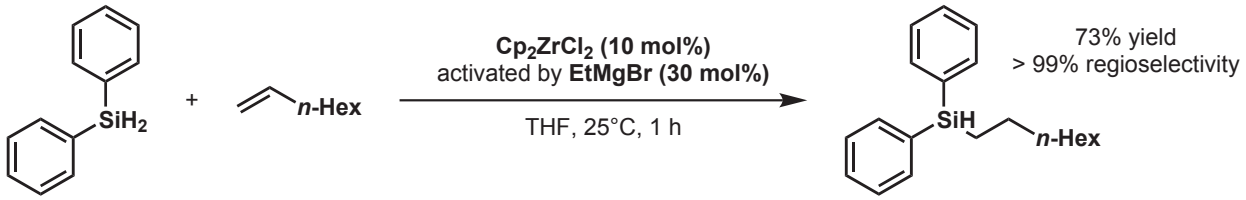


Figure 1.52: Hydrosilylation of 1-octene by diphenylsilane catalyzed by a zirconocene catalyst.[125]

In a theoretical study from 2004, Sakaki *et al.* studied the mechanism that such catalysts could follow, with the model reaction of ethylene and SiH_4.[126] They proposed a $Cp_2Zr(C_2H_4)$ resting state (Figure 1.53), undergoing an unprecedented σ-bond metathesis with SiH_4 giving the alkylsilyl zirconium complex, followed by an ethylene-assisted C-H reductive elimination.

[126] S. Sakaki et al., *J. Am. Chem. Soc.* **2004**, 126, 3332–3348.

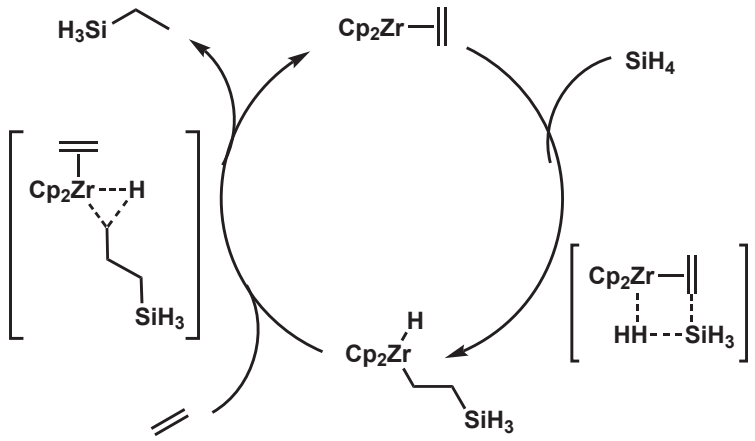


Figure 1.53: Mechanism proposed by Sakaki *et al.*[126]

Complexes of early main-group metals (Ca, Sr and K) have also been studied as catalysts.[127] For example Buch *et al.* were the first to develop a calcium complex (Figure 1.54) which once converted *in situ* to the corresponding hydride was able to hydrosilylate 1,1-diphenylethylene with phenylsilane.[128]

[127] S. Harder, *Chem. Rev.* **2010**, 110, 3852–3876.

[128] F. Buch, J. Brettar and S. Harder, *Angew. Chem. Int. Ed.* **2006**, 45, 2741–2745.

Remarkably, the catalyst was Markovnikov-selective, and did not lead to the formation of insoluble CaH_2 in the medium, a potential deactivation pathway.

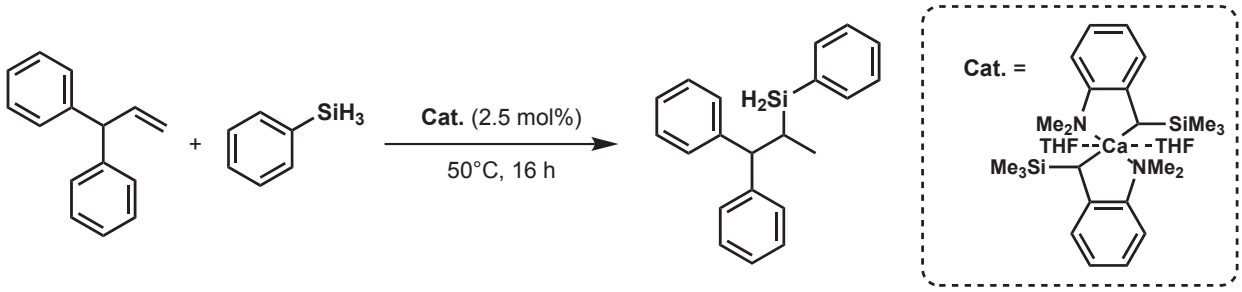


Figure 1.54: Hydrosilylation of 1,1-diphenylethylene by phenylsilane catalyzed by a Ca(II) complex.[128]

Several lanthanide and actinide complexes have been reported to catalyze alkene hydrosilylation, but only with primary silanes.[13] Nonetheless, these complexes can have original reactivity, owing to some of their original features, such as the impossibility to undergo oxidative addition or reductive elimination and their high electrophilicity.[129] They usually favor Markovnikov addition. A proposed mechanism involve alkene 2,1-insertion in a Ln – H bond followed by a σ-bond metathesis regenerating the hydride (Figure 1.55).[129]

[129] P. Fu et al., *J. Am. Chem. Soc.* **1995**, 117, 7157–7168.

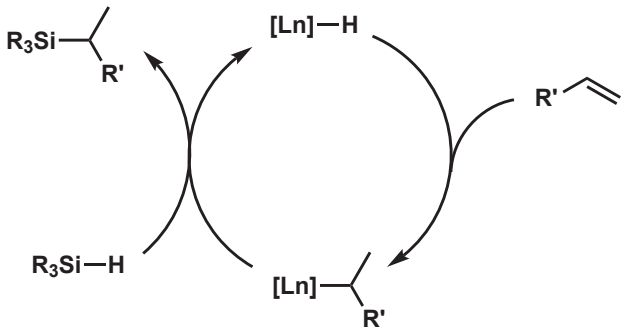


Figure 1.55: Proposed mechanism for alkene hydrosilylation by lanthanide complexes.[129]

Lewis acids also interesting catalytic properties. For example, the dicationic salt $[(SIMes)PFPh_2][B(C_6F_5)_4]_2$ can catalyze hydrosilylation of terminal and internal alkenes with triethylsilane (Figure 1.56).[130] Terminal alkenes were hydrosilylated on the terminal position (anti-Markovnikov), but very interestingly *Z*-2-octene was hydrosilylated on the 2-position, meaning that alkene isomerization to the terminal position did not happen prior to hydrosilylation, as was observed with several metallic catalysts.[38,88]

[130] M. H. Holthausen, M. Mehta and D. W. Stephan, *Angew. Chem. Int. Ed.* **2014**, 53, 6538–6541.

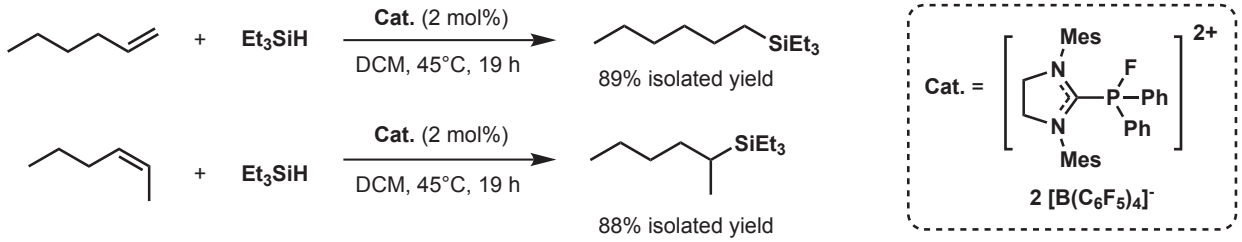


Figure 1.56: Hydrosilylation of 1-octene and *Z*-2-octene by triethylsilane with a dicationic Lewis acid catalyst.[130]

Molander and Nichols took advantage of the ability of yttrium complexes

to catalyze dienes cyclizations and alkene hydrosilylation to develop a diastereoselective tandem cyclization-silylation of 1,5-dienes and 1,6-dienes (Figure 1.57).[131] The obtained silane could then be oxidized to the corresponding alcohol.

[131] G. A. Molander and P. J. Nichols, *J. Am. Chem. Soc.* **1995**, 117, 4415–4416.

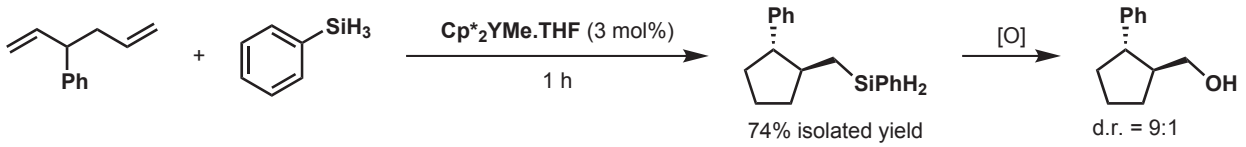


Figure 1.57: Tandem diastereoselective diene cyclization/hydrosilylation with an yttrium complex.[131]

A recent research area that deserves to be mentionned is the development of catalytic systems for transfer hydrosilylation.[132] This transfer hydrosilylation chemistry aims to replace light silanes such as Me_3SiH[133] or SiH_4[134], that are pyrophoric and thus very difficult and dangerous to handle, by stable surrogates (Figure 1.58).

[132] M. Oestreich, *Angew. Chem. Int. Ed.* **2016**, 55, 494–499.
[133] A. Simonneau and M. Oestreich, *Angew. Chem. Int. Ed.* **2013**, 52, 11905–11907.
[134] A. Simonneau and M. Oestreich, *Nat. Chem.* **2015**, 7, 816–822.

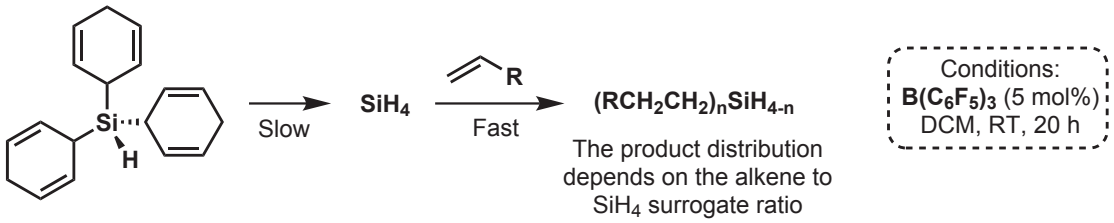


Figure 1.58: A stable SiH_4 surrogate enables the slow release of SiH_4 in the reaction medium.[134]

1.5.11 Perspective

Replacing Pt complexes is at the heart of current research in alkene hydrosilylation. Non-innocent ligands have enabled researchers to develop complexes of cheap and abundant metals such as iron, cobalt and nickel that are active in alkene hydrosilylation.

Criteria that are desired for such complexes include: high activity, high stability (enabling to reach high TONs), selectivity (absence of alkene isomerization or other side-reactions), chemoselectivity (tolerance towards functional groups such as epoxides, alcohols or carbonyl groups) and reactivity with tertiary silanes (that are industrially relevant). Some non-noble metal complexes have matched some of these criteria, and have even surpassed platinum complexes in a few cases!

It seems that the key to these successes is a combination of trial-and-error, thorough mechanistic study of the discovered catalysts (including kinetic studies) followed by rational design of more efficient catalysts based on the acquired knowledge.

Research on metallic complexes completely dominates the hydrosilylation literature, and heterogeneous catalysts or nanoparticles-based catalysts are almost absent of it. Given that nanoparticles can have original reactivities compared to metallic complexes,[135] it appears judicious to explore this vast part of the chemical space.

[135] A. Roucoux, J. Schulz and H. Patin, *Chem. Rev.* **2002**, 102, 3757–3778.

1.6 The research project

1.6.1 Background and objective

This PhD project is based on results obtained in a previous research project, called "Hexosic", funded by the french "Agence Nationale de la Recherche". Its first aim was to identify solid catalysts adapted for alkene hydrosilylation in continuous reactors, with criteria of high activity, low Pt leaching and high stability. The second aim was to study the behaviour of the selected catalysts in continuous reactors manufactured in silicon carbide (for an effective heat dissipation of this very exothermic reaction).

The results on the reactor engineering part of the Hexosic won't be commented here, but some results on the chemistry part are the starting point for the current project and will be discussed here.

It was proven using ^{29}Si NMR that during hydrosilylation of 1-octene by a polymethylhydrosiloxane, the functionalization of adjacent Si – H bonds was more frequent than if it was random, but only at the beginning of the reaction.[136] This effect faded away when conversion increased, and was not observed for other Pt catalysts than Karstedt's complex. It thus showed that there were at least two catalytic species arising from Karstedt's complex, each one having a different mechanism.

[136] V. Meille et al., *Silicon* **2014**, 6, 247–255.

Preliminary experiments showed that preformed Pt nanoparticles had comparable activity and selectivity with Karstedt's complex, surprisingly, despite having a metallic dispersion of about 50%. It thus showed that metallic nanoparticles were interesting precatalysts, with singular behaviours, and that their study could open new paths in alkene hydrosilylation catalysis.

Finally, it was demonstrated that the immobilization of Pt nanoparticles in the silica walls of a mesostructured silica, SBA-15, yielded a non-leaching catalyst,[137] knowing that Pt leaching is a recurring problem for heterogeneous alkene hydrosilylation catalysts. It appeared that the development of heterogeneous Pt catalysts comprised important challenges to be tackled.

[137] C. Thieuleux et al. *Hydrosilylation method* WO Patent App. PCT/EP2013/077,581 2014

The current project, called "Hysinano" and also funded by the french "Agence Nationale de la Recherche", is focused on the **study of catalysts based on metallic nanoparticles for alkene hydrosilylation**, in a quest to sustainable alternatives to platinum complexes.

1.6.2 Why metal nanoparticles?

Metal nanoparticles (NPs) have attracted a lot of attention as catalysts since approximately the end of the 1980s.[135,138–141]

[138] A. T. Bell, *Science* **2003**, 299, 1688–1691.
[139] D. Astruc, F. Lu and J. R. Aranzaes, *Angew. Chem. Int. Ed.* **2005**, 44, 7852–7872.
[140] D. Astruc, ed. *Nanoparticles and Catalysis*. Wiley-VCH, 2008.
[141] C. Jia and F. Schüth, *Phys. Chem. Chem. Phys.* **2011**, 13, 2457–2487.

The NP synthesis approach which is usually used for catalysis, called "bottom-up approach" (Figure 1.59), involves a synthesis starting from smaller species such as salts, complexes or clusters, which are reduced or decomposed. It generally allows to get a precise control over the size, dispersity, composition and shape of the NPs, which is not always the case for heterogeneous catalysts synthesized by conventional impregnation methods and for top-down approaches of NPs preparation (mechanical subdivision of bigger particles).[135,141]

The control over the size of the particles can be important for some reactions. Indeed, not all sites are equal on a nanoparticle: sites located on NP corners or edges have higher surface energy than sites on facets, and thus have different

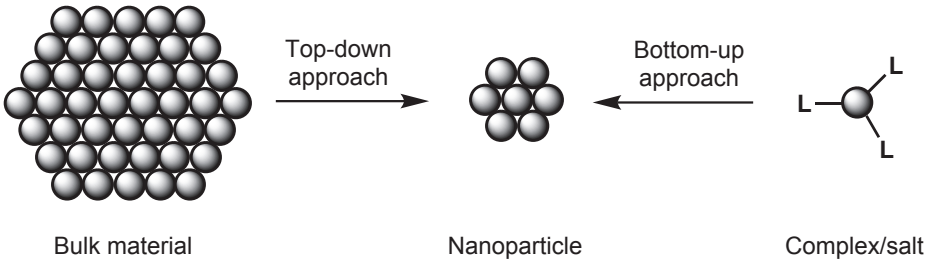


Figure 1.59: Top-down and bottom-up approaches for nanoparticle synthesis. L = ligand.

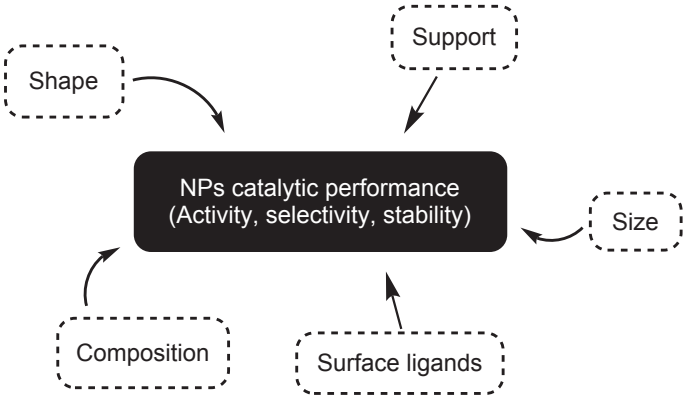


Figure 1.60: Properties of metallic nanoparticles influencing their catalytic performances.

catalytic properties. Depending on which sites one wants to favour, an optimal NP size for a given catalytic reaction exists.[142]

Metal NPs of different shapes can be synthesized,[143–146] which expose different crystalline facets and often have different catalytic reactivities. Thus, by synthesizing nanoparticles with well-defined shapes, it is possible to modulate activities and selectivities.[146] The shape of the nanoparticles depends on the interplay between thermodynamical and kinetic factors during their growth. In practice, factors such as reaction temperature, nature and concentration of the metallic precursors and the nature of stabilizers and additives used will have an influence on the final shape of the NPs.

Recently, efforts have been made to functionalize metallic nanoparticles with organic ligands, particularly with enantiopure ligands, for enantioselective catalysis.[147] We can suppose that original reactivities could be obtained by modifying metallic NPs with ligands.

There are some examples of catalysis by platinum nanoparticles in alkene hydrosilylation, mostly in the context of a controversy concerning the nature of the active species when using metal salts such as H_2PtCl_6 (Speier's catalyst) has been active since 1986.[55] In this paper, Lewis suggests that a Pt colloid, formed from the Pt salt used as precatalyst, is the actual active species. Since this, other papers discussing that matter were published, and it seems that the issue is not definitely solved. But still, it seems that in several cases, even for the well-known Karstedt's catalyst, a lot of people have done alkene hydrosilylation reactions with nanostructured catalysts without knowing it! However very few examples of deliberately synthesized nanostructured precatalysts can be found in the alkene hydrosilylation literature.[148,149]

[142] V. Iablokov et al., *ACS Catal.* **2016**, 6, 2496–2500.

[147] S. Roy and M. A. Pericàs, *Org. Biomol. Chem.* **2009**, 7, 2669–2677.

[148] B. P. S. Chauhan and J. S. Rathore, *J. Am. Chem. Soc.* **2005**, 127, 5790–5791.

[149] B. P. S. Chauhan and B. Balagam, *Macromolecules* **2006**, 39, 2010–2012.

1.6.3 Strategy

Our strategy is to study metallic nanoparticles of different metals, in the 0 oxidation state, because the principal hydrosilylation mechanisms usually involve a M(0)/M(II) redox cycle (Figure 1.61).

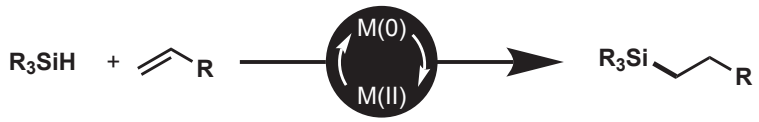


Figure 1.61: Hydrosilylation catalysts usually oscillate between M(0) and M(II) oxidation states.

The first research line (Table 1.2), with platinum catalysts, is based on preliminary results of the Hexosic project, funded by the Agence Nationale de la Recherche. It aims at maximizing the number of turnovers that each platinum atom can reach, in order to decrease the quantity of platinum needed in hydrosilylation processes, and to search for catalysts giving platinum-free products. This part of the project is the most applied.

The second research line (Table 1.2), with non-noble metal nanoparticles, aims at completely replacing platinum in hydrosilylation catalysts. This axis is much more fundamental, given the paucity of hydrosilylation catalysts based on non-noble nanoparticles in the literature, and intends to identify potential catalyst candidates for further development. We have chosen to work with iron and nickel because there were many complexes of these non-noble metals in the alkene hydrosilylation literature. Even if they were often much less active than noble metal complexes, it was proven that by finely tuning the environment of the metal center of these complexes, it was possible to greatly enhance catalytic performances. We expect that the same approach of optimization could also lead to active and selective non-noble metal-based nanoparticles.

Axis 1	Axis 2
Pt	Abundant metals
Shorter term	Longer term
More applied	More fundamental
Maximize TONs	Identify candidates
Obtain platinum-free products	for further development

Table 1.2: Research lines of the Hysinano project.

Various substrates have been used during catalytic tests, because the reaction is known to be very substrate-sensitive, and catalysts may be active with certain substrate combinations while being inactive/slow with other substrates. For example, the hydrosilylation of 1-octene by MD'$_{50}$M (Figure 1.62, top) is a reaction performed industrially, was used to get an overview of how a catalyst would perform in industrially relevant conditions. The hydrosilylation of 1-octene by MD'M (Figure 1.62, middle) has a similar behaviour, even if the kinetics is usually slower because of the steric hinderance caused by the two M groups around the Si – H bond. This reaction is very convenient because it can be monitored by gas chromatography, unlike the first reaction (because long-chain siloxanes are not volatile enough). Other substrates, triethoxysilane, triethoxyvinylsilane, triethylsilane and triethoxyvinylsilane have also been used (Figure 1.62, bottom) because they can sometimes be reactive when the

reagents of the first two reactions would not.

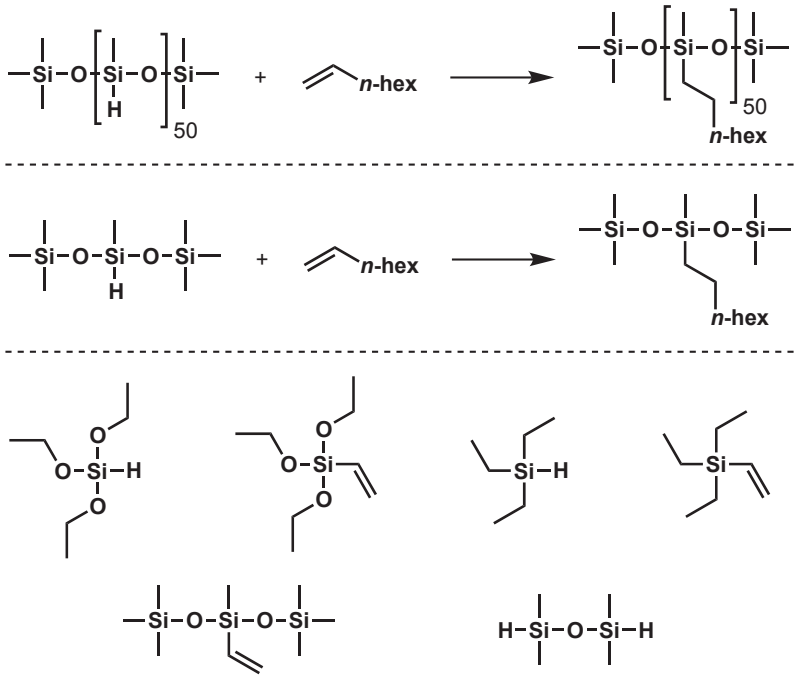


Figure 1.62: Top: hydrosilylation of 1-octene by a PMHS containing 50 Si – H units. Middle: hydrosilylation of 1-octene by MD'M. Bottom: other substrates used in catalytic tests.

Globally, our strategy is to adopt a fundamental approach, to explore reactivities of different metal nanoparticles and to provide bases for kinetic/mechanistic studies, which themselves will allow to optimize catalysts. During this project, we postulated several mechanisms that account for the formation of the observed products. These mechanisms are not backed by proper mechanistic studies, but are nevertheless inserted in this manuscript and commented, because they can stimulate thought about future studies, including mechanistic studies.

Four partners participated to the project (Figure 1.63): the "Laboratoire de Génie des Procédés Catalytiques", where catalytic tests were performed, the "Laboratoire de Chimie, Catalyse, Polymères et Procédés", where catalysts are synthesized, characterized and tested, CPE FCR and Bluestar Silicones France SAS, which brought industrial expertise on alkene hydrosilylation and raw materials.

Figure 1.63: Partners for the Hysinano project.

1.6.4 Catalyst comparison criteria

Several criteria will be used in this manuscript to compare catalysts, their economic potential and their sustainability. They are presented here.

When working with metallic NPs, a sustainable catalyst must be made of a cheap and abundant metal (see Table 1.3). The price of a metal and its abundance are usually linked (see Figure 1.64), but the price is most of all determined by its supply and demand. For example, ruthenium is not very expensive despite being very rare, because its demand is low and is exceeded by its supply.[d]

[d] A risk is that if demand for ruthenium increases, its price may increase a lot. Hence, ruthenium is a rather cheap ressource, but not sustainable.

Metal	Price (€/kg)	M (g/mol)	Price (€/mol)
Fe (ore)	0.04	55.8	0.7
Co	21	58.9	360
Ni	8	58.7	140
Ru	1200	101.1	12 000
Pt	29 000	195.1	149 000

Table 1.3: Order of magnitude of the prices of metals commonly used for the fabrication of hydrosilylation catalysts on April 24th, 2016.

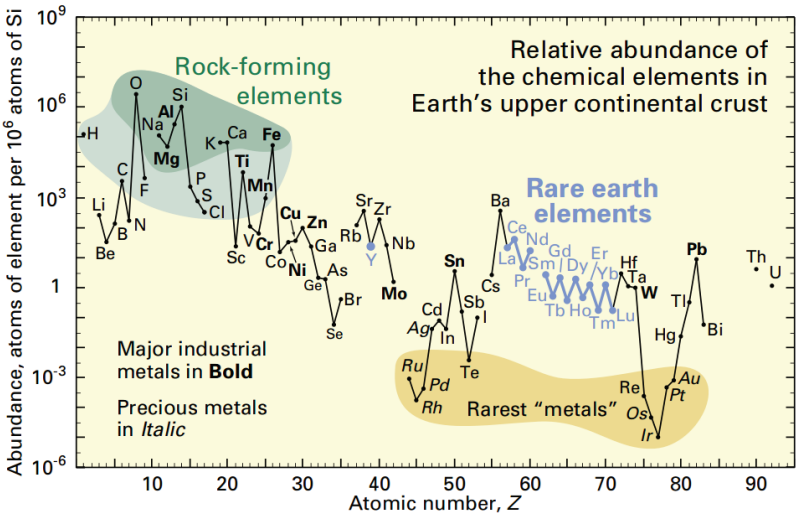


Figure 1.64: Relative abundance of chemical elements in earth's upper continental crust.[150]

However, besides considering the cost of the metal, one should consider the cost of the whole catalyst. In the case of homogeneous catalysts, expensive ligands may represent a higher part of the cost of the catalyst than the metal itself. This is particularly relevant for complex ligands that require lengthy syntheses or enantiopure ligands for asymetric catalysis.

The turnover number (TON), a unitless number defined as

$$\mathrm{TON} = \frac{n_{\text{converted substrate}}}{n_{\text{metal}}}$$

is especially important to look at in the case of expensive metals such as Pt. Indeed, the higher the TON, the less metal is needed to convert a given quantity of substrate. The TON can either be calculated relatively to the total quantity of metal in the system, or relatively to the amount of surface metal in the catalyst, knowing that

$$n_{\text{metal,surface}} = n_{\text{metal,total}} \times \text{metallic dispersion}$$

In the present manuscript, unless otherwise noted, we will consider TONs relative to the total metal amount. In the case of polymethylhydrosiloxane, that

contain multiple Si – H bonds, the TON is calculated with respect to the quantity of Si – H bonds converted. If the catalyst is reusable over several batches, then a total TON over these batches should be calculated. In a continuous reactor, a TON can likewise be calculated.

The turnover frequency (TOF) is a related quantity, in s^{-1}, expressing the activity of the catalyst. For a batch reaction, it is either instantaneous and defined as

$$\mathrm{TOF} = \frac{d(n_{\text{converted substrate}})}{n_{\text{metal}} \cdot dt}$$

or averaged over a period of time and defined as

$$\mathrm{TOF} = \frac{n_{\text{converted substrate}}}{n_{\text{metal}} \cdot t}$$

with t being the reaction time. If an initial or instantaneous TOF is not easily calculable, an average TOF at 50% conversion can be calculated, for example.

Some process variables that are imposed by the catalyst, for example the reaction temperature, can strongly influence the process cost. For example, a catalyst that works at room temperature is more advantageous than a catalyst which requires high temperatures (leading to high energy costs).

For a batch reaction $R \rightarrow P + BP$ (reagent R, desired product P and byproduct BP) starting at time $t0$, the conversion of R at time t is defined as

$$\mathrm{Conversion}_R(t) = \frac{n_R(t0) - n_R(t)}{n_R(t0)}$$

the yield of P at time t is defined as

$$\mathrm{Yield}_P(t) = \frac{n_P(t)}{n_R(t0)}$$

and the selectivity for P at time t is defined as

$$\mathrm{Selectivity}_P(t) = \frac{\mathrm{Yield}_P(t)}{\mathrm{Conversion}_R(t)}$$

The selectivity represents the efficacy of the reaction to convert the reagent R in the desired product P. A low selectivity means that a purification process is needed to remove the byproducts, leading to expenses for waste treatment, and higher quantities of reagents needed to produce a given quantity of product. Therefore, selectivity should be maximized.

The ease of recovery of the metal is another important parameter, especially for precious metals. If a catalyst based on a precious metal is deactivated, but the metal is recoverable, it can then be refined, and a new catalyst can be prepared with it. For heterogeneous catalysts, this is generally easier than for homogeneous catalysts, except if metal leaching from the support happens.

1.6.5 Manuscript organization

After this introductive first chapter, the second chapter concerns the study of platinum nanoparticles in suspension, their comparison with Karstedt's complex, and the implications regarding the nature of the active species when using Karstedt's complex as precatalyst. The third chapter concerns the synthesis and test of solid Pt-based catalysts using two sets of supports: silicas and carbons. Their reusability, total TON reached and nature of the active

species (dissolved or truly heterogeneous) are discussed. The fourth chapter describes the results that we obtained while studying nickel-based nanostructured catalysts: a Ni/SiO_2 solid and a Ni_3Si_2 colloid, in particular with respect to selectivity, which we show is greatly affected by the chemical environment of the nickel centers. Finally, the fifth chapter treats with iron nanoparticles of several kinds, and constitutes a first exploration of the reactivity towards hydrosilylation of iron-based nanoparticles.

2

Platinum nanoparticles in suspension

Most of the results presented in this chapter have been published as:

Thomas Galeandro-Diamant, Marie-Line Zanota, Reine Sayah, Laurent Veyre, Clémence Nikitine, Claude de Bellefon, Sébastien Marrot, Valérie Meille and Chloé Thieuleux, *Chem. Comm.* **2015**, 51, 16194–16196.

Antoine Degenne (CPE Lyon) is thanked for his participation to some experiments appearing in this chapter.

2.1 Introduction

Given the very high and unstable price of platinum, it is crucial to improve the performances of the platinum-based catalysts to reduce the quantities of platinum used.[5] For that purpose, important efforts have been directed to the better understanding of the reaction mechanism and to the determination of the structure of the active species—homogeneous or NPs—, a subject which has been controversial for almost thirty years and also concerns other catalytic reactions.[151]

Several examples of platinum colloids have been reported to be catalytically active for alkene hydrosilylation,[148,152,153] thus showing that their formation is not responsible for the deactivation of homogeneous catalysts, as it has been thought for a long time. At the reverse, several truly homogeneous platinum catalysts were also described,[43,56,57,154] meaning that colloid formation does not happen for all catalysts, contrary to the conclusions of several authors.[39,55,122,155] Thus, it seems that both can catalyze hydrosilylation.

For Karstedt's catalyst, the benchmark in the silicone industry, the exact nature of the active species is still unknown. Lewis and co-workers have suspected for a long time that platinum colloids could be the actual active species of hydrosilylation reactions in general, and that their formation was at the origin of the induction period observed.[39,55,122] These results however lacked *in situ* data. More recently, they challenged their own conclusions by using *in situ* Extended X-Ray Absorption Fine Structure (EXAFS) to show that in the case of Karstedt's catalyst, the active Pt presented Pt – C and Pt – Si bonds, but no Pt – Pt bonds, thus demonstrating that the catalyst was truly homogeneous.[56] Their Tunover Numbers (TONs, expressed in mol of transformed SiH per mol of platinum) were about 1000, because their set up only allowed to work with

[151] R. H. Crabtree, *Chem. Rev.* **2012**, 112, 1536–1554.

[152] M. A. Brook et al., *Inorg. Chim. Acta* **1997**, 264, 125–135.

[153] Y. Bai et al., *J. Colloid Interface Sci.* **2013**, 394, 428–433.

[154] P. Steffanut et al., *Chem. Eur. J.* **1998**, 4, 2008–2017.

[155] L. N. Lewis and R. J. Uriarte, *Organometallics* **1990**, 9, 621–625.

low substrate/catalyst ratios, ie. high Pt loadings. In constrast, industrial TONs for this reaction are about 10^5, so there is still a need to further examine what is occurring at TONs higher than 1000.

Besides providing mechanistic insights, studying platinum colloids as a catalyst for alkene hydrosilylation opens the way for reusable platinum catalysts. Up to now, none of the published platinum NPs catalysts for alkene hydrosilylation could compete with Karstedt's catalyst in terms of TON.[148,152,153]

In the present work, we prepared three kinds of platinum nanoparticle suspensions and used them to catalyze the hydrosilylation of 1-octene with a polymethylhydrosiloxane (PMHS) containing approximately 50 SiH units (Figure 2.1). TONs higher than 10^5 were rapidly reached without significant deactivation, demonstrating that platinum nanoparticles could be as efficient as Karstedt's complex. We also reactivated the debate on whether Karstedt's catalyst is truly homogeneous or colloidal during catalysis.

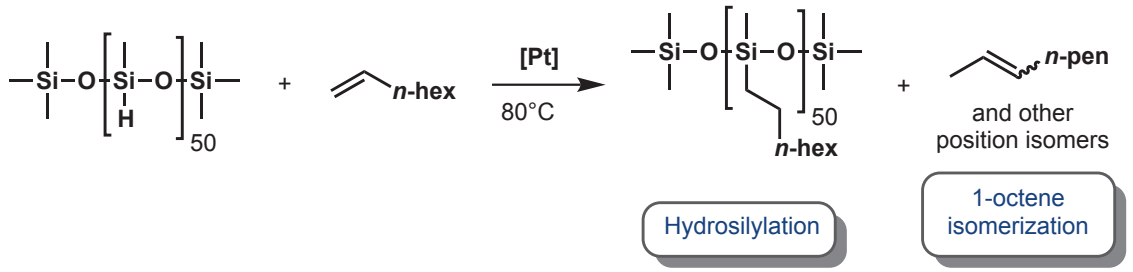


Figure 2.1: Hydrosilylation of 1-octene by a PMHS.

2.2 Results

Three kinds of platinum nanoparticles were synthesized using an experimental procedure developed in our laboratory for the synthesis of NPs of platinum,[156] ruthenium,[157] gold[158] and nickel.[159] A typical procedure comprises dissolution of 0.015 mmol of $Pt(dba)_2$ (dba = dibenzylideneacetone) or Karstedt's catalyst in 43 mL of toluene, adding a quantity of *n*-octylsilane or PMHS corresponding to 1 equivalent of SiH_3 (or SiH, respectively) and stirring overnight at room temperature under 4 bars of hydrogen. It should be noted that only one example of platinum nanoparticles stabilized by polymethylhydrosiloxanes was reported in the literature.[148]

We assessed that the decomposition of the Pt(0) precursor was quantitative using UV/visible spectroscopy (Figure 2.2). Indeed, the spectrum of the colloidal solution shows the absence of the $Pt(dba)_2$ absorption band, indicating a total conversion of the Pt complex.

The colloids were characterized by transmission electron microscopy (TEM), as shown in Figure 2.3. The nanoparticles were found to be small, isolated and crystalline. Their mean diameter was calculated by averaging the size of at least 200 particles per colloid, measured from the TEM images. It was of 1.6 nm for Colloid1, and 1.7 nm for Colloid2 and Colloid3 (Table 2.1).

Catalytic tests were performed to compare the activities of platinum nanoparticles and their homogeneous precursors at 0.5 ppm and 7 ppm of platinum in the reaction mixture (Table 2.1). A typical procedure involves preheating a

[156] M. Boualleg et al., *Chem. Mater.* **2009**, 21, 775–777.
[157] K. Pelzer et al., *Chem. Mater.* **2004**, 16, 4937–4941.
[158] M. Boualleg et al., *Chem. Comm.* **2010**, 46, 5361–5363.
[159] D. Baudouin et al., *J. Am. Chem. Soc.* **2012**, 134, 20624–20627.

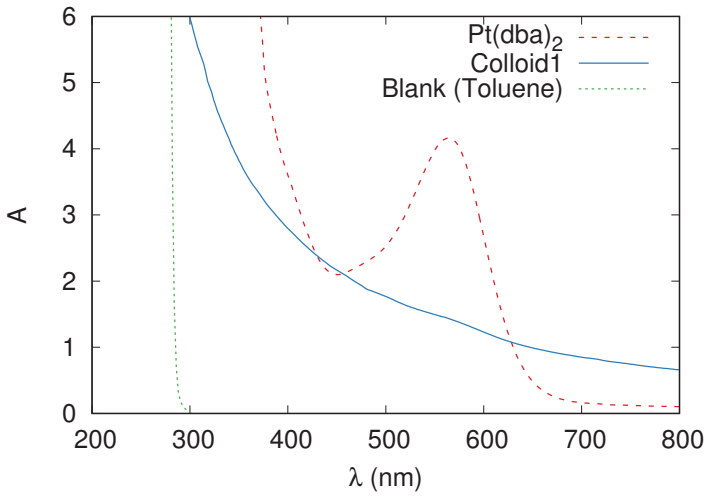


Figure 2.2: UV/Visible spectra of Colloid1 and a $Pt(dba)_2$ solution at identical total platinum concentration.

Catalyst	Pt precursor	Stabilizer	Average diameter (nm)	SiH conv. (TON) 0.5 ppm total Pt	SiH conv. (TON) 7 ppm total Pt	1-octene isomerization
Karstedt	-	-	-	87% (1.5×10^6)	96% (1.0×10^5)	12%
$Pt(dba)_2$	-	-	-	86% (1.5×10^6)	98% (1.1×10^5)	12%
Colloid1	$Pt(dba)_2$	*n*-octylsilane	1.6	77% (1.3×10^6)	98% (1.1×10^5)	11%
Colloid2	Karstedt	PMHS	1.7	84% (1.5×10^6)	97% (1.0×10^5)	11%
Colloid3	Karstedt	*n*-octylsilane	1.7	81% (1.4×10^6)	99% (1.1×10^5)	11%

Table 2.1: Characteristics of the colloids and results of catalytic tests with the colloids and their platinum precursors. The SiH conversions were measured 30 minutes after the end of PMHS addition.

mixture of 1-octene and the colloidal suspension at 75°C and then adding a quantity of PMHS corresponding to 0.7 equivalent of SiH over 52 minutes. The SiH conversions were determined by ^{1}H NMR at regular intervals after the end of the addition of PMHS. Blank experiments were performed at various points of the project and showed that the catalytic test setup was not contaminated by any trace of catalyst.

SiH conversions are compared 30 minutes after the end of the addition of PMHS in the Table 2.1. At 7 ppm of platinum, conversions are almost quantitative (> 96%) for all catalysts. At 0.5 ppm of platinum, the colloidal catalyst gave 77%–84% conversion while Karstedt's catalyst gave 87% conversion. At 7 ppm platinum, full conversion of the PMHS could easily be reached with longer reaction times, but at 0.5 ppm, conversions never reached more than 90%. We suspected a deactivation of the catalysts due to traces of contaminant in the reactants, given the very small platinum concentrations used.

Colloidal catalysts were found to be as selective as Karstedt's catalyst, and showed only anti-Markovnikov addition of the SiH on the C=C bond (like most platinum catalysts). The proportion of isomerization of 1-octene to 2-octene, a side reaction very common in hydrosilylation with platinum catalysts, was between 10% and 12% for all catalysts.

These results (rate, conversion, amount of isomerization) clearly show that well-stabilized nanoparticles are very active catalysts, as efficient as Karstedt's complex, and not a deactivation form of Pt complexes. Noteworthy, if colloids were not well-stabilized (for example because of a lack of stabilizer) and started to agglomerate, their catalytic performance dropped.

We then used Celite to selectively adsorb Pt NPs but not Pt complexes such

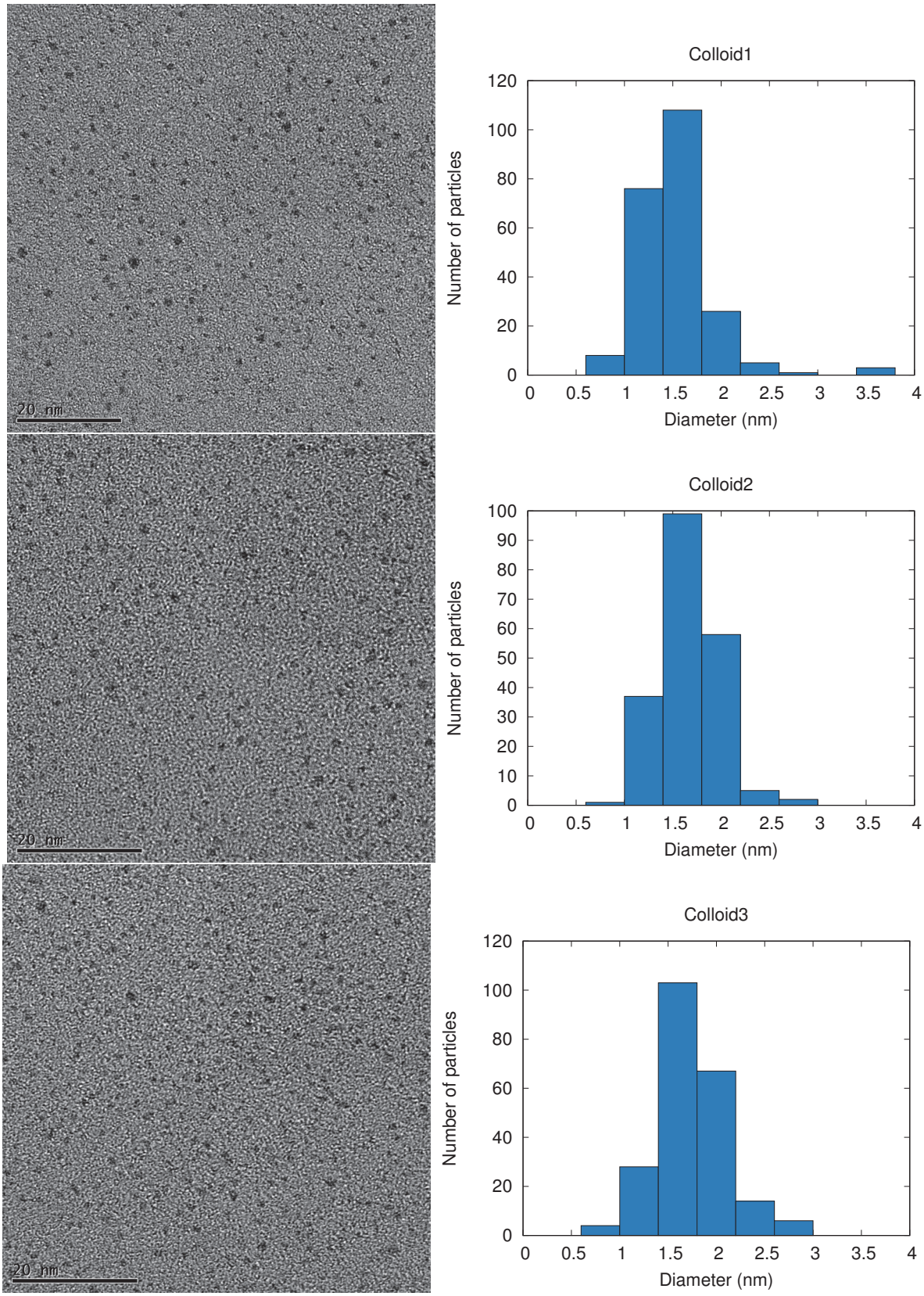


Figure 2.3: Transmission Electron Micrograph and particle size distribution of the colloids. Top : Colloid1, Middle : Colloid2, Bottom : Colloid3.

as $Pt(dba)_2$ to probe the homogeneous/colloidal nature of the active species when using Pt NPs as precatalyst.

We started by checking visually that a Celite® plug could selectively adsorb platinum nanoparticles but not platinum complexes such as $Pt(dba)_2$, as shown in Figure 2.4.



Figure 2.4: Adsorption experiments of a solution of Pt nanoparticles (left) and $Pt(dba)_2$ (right) on a Celite® plug.

We then performed a semi-batch experiment at 60 °C with a low quantity of PMHS with respect to 1-octene in order to ensure a low conversion (2 g PMHS added over 5 min in 42 g of 1-octene containing 7 ppm of Pt NPs). Immediately after the PMHS addition, we took an aliquot of the reaction medium. We filtrated this sample on a celite plug (4 cm Celite in a glass pipette). The SiH conversion in the filtrate was 57%. The filtrate was put at 60°C during 1 h, after which the SiH conversion was 62%. In the same amount of time, the SiH conversion in the reactor had progressed to 80%. That test supported the hypothesis that when using Pt NPs as precatalysts, the catalytic activity was essentially due to the NPs themselves and not a dissolved Pt species.

On Figure 2.5, the SiH conversion is plotted vs. time at 0.5 ppm of total Pt for different catalysts. The tendency is that homogeneous Pt(0) precatalysts such as Karstedt's complex or $Pt(dba)_2$ are more active than Pt nanoparticles in the first minutes of reaction, but that all catalyst tend to have similar activities in the late stage of the reaction.

The difference of initial activity may be explained by the fact that in a SiH-rich medium, that is able to stabilize Pt nanoparticles (see the synthesis of Colloid2), Karstedt's complex decomposes into clusters or very small and well-stabilized nanoparticles, and is thus more active than preformed nanoparticles of larger size (1.7 nm in our case). Then, when the reaction progresses, the SiH content of the medium decreases and these Pt clusters or very small nanoparticles grow to reach a size close to that of the preformed nanoparticles (1.5–2 nm), thus being slightly less active. One other explanation may be that for preformed Pt nanoparticles there is an induction period due to the time needed to displace the ligands stabilizing the nanoparticles, leaving their surface accessible for catalysis.

The similar activities and final selectivities towards 1-octene isomerization

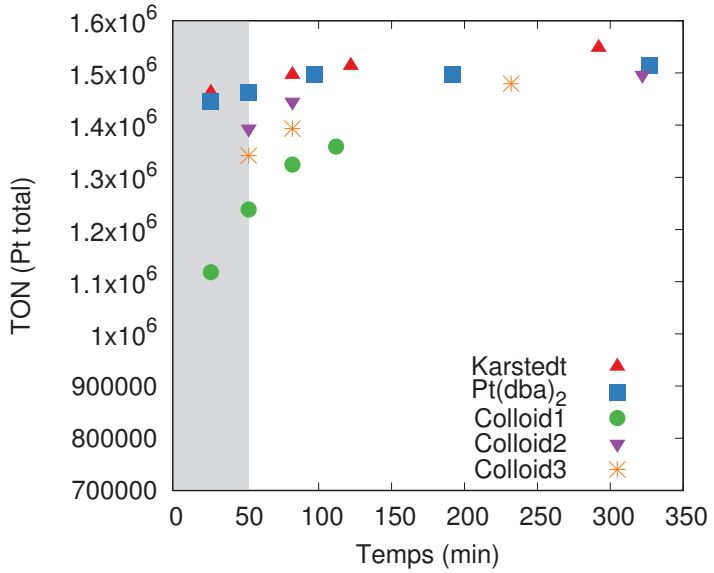


Figure 2.5: SiH conversion as a function of time, in batch tests (0.5 ppm total Pt). The period in grey, from 0 to 52 minutes, is the addition of PMHS in the reactor.

of all catalysts in the late stages of the reaction also support the hypothesis that Karstedt's catalyst is rapidly transformed into Pt nanoparticles during the reaction.

To summarize, all these observations suggest that depending on the reaction conditions, the nature of the active species are different: at very low TONs (< 1000), Karstedt's catalyst is truly homogeneous, as demonstrated by the group of Lewis with *in situ* EXAFS experiments,[56] and that at higher TONs, it is rapidly transformed into Pt nanoparticles. Our group recently used ^{1}H and ^{29}Si NMR to show that Karstedt's complex had a tendency to functionalize PMHS polymers with a high proportion of block units (three consecutive D^{oct} units) at low TONs, and that this tendency disappeared at higher TONs.[136] This was interpreted as a progressive transformation of Karstedt's complex into a different active species at TONs of 10^3–10^4. This result had already been suggested by Steffanut and co-workers in 1998.[154]

2.3 Conclusion

In conclusion, we showed that platinum nanoparticles used in same concentration as Karstedt's catalyst, the benchmark in the silicone industry, gave equal to superior performances, and could reach full conversions even at concentrations as low as 7 ppm. These results tend to prove that Karstedt's complex is rapidly transformed into colloids, which are the active species during the rest of the reaction. These results also open the way towards the development of nanostructured heterogeneous platinum catalysts for alkene hydrosilylation.[135,141] Indeed, immobilizing Pt nanoparticles on solid supports would allow to reuse catalysts and to obtain platinum-free and colorless hydrosilylation products, two highly desirable qualities for the silicone industry.[53] One important challenge will be to develop a heterogeneous catalyst which is extremely stable towards deactivation and platinum leaching, in order to outperform homogeneous catalysts in terms of TONs. Since the nanoparticles presented herein have already reached TONs as high as Karstedt's catalyst,

once immobilized they would be recyclable and could give even higher TONs. It would allow the development of hydrosilylation processes with reduced platinum consumption, thus more sustainable.

2.4 Experimental

All experiments were run in duplicate. Platinum concentrations are expressed in ppm (microgram of platinum per gram of reaction mixture).

2.4.1 Chemicals

Dibenzylideneacetone (dba), potassium tetrachloroplatinate (K_2PtCl_4) and 1-octene were bought from Sigma-Aldrich. The polymethylhydrosiloxane (PMHS) containing approximately 50 SiH units and Karstedt's catalyst (10% w/w Pt solution in a neutral silicone oil) were generously provided by Bluestar Silicones France SAS. *n*-octylsilane was bought from ABCR. $CDCl_3$ was bought from Alfa Aesar. Toluene was bought from Carlo Erba, dried in a MBraun SPS-800 system, and degassed using the freeze-pump-thaw method.

2.4.2 Synthesis of $Pt(dba)_2$

This synthesis is based on a procedure from the literature.[160]

[160] K. Moseley and P. M. Maitlis, *J. Chem. Soc. D: Chem. Comm.* **1971**, 982–983.

In a Schlenk tube equipped with a magnetic stirbar was introduced potassium tetrachloroplatinate (1000 mg, 2.4 mmol, 1 eq.) and 6 mL of distilled water. The red solution was stirred 20 minutes, degassed by applying vaccum and shaking vigorously, and put under argon.

In another Schlenk tube equipped with a magnetic stirbar was introduced dibenzylideneacetone (1500 mg, 6,4 mmol, 2.6 eq.), sodium acetate (1560 mg, 19 mmol, 7.9 eq.) and absolute ethanol (40 mL). The suspension was stirred during 30 min, degassed by applying vaccum and shaking vigorously, and put under argon.

The potassium tetrachloroplatinate solution was transferred to the Schlenk tube containing the dba and sodium acetate solution, causing the mixture to precipitate. The mixture was heated under reflux (oil bath at 90°C) under argon during 2 h. It was let cool down during 2 h, and then filtered under argon. The black solid was washed with 2*20 mL of distilled water, and 2*20 mL of pentane, and dried under vaccuum.

2.4.3 Synthesis of the colloidal suspensions

General procedure

43 mL of toluene and 0.015 mmol of the platinum precursor were introduced in a dry schlenk tube under argon. The solution was transferred into a dry Fisher-Porter vessel under argon using a canula. 1.5 equivalent of stabilizer was added. The solution was put under 4 bars of H_2, and stirred at room temperature overnight. The resulting colloidal solutions contained 80 ppm of platinum.

Colloid1

The general procedure was used, with $Pt(dba)_2$ (10 mg, 0,015 mmol) as platinum precursor and *n*-octylsilane (3.3 mg, 0,023 mmol) as stabilizer. This synthesis has already been published.[156]

Colloid2

The general procedure was used, with Karstedt's catalyst (29.4 mg of a 10% solution, corresponding to 2.9 mg of platinum, 0.015 mmol of Pt) as platinum precursor and the PMHS (4.2 mg, 0.023 mmol) as stabilizer.

Colloid3

The general procedure was used, with Karstedt's catalyst (29.4 mg of a 10% solution, corresponding to 2.9 mg of platinum, 0.015 mmol of Pt) as platinum precursor and *n*-octylsilane (3.3 mg, 0.023 mmol) as stabilizer.

2.4.4 Transmission Electron Microscopy

Transmission Electron Microscopy (TEM) of the platinum colloids was performed at the "Centre Technologique des Microstructures", Université Lyon 1, Villeurbanne, France, with a JEOL2100F transmission electron microscope, using an acceleration voltage of 200 kV. The samples were prepared by depositing a drop of colloidal solution on a copper grid covered by a carbon film and letting it dry.

2.4.5 Catalytic tests

Warning: the hydrosilylation reaction is very exothermic! The reaction medium temperature must be monitored carefully to prevent a runaway.

Blank tests were performed at several points of the study and indicated that the reactor was not contaminated by traces of catalysts.

The hydrosilylation catalysts were found to be very sensitive to the grade of the octene used. When using octene of industrial grade, conversions significantly lower were obtained, and the presence of traces of poisons in the octene were suspected to be at the origin of these lower performances.

The catalytic tests were run under an atmosphere of air, in a classic 300 mL glass reactor equipped with a glass impeller and baffles. The stirring rate was 1000 rpm. At the beginning of the reaction, the reactor was filled with 43 g of 1-octene (1.4 equivalent respective to SiH, to compensate for alkene isomerization). For 7 ppm tests, 6 g (6.9 mL) of colloidal solution were added. For 0.5 ppm tests, 0.37 g (0.43 mL) of colloidal solution were added. When Karstedt's catalyst was used, it was diluted with toluene to reach the same Pt concentration in the reaction medium. The 1-octene/catalyst mixture was heated to 75°C. Then, 17 g of PMHS were added at 0.3 mL/min with a syringe pump. The temperature of the reaction medium was maintained between 75°C and 85°C by removing partly or totally the heating bath. After the end of the PMHS addition, samples were regularly collected, diluted in $CDCl_3$ and analysed by ^1H NMR to get the SiH conversion.

We observed that when colloids were not perfectly dispersed (presence of some aggregates on the TEM), the SiH conversions were significantly lower. The presence of aggregates may indicate that the particles are not perfectly

stabilized, for example because of a lack of silane stabilizer, and the particles may aggregate further when heated in the reaction medium, thus decreasing their activity.

2.4.6 SiH conversion calculation

An example of proton NMR spectrum of the reaction mixture of a catalytic test is given in Figure 2.6.

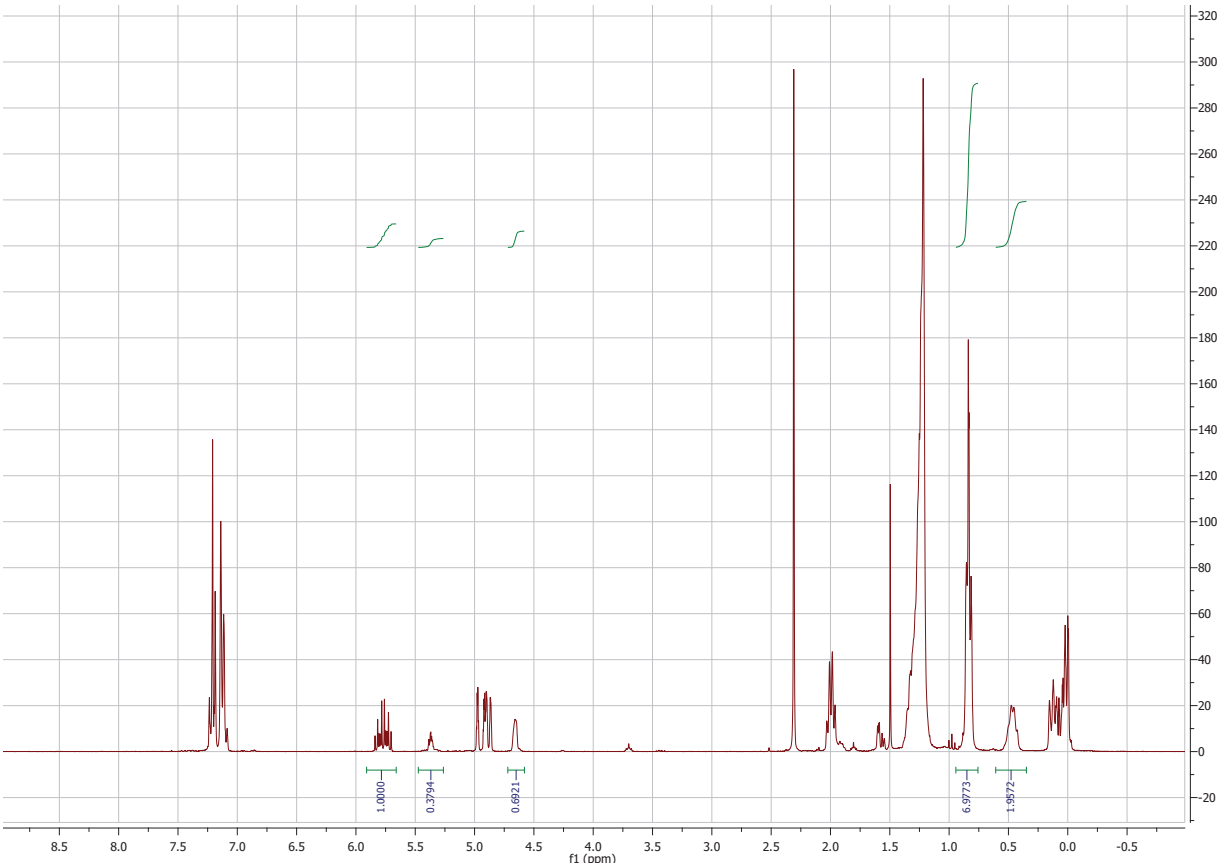


Figure 2.6: Example proton NMR spectrum of the crude of a catalytic test.

The signal at $\delta = 0.5$ ppm corresponds to the $C\underline{H_2}Si$ of hydrosilylated SiH, the signal at $\delta = 0.85$ ppm corresponds to the $CH_2C\underline{H_3}$ of all octyl chains and 2-ethyl-1-hexene, the signal at $\delta = 4.7$ ppm corresponds to the $Si\underline{H}$ protons plus 1-ethyl-2-hexene, an impurity contained in 1-octene, the signal at $\delta = 5.3$ ppm corresponds to both $C\underline{H}$ of 2-octene (formed in the medium by isomerization of 1-octene) and the signal at $\delta = 5.7$ ppm corresponds to the $C\underline{H}$ of 1-octene.

The quantity of 2-ethyl-1-hexene is

$$\text{ethylhexene} = \frac{I_{0.85\,\text{ppm}}/3 - I_{5.7\,\text{ppm}} - I_{5.3\,\text{ppm}}/2 - I_{0.5\,\text{ppm}}/2}{3}$$

The SiH conversion is

$$\text{Conv}_{\text{SiH}} = \frac{\text{functionnalized SiH}}{\text{functionnalized SiH} + \text{unfunctionnalized SiH}}$$

hence

$$\text{Conv}_{\text{SiH}} = \frac{I_{0.5\,\text{ppm}}/2}{I_{0.5\,\text{ppm}}/2 + (I_{4.7\,\text{ppm}} - \text{ethylhexene}/2)}$$

2.4.7 Metallic dispersion

From TEM images of platinum nanoparticles, by measuring the diameter of at least 200 particles per colloid, a particle diameter histogram is drawn, and a medium diameter is calculated.

From this medium diameter d, the metallic dispersion D can be calculated using the formula:

$$D = \frac{6M}{N_A \rho S_a d}.$$

Assuming a surface concentration of platinum atoms $1/S_a$ of 1.25×10^{19} atoms/m^2,[161] we get for platinum the equation

$$D = \frac{1.137}{d}$$

which is plotted in the Figure 2.7.

[161] J. Anderson. *Structure of Metallic Catalysts*. Academic Press, 1975. 296

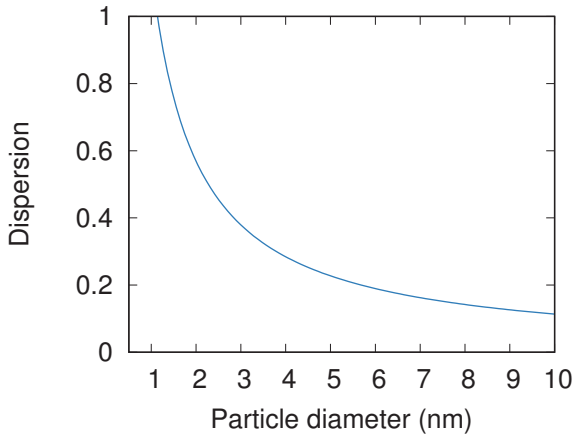


Figure 2.7: Metallic dispersion of platinum colloids as a function of the medium particle diameter.

2.5 Appendices

2.5.1 Dynamic Light Scattering

We attempted to measure the NPs size and concentration in the reaction medium by Dynamic Light Scattering (DLS) on a Nano ZS zetameter (Malvern Instruments). While the nanoparticle size was above the detection limit of 0.6 nm, the very low NP concentration and the heterogeneity of the liquid phase (micro-emulsion of silicone oil with 1-octene) prevented us from using this analytical method.

2.5.2 ^{195}Pt NMR

We performed several ^{195}Pt NMR experiments in order to observe precatalysts or catalytic intermediates.

The spectrum of a 10 mM solution of Karstedt's complex in toluene took several hours to acquire and yielded one peak at $\delta = -6124$ ppm (Figure 2.8), as described in the literature.[60]

A Pt colloidal solution that was concentrated under reduced pressure to 19 mM Pt yielded no signal (2.9, top), even after several hours of acquisition.

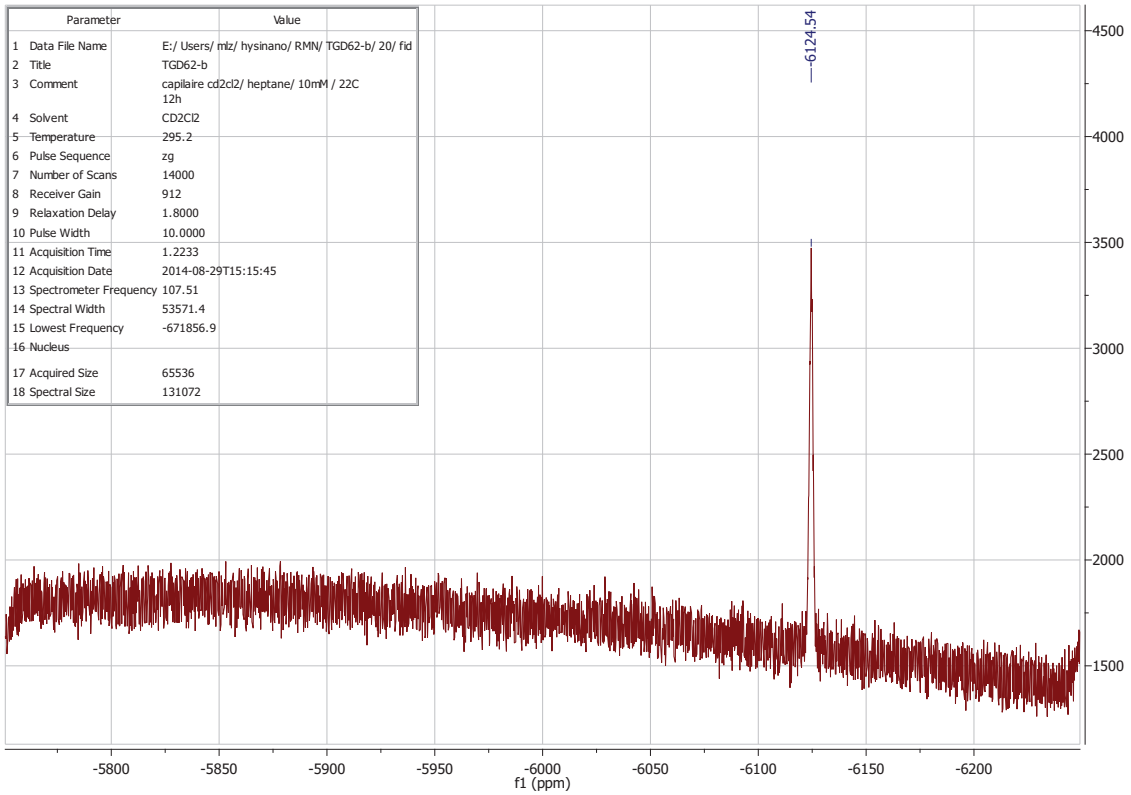


Figure 2.8: Karstedt's complex ^{195}Pt NMR spectrum (10 mM in toluene).

The two bands around $\delta = -3400$ ppm and $\delta = -4200$ ppm are artifacts due the spectrometer, as shown by a blank spectrum acquired without NMR tube (2.9, bottom). This is in agreement with a study of the synthesis of Pt NPs with SiH reducing agents by Lewis *et al.*,[162] who wrote: "Note that no ^{195}Pt NMR signals have been observed for any of the colloid preparations. A colloid is expected to have a multitude of states, so that failure to observe a single ^{195}Pt resonance or any M-^{195}Pt coupling is not surprising."

Overall, the low sensitivity of ^{195}Pt NMR makes the acquisition times prohibitively long and thus precludes an observation of dissolved catalytic intermediates (if they exist) and their evolution over the course of a catalysis experiment, even at relatively high concentrations (10 mM).

We envisage to perform Dynamic Nuclear Polarization (DNP) experiments to mitigate this low sensitivity problem. DNP is a technique that allows to record NMR spectra with much higher sensitivity than classical NMR experiments, thus reducing greatly the acquisition times (typically by several orders of magnitude). It is based on the polarization of electron spins of paramagnetic species (such as free radicals), which are much easier to polarize than nuclar spins, followed by a polarization transfer from electrons to nuclei. We have found one example of utilization of DNP with ^{195}Pt, for the study of coordination of Pt in metal-organic frameworks (MOFs) in the solid state.[163]

[162] L. N. Lewis and N. Lewis, *Chem. Mater.* **1989**, 1, 106–114.

[163] T. Kobayashi et al., *J. Phys. Chem. Lett.* **2016**, 7, 2322–2327.

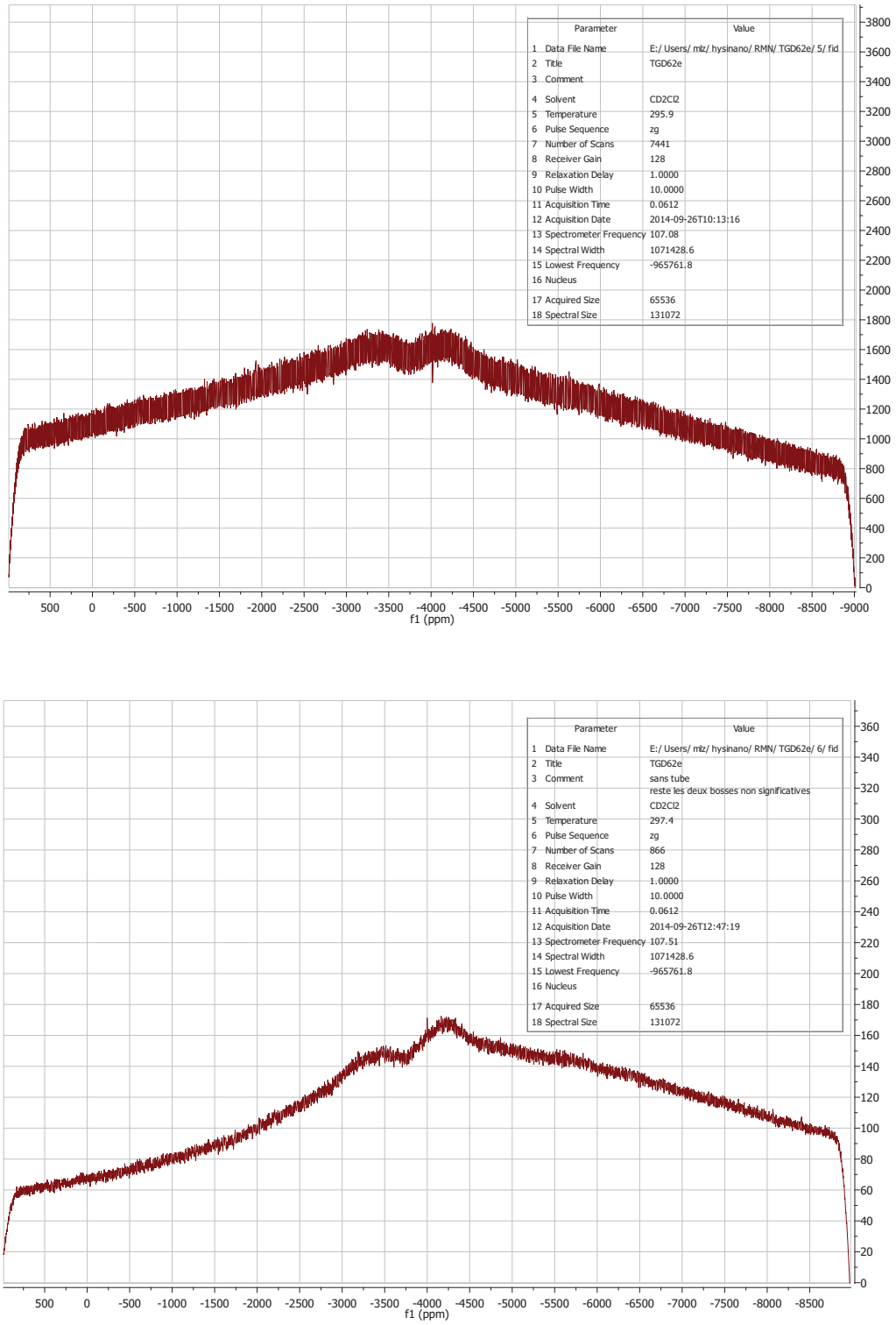


Figure 2.9: Top: Pt colloid ^{195}Pt NMR spectrum. Bottom: blank ^{195}Pt NMR spectrum (without NMR tube).

3

Heterogeneous Pt catalysts: two strategies to improve platinum recovery

The development of the Pt/SBA-15 catalyst was performed by Reine Sayah (C2P2) and its testing was carried out by Marie-Line Zanota (LGPC) and Valérie Meille (LGPC), resulting in a patent application.[137] Most of the experimental work concerning the Pt NPs on carbon nanotubes has been performed by Briony Munslow (Cardiff University) and Alice Relave (Université de Lyon) under my supervision during internships at the LGPC.

3.1 Introduction on heterogeneous Pt catalysts

As we have seen in chapter 2, homogeneous platinum catalysts are extremely active for alkene hydrosilylation, and are able to reach very high TONs. As a consequence of these advantageous characteristics, they are used in very low concentrations (typically 1 ppm to 10 ppm), which makes the catalyst recovery (for reusing or recycling) very difficult and expensive. Furthermore, the presence of platinum in the reaction products can give a yellow-brown color to the reaction products,[5,53] and be a problem for medical or pharmaceutical applications, where the tolerance for heavy metal contamination is low.[e]

Heterogeneous Pt catalysts have been studied as a means of facilitating Pt recovery in hydrosilylation processes, but suffer from leaching issues and poor catalytic performances compared to Pt complexes in solution.[6]

The first type of heterogeneous catalysts for alkene hydrosilylation encountered in the literature comprises supported Pt(0) complexes.[165–167] These complexes often reached maximum TONs of 10^4 (ie. one to two orders of magnitude lower than Karstedt's complex, see Chapter 2), even with several catalyst reuses. These poor catalytic performances were often attributed to the low stability of the catalysts, presumably because Pt atoms were weakly bound to the support.

A second type of solid catalysts that was investigated was based on supported Pt nanoparticles. These catalysts usually exhibited better catalytic performances than supported complexes. In fact, the first alkene hydrosilylation catalyst that has been published, in 1953, was a Pt/C catalyst.[29] It reached impressive TONs of 2×10^6 but required harsh reaction conditions (temperatures of 130 °C to 160 °C), leading to selectivity issues. To cite a few other examples, in 2011 Wawrzyńczak *et al.* showed that a Pt/PS-DVB (PS = polystyrene,

[e] For active pharmaceutical ingredients (APIs), the concentration limit for elemental impurities such as platinum depends on the route of administration and the daily dose of the API.[164]

[165] L. Wang and Y. Jiang, *J. Organomet. Chem.* **1983**, 251, 39–44.
[166] Q. J. Miao, Z. Fang and G. P. Cai, *Catal. Comm.* **2003**, 4, 637–639.
[167] Z. M. Michalska et al., *J. Mol. Catal. A: Chem.* **2004**, 208, 187–194.

DVB = divinylbenzene) was stable over several uses, but unfortunately this catalyst reached a cumulated TON of only about 2×10^4 after 5 catalytic runs, making this catalyst less advantageous than classical Pt complexes. In 2012 Bandari *et al.* reported the preparation of polymeric monolith-supported Pt nanoparticles.[168] Platinum leaching in the final product was high: around 4 ppm. Ciriminna *et al.* reached in 2013 similar levels of leaching using platinum nanoparticles entrapped in organo-silica xerogels, but reached TONs of only 200.[50] In 2014, Bai presented the use of several heterogeneous platinum catalysts in batch and continuous operations.[53] In batch, low Pt concentrations in the filtered liquid product were reported (less than 1 ppm). However, these concentrations accounted for 5 to 10% of the total Pt amount. Likewise, in continuous operation, 0.24 ppm Pt was analyzed in the product, causing a premature need to renew the catalyst bed.

[168] R. Bandari and M. R. Buchmeiser, *Catal. Sci. Tech.* **2012**, 2, 220–226.

In this chapter we present two strategies to tackle the problem of platinum separation from hydrosilylation products, one based on the physical entrapment of Pt NPs in a mesostructured silica matrix, SBA-15, and the other based on the deposition of Pt NPs on carbon nanotubes (CNTs) and active carbon (AC).

3.2 Pt nanoparticles in SBA-15 mesostructured silica matrices

3.2.1 Introduction

Mesostructured materials are characterized by the presence of an ordered network of mesopores (2 nm to 50 nm).[169] They are usually synthesized by a sol-gel process using a templating route. Depending on the experimental conditions, three distinct mechanisms are observed: liquid crystal templating (assembly happens before condensation) cooperative self-assembly (assembly during condensation) or hard sphere packing (assembly after condensation).[170] Mesostructured materials have found applications in many fields such as catalysis, adsorption, electrochemistry and biology.

[169] D. Zhao, Y. Wan and W. Zhou. *Ordered Mesoporous Materials*. John Wiley & Sons, 2012.

[170] J. Tang et al., *J. Am. Chem. Soc.* **2007**, 129, 9044–9048.

We report herein the use of a Pt-based heterogeneous catalyst containing Pt nanoparticles (NPs) embedded into the walls of a mesostructured silica framework (Pt@{walls}SBA-15) as a highly active and leaching-resistant alkene hydrosilylation catalyst.

3.2.2 Results

This solid catalyst was prepared by the controlled growth of a silica framework around chloropropylsilane-stabilized hydrophilic Pt NPs using Pluronic®123 surfactant as structure-directing agent, followed by calcination under a flow of dry air at 320 °C (Figure 3.1, see experimental part for detailed protocol).[171] This methodology reported by our group allowed the controlled localization of the Pt NPs in the silica pores[156] or walls[171] depending on the hydrophilic/hydrophobic character of these NPs.

[171] M. Boualleg et al., *J. Catal.* **2011**, 284, 184–193.

The obtained solid, containing a Pt loading of 0.3% w/w, was characterized by N_2 adsorption at 77 K (Figure 3.2), which showed that the material was mesostructured (type IV isotherm) with mesopores of about 6 nm diameter

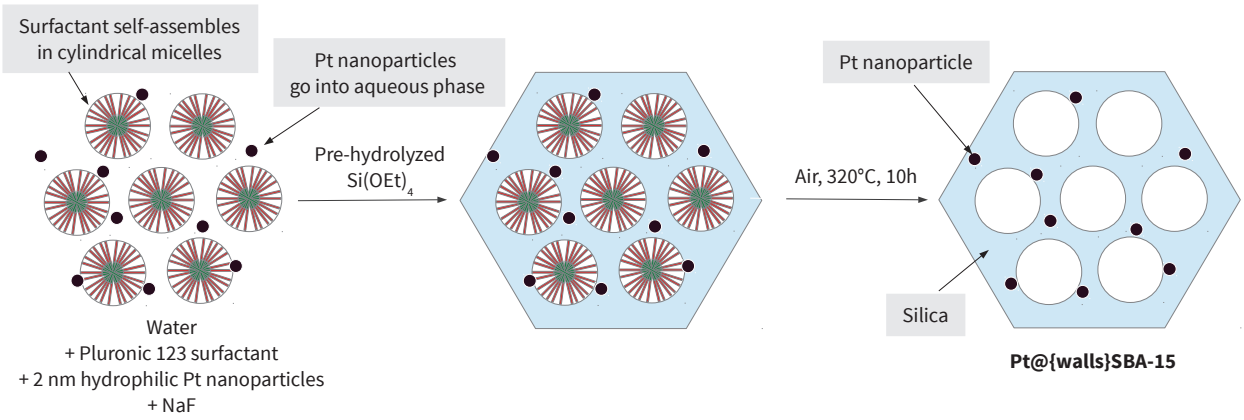


Figure 3.1: Synthesis of Pt@{walls}SBA-15. Adapted from reference [171].

and a specific surface area of about 1000 $m^2\ g^{-1}$. H_2 chemisorption showed a Pt dispersion of about 40 %, corresponding to a Pt NPs average diameter of 2.8 nm, indicating that no significant Pt NPs sintering had occured during the material synthesis and calcination. TEM and STEM-HAADF characterization of the material confirmed these features (Fig. 3.3 and 3.4), and showed that Pt NPs were located in the silica walls of the material.

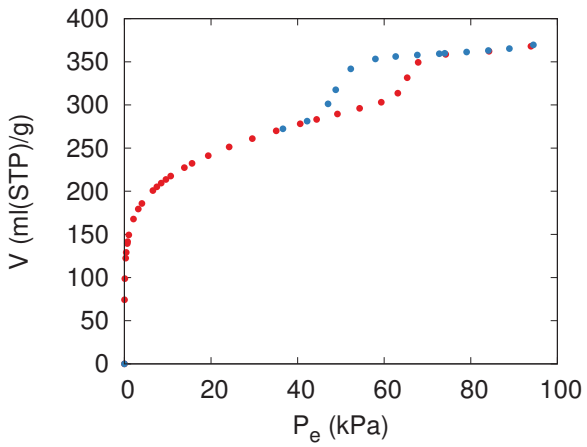


Figure 3.2: Nitrogen adsorption isotherm of the Pt@{walls}SBA-15 solid at 77 K.

First, semi-batch catalytic tests were performed to explore the activity and stability of this catalyst. The hydrosilylation of 1-octene with a polymethylhydrosiloxane (PMHS) containing 50 Si – H units was used as a model reaction (Fig. 3.5). A glass reactor equipped with a mechanical stirrer was loaded with 1-octene and the catalyst powder. The suspension was preheated at 75 °C and the PMHS (0.7 equivalent of SiH vs. 1-octene) was added drop-by-drop over 52 minutes with a syringe pump. The SiH conversion was monitored by ^1H NMR.

Additionally, for assessing for Pt leaching, we performed split tests (ie. hot filtration tests) at the end of the PMHS addition: an aliquot of the reaction mixture was taken, hot-filtered with a 0.45 µm syringe filter to remove the solid catalyst, and placed at 75 °C to continue the reaction. From such an experiment, as shown in Figure 3.6, it can be determined a TON at the end of SiH addition, which has both homogeneous and heterogeneous components,

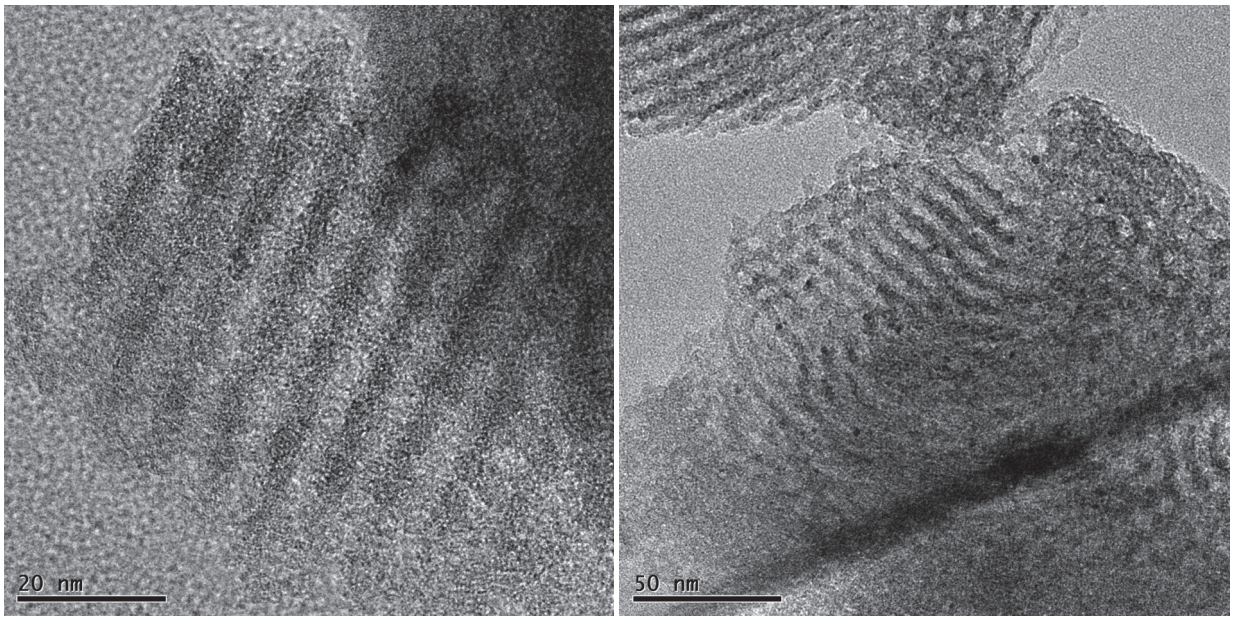


Figure 3.3: TEM micrograph of Pt@{walls}SBA-15.

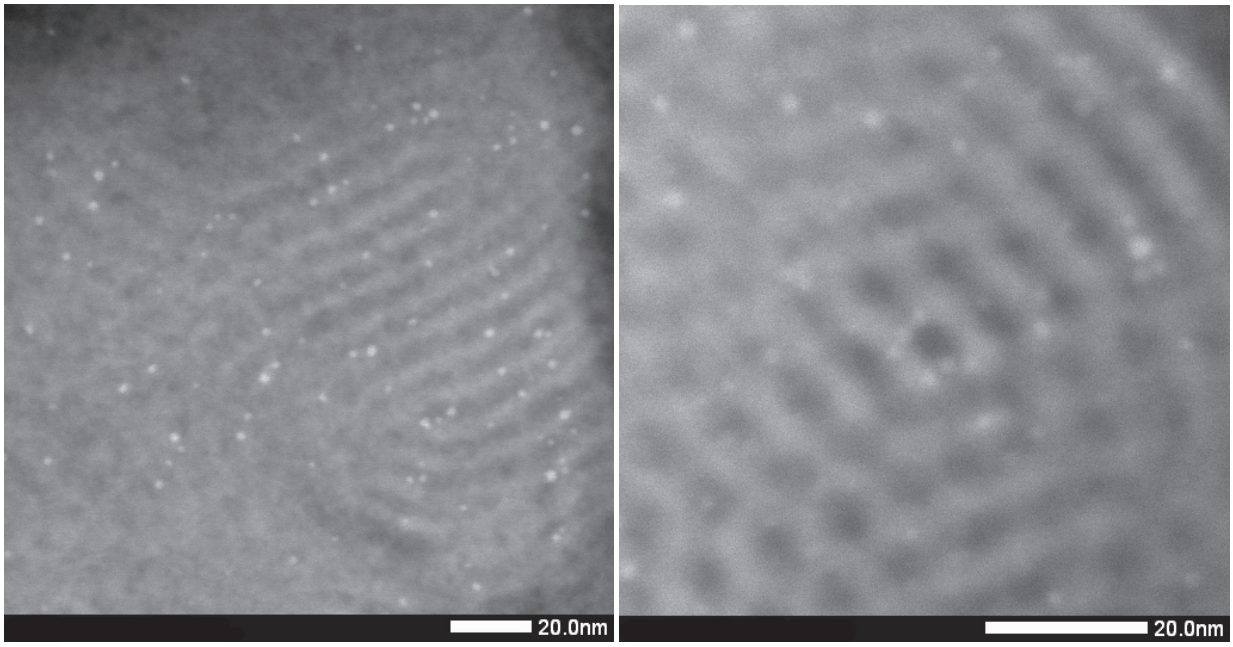


Figure 3.4: STEM-HAADF micrograph of Pt@{walls}SBA-15.

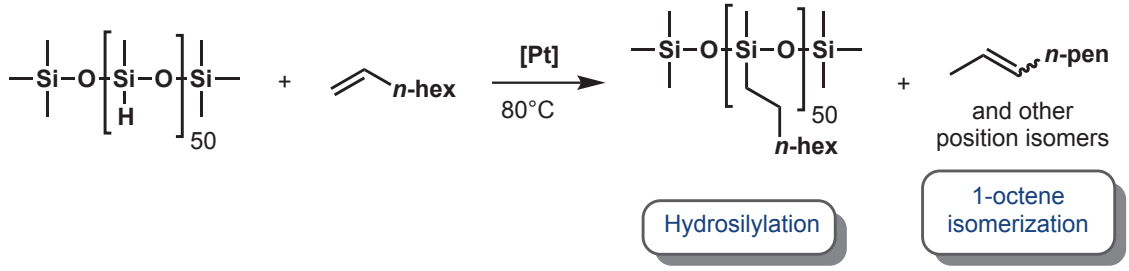


Figure 3.5: The model reaction used for this study: hydrosilylation of 1-octene with a PMHS.

a homogeneous TON, which corresponds to the TON progression in the filtered sample, and a heterogeneous TON, which is the difference between the progression of the TON in the reactor after the end of SiH addition and the homogeneous TON. Note that it is important to perform the split test at a conversion which is neither too low (because there is a risk that the Pt hasn't leached yet) nor too high (because there is a risk of redeposition of the leached Pt on the catalyst), as observed for other reactions such as the Heck reaction with Pd catalysts.[172,173]

[172] L. Djakovitch, H. Heise and K. Köhler, *J. Organomet. Chem.* **1999**, 584, 16–26.

[173] R. G. Heidenreich et al., *J. Mol. Catal. A: Chem.* **2002**, 182–183, 499–509.

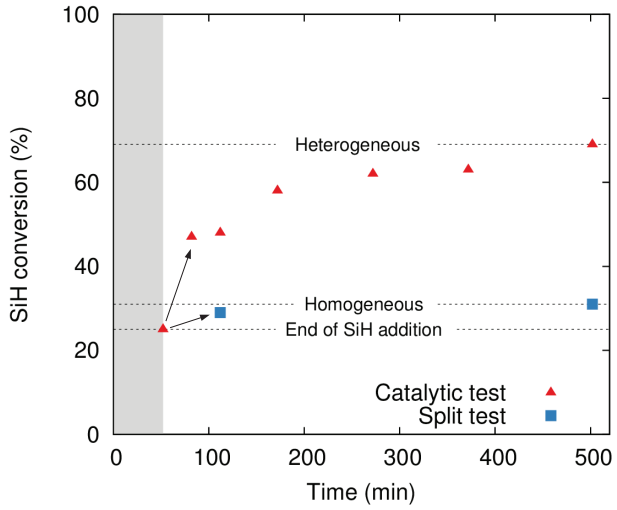


Figure 3.6: Split test (hot filtration) during a semi-batch test of Pt@{walls}SBA-15. The period in grey, from 0 to 52 minutes, is the addition of PMHS in the reactor.

The results of the catalytic tests are presented in Fig. 3.7. The first catalyst, Pt@{walls}SBA-15, showed very little leaching, as seen from the heterogeneous TON after SiH addition: 57 100, much higher than the homogeneous TON after SiH addition of 4900. The final TON of 10^5 is very close to TONs reached routinely with Karstedt's complex (see chapter 2). An elemental analysis by ICP-AES of an aliquot of the split test was performed by Solvay in St Fons (*via* Bluestar Silicones), who are specialists of Pt traces analysis in silicone matrices. It revealed a Pt content lower than the quantification limit of 1 ppm. Pt concentration measurements will be performed by another company, in order to try to reach lower quantification limits.

The second catalyst, Pt@{pores}SBA-15, where the Pt NPs are located inside the mesopores of the material, was slightly more active than Pt@{walls}SBA-15, but showed a heterogeneous TON after SiH addition of 28 400, lower than the homogeneous TON after SiH addition of 55 400, indicating a much higher Pt leaching.

The third catalyst, prepared by incipient wetness impregnation of low surface area silica with a suspension of Pt nanoparticles followed by calcination under air at 320 °C, was highly active but displayed a high Pt leaching, as shown by the high heterogeneous TON after SiH addition of 45 700 compared to the heterogeneous TON after SiH addition of 7100.

To summarize, Pt@{walls}SBA-15 successfully combined high activity with very low Pt leaching. This very low leaching is attributed to the physical entrapment of the NPs inside the silica walls, while still being accessible to the reactants through the micropores of the silica. Interestingly, for all these heterogeneous Pt catalysts, the proportion of 1-octene isomerization in these

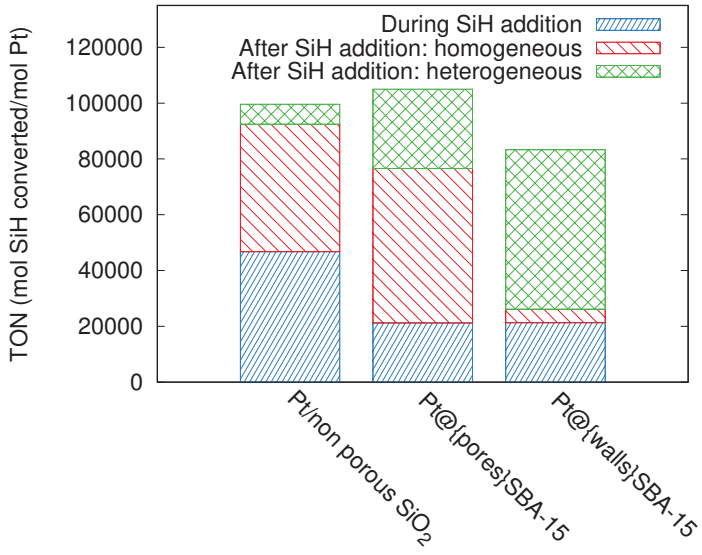


Figure 3.7: TON and Pt leaching comparaison for various heterogeneous Pt catalysts, after 5 h.

reaction conditions was around 10-12%, as observed with Karstedt's catalyst (see Chapter 2), showing no particular behaviour of heterogeneous Pt catalysts in that regard.

We then explored an industrially interesting feature of non-leaching catalysts: the possibility to partially functionalize multi-functional substrates such as PMHS fluids. When using a homogeneous catalyst or a leaching heterogeneous Pt catalyst, such a partial functionalization is not practically feasible, because the reaction product contains Pt, which then catalyzes the reticulation of the remaining SiH functionalities when exposed to moisture, leading to gelification of the fluid. We conducted the hydrosilylation of a PMHS containing 50 Si-H units and 1-octene as limiting reagent (0.1 eq. 1-octene relative to SiH) with Pt@{walls}SBA-15 as catalyst.[137] After the conversion stopped evolving, the reaction medium was filtered to remove the catalyst and devolatilized under partial vaccuum (15 mbar) at 80 °C. The partially functionalized product was stored under air at room temperature, and was stable towards gelification. In comparison, the same product prepared with Karstedt's complex gelified at the surface in less than 15 minutes, and a treatment with carbon black didn't increase its stability towards gelification in the presence of moisture.

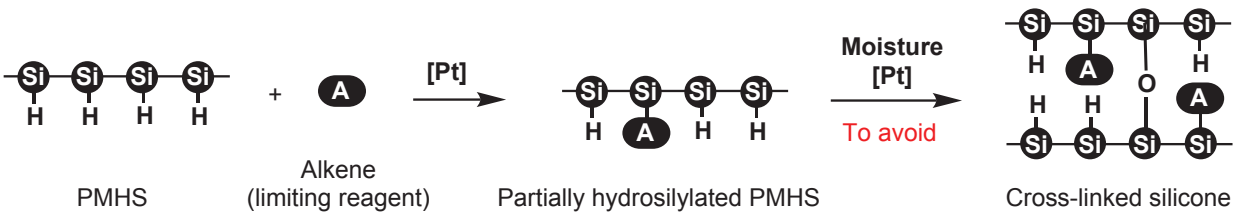


Figure 3.8: During the partial functionalization of a PMHS, traces of platinum in the product lead to product gelification when exposed to moisture.

In conclusion, we have demonstrated here that a tailored solid catalyst composed of Pt nanoparticles in the walls of a mesostructured silica, called Pt@{walls}SBA-15, was able to reach high TONs of 10^5 in alkene hydrosilylation

without Pt leaching. The absence of leaching was attributed to the physical entrapment of the Pt NPs in the silica matrix, while still being accessible for the reactants *via* the microporosity. This catalyst is thus advantageous for applications where the absence of Pt in the product is necessary, for example in the pharmaceutical industry or for the production of silicone medical devices. We have also shown that it was possible to use this catalyst to partially functionalize PMHS substrates with no risk of gelification of the product, which is not possible with a leaching heterogeneous Pt catalyst or a Pt complex. Finally, the combination of the high activity and the absence of Pt leaching makes this catalyst a good candidate for reuse in batch reactors, by decantation or filtration, or for utilization in a continuous reactor, with the aim of outperforming the TONs of homogeneous Pt catalysts (typically 10^5) and decreasing the Pt consumption of alkene hydrosilylation processes. We are currently working towards this objective. The fact that Pt doesn't leach in the reaction products also allows the easy recovery of Pt from spent catalysts for recycling.

3.3 Pt nanoparticles on carbon nanotubes

3.3.1 Introduction

Carbon nanotubes

Carbon nanotubes (CNTs) are constituted of one or several graphitic sheets (ie. made of sp^2 carbon atoms) that are rolled in a cylindrical shape. Multi-wall CNTs were discovered by Iijima in 1991,[174] and single-wall CNTs were reported two years later.[175,176] There is a great variety of CNTs, varying by the number of concentric graphitic sheets, diameter, length, arrangement of the hexagonal carbon rings and chemical composition (including doping, presence of defects and surface functionalization).

[174] S. Iijima, *Nature* **1991**, 354, 56–58.

[175] S. Iijima and T. Ichihashi, *Nature* **1993**, 363, 603–605.
[176] D. S. Bethune et al., *Nature* **1993**, 363, 605–607.

Owing to their extraordinary high mechanical strength, thermal conductivity and electrical conductivity (Table 3.1),[177] they have found applications as fillers in composite materials (associated with polymers), and several other applications have been envisioned, such as catalyst support or electronic component.[178,179]

[177] S. Bordere et al., *Industrial Production and Applications of Carbon Nanotubes - Technical document by Arkema* **2007**.

[178] J. M. Schnorr and T. M. Swager, *Chem. Mater.* **2011**, 23, 646–657.
[179] Q. Zhang et al., *Small* **2013**, 9, 1237–1265.

	MWCNTs	Steel
Young's modulus (GPa)	1000	1200
Tensile strength (GPa)	150	0.4
Density	2.6	7.9
Thermal conductivity ($W\,m^{-1}\,K^{-1}$)	3000	15 to 55
Electrical conductivity ($S\,m^{-1}$)	10^5 to 10^7	10^6 to 10^7

Table 3.1: Some physical properties of CNTs and steel. Adapted from reference [177].

They are produced industrially at a multi-ton scale by companies such as Arkema, Zeon Corp., Nanocyl and many others. For example, in the Arkema process,[177] implemented at a 10 t/year scale, they are produced by decomposition of ethylene on a Fe/Al_2O_3 catalyst in a fluidized bed at 650 °C.

Carbon nanotubes as catalyst support

Carbons have been largely used as catalyst supports,[180] mainly as active carbon

[180] F. Rodríguez-reinoso, *Carbon* **1998**, 36, 159–175.

(AC). Interestingly, they are quite chemically inert (in particular in acidic or basic media), the active phase (often metallic nanoparticles) can be easily recovered by burning the carbon support and it is possible to control their porosity and surface functionalization to a certain extent. However, they cannot be used at high temperatures under hydrogen or oxidizing atmospheres.

In the family of carbon catalyst supports, CNTs often display original and advantageous properties.[181] For example, they allow a better structure control (including quantity of defects and impurities) than active carbons produced from natural sources. Their high mechanical resistance is ideal for the fabrication of catalysts beads or pellets for utilization in industrial reactors. Their high thermal conductivity allows for better heat transfer and can thus increase selectivity by impeding the formation of hotspots with exothermic reactions. The absence of microporosity can also eliminate internal mass transfer limitations that are often observed with microporous materials such as active carbons. As an example, in 2006 Serp *et al.* showed that PtRu/CNTs catalysts were more active and selective than their active carbon analogs for the hydrogenation of cinnamaldehyde to cinnamyl alcohol.[182] They attributed the higher activity of CNT-based catalysts to lower mass transfer limitations. A rather recent research line is the confinement of metal nanoparticles inside the CNTs, which allows to obtain catalysts with different reactivities than when the metal NPs are located on the outer surfaces of the CNTs, as explained in a review by Serp and Castillejos in 2010.[183] This modification of the catalyst reactivity can arise from confinement-induced variations of the physical properties of the medium (eg. viscosity or density) or by geometric effects due to the curvature of the CNT. Interestingly, higher catalytic activities have generally been reported when confining active phases inside CNTs,[f] despite the mass transfer limitations that could be expected. Finally, CNTs can be inherently catalytically active, especially when they are doped with atoms such as nitrogen or boron.[184]

Despite the apparent advantages and original properties of CNTs, their price have been for long prohibitively high for any industrial application as catalyst supports. However, in their review from 2013, Su *et al.* highlighted that "with the actual possibility of mass-production for example of CNTs at costs well-comparable with that of the oxide supports in catalysis applications (alumina, silica) or even of [active carbon], the industrial interest in developing catalysts based on nanocarbons is rapidly raising".[185] It should be noted that the price of multi-wall CNTs is much lower than single-wall CNTs, motivating our choice to work with multi-wall CNTs.

Pt/CNTs synthesis and use in alkene hydrosilylation

Syntheses of Pt/CNTs solids have already been reported, and are often based on impregnation of a Pt salt such as $Pt(NO_2)_2(NH_3)_2$ or H_2PtCl_6 followed by a H_2 treatment at high temperature (>200 °C) to yield Pt NPs.[186,187]

In the state of the art of alkene hydrosilylation, there are two examples of utilization of Pt/CNTs solids. The first article was published by Dai *et al.* in 2005,[188] but unfortunately we couldn't access it. From the abstract, it can be read that the solid was prepared by impregnation of chitosan-functionalized CNTs with an unreported Pt source. The solid was then applied in the hydrosilylation of allyl glycidyl ether with triethoxysilane at 130 °C with a yield of 70%, and after 4 reuses of the catalyst, the yield dropped to 24%.

[181] P. Serp, M. Corrias and P. Kalck, *Appl. Catal. A: General* **2003**, 253, 337–358.

[182] H. Vu et al., *J. Catal.* **2006**, 240, 18–22.

[183] P. Serp and E. Castillejos, *ChemCatChem* **2010**, 2, 41–47.

[f] This might be simply explained by a selection bias, because when confinement of the active phase decreases the activity of a catalyst, there is little interest to publish it.

[184] K. Gong et al., *Science* **2009**, 323, 760–764.

[185] D. S. Su, S. Perathoner and G. Centi, *Chem. Rev.* **2013**, 113, 5782–5816.

[186] A. Muneendra Prasad, C. Santhosh and A. Nirmala Grace, *Appl. Nanosci.* **2012**, 2, 457–466.

[187] S. Takenaka et al., *J. Phys. Chem. C* **2014**, 118, 774–783.

[188] Y.-F. Dai, F.-Y. Li and B. Xiao, *Organic Chemistry: An Indian Journal* **2005**, 1,

Jian-Bo *et al.*[189] published another article in 2010, but the text is in mandarin. From the abstract in english, it can be read that the solid was prepared by impregnation of polyethylene glycol-functionalized CNTs with H_2PtCl_6. The authors claimed to achieve a "remarkably improved β-addition selectivity and excellent recyclability relative to Speier's catalyst" for the reaction of styrene with methyldichlorosilane.

These two articles are lacking a comparison with active carbon to determine whether the use of CNTs is advantageous. Indeed, Serp *et al.* stated that "unfortunately, a lack of systematic comparison with activated carbon based catalytic systems has to be noted and should be considered in the future studies as it is a necessary step towards an extensive use of these new materials."[181]

[189] Z. Jian-bo et al., *China Surfactant Detergent & Cosmetics* **2010**, 40, 427–431.

Objectives and methodology

In the present study, we synthesized Pt/CNTs and Pt/AC solids and compared their catalytic performances, including activity, total TON over several uses and selectivity. We also studied their Pt leaching behaviour, which is a key point for heterogeneous Pt catalysts. We specifically studied the effects of the thermal treatment under H_2 at 320 °C or 450 °C on Pt leaching and reusability.

The catalysts were mainly tested on a 10 mmol scale in batch reactors, at 80 °C, in the reaction between MD'M and 1-octene (1 eq), as shown on Figure 3.9, a model reaction for the industrially relevant functionalization of polymethylhydrosiloxanes. The reaction was performed with dodecane as internal standard, and monitored by gas chromatography.

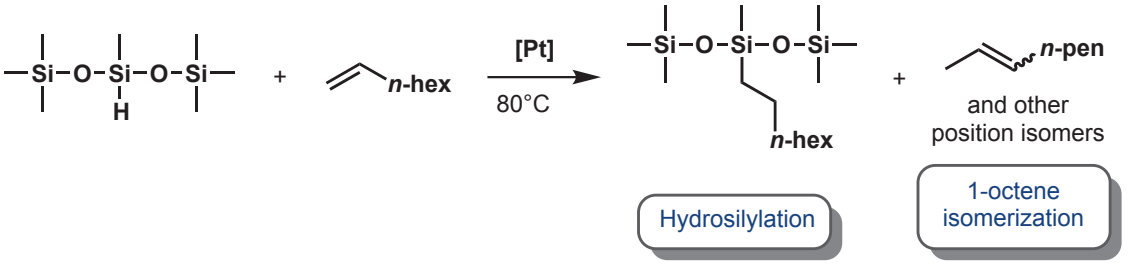


Figure 3.9: Model reaction used in this study: hydrosilylation of 1-octene by MD'M.

Some catalytic tests were also performed on a 300 mmol scale on the hydrosilylation of 1-octene (1.4 eq relative to the SiH quantity) by MD'$_{50}$M (Figure 3.10).

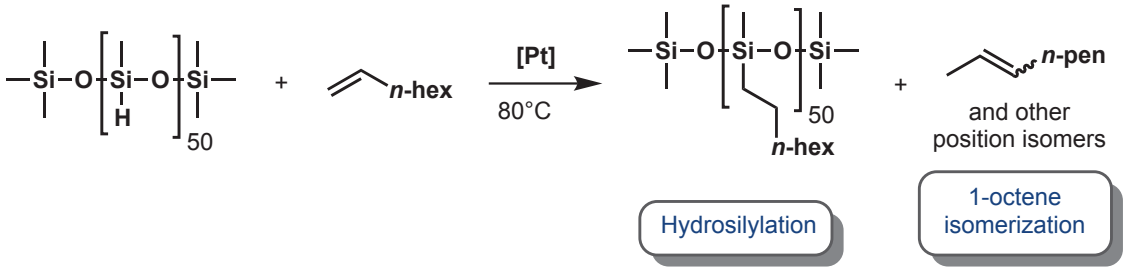


Figure 3.10: Model reaction used in this study: hydrosilylation of 1-octene by MD'$_{50}$M.

3.3.2 Results

CNTs pretreatments

We used multi-wall CNTs of the brand Graphistrength® C100, manufactured by Arkema. Their specifications were the following: nanotube diameter from 10 nm to 15 nm, length from 0.1 µm to 10 µm, aggregates from 50 µm to 150 µm. A SEM micrograph is shown in Figure 3.11.[190]

[190] F. Simescu-Lazar et al., *Appl. Catal. A: General* **2015**, 508, 45–51.

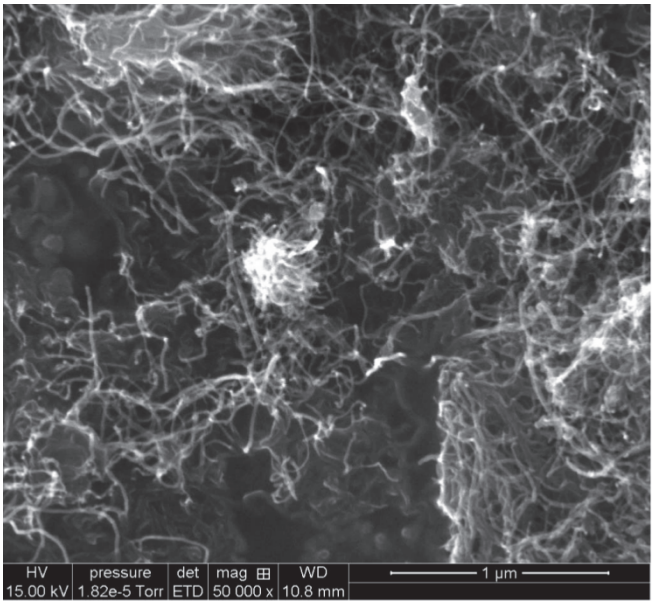


Figure 3.11: SEM of CNTs used in this project.[190]

We started by purifying CNTs, by a sulfuric acid treatment at 140 °C (Figure 3.12). This acid treatment dissolves the Fe/Al_2O_3 catalyst used to synthesize nanotubes, even if some catalyst particles that are not easily accessible inside the nanotubes can be left intact by this treatment, as reported by our group.[190]

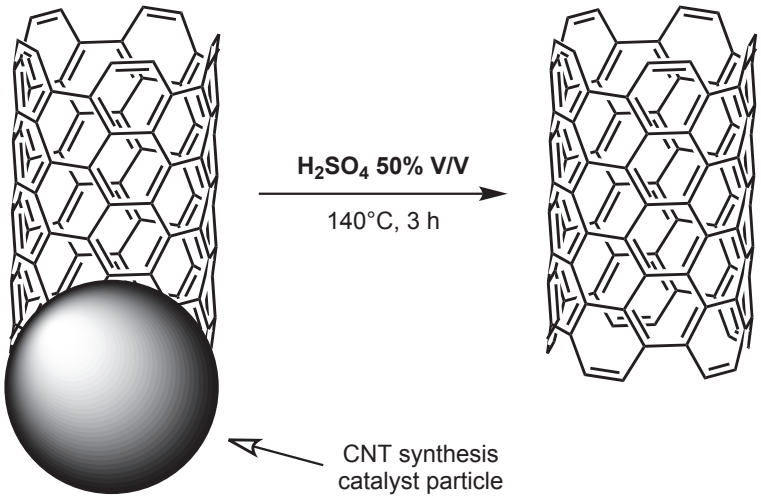


Figure 3.12: Carbon nanotubes purification to remove the iron-based catalyst used for their synthesis.

The surface chemistry of CNTs is well-developed,[191] and methods are available to introduce a lot of different surface functionalities. We have used a simple and well-known procedure to introduce coordinating oxygenated functionalities at the surface of the CNTs, by heating a suspension of purified CNTs in nitric acid under reflux (Figure 3.13). In a recent review on carbon

[191] D. Tasis et al., *Chem. Rev.* **2006**, 106, 1105–1136.

coordination chemistry, Serp *et al.* stated that "oxidation with strong oxidants such as nitric acid leads to carbons with a predominant population of surface carboxylic groups".[192] This introduction of oxygenated coordinating groups was reported to improve the metallic dispersion of impregnated CNTs catalysts.[190,193]

[192] M. R. Axet et al., *Coord. Chem. Rev.* **2016**, 308, Part 2, 236–345.

[193] A. Solhy et al., *Carbon* **2008**, 46, 1194–1207.

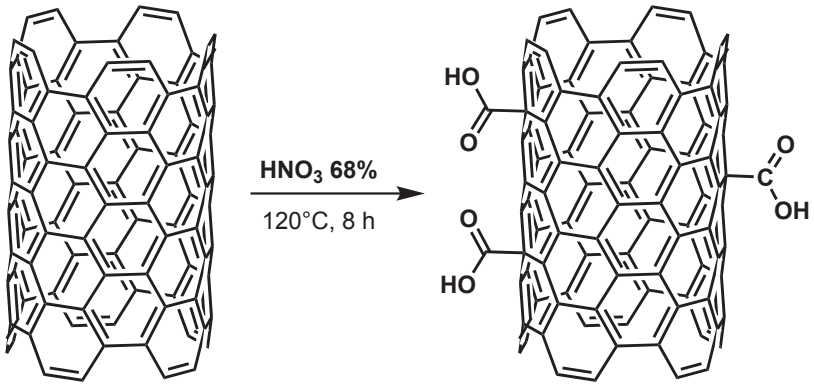


Figure 3.13: Carbon nanotubes functionalization, with mainly carboxylic acid functionalities.

Impregnation and N_2 treatment

Active carbon and CNTs were impregnated with an ethanolic solution of $H_2PtCl_6 \cdot 6\,H_2O$ by using the incipient wetness impregnation (IWI) method. The porous volume of both solids was determined by adding ethanol to a known mass of solid under stirring until the powder became sticky, indicating that the porous volume of the solid was filled with ethanol. Porous volumes of 1.2 mL g^{-1} for active carbon and 3.5 mL g^{-1} for CNTs were found. The impregnated solids contained 0.3% Pt w/w.

The impregnated solids were then treated under N_2 flow at 120 °C during 4 h for drying them, then at 450 °C during 4 h. Elemental analysis of the reduced solids gave Pt contents of 0.30% for Pt/CNTs and 0.31% for Pt/AC.

Non-reduced solids

A catalytic test with the non-reduced Pt/CNTs catalyst was performed (Figure 3.15). Interestingly, the Pt/CNTs was much better dispersed in the reaction medium than Pt/SBA-15 catalysts, probably because of the hydrophobic nature of carbon supports (this was also the case for Pt/AC solids). A high activity was recorded, with a half-conversion time of about one hour. After 15 min of reaction, a split test (hot-filtration test, see Figure 3.14) was performed. The conversion in the filtered reaction mixture was almost as high as in the original mixture, indicating that Pt had significantly leached.

For the non-reduced Pt/AC solid (Figure 3.16, left), a split-test also showed a very high Pt leaching. Attempts to reuse the catalyst by decanting the reaction mixture, eliminating the supernatant and adding a new reaction mixture showed a drastic decrease in activity (Figure 3.16, right), with a quasi-null activity in the third run.

Solids reduced at 450 °C

We decided to reduce both solids under H_2, in an attempt to decrease leaching and improve the reusability of our catalysts. We performed the reduction at

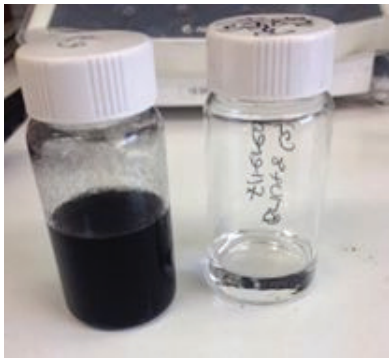


Figure 3.14: Left: a batch catalytic test mixture. Right: a hot-filterered sample of a catalytic test.

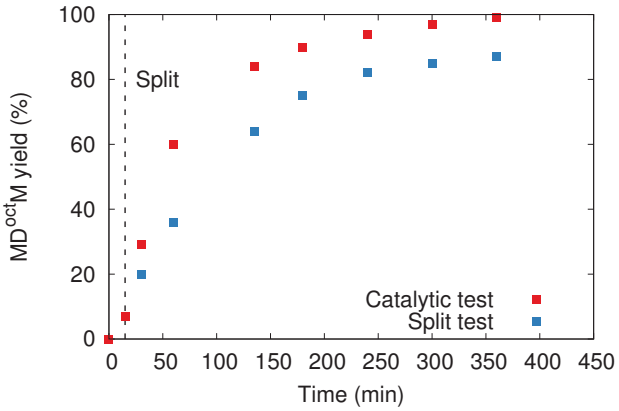


Figure 3.15: Catalytic test of Pt/CNTs non-reduced solid. SiH/Pt = 10^5.

450 °C during 4 h under H_2 flow in a tubular oven. These solids are called Pt/CNTs(450) and Pt/AC(450).

Samples for TEM analysis were prepared by suspending some milligrams of solid in ethanol, followed by ultrasonication during 5 min. A drop of this suspension was then deposited on a microscopy grid and left to dry. This step of ultrasonication in ethanol is crucial to partially unfold the nanotubes and allow to have zones on the microscopy grid where nanotubes are not superposed.

TEM analysis of Pt/CNTs or Pt/AC solids yielded a low contrast between the carbon support and Pt nanoparticles (see Figure 3.17 for an example with Pt/CNTs), making the measurement of particle sizes difficult and imprecise.

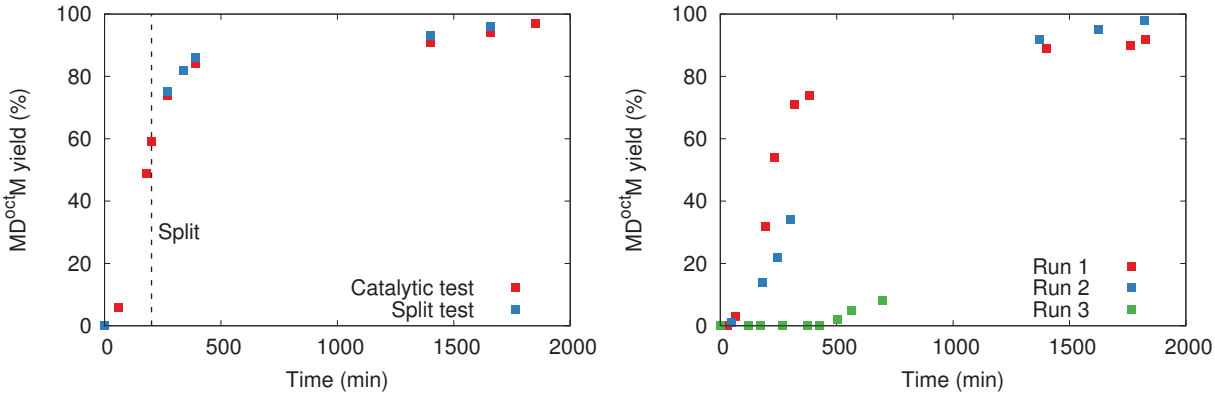


Figure 3.16: Catalytic test of Pt/AC non-reduced solid, with split test. SiH/Pt = 10^5.

However, it allowed to confirm the CNTs diameter specification of 10 nm to 20 nm, and allowed to see very well the multiple walls of the CNTs. Some Fe/Al_2O_3 particles that were not dissolved during the CNTs purification could also be observed. On the other hand, STEM allowed to acquire images with much better contrast between CNTs and Pt NPs, and was used for the determination of particle size histograms.

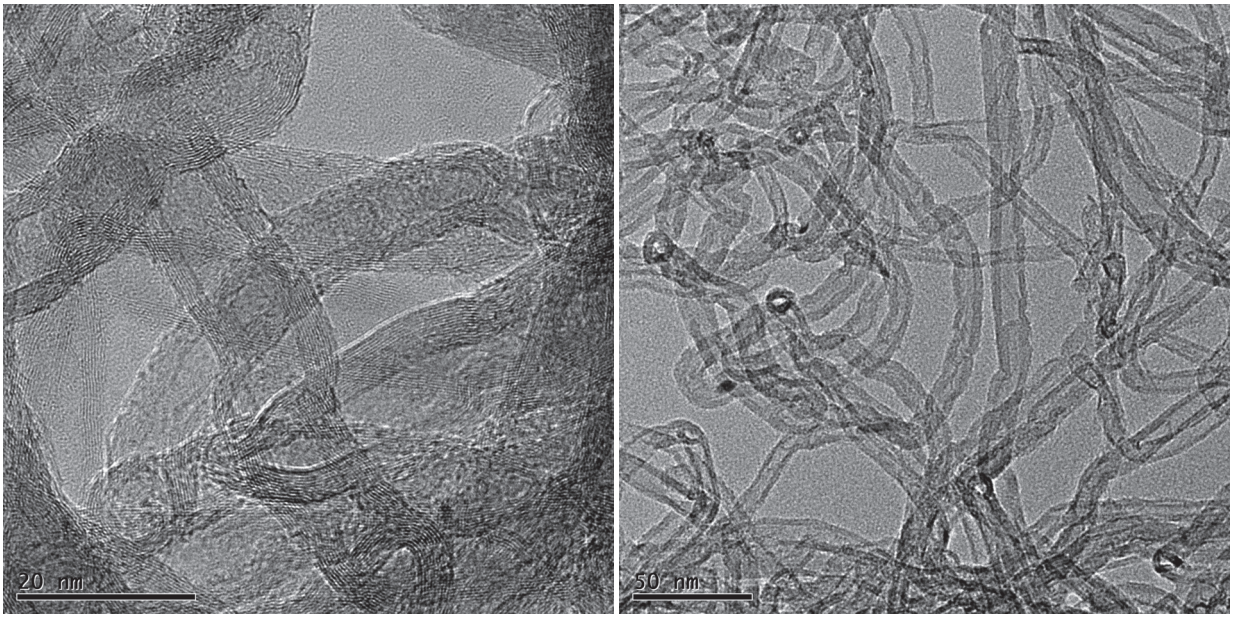


Figure 3.17: TEM of a Pt/CNTs catalyst, reduced at 450 °C.

STEM analysis of the Pt/AC(450) solid (Figure 3.18) showed the presence of many small (1 nm to 4 nm) particles and some much bigger particles (10 nm to 20 nm). We supposed that these very large particles were Pt particles which were formed by sintering of small Pt particles during the H_2 treatment at 450 °C. Indeed, EDX analysis of one of these large particles showed signals at 2.05 keV, 9.44 keV and 11.25 keV that are characteristic of Pt (Figure 3.19).

In this kind of samples, where the size distribution is not uniform (a high number of small particles plus some much larger particles), the average NP size does not reflect the average metal dispersion of the sample.

A particle size histogram of the Pt/CNTs(450) solid (Figure 3.20) showed that Pt NPs had an average size of 2.4 nm, corresponding to a metallic dispersion of 47%.

From the STEM images of this Pt/CNTs(450) solid, and for any other Pt/CNTs solids studied in this project, it was not possible to determine if the Pt NPs were located specifically inside or outside the CNTs or both, because the STEM images are 2-dimensional projections of a 3-dimensional solid. To perform such a determination, it would be necessary to use TEM tomography[g] (also called 3D TEM).[183]

[g] This technique is based on the acquisition of several images of a CNT at different tilt angles, followed by the reconstruction of the CNT volume from these images with a computer program.

Solid	Average NP size (TEM)	Pt dispersion (TEM)
Pt/AC(320)	2.8 nm	41%
Pt/AC(450)	2.9 nm	39%
Pt/CNTs(320)	1.9 nm	60%
Pt/CNTs(450)	2.4 nm	47%

Table 3.2: Characteristics of the catalysts of this study.

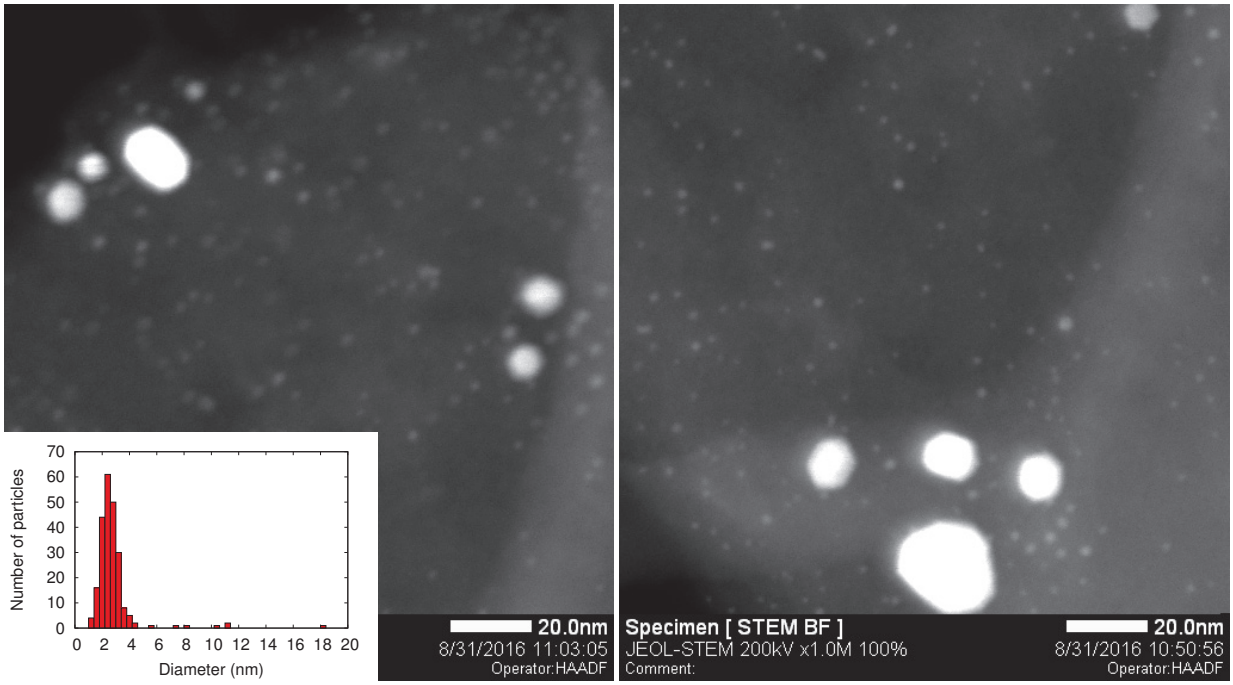


Figure 3.18: STEM of Pt/AC catalyst reduced at 450 °C.

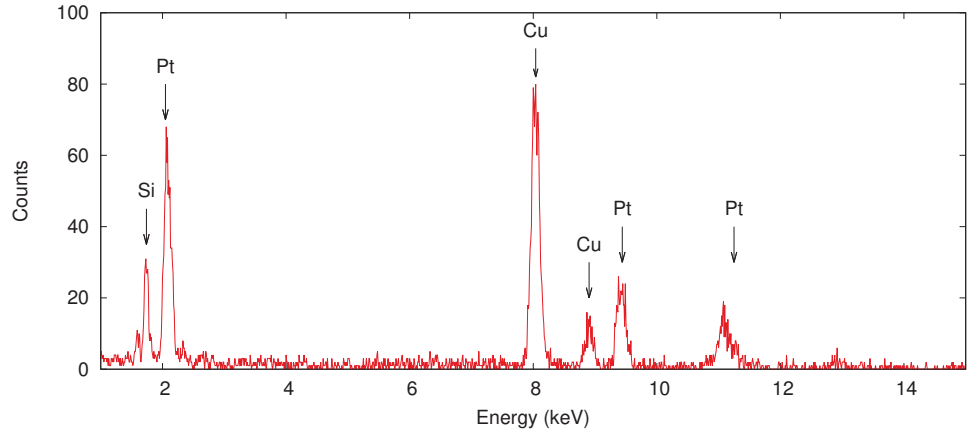


Figure 3.19: EDX of a large particle seen by STEM on a Pt/AC(450) sample.

From these analyses, it seems that CNTs stabilize much better Pt NPs towards sintering under H_2 at 450 °C. This is in agreement with a recent publication of our group, in which it has been shown that Pd/CNTs solids were much more stable towards palladium sintering at high temperatures than their active carbon analogues.[190]

A catalytic test using Pt/CNTs(450) with a SiH/Pt ratio of 10^5 (Figure 3.21) showed that the catalyst was much less active than the non-reduced Pt/CNTs solid. Indeed, the half-reaction time was about 290 min for the reduced solid and about 60 min for the non-reduced solid. A split test performed at 35% yield showed that activity in the filtered sample was as high as in the original reacting mixture, indicating that leaching was high.

Despite this very high leaching, we tried to reuse the catalyst (Figure 3.22). Very surprisingly, at a SiH/Pt ratio of 10^4, it was used for 7 consecutive runs with no significant difference of activity, except for a slightly lower activity

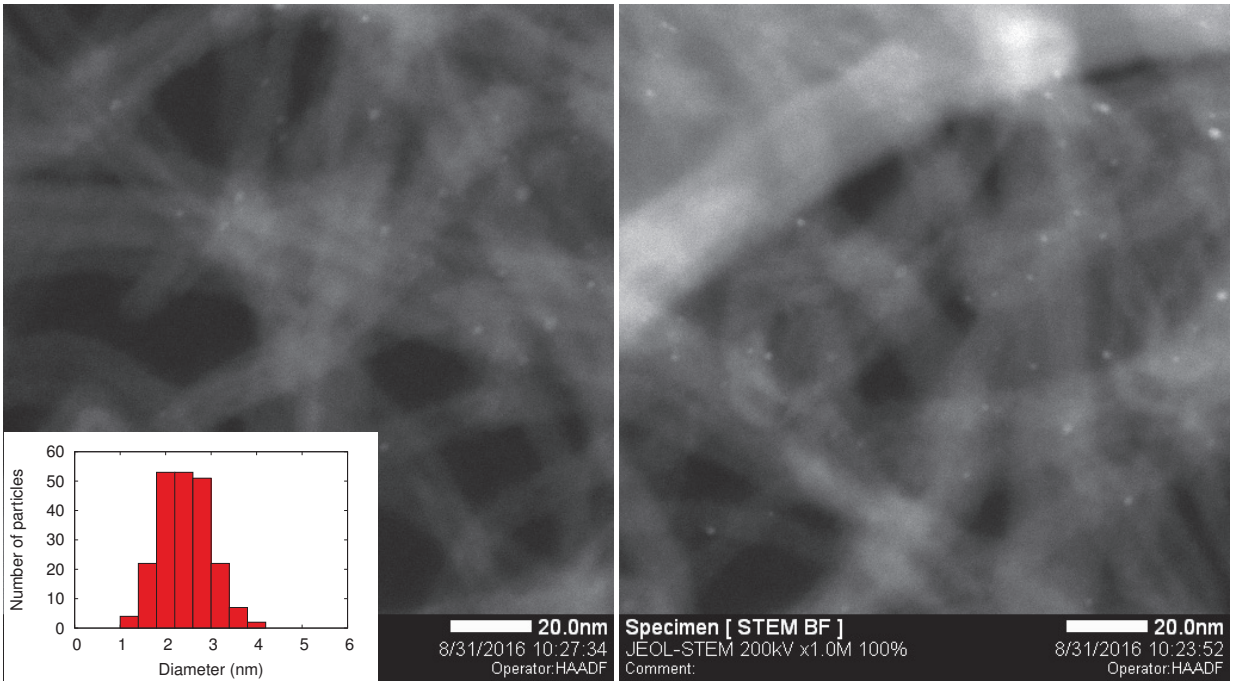


Figure 3.20: STEM of Pt/CNTs catalyst reduced at 450 °C.

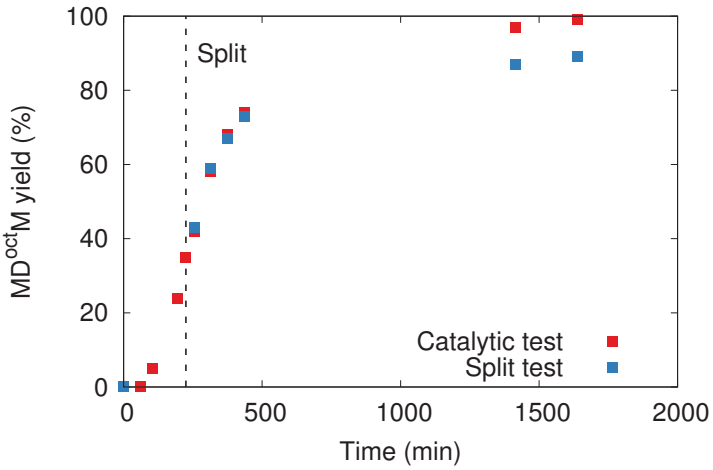


Figure 3.21: Catalytic test of Pt/CNTs(450), with a split test. SiH/Pt = 10^5.

during the first run, suggesting an activation of the catalyst by the reagents. To probe the limits of the solid, we reduced the amount of Pt by a factor of ten, and performed reuse tests with a SiH/Pt ratio of 10^5. During the first three runs, the catalytic activity is very similar. The fourth and fifth runs show that the catalyst is still active, even if too few GC analyses were performed to be able to compare activity with the other runs. A remarkable cumulated TON of 3.9×10^5 was reached over these five runs.

Surprisingly, despite the factor 10 between the SiH/Pt ratios in both series of tests, the reaction kinetics is not 10 times higher for the tests with SiH/Pt = 10^4. Indeed, for tests with SiH/Pt = 10^4 the half-reaction time was around 110 min whereas for for tests with SiH/Pt = 10^5 the half-reaction time was about 200 min. This apparent order in total Pt lower than 1 might be explained by a saturation by leached (and active) Pt species.

To explain the apparent contradiction between a high Pt leaching, which should decrease the Pt content of the solid (and thus the catalytic activity)

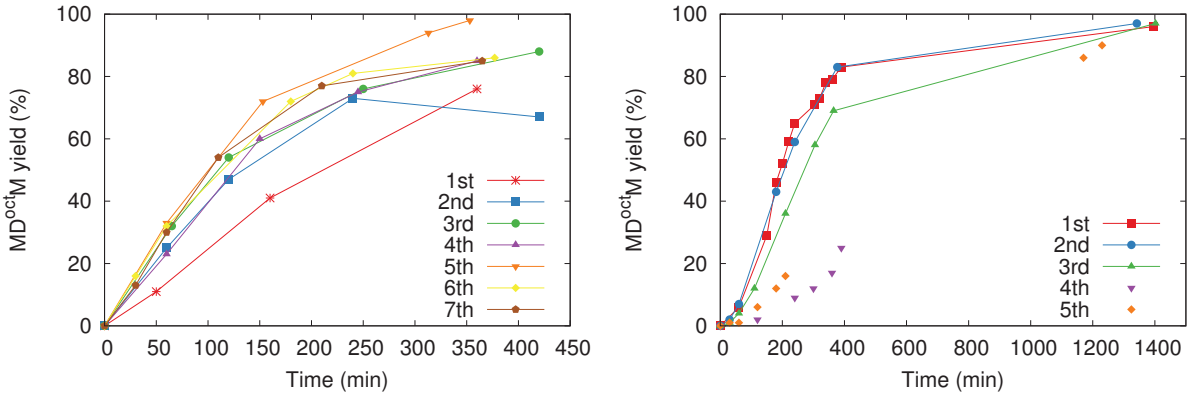


Figure 3.22: Left: reuses of the reduced Pt/CNTs solid with SiH/Pt = 10^4, right: reuses of the reduced Pt/CNTs solid with SiH/Pt = 10^5. Lines are guide to the eye.

over time, and a catalytic activity which remains stable for numerous runs, we hypothesized that leaching may arise from dissolution of Pt species stabilized by 1-octene and MD'M ligands, and that the decrease of 1-octene and MD'M concentrations at the end of the reaction would destabilize these dissolved Pt species and favour their redeposition on the support (Figure 3.23). Such a phenomenon has already been observed for the palladium-catalyzed Heck and Suzuki C – C coupling reactions,[151,194–198] and is sometimes called "release and catch" phenomenon or "boomerang effect".

[194] F. Zhao et al., *Chem. Eur. J.* **2000**, 6, 843–848.
[195] B. H. Lipshutz et al., *J. Org. Chem.* **2003**, 68, 1177–1189.
[196] D. Astruc, *Inorg. Chem.* **2007**, 46, 1884–1894.
[197] K. Köhler et al., *Adv. Synth. Catal.* **2008**, 350, 2930–2936.
[198] M. Gruttadauria, F. Giacalone and R. Noto, *Green Chem.* **2013**, 15, 2608–2618.

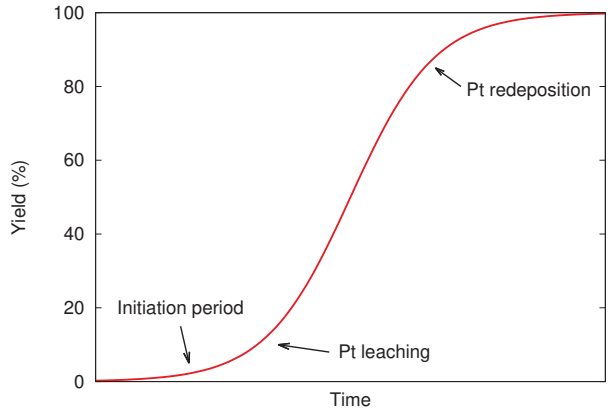


Figure 3.23: Artist's impression of the proposed dissolution-redeposition phenomenon, with Pt leaching at low conversions (ie. high reagents concentrations) and Pt redepositions at high conversions (ie. low reagents concentrations).

To test this hypothesis, we performed "redeposition tests": we conducted a test until >95% yield was reached, then took half the mixture, filtered and mixed with fresh reactants. If there was catalytic activity, it would mean that Pt was still present in the liquid phase. If not, either redeposition happened, or Pt was present but inactive. It should be noted that this addition of new reagents dilutes the possibly present Pt by a factor of 2, and that the kinetics may be slowed down by this dilution.

A redeposition test conducted with a SiH/Pt ratio of 10^4 (Figure 3.24, left) showed a much lower activity (but still significant) in the redeposition test than in the original test, indicating the presence of active Pt in the liquid phase. The same test with a SiH/Pt ratio of 10^5 showed an absence of catalytic activity during the redeposition test, which can be explained by either a full redeposition of Pt or the presence of inactive Pt species in the liquid phase. ICP-AES analysis of the liquid phase revealed that the Pt concentration was

below the quantification limit (1 ppm).

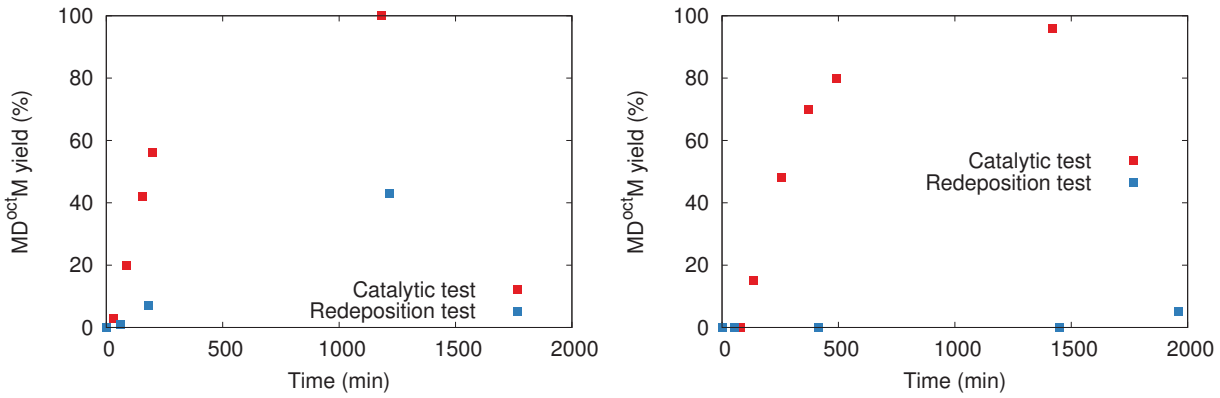


Figure 3.24: Left: redeposition test with SiH/Pt = 10^4, right: redeposition test with SiH/Pt = 10^5.

Solids reduced at 320 °C

To mitigate the sintering for Pt/AC solids, and to allow a proper comparison of catalytic performances between Pt/AC and Pt/CNTs solids, we also reduced these two solids under H_2 flow at 320 °C instead of 450 °C. These solids are called Pt/CNTs(320) and Pt/AC(320).

STEM analysis of the Pt/CNTS(320) solid (Figure 3.25) showed well-dispersed Pt NPs with an average diameter of 1.9 nm, corresponding to a Pt dispersion of 60%.

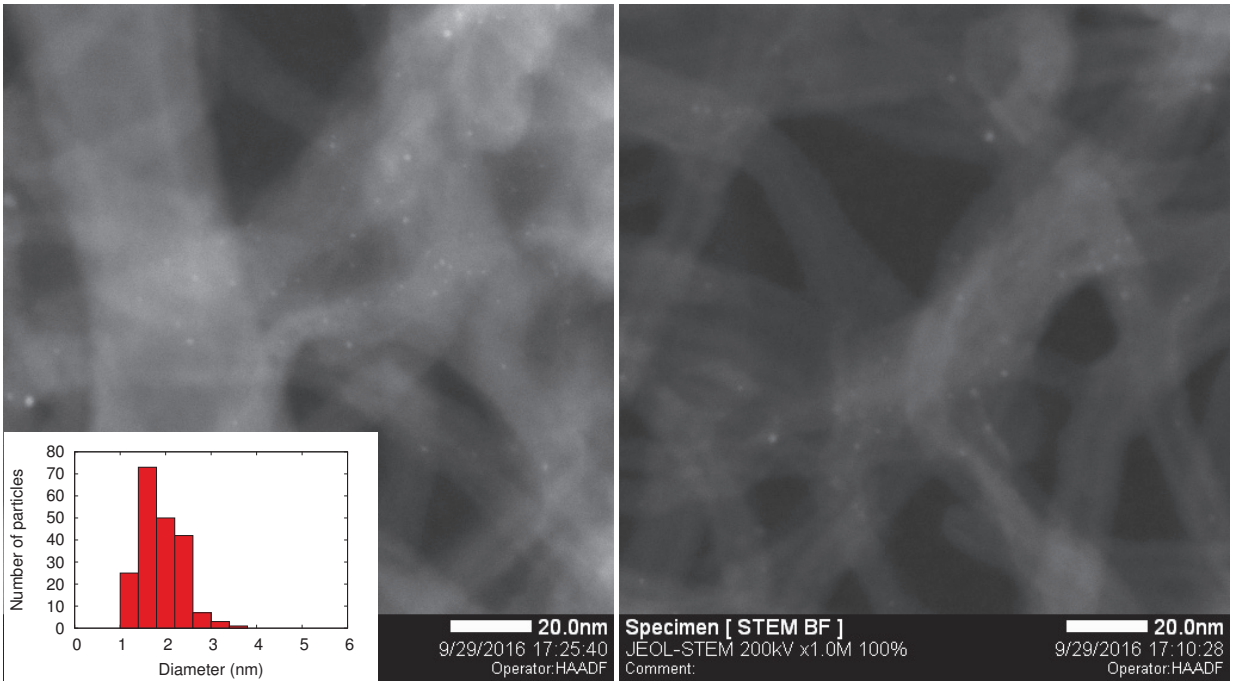


Figure 3.25: STEM of Pt/CNTs catalyst reduced at 320 °C.

STEM images of Pt/AC solid reduced at 320 °C (Figure 3.26) showed Pt particles of rather uniform size, with an average diameter of 2.8 nm, and the absence of very large particles as observed for the solid reduced at 450 °C, confirming the effect of high reduction temperature on Pt sintering.

The catalytic activity of Pt/CNTs(320) was much higher than that of Pt/CNTs(450) (Figure 3.27), very close to the activity of the unreduced solid. Moreover, there

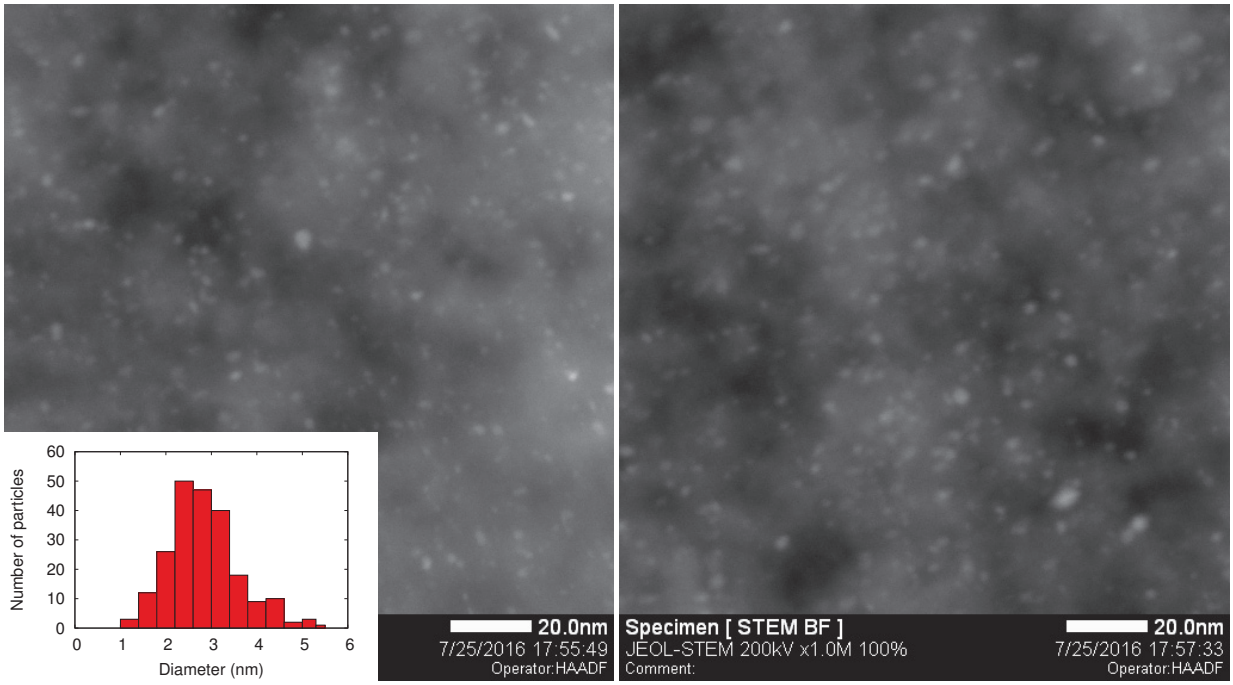
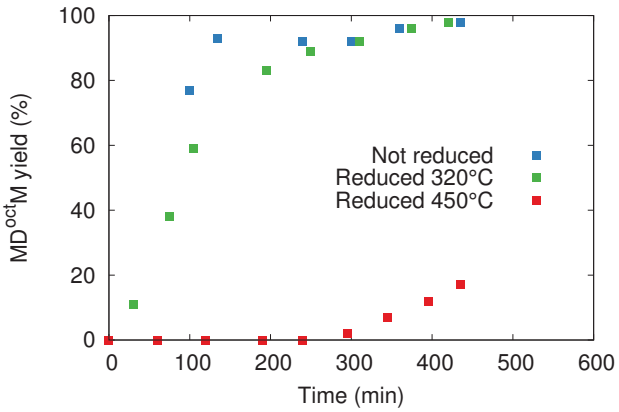


Figure 3.26: STEM of Pt/AC catalyst reduced at 320 °C.

was almost no induction period, as for the unreduced solid. Analysis of a filtered aliquot of the reaction mixture (taken around 40% conversion) by ICP-AES indicated a Pt content lower that the quantification limit (1 ppm).

It would be interesting to perform XPS analysis on the three solids (not reduced, reduced at 320 °C and reduced at 450 °C) to probe the oxidation state of Pt. This would give a hint on if the much higher activity of Pt/CNTs(320) relative to Pt/CNTs(450) is due to an incomplete reduction to metallic Pt (thus allowing faster leaching) or some other reasons. These analyses are planned.

Figure 3.27: Influence of the reduction of a Pt/CNTs solid on its activity.



A catalytic test of Pt/CNTs(320) was performed with split tests at reaction times (Figure 3.28). The conversion observed during the split tests at 30 min, 50 min and 100 min all stagnate after some progression, indicating a deactivation of the leached Pt species. Such a deactivation is not observed for the split test at 200 min, which might be explained by the fact that the yield was already 74% when the split test was performed, and that an almost quantitative yield was reached before active species deactivation. For the split tests at 30 min,

50 min and 100 min, the conversion progression between splitting and deactivation was respectively of 8%, 18% and 29%. This supports the hypothesis that the leached Pt quantity increases throughout the test, but it doesn't indicate anything about a possible redeposition at the end of the test.

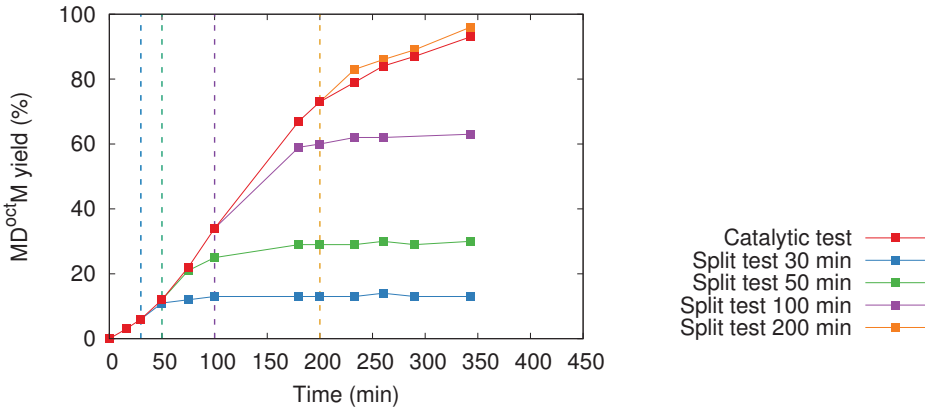


Figure 3.28: Multiple split tests performed at different moments during a single catalytic test. The main reactor is drawn in red. Each vertical dashed line represents a split test. Lines are guide to the eye.

We reused Pt/CNTs(320) and Pt/AC(320) several times (Figure 3.29). They displayed comparable activities, but a slightly different behaviour: the activity of Pt/CNTs(320) slightly decreased at each cycle, whereas a sharp activity drop was observed for Pt/AC(320) between the first and the second cycle and the activity remained stable for the next 3 runs. The total TONs were 4.7×10^5 for Pt/CNTs(320) (over 6 runs) and 3.1×10^5 for Pt/AC(320) (over 5 runs).

Redeposition tests were performed with both catalysts, as shown in Figure 3.30. For both catalysts some catalytic activity was observed, meaning that there was still active Pt in solution at the end of the first catalytic tests. The catalytic activity was significantly higher for Pt/AC(320), but the yield at the end of the first run was lower for this catalyst, meaning that Pt might have redeposited more when a yield closer to 100% was reached.

To summarize, the solids reduced at 320 °C were more active than those reduced at 450 °C and almost as active as unreduced catalysts. Their activity seemed to decrease faster on reuse, but this observation should be confirmed with runs that are carried out at yields close to 100% to ensure maximum redeposition of Pt.

Catalytic tests with a PHMS

We tested the Pt/CNTs(450) solid in the hydrosilylation of 1-octene with MD'$_{50}$M (Figure 3.10). In the first run, the SiH conversion stagnated at about 80% (Figure 3.31). The catalyst was reused after being separated from the reaction mixture by decantation, and in the second run, the activity was significantly lower than that reached during the first run. A more detailed study could determine if redeposition also happens in this catalytic system, knowing that even if the SiH conversion was quantitative, there would still be 0.4 eq of octenes in the reaction medium, which could prevent Pt redeposition.

We also analyzed the reaction mixture by ^{1}H NMR, which allowed us to determine the amount of 1-octene isomerization at similar SiH conversions (Table 3.3). Interestingly, this amount was of 5% for Pt/CNTs(450), much lower than for Karstedt's catalyst (12%) or unsupported Pt NPs (11%) in the same conditions. For Pt/CNTs(320), the amount of isomerization was of 8%,

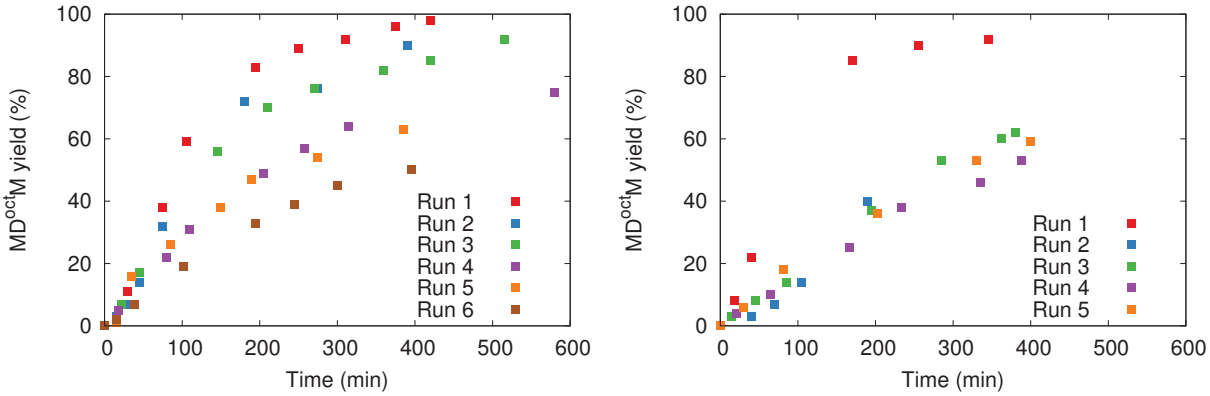


Figure 3.29: Left: reuses of Pt/CNTs reduced at 320 °C, right: reuses of Pt/AC reduced at 320 °C

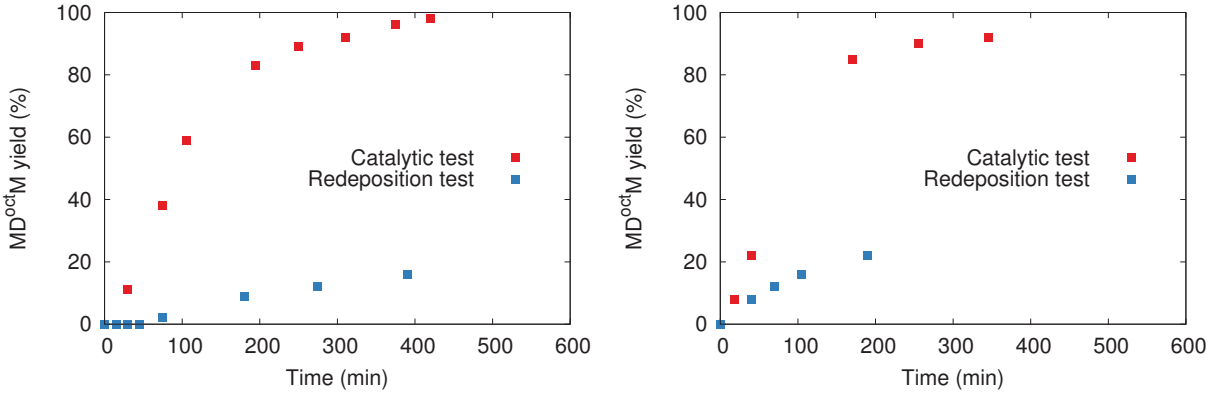


Figure 3.30: Left: redeposition test with Pt/CNTs reduced at 320 °C, right: redeposition test with Pt/AC reduced at 320 °C

intermediate between Pt/CNTs(450) and Karstedt's complex or a Pt colloid.

When looking at the relative activities of different homogeneous and heterogeneous Pt-based catalysts (Figure 3.32), a direct correlation between hydrosilylation rate and isomerization proportion can be established.

In fact, such a correlation has already been observed by Markó *et al.* when they studied the effect of different NHC substituents ("R" substituents in Figure 3.33) on hydrosilylation and isomerization selectivities for the reaction between

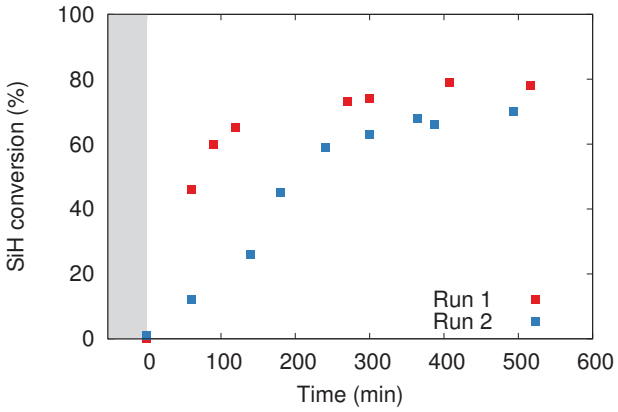


Figure 3.31: Catalytic tests with Pt/CNTs solid reduced at 450 °C (6 ppm Pt, SiH/Pt = 1.5×10^5, 1-octene/SiH = 1.4). The period in grey is the addition of $MD'_{50}M$ into the reactor.

Catalyst	1-octene fraction isomerized	SiH conversion
Karstedt's complex	12%	87%
Pt colloid	11%	84%
Pt-NHC complex	8%	84%
Pt@{walls}SBA-15	9%	73%
Pt/CNTs(320)	**8%**	**78%**
Pt/CNTs(450)	**5%**	**81%**

Table 3.3: Fraction of 1-octene isomerized for various Pt-based catalysts and the corresponding SiH conversion.

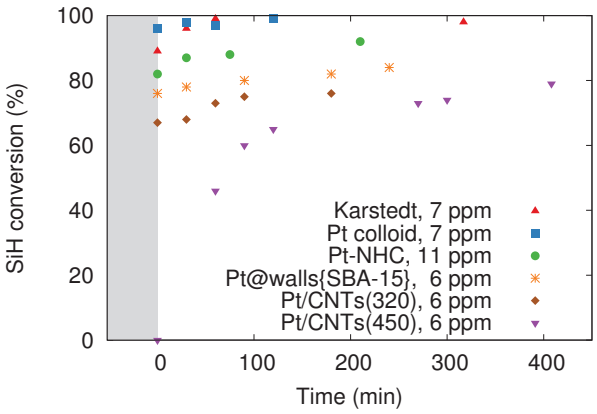


Figure 3.32: Comparison of homogeneous and heterogeneous Pt catalysts for the reaction between MD'$_{50}$M and 1-octene. The period in grey is the addition of MD'$_{50}$M into the reactor.

MD'M and 1-octene.[48]

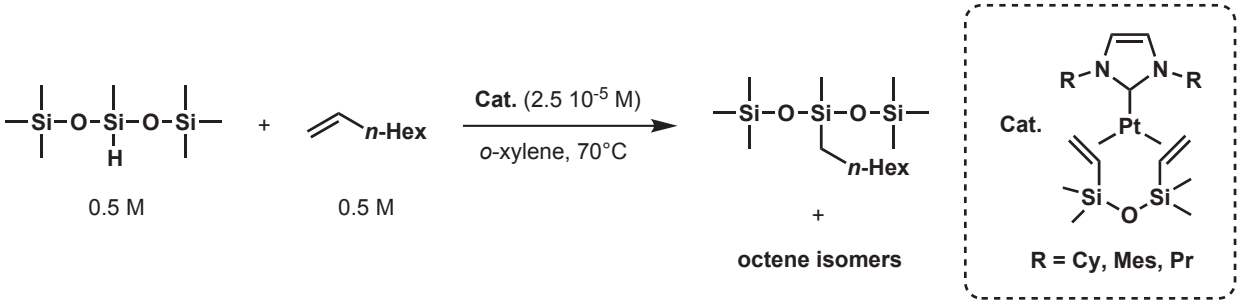


Figure 3.33: Reaction used by Markó *et al.* to study the effect of NHC substituents ("R") on the isomerization proportion.[48] Cy = cyclohexyl, Mes = mesityl, Pr = propyl.

They remarked that the NHC substituents had a significant effect on the reaction rate, that the rate of isomerization was proportional to the rate of hydrosilylation to the power 1.4, and that "slow release [of the active Pt species was] a key prerequisite for minimizing the amount of isomerized olefins". Note that for all catalysts, the selectivities were almost constant with the SiH conversion (but different for all catalysts). Even if in our case we didn't measure isomerization rates but selectivities,[h] we see qualitatively that the correlation seems to be valid.

In our case, more experiments are needed to identify the cause of this low isomerization rate and to determine whether there is a correlation between the amount of Pt leached and the rate of isomerization. However, we can already see that the Pt/CNTs(450) catalyst is advantageous from the point of view of selectivity with respect to Karstedt's complex or a Pt colloid.

[h] To have an equivalence between the ratio of isomerization and hydrosilylation rates with the ratio of selectivities, it would be necessary to show that selectivities are constant throughout the reaction.

Conclusion for CNTs

In conclusion, we have studied Pt/CNTs and Pt/AC solids prepared from impregnation with H_2PtCl_6 as catalysts for the model reaction of MD'M and 1-octene. We have given evidence that a dissolution-redeposition phenomenon was happening in these conditions, suggesting that activity was —at least partially— due to leached Pt species, and that at very high yields (typically >90%) the concentrations of both reagents become too low to stabilize the leached Pt species, leading to the redeposition of Pt on the support. Such a mechanism had already been observed for other reactions such as the Heck reaction, but we are the first to mention it for alkene hydrosilylation, to our knowledge.

One important question is the nature of the leached Pt species. We can envision that they are either whole Pt NPs that detached from their support, or Pt complexes formed by dissolution of Pt NPs of the solid and stabilized by the SiH reagent and/or the alkene. Selective poisoning tests with mercury could give valuable insights about this question.

We have also shown that there was an important effect of H_2 reduction and the reduction temperature on the presence of an induction period, the catalytic activity and reusability.

Given that this dissolution-redeposition phenomenon happens, a batch reactor is more adapted for using these catalysts than a continuous flow reactor. Indeed, in a continuous flow reactor, Pt would progressively migrate towards the outlet of the reactor and would be lost in the reaction product. Redeposition of Pt advantageously allows to obtain reaction products with very low Pt concentration, to reuse the catalyst, and to easily recycle Pt from spent catalysts once they are deactivated.

For the catalysts reduced at 450 °C, CNTs stabilized better the Pt NPs than AC, thus limiting Pt sintering. At 320 °C, both supports gave catalysts that behaved very similarly in catalysis, showing no particular influence of CNTs with respect to AC in these conditions.

The impregnation method could be optimized in the case of CNTs in order to ensure a homogeneous distribution of Pt NPs on CNTs. XPS could be used to determine if Pt reduction is complete for the solids reduced at 320 °C. If it is the case, it means that the much higher induction period observed for Pt/CNTs(450) has another cause than the partial oxidation of Pt.

A more systematic study of dissolution-redeposition could be conducted. We suggest to measure Pt concentrations in the liquid phase at various yields, which would allow to know at which yield Pt starts to redeposit. A more precise quantification of Pt in the liquid phase would be necessary, with quantification limits of 0.1 ppm, for example. Tests could be done with different substrates, eg. with more coordinating alkenes (for example bearing an alcohol function), and see if leaching is faster and if there is still redeposition or not, knowing that the coordinating functions of the alkene (ie. the alcohol, in our example) would still be present in the reaction product.

3.4 Conclusion

Pt@{walls}SBA-15 apparently operates by a heterogeneous mechanism, while Pt/AC and Pt/CNTs probably operate by a homogeneous mechanism with a Pt active species arising from Pt dissolution from Pt NPs. This conclusion is very surprising, since both catalysts are based on Pt NPs. This difference might arise from the nature of the support (polar for SBA-15 and apolar for carbon supports), from the method of preparation (using preformed Pt NPs for SBA-15 and a Pt salt for carbon supports) or from the thermal treatments of the solids (calcination under air for SBA-15 and reduction under H_2 for carbon supports).

As shown in Chapter 2, the problem of distinguishing between homogeneous and heterogeneous active species is very difficult,[151] especially when minute quantities of active phase are present in the reaction medium as in our case with Pt.

Both the heterogeneous mechanism and the homogeneous mechanism accompanied by redeposition at the end of the reaction facilitate the separation of Pt from the reaction products, allowing its reuse or recycling, which are two routes to more sustainable hydrosilylation processes.

3.5 Experimental

Syringe filters comprise a PTFE membrane with a pore size of 0.45 µm.

3.5.1 Hydrophilic Pt colloid synthesis

100 mg (0.15 mmol) of $Pt(dba)_2$ (dba = dibenzylideneacetone) and 90 mL of THF were introduced in a Fischer-Porter glass reactor under Ar, giving a deep purple solution. A solution of 25 mg of 3-chloropropylsilane (0.23 mmol, 1.5 eq) in 10 mL of THF was prepared under Ar and introduced in the Fischer-Porter reactor, which was then evacuated, pressurized at 3 bar of H_2 under stirring during 12 hours. A deep brown colloid was obtained, and stored under Ar.

3.5.2 Pt@walls{SBA-15} (0.3% Pt w/w) synthesis

In a 150 mL erlenmeyer, 0.5 g (86 µmol) of Pluronic®123, 50 mL of distilled water and 20 mg of NaF were vigorously stirred during 1 h. 20 mL of a Pt colloid (24 µmol Pt) was then added, and the mixture is stirred 2 h more. The THF was then fully evaporated under reduced pressure.

In another erlenmeyer, 5 mL of water, 170 mg of HCl 37% w/w and 5 g (24 mmol) of tetraethylorthosilicate were stirred at 35 °C during 3 h.

The contents of both erlenmeyer were mixed together at 35 °C during 48 h. The grey solid was filtered, then washed with 2 × 20 mL of water, 2 × 20 mL of ethanol and 2 × 20 mL of diethylic ether. The solid was calcined under a flow of dry air (40 mL min^{-1}) at 350 °C during 10 h, with a ramp of 2 °C min^{-1}.

3.5.3 Catalytic tests (semibatch)

Warning: the hydrosilylation reaction is very exothermic ! The reaction medium temperature must be monitored carefully to prevent a runaway.

Blank tests were performed at several points of the study and indicated that the reactor was not contaminated by traces of catalysts.

The hydrosilylation catalysts were found to be very sensitive to the grade of the octene used. When using octene of industrial grade, conversions significantly lower were obtained, and the presence of traces of poisons in the octene were suspected to be at the origin of these lower performances.

The catalytic tests were run under an atmosphere of air, in a classic 300 mL glass reactor equipped with a glass impeller and baffles. The stirring rate was 1000 rpm. At the beginning of the reaction, the reactor was filled with 43 g of 1-octene (1.4 equivalent respective to SiH, to compensate for alkene isomerization) and 114 mg of Pt@walls{SBA-15}(6 ppm Pt).

The 1-octene/catalyst mixture was heated to 75 °C. Then, 17 g of PMHS were added at 0.3 mL min^{-1} with a syringe pump. The temperature of the reaction medium was maintained between 75 °C and 85 °C by removing partly or totally the heating bath. After the end of the PMHS addition, samples were regularly collected, diluted in $CDCl_3$ and analysed by ^1H NMR to get the SiH conversion.

3.5.4 CNTs purification

500 mL of H_2SO_4 95% were added drop-wise over 1 h under constant stirring into a suspension of 20 g of CNTs in 500 mL of demineralized water. The suspension was then refluxed at 140 °C for 3 h. Then, without cooling, the suspension was filtered on a fritted glass funnel and washed with demineralized water until a filtrate pH of 5 was reached. The CNTs were then dried at 110 °C for 24 h.

3.5.5 N_2 adsorption

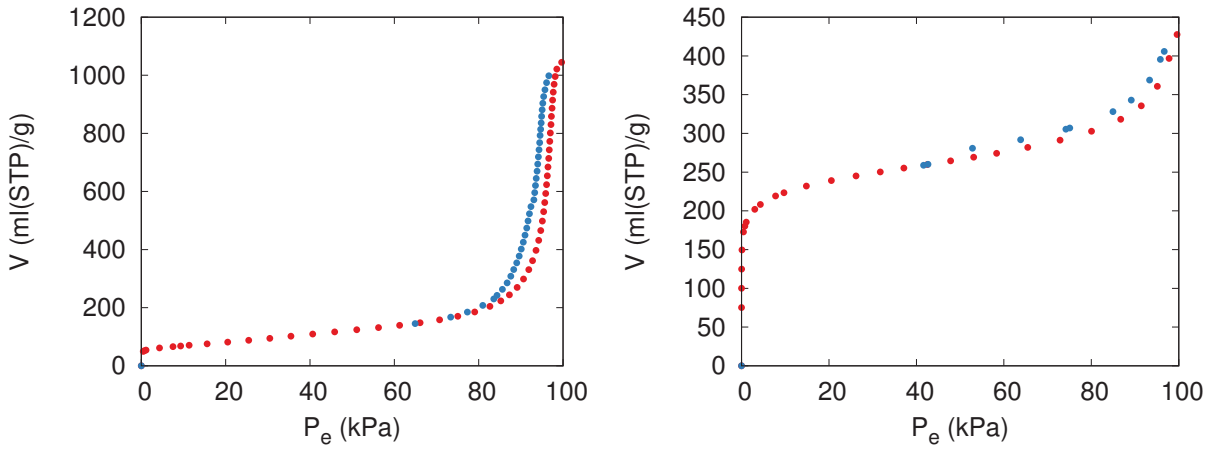


Figure 3.34: N_2 adsorption isotherms at 77 K for CNTs (left) and AC (right).

3.5.6 CNTs functionalization

10 g of purified CNTs were mixed with 500 mL of HNO_3 68% and refluxed at 120 °C for 8 h under stirring. The CNTs were then filtered on a fritted glass funnel and washed with demineralized water until a filtrate pH of 5 was reached. The CNTs were then dried at 110 °C for 24 h.

3.5.7 Incipient wetness impregnation and nitrogen treatment

7.8 mg of $H_2PtCl_6 \cdot 6\,H_2O$ were dissolved in 3.5 mL (for CNTs) or 1.2 mL (for active carbon) of absolute anhydrous EtOH. The solution was added dropwise to 1 g of functionalized CNTs or active carbon, while stirring with a glass rod, until the powder became sticky with particles attaching to the glass wall of the vial.

A horizontal tubular oven was then programmed as follows to dry and calcine the solid: ramp to 120 °C in 1 h 40, 120 °C for 4 h, ramp to 450 °C in 3 h, 450 °C for 4 h. The oven was under a nitrogen flow of 200 mL min^{-1}. A solid containing 0.3% Pt w/w was obtained.

3.5.8 Catalyst reduction

A glass tube containing the dried and calcined solid was flushed with argon, then placed in a vertical tubular oven under hydrogen flow 40 mL min^{-1}.

The vertical tubular oven was then programmed as follows: ramp to 450 °C in 2 h, 450 °C for 4 h.

3.5.9 Catalytic test (batch)

Small cylindrical glass vials (45 mm height, 25 mm diameter) with a screw-cap lid were equipped with a PTFE magnetic stirrer (14 mm length, 2 mm diameter). 1.7 g of dodecane (10 mmol, 0.5 eq), 4.45 g of MD'M (20 mmol, 1 eq) and 2.24 g of 1-octene (20 mmol, 1 eq) were then introduced into the vial. At this point, a sample of starting mixture (0.1 mL) was analyzed. A specified mass of catalyst was then added to the solution. For example, for a Pt/SiH ratio of 10^{-5}, a mass of 13 mg of catalyst (0.3% Pt w/w) would be added, which corresponds to 39 µg or 2×10^{-4} mmol of Pt.

The reaction mixture was then placed in an oil bath at 80 °C and agitation 500 rpm. The catalyst was well suspended in the reaction medium. Further samples (0.2 mL) were taken and analysed by gas chromatography throughout the experiment. t = 0 was defined as the moment when the glass vial (containing the reaction mixture) was placed in the pre-heated oil bath.

3.5.10 Samples preparation for gas chromatography

Samples were taken with a syringe, filtered through a syringe filter and diluted with 0.4 mL of toluene.

3.5.11 Split test (batch)

A catalytic test was run to 20-30% $MD^{oct}M$ yield. At that point, half of the reaction mixture (4 mL) was taken using a syringe, filtered through a syringe filter and added to a new glass vial containing a PTFE magnetic stirrer. This

filtered reaction mixture was then placed in the same conditions that the original reaction and monitored.

3.5.12 Pre-leaching test (batch)

A catalytic test was conducted as described in subsection 3.5.9, except that one of the reagents (MD'M or 1-octene) was added to the medium only after 1 h of contact of the other components at 80 °C. t = 0 was defined as the time when the missing reagent was added to the reaction medium.

3.5.13 Redeposition test (batch)

A catalytic test was run to completion (> 95% yield). 4 mL of the liquid phase was then taken using a syringe, filtered using a syringe filter and introduced in a vial containing a magnetic stirrer. 0.85 g of dodecane (5 mmol, 0.5 eq), 2.23 g of MD'M (10 mmol, 1 eq) and 1.12 g of 1-octene (10 mmol, 1 eq) were added into the vial. A sample of the resulting mixture (0.1 mL) was analyzed. The vial was then placed in an oil bath at 80 °C and agitation 500 rpm.

3.5.14 Catalyst reusing (batch)

A catalytic test was run to completion (> 95% yield). The mixture was decanted at room temperature and the liquid phase removed with a syringe. A new mixture containing dodecane, 1-octene and MD'M was then added, and the catalytic test conducted as written in subsection 3.5.9.

3.5.15 Gas chromatography

See Appendix C at the end of the manuscript.

4

Nickel nanoparticles

4.1 Introduction

Ni has been studied as an alkene hydrosilylation catalyst, but mostly in the form of complexes of Ni(0) or Ni(II), as discussed in subsection 1.5.5.[38,70,94,103,105,107] Most of these catalytic systems often involve high temperature, poor catalytic performances and the necessity of using primary or secondary silanes, which are intrinsically more reactive than tertiary silanes, but which give less interesting products.[38,70,94,103,105] However, very recently, a complex featuring a non-innocent ligand was shown by Chirik *et al.* to be able to functionalize several tertiary silanes that are of industrial interest, in mild conditions.[107]

A few example of heterogeneous Ni catalysts have also been found in the literature. For example, Raney nickel was studied in 1956,[92] but needed harsh reaction conditions (160 °C), and led to a yield of about 10% in 4 h of reaction. In 1991, Boudjouk *et al.* published the synthesis of an activated nickel powder by lithium reduction of nickel iodide in tetrahydrofuran and its use as catalyst.[199] Unfortunately, it reached only 6 turnovers, no characterization of the powder was provided, and we can presume that it was constituted of large particles, because no stabilizer was used during the synthesis.

It is only very recently that the first example of utilization of small nickel nanoparticles as alkene hydrosilylation catalysts was published by Hu *et al.*,[109] despite the fact that metallic nanoparticles of noble metal such as platinum or rhodium have been proven to be catalytically active several decades ago (see Chapter 2 and references [55, 155]).

Given that metallic NPs constitute a part of the chemical space that is complementary to organometallic complexes, and can show some original reactivity,[135,141] in this Chapter we report the utilization of Ni NPs as alkene hydrosilylation catalysts. Ni NPs are often synthesized starting from Ni(II) complexes such as $Ni(acac)_2$ (acac = acetylacetonate), by reduction by a polyol,[200] a hydride source[201] or oleylamine.[202,203] They can also be synthesized by decomposition of a Ni(0) complex.[204] In this work, we used the latter route to synthesize three kinds of Ni NPs, using a protocol developed in our laboratory:[159] Ni(0) silicide nanoparticles, Ni oxide nanoparticles, and metallic Ni(0) nanoparticles on silica.[i] We then tested these nanoparticles on various hydrosilylation reactions, and obtained very different results depending on

[199] P. Boudjouk et al., *J. Chem. Soc., Chem. Comm.* **1991**, 1424–1425.

[200] T. Hinotsu et al., *J. Appl. Phys.* **2004**, 95, 7477–7479.
[201] Y. Hou and S. Gao, *J. Mater. Chem.* **2003**, 13, 1510–1512.
[202] Y. Chen et al., **2007**, 18, 505703.
[203] S. Carenco et al., *Chem. Mater.* **2010**, 22, 1340–1349.
[204] J. Park et al., *Adv. Mater.* **2005**, 17, 429–434.
[i] The chemical nature of these three kind of NPs was determined by EXAFS in a previous study by our group.[159]

the substrates and the environment of nickel atoms in the NPs.

4.2 Results

4.2.1 Catalysts synthesis and characterization

First, a colloidal solution of Ni_3Si_2 NPs was prepared by decomposition of $Ni(COD)_2$ in toluene (light yellow solution) in presence of *n*-octylsilane as stabilizer under 3 bar of hydrogen at 55 °C (Figure 4.1), leading to a black solution.

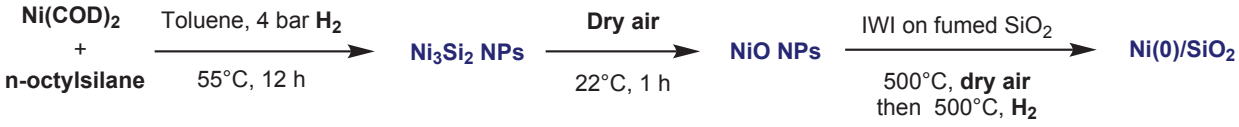


Figure 4.1: Synthesis of the Ni colloids used as catalysts. IWI = Incipient wetness impregnation.

The obtained Ni_3Si_2 colloid was characterized by STEM. For all electronic microscopy in this chapter, samples were prepared under inert atmosphere and loaded in the microscope with a specific sample holder which keeps the sample under inert atmosphere. This allows to observe NPs without any oxidation caused by a contact with air. For this Ni_3Si_2 colloid, very small and well-dispersed NPs were observed (Figure 4.2).

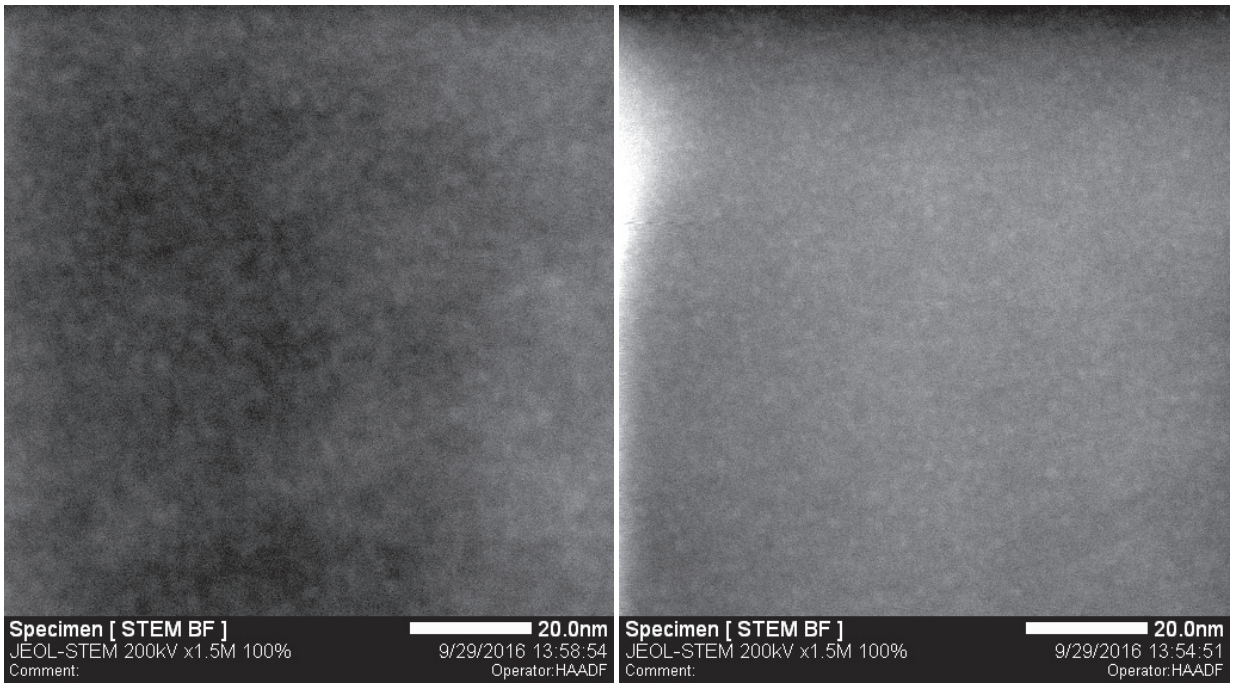


Figure 4.2: STEM images of the Ni_3Si_2 colloid.

We performed a diffusion-ordered spectroscopy (DOSY) NMR experiment with this colloidal solution of Ni_3Si_2 NPs, after toluene evaporation and redissolution in C_6D_6 (Figure 4.3).

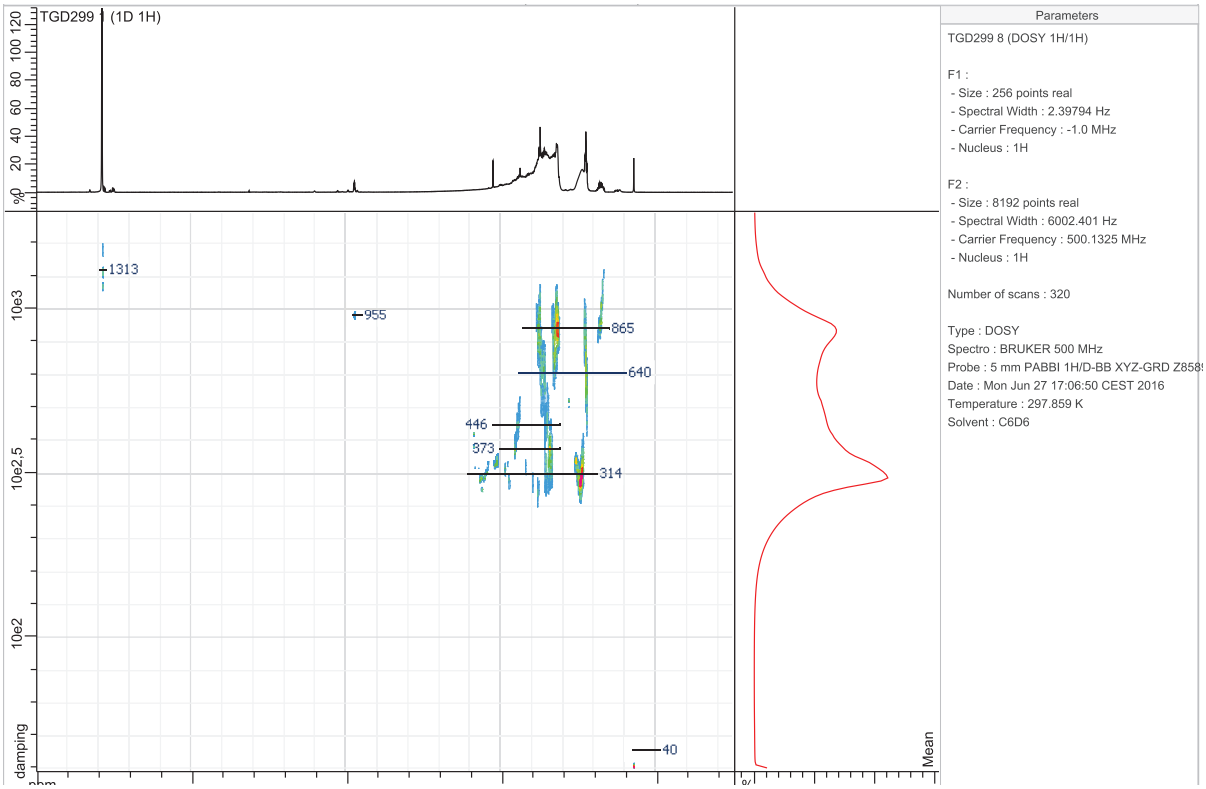


Figure 4.3: ^{1}H-DOSY spectrum of Ni_3Si_2 colloidal solution in C_6D_6.

Using the Stokes-Einstein law:

$$D = \frac{k_B T}{6\pi\eta r}$$

the hydrodynamic radius can be estimated as

$$r = \frac{k_B T}{6\pi\eta D}$$

with $k_B = 1.381 \times 10^{-23}$ J K^{-1}, $T = 298$ K and $\eta = 0.636$ cP (viscosity of C_6D_6 at 298 K)[205]. The signal attributed to the Ni_3Si_2 nanoparticles has a diffusion coefficient of 314 µm^2 s^{-1}, corresponding to a hydrodynamic radius of 1.1 nm and thus to a hydrodynamic diameter of 2.2 nm.

From the Ni_3Si_2 colloidal solution, a second type of nickel nanoparticles was prepared by exposing it to dry air, leading to oxidation of the Ni_3Si_2 nanoparticles to NiO.

Finally, a third kind of nanoparticles was obtained by impregnation of the NiO colloid on fumed silica by incipent wetness impregnation, followed by calcination and reduction under hydrogen at 500 °C.

TEM analysis of this solid (Figure 4.4) showed NPs that were well-dispersed on the surface of silica. The low contrast prevented from accurately determining a particle size histogram.

However, STEM analysis (Figure 4.5 for STEM images and Figure 4.6 for EDX analysis of a Ni particle.) gave a better contrast and showed the presence of small (1 nm to 2 nm) along with some large NPs (5 nm to 10 nm), and an average size of 1.4 nm, in accordance with the original synthesis reported by our group.[159]

[205] M. Holz et al., *J. Chem. Phys.* **1996**, 104, 669–679.

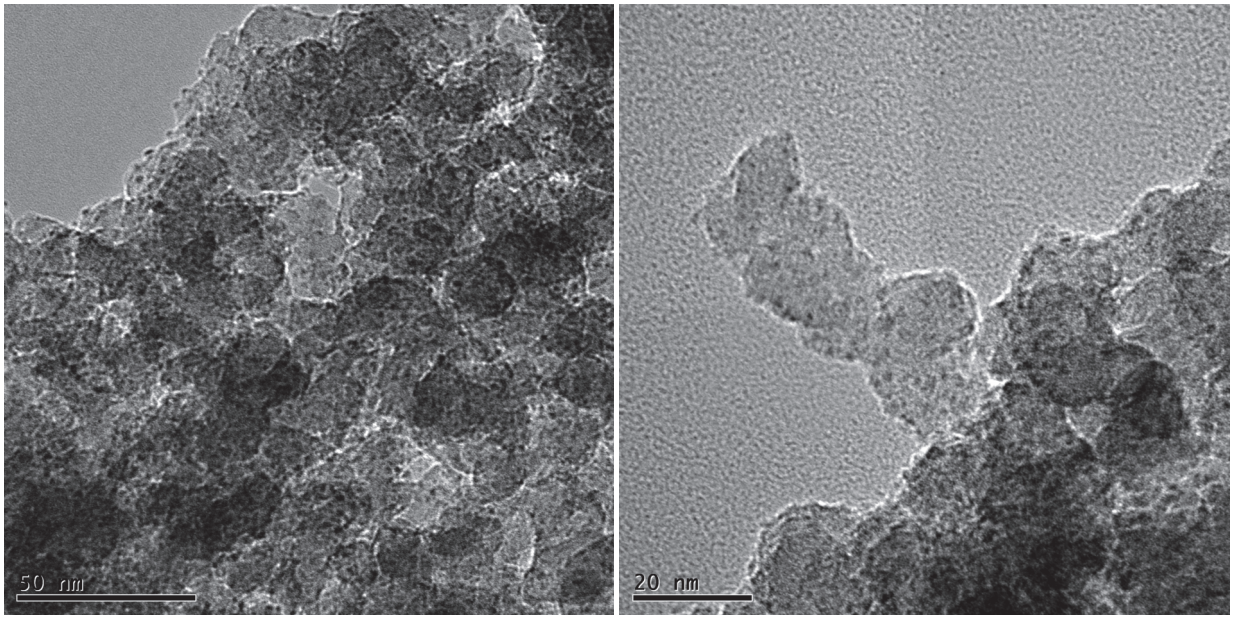


Figure 4.4: TEM of the Ni(0)/SiO_2 solid.

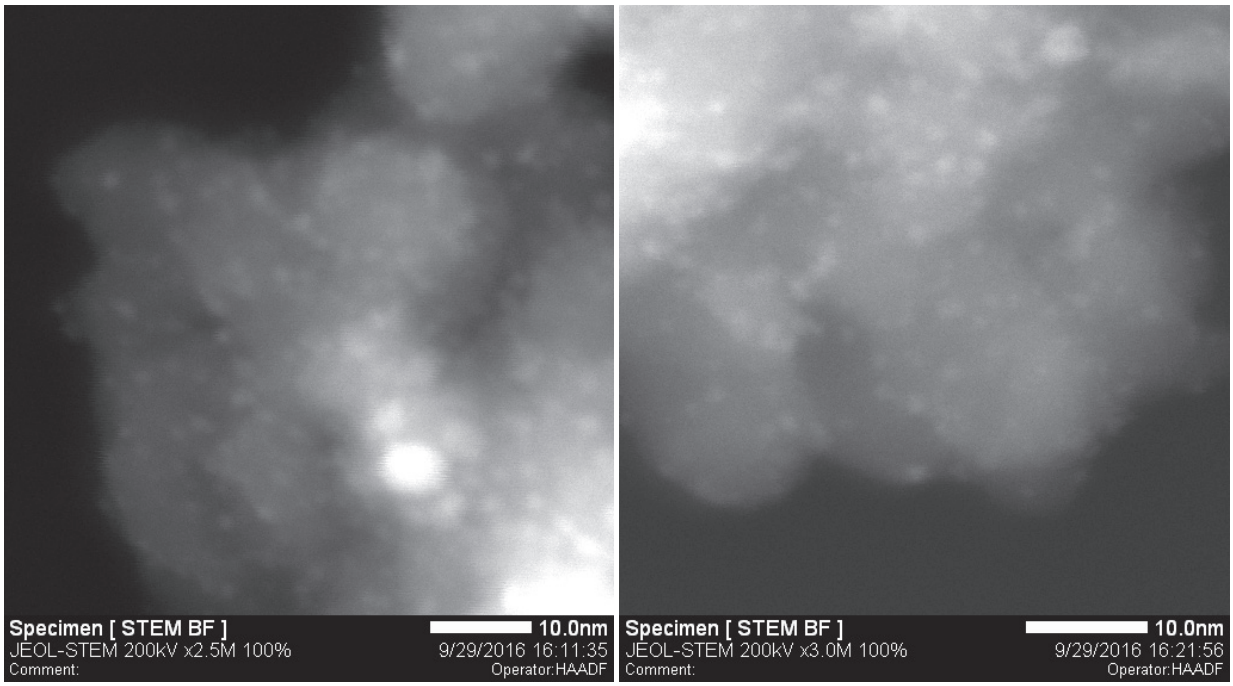


Figure 4.5: STEM of the Ni(0)/SiO_2 solid.

H_2 chemisorption at 25 °C yielded a Ni dispersion of 39%, corresponding to a particle size of 2.9 nm. This result is in disagreement with the average particle size obtained by STEM. This contradiction may arise from the non-uniform NP size repartition and the presence of large NPs as shown on the STEM images.

4.2.2 Tests with triethoxysilane and triethoxyvinylsilane

The three types of NPs were tested in the hydrosilylation of triethoxyvinylsilane by triethoxysilane, a reaction with selectivity challenges.[98] Apart from the

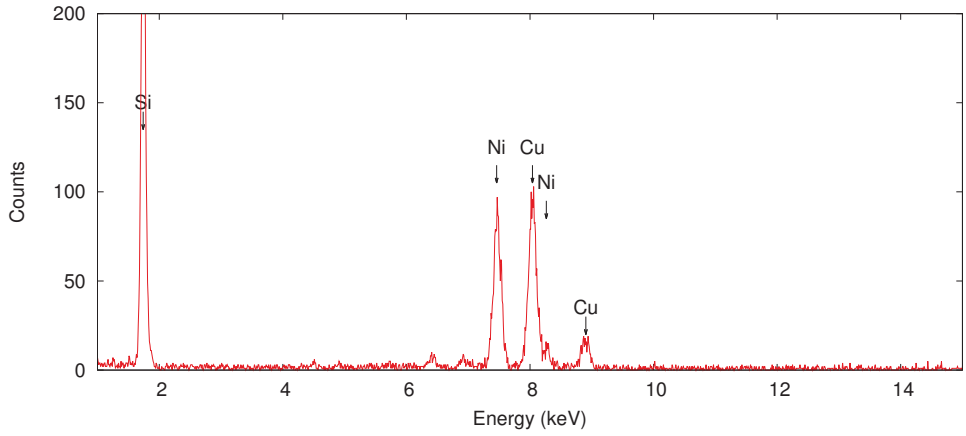


Figure 4.6: EDX of a Ni particle.

hydrosilylation product, the products of dehydrogenative silylation, vinylsilane hydrogenation, silane substituents redistribution and vinylsilane dimerization can also be formed (Figure 4.7). The reaction was conducted in batch reactor, in toluene, using dodecane as internal standard and monitoring the reaction with gas chromatography.

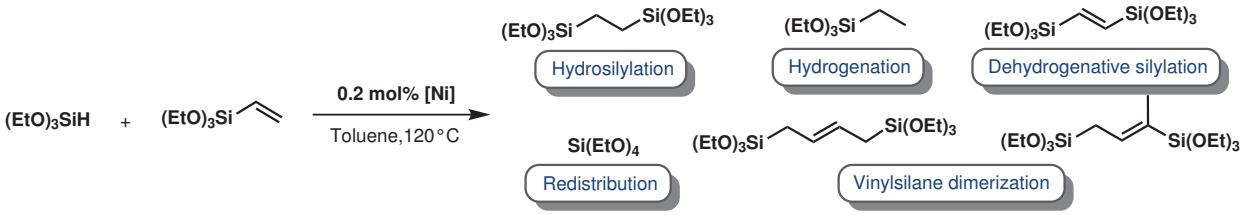


Figure 4.7: Reaction between triethoxysilane and triethoxyvinylsilane.

We first tested two Ni complexes that were used to catalyze this reaction in the literature: $Ni(acac)_2$ and $Ni(COD)_2$,[98–100] in order to validate our experimental setup. Indeed, we obtained results rather close to those of the literature (Table 4.1). In our tests, $Ni(acac)_2$ gave predominantly the products of vinylsilane dimerization (33% yield) and dehydrogenative silylation (27% yield), while $Ni(COD)_2$ gave mainly dehydrogenative silylation (25% yield) and vinylsilane dimerization (17% yield). Hydrosilylation was a minor product in both cases, with 4% yield for $Ni(acac)_2$ and 2% yield for $Ni(COD)_2$.

Cat.	Conv. $(EtO)_3SiH$	Conv. $(EtO)_3Sivi$	Yield $(EtO)_3SiEt$	Yield TEOS	Yield DHSI	Yield HSI	Yield Dimers
$Ni(acac)_2$ (literature)	64%	100%	14%	5%	19%	9%	23%
$Ni(acac)_2$	49%	99%	11%	7%	27%	4%	33%
$Ni(COD)_2$ (literature)	64%	100%	28%	6%	15%	8%	17%
$Ni(COD)_2$	36%	74%	15%	7%	25%	2%	17%

Table 4.1: Comparison of our results with results of the literature for for the reaction between triethoxysilane and triethoxyvinylsilane catalyzed by $Ni(COD)_2$ and $Ni(acac)_2$. 120 °C, 2 h, SiH/vinyl/Ni = 1/1/0.001, DHSI = dehydrogenative silylation, HSI = hydrosilylation.

Since these experiments effectively validated our catalytic test setup, we tested our Ni catalysts. Both Ni(0) catalysts (Ni_3Si_2 colloid and Ni/SiO_2) showed conversion of the substrates, whereas NiO colloid did not show any catalytic activity, indicating that the resting state of the catalyst is probably a Ni(0) center, and that the Ni(II) centers of NiO cannot be reduced to Ni(0) by

the hydrosilane in these conditions.

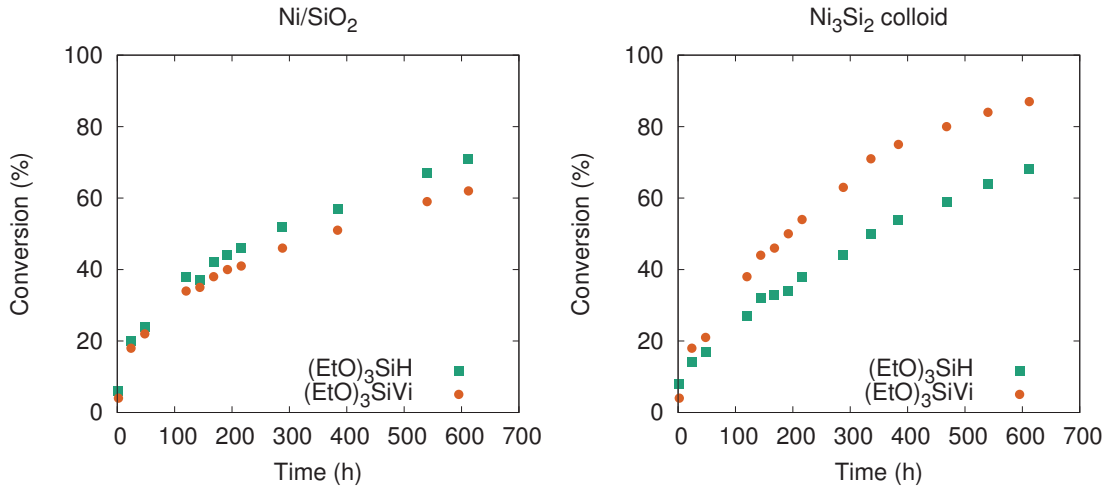


Figure 4.8: Kinetic profiles of the conversions.

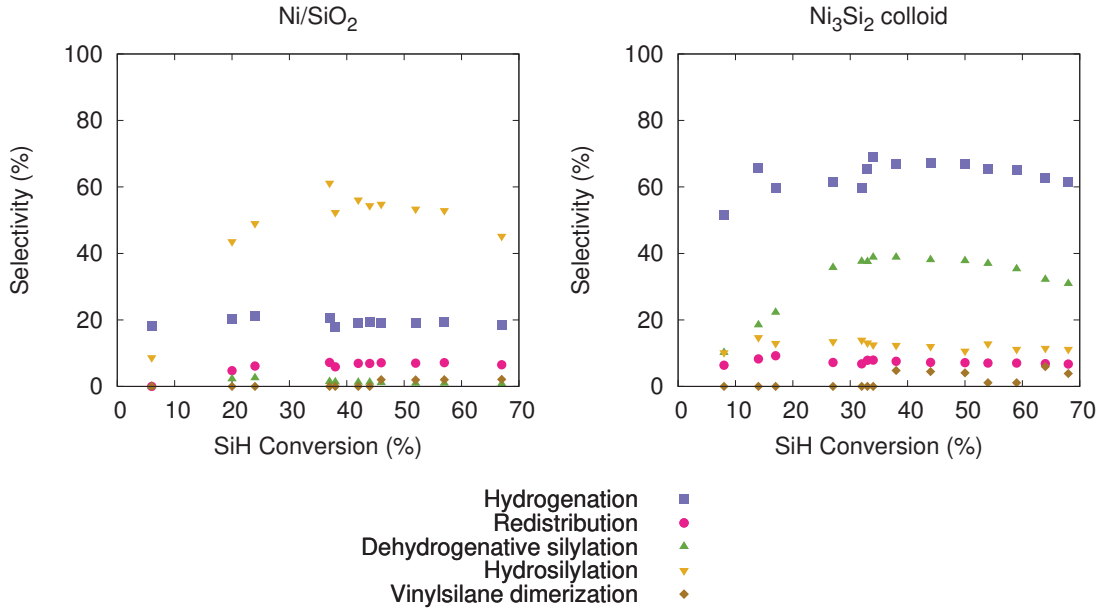


Figure 4.9: Evolution of the selectivity with the conversion.

We observed that both Ni(0) catalysts had similar activities (Figure 4.8), but completely different selectivities (Figure 4.9). The Ni/SiO_2 solid favored hydrosilylation, the desired reaction, with a selectivity of almost 60%. On the contrary, the nickel silicide colloid favored dehydrogenative silylation (around 60% selectivity), accompanied by hydrogenation of the vinylsilane (around 40% selectivity). These results clearly show that even if both catalysts comprise Ni(0) atoms, the chemical environment of these atom is a key factor to control the selectivity of the catalyst. Interestingly, the selectivities did not evolve significantly throughout the reaction (Figure 4.9), which indicates that no change in the structure of the catalysts happened during the tests. It can also

be noted that our nanoparticles were stable for many days at 120 °C, even the unsupported nickel silicide colloid.

A silicon balance was calculated for both catalytic tests by dividing the sum of all detected Si atoms in the reaction mixture per the sum of all Si atoms in the starting mixture:

$$\text{Si balance} = \frac{\sum n_{\text{Si(products)}}}{\sum n_{\text{Si(starting mixture)}}}$$

For both catalytic tests, the Si balance decreased over time (Figure 4.10), and reached 80% after 700 h of reaction, meaning that not all products were dectected. This could be due to the lighter products of silane redistribution that could be neither detected nor quantified. These lighter redistribution production may also have oligomerized or polymerized to heavier products, not detectable by gas chromatography. Indeed, the formation of Si – Si bonds from Si – H bonds by dehydrogenative condensation in the presence of hydrosilylation catalysts is known.[206] This mass balance decrease may also have arised from evaporation/leaking of volatile products, because the reactor was at a slightly positive pressure at 120 °C and the reaction times were very long.

[206] K. A. Brown-Wensley, *Organometallics* **1987**, 6, 1590–1591.

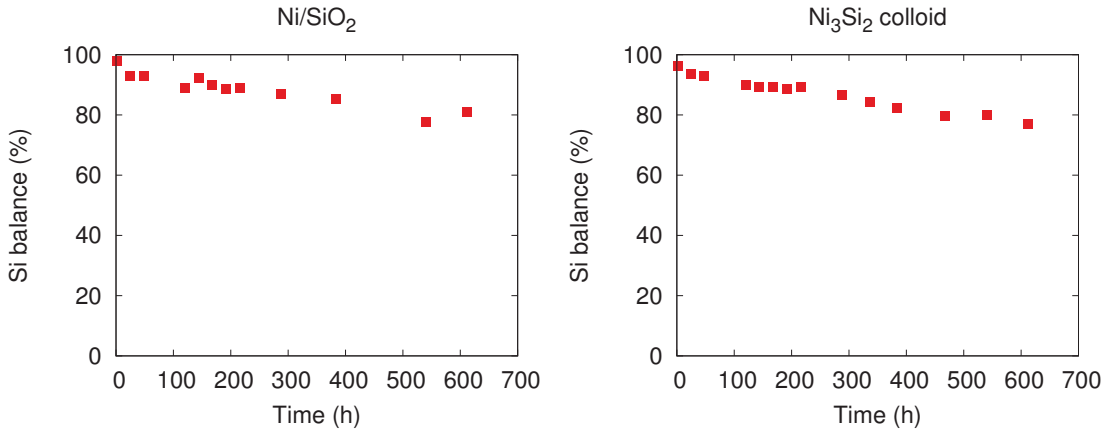


Figure 4.10: Evolution of the Si balance with time.

4.2.3 Tests with MD'M and 1-octene

We then tested our nickel catalysts in the reaction between MD'M and 1-octene (Figure 4.11), a model reaction for the functionalization of polymethylhydrosiloxanes.

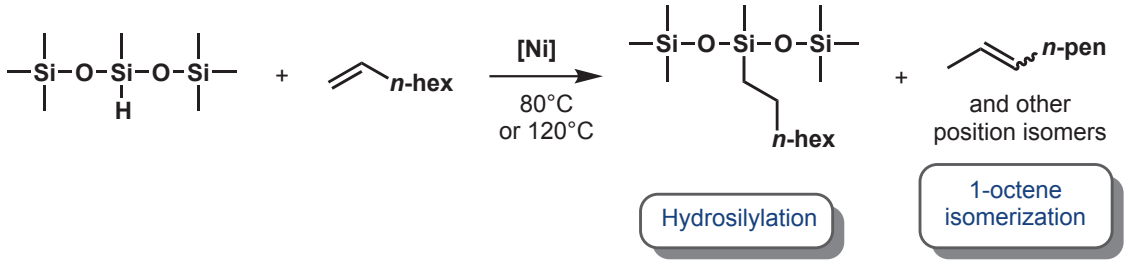


Figure 4.11: Reaction between MD'M and 1-octene.

We didn't observe any formation of hydrosilylation product, but 1-octene isomerization to 2-octenes, 3-octenes and 4-octenes, as determined by GC-MS. This isomerization of terminal alkenes to more thermodynamically stable

alkenes is common in hydrosilylation reactions, and has already been observed for nickel catalysts.[96,107]

The Ni_3Si_2 colloid was more active than Ni/SiO_2 at identical total Ni concentration, as shown in Figure 4.12. In all our catalytic tests with 1-octene and MD'M, it was observed that 1-octene conversion never reached more than 97%, which may be the thermodynamical equilibrium.

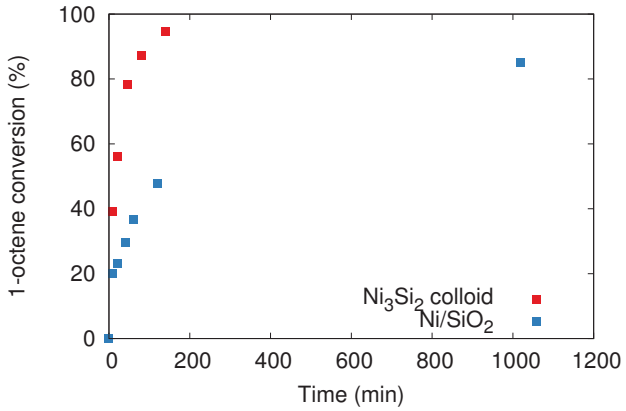


Figure 4.12: Kinetic profile of 1-octene isomerization. 1-octene/Ni = 1/0.01, 80 °C.

We observed that isomerization did not happen in absence of MD'M (Table 4.2, entry 2), meaning that a Ni hydride intermediate is involved in the isomerization mechanism, and that the Lewis acidity of Ni alone is not sufficient to allow isomerization. Moreover, no reaction at all was observed with NiO NPs, meaning that a Ni(0) precatalyst is needed, and that NiO could not be reduced to metallic Ni(0) by MD'M in these conditions.

Table 4.2: Catalytic tests with nickel catalysts. 1 mol% Ni, 50 °C, 1 h.

Entry	Cat.	Conv. SiH	Conv. 1-oct	Comments
1	Ni_3Si_2	<1%	34%	MD'M
2	Ni_3Si_2	-	2%	No MD'M
3	NiO	<1%	<1%	MD'M

In table 4.3, it is shown that Ni_3Si_2 NPs are able to reach almost isomerization equilibrium at room temperature (entry 1). It is also shown that with only 0.1 eq of MD'M it is possible to isomerize about 90% of 1-octene at room temperature (entry 3) or 80 °C (entry 4), further confirming that the role of MD'M is solely to activate nickel as Ni – H.

Table 4.3: Tests with Ni_3Si_2 colloid on the MD'M + 1-octene reaction. 18 h, Ni/SiH = 1%.

Entry	Temp.	Conv. SiH	Conv. 1-oct	Comments
1	RT	0%	95%	1 eq MD'M
2	80 °C	0%	97%	1 eq MD'M
3	RT	0%	87%	0.1 eq. MD'M
4	80 °C	0%	92%	0.1 eq MD'M

4.2.4 Other catalytic tests

We used triethylsilane (Et_3SiH) and 1-octene (Figure 4.13 and Table 4.4), to see if alkylsilanes had a different reactivity from hydrosiloxanes. We observed no

hydrosilylation product, but we did see 1-octene isomerisation as when using MD'M as SiH reagent, along with a small triethylsilane conversion (13–28%), without seeing any product appearing in the GC chromatograms at higher retention times. This apparent conversion may be due to some evaporation (the boiling point of triethylsilane is 107 °C, close to the reaction temperature of 80 °C) during the sampling for GC analysis.

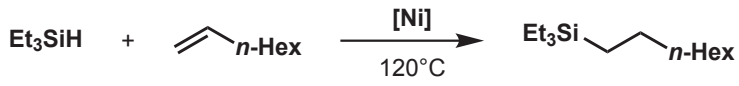


Figure 4.13: Reaction between triethylsilane and 1-octene.

Cat.	Conv. Et_3SiH	Conv. 1-octene	Yield octene isomers
Ni/SiO_2	28%	73%	69%
Ni_3Si_2	13%	93%	92%

Table 4.4: Nanostructured nickel catalysts tested with Et_3SiH and 1-octene. 1 mol% Ni, 80°C, 18 h.

We hypothesized that no hydrosilylation was observed with 1-octene because the rate of isomerization was much higher than the rate of hydrosilylation. Therefore, we used MD'M and $MD^{vi}M$ instead of 1-octene (Figure 4.14, Table 4.5), in order to determine if using a non-isomerizable alkene would allow us to observe hydrosilylation activity. Moreover, vinylsilanes are known to have different reactivities than alkenes. Unfortunately, we observed no catalytic activity at all.

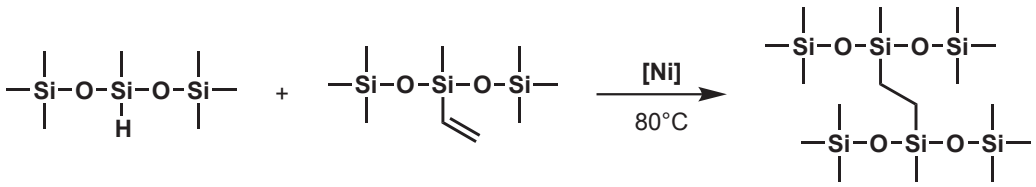


Figure 4.14: Reaction between $MD^{vi}M$ and MD'M.

Cat.	Conv. MD'M	Conv. $MD^{vi}M$
Ni/SiO_2	1%	4%
Ni_3Si_2	0%	1%

Table 4.5: Tests with nanostructured nickel catalysts with MD'M and $MD^{vi}M$. 1 mol% Ni, 80°C, 18 h.

Finally, we tested M'_2 (Figure 4.15), a siloxane with two adjacent SiH functionnalities, a property which is known to influence the catalytic activity in some cases.[40] We also observed 1-octene isomerization, along with a significant M'_2 apparent conversion (32–53%) but no formation of the hydrosilylation product (Table 4.6). As with triethylsilane, we strongly suspect that this is due to evaporation of M'_2 (boiling point : 70 °C) during sampling and not because of a chemical reaction.

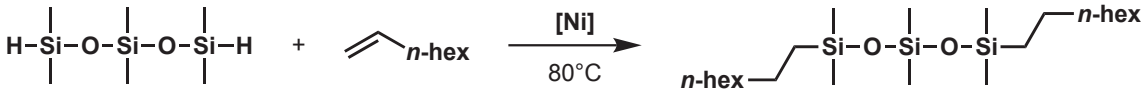


Figure 4.15: Reaction between M'_2 and 1-octene.

Table 4.6: Nanostructured nickel catalysts tested with M'_2 and 1-octene. 1 mol% Ni, 80°C, 18 h.

Cat.	Conv. M'_2	Conv. 1-oct	Yield octene isomers
Ni/SiO_2	32	10	10
Ni_3Si_2	53	97	97

4.2.5 Postulated mechanisms

We have postulated mechanisms to account for the formation of each of these products. They are not backed by mechanistic studies, but can serve at a basis for further studies, and are constructed with mechanistic steps that are common with metals such as nickel and the substrates that we have used.

Alkene isomerization, hydrosilylation, dehydrogenative silylation and hydrogenation

The most common hydrosilylation mechanisms, Chalk-Harrod (developed for noble metals such as Pt) and modified Chalk-Harrod (developed for Cobalt), differ by the mode of insertion of the alkene, as discussed in Chapter 1.

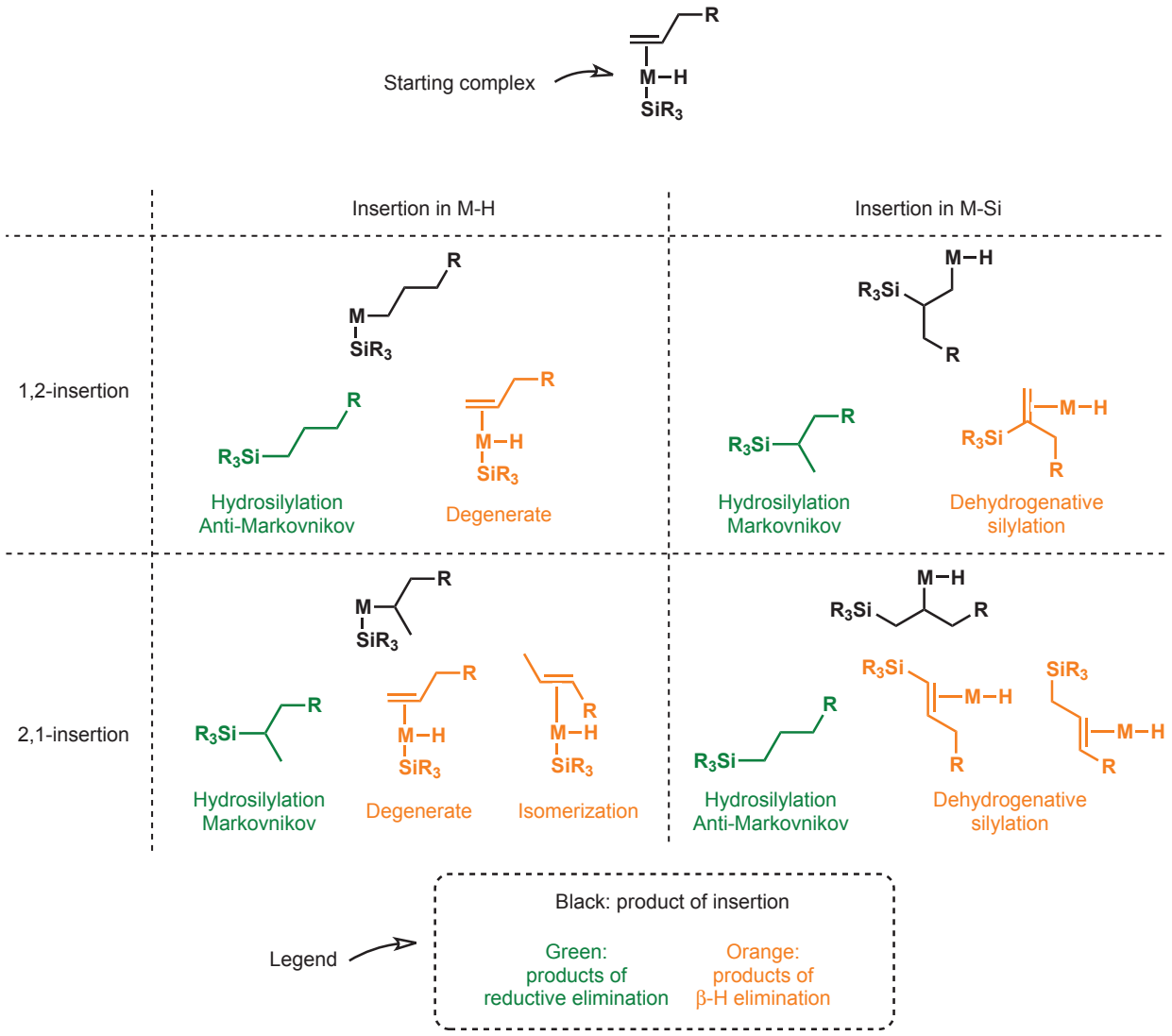


Figure 4.16: Possible alkene insertion modes for a $Ni(H)(SiR_3)$(alkene) complex, and subsequent products of reductive elimination or β-H elimination.

In Figure 4.16, we have drawn all the complexes that could result from insertion of 1-octene in a Ni(H)(SiR_3)(alkene) (obtained by oxidative addition of a SiH reagent and coordination of an alkene molecule) and the subsequent products of β-H elimination and reductive elimination of these complexes. From the products obtained in a catalytic test, we can then suggest which insertion modes are more or less plausible.

If the alkene undergoes 1,2-insertion in the Ni – H bond, the reductive elimination gives the anti-Markovnikov hydrosilylation product and the β-H elimination is degenerate (it gives back the starting complex). If it undergoes 2,1-insertion in the Ni – H bond, it can give the Markovnikov product by reductive elimination, and the β-H elimination can either be degenerate or give the isomerized alkene. If the alkene undergoes 1,2-insertion in the Ni – Si bond, it can either give the Markovnikov hydrosilylation product by reductive elimination or the dehydrogenative silylation product bearing a 1,1-disubstituted C = C bond. Finally, if the alkene undergoes 2,1-insertion in the Ni – Si bond, it can give either the anti-Markovnikov hydrosilylation product by reductive elimination, or two different dehydrogenative silylation products by β-H elimination.

We then postulated a mechanism for the observed octene isomerization (Figure 4.17), where the resting state is a Ni(H)(SiR_3) species, the alkene undergoes 2,1-insertion in the Ni – H bond, followed by β-H elimination.

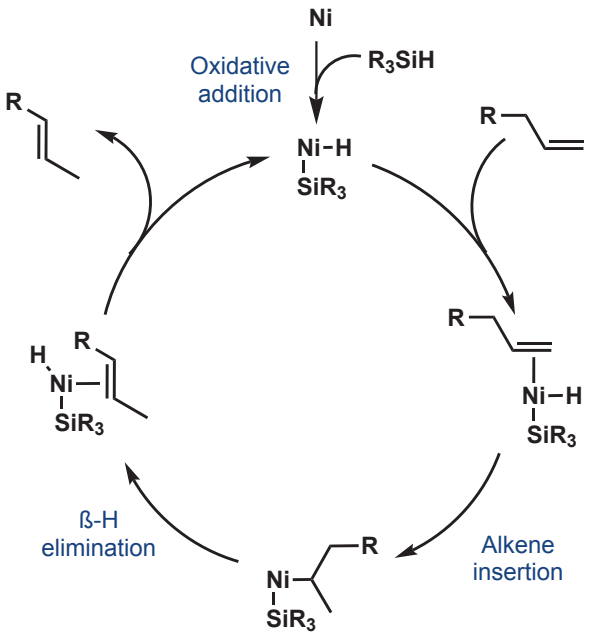


Figure 4.17: Postulated mechanism for alkene isomerization.

Interestingly, given that 3-octene and 4-octene were observed, it suggests that insertion of internal alkenes in the Ni – H bond could happen, and that the absence of products of hydrosilylation of internal alkenes would be caused by the inability to perform reductive elimination from a Ni(alkyl)(silyl) intermediate when the alkyl group is not linear.

For the observed anti-Markovnikov hydrosilylation, after oxidative addition of the SiH reagent and coordination of the alkene, the complex would either undergo 1,2-insertion of the alkene in the Ni – H bond or 2,1-insertion in the Ni – Si bond, followed in both case by reductive elimination (Figure 4.18).

Since the isomerization is much faster than hydrosilylation for our Ni catalysts, we can hypothesize that if 1,2-insertion in the Ni – H bond happens, the β-H elimination is largely favoured. Thus, to account for hydrosilylation, the 2,1-insertion in the Ni – Si bond seems more plausible. This is also coherent with the modified Chalk-Harrod mechanism (see Figure 1.25 in Chapter 1), which has been developed for cobalt (which is just near nickel in the periodic table) and features an alkene insertion in the M – Si bond.

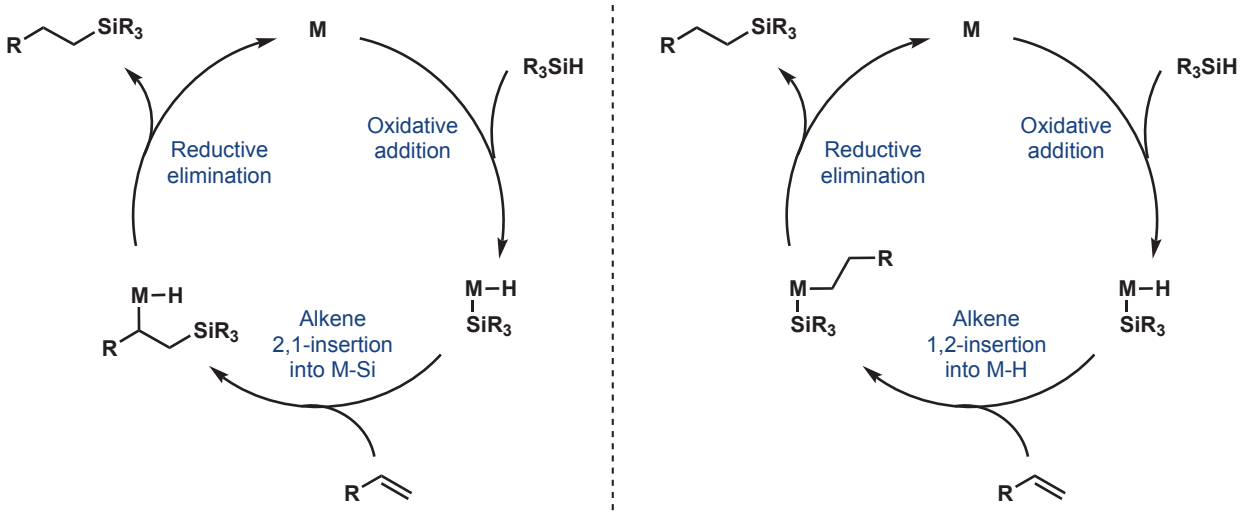


Figure 4.18: Two possible mechanisms for hydrosilylation.

For dehydrogenative silylation (Figure 4.19), we postulate that a Ni(0) center undergoes oxidative addition of the SiH reagent and coordination of the alkene, 2,1-insertion of the alkene into the Ni – Si bond and β-H elimination to give the dehydrogenative silylation product and a $Ni(H)_2$ center. This $Ni(H)_2$ center can either produce molecular H_2 by reductive elimination or hydrogenate an alkene molecule. In our case, the hydrogenation product is formed in significant quantities.

It suggests that controlling the relative rates of these insertion reactions and the following β-H elimination or reductive elimination would be the key to obtaining selectively hydrosilylation.

Silane substituent metathesis

For the silane substituent metathesis, we envisionned two mechanisms (Figure 4.20). The first mechanism involves oxidative additions of both an SiH bond and a Si-OR bond on the Ni center, followed by reductive eliminations of a tetraalkoxysilane and a dialkoxysilane. This mechanism involves a Ni(IV) center, which is seldom observed. The second mechanism, which seems more plausible, involves oxidative addition of an SiH bond on the Ni, followed by σ-bond metathesis and reductive elimination of a tetraalkoxysilane molecule.

Vinylsilane dimerization

The mechanism that we postulate for vinylsilane dimerization (Figure 4.21) involves a $Ni(H)(SiR_3)$ resting state, obtained by oxidative addition of a SiH on a Ni(0) center. The first step of the cycle is an insertion of a vinylsilane in a

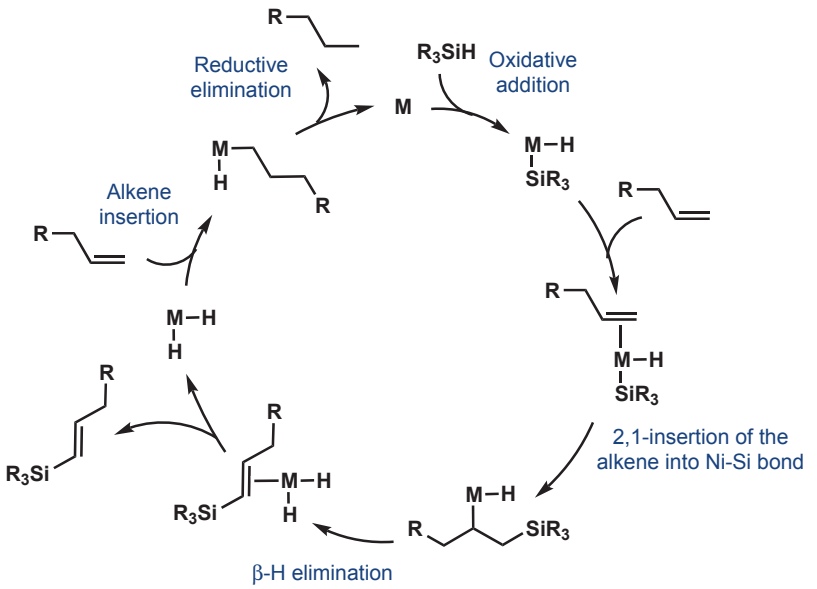


Figure 4.19: Postulated mechanism for dehydrogenative silylation, accompanied by production of H_2 or alkene hydrogenation.

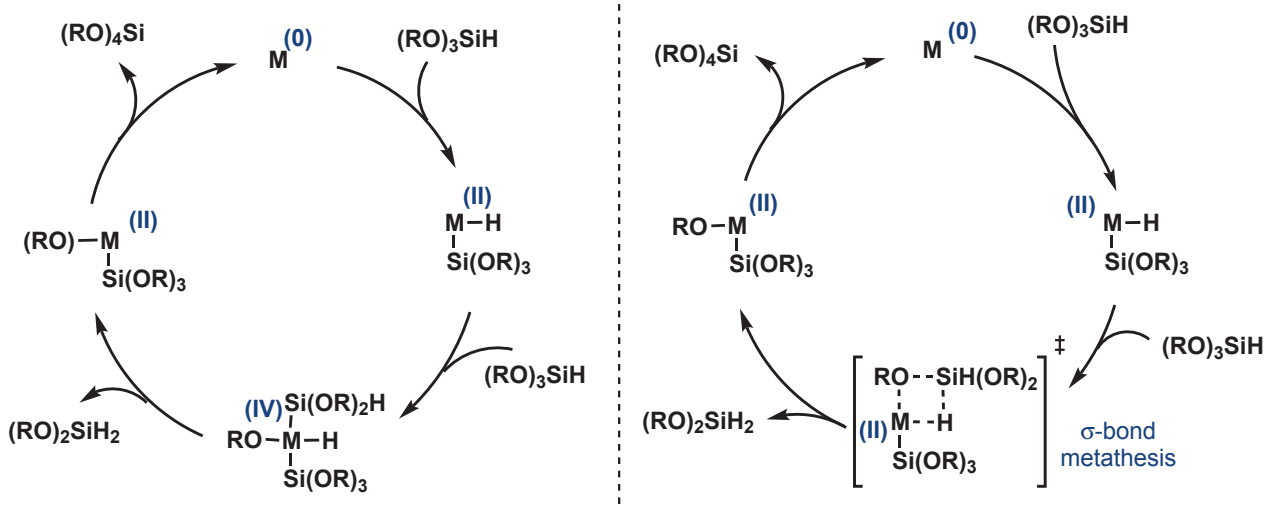


Figure 4.20: Postulated mechanisms for silane substituents metathesis.

Ni – H bond, followed by the insertion of a second vinylsilane molecule in the newly formed Ni – C bond and β-H elimination. Both linear and branched products of dimerization are detected, meaning that vinylsilane insertion can happen in 1,2- or 2,1- fashion.

4.2.6 1-octene hydrogenation

Nickel is a well known catalyst for the hydrogenation of various functional groups, with a history that is more than centenary.[207,208]

As our Ni/SiO_2 solid comprises Ni(0) NPs, we expected that it would be active in the hydrogenation of alkenes such as 1-octene (Figure 4.22). Indeed, after 17 h at 80 °C, with 3 bar of H_2 and a Ni/1-octene ratio of 0.05%, full conversion of 1-octene to *n*-octane was obtained, corresponding to a TON of 2000.

[207] P. Sabatier. *La Catalyse en chimie organique*. ed. by C. Béranger (Paris ; Liège) 1913.
[208] M. Raney *Method of producing finely-divided nickel* 1927

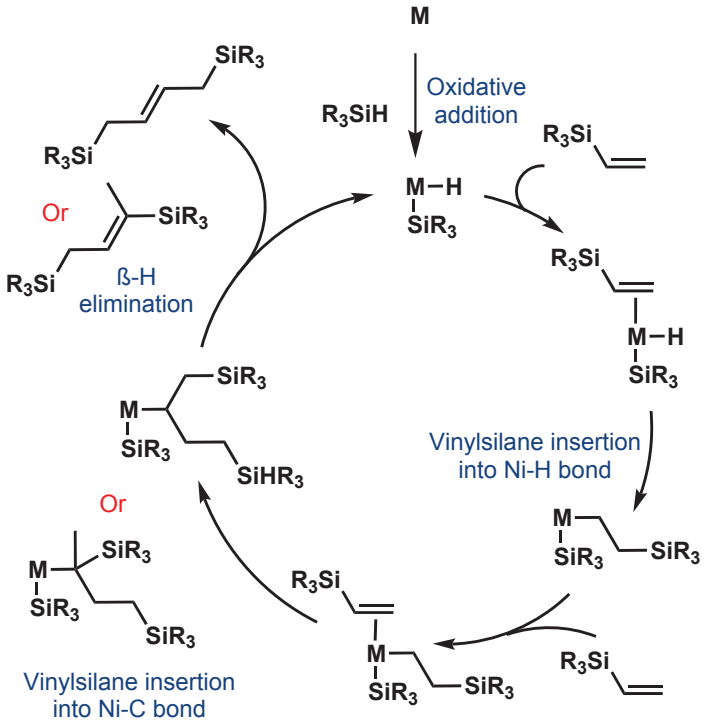


Figure 4.21: Postulated mechanism for vinylsilane dimerization.

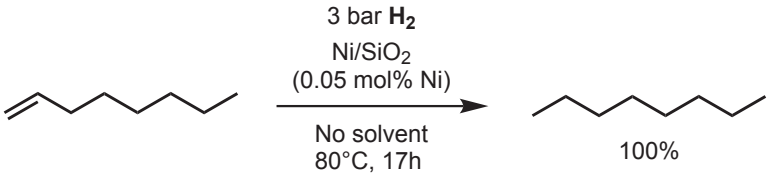


Figure 4.22: 1-octene hydrogenation with our Ni/SiO_2 catalyst.

Although this experiment alone does not allow to compare our catalyst with the state of the art, it shows that it is active as expected. A study dedicated to the comparison of various kinds of Ni NPs, including this one, is underway in our laboratory.

4.3 Conclusion

To conclude, we reported an application of small and well-defined Ni nanoparticles as catalysts for alkene hydrosilylation. Using a model reaction of triethoxyvinylsilane with triethoxysilane, a challenging reaction from a selectivity standpoint, we showed that completely different selectivities could be obtained depending on the environment of Ni atoms. These results suggest that exploring diverse environments for Ni atoms could lead to improved selectivities and/or activities, for example by alloying nickel with other transition metals or other elements.

With the MD'M + 1-octene catalytic test, only octene isomerization was observed. The reaction was fast, needing only substoichiometric quantities of MD'M to proceed but didn't happen when MD'M was absent, suggesting that nickel needs to be activated to Ni-hydride by MD'M in order to be active.

Other substrates were also tested, but led to either 1-octene isomerization (when it was used as the alkene) or no reaction at all.

This work opens a new path for durable alkene hydrosilylation catalysts, based on non-noble nickel nanoparticles. To achieve practically usable nickel NP catalysts, it will be necessary to explore a variety of other nickel phases, and it will also be important to study and understand the mechanism of the reaction (using for instance deuterated silanes) to be able to rationally design more selective and active catalysts.

4.4 Experimental

All the catalysts were synthesized based on protocols published by our group.[159]

4.4.1 Synthesis of NiSi nanoparticles

$Ni(COD)_2$ (45 mg, 164 μmol) was weighed in a Fischer-Porter reactor in a glovebox. The reactor was taken out of the glovebox, and toluene (48 mL) was added. Once the $Ni(COD)_2$ was dissolved (light yellow solution), a 20 mg/mL solution of *n*-octylsilane in toluene was prepared, and 2.4 mL of this solution (48 mg of *n*-octylsilane, 330 μmol) were introduced in the reactor. The solution was stirred 30 min. at room temperature, turning lightly brown, then heated at 55°C and pressurized with 4 bar of hydrogen (absolute pressure) and stirred overnight. A dark brown solution (3.28 μmol Ni/mL) was obtained.

4.4.2 Synthesis of NiO nanoparticles

20 mL of a NiSi nanoparticle suspension were gently bubbled with dry air during 2 min., giving an almost transparent solution.

4.4.3 Silica preparation

15 g of hydrophilic fumed silica Evonik Aerosil® 200 (specific surface area 200 m^2/g) were suspended in deionized water to form a gel. Once visually homogeneous, the gel was put into a 100°C oven during 5 days, then crushed and sieved (40–90 μm). The powder was calcined at 500°C under a flow of 40 mL/min. of dry air during 8 h.

4.4.4 Synthesis of Ni(0) nanoparticles on silica

25 mL of a NiO nanoparticles solution (3.28 μmol Ni/mL) were concentrated under reduced pressure to 2.2 mL. 1.8 mL of this solution was used to impregnate (incipient wetness impregnation) 1 g of prepared silica. The powder was dried under an argon flow overnight, then calcinated under dry air (80 mL/min, 2°C/min ramp, 500°C during 1h), and finally reduced under a hydrogen flow (80 mL/min, 2°C/min ramp, 500°C during 4h).

4.4.5 Ni_3Si_2 colloidal solution DOSY

The diffusion-ordered spectroscopy spectrum was acquired at the Centre Commun de RMN of Université Lyon 1 at 298 K on a AV 500 MHz Avance III Bruker spectrometer.

The Ni_3Si_2 colloidal solution was evaporated to dryness, then redissolved in C_6D_6 and transferred in a NMR tube equipped with a J. Young valve under argon.

4.4.6 Catalytic tests

Catalytic tests were performed in Schlenk tubes, under an atmosphere of argon. All reagents/solvents were dried on activated 3 angström molecular sieves. The reactive mixture was prepared in a schlenk tube by mixing the internal standard, solvent, SiH and alkene. This mixture was degassed with three freeze-pump-thaw cycles. A known quantity of this mixture was then introduced in a Shlenk tube containing the catalyst. Aliquots of the reaction mixture were taken regularly, exposed to air to quench the catalyst, filtered on 200-300 nm syringe filters in the case of heterogeneous catalysts, and analyzed by gas chromatography.

4.4.7 Gas chromatography

See Appendix C at the end of the manuscript.

4.5 Appendices

4.5.1 Hydrogen chemisorption

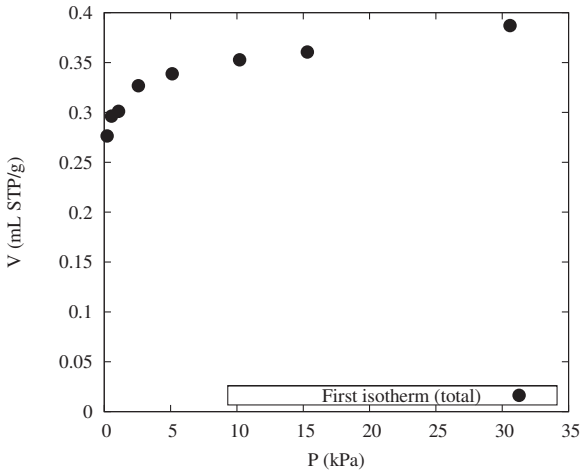


Figure 4.23: Hydrogen chemisorption isotherm of a Ni/SiO_2 0.5% solid. The corresponding dispersion was calculated to be 39%, corresponding to a mean size of Ni particles of 2.9 nm.

4.5.2 Particle size histogram

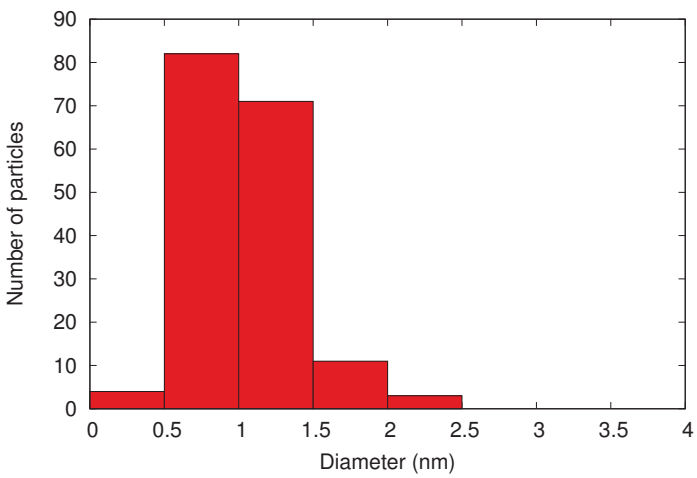


Figure 4.24: Particle size histogram of the Ni/SiO_2 solid, from STEM images.

5

Iron nanoparticles

Mössbauer spectroscopy was performed by Moulay-Tahar Sougrati (Institut Charles Gerhardt, Montpellier).

5.1 Introduction

In alkene hydrosilylation catalysis, iron has been mostly studied as complexes, as shown in subsection 1.5.3. Early examples involved iron carbonyls, often photoexcitated to create a vacancy by loss of a CO ligand.[71–74] The catalytic performances of these complexes were rather poor. A breakthrough came in 2004 when Chirik *et al.* used an iron-bisiminopyridine complex as catalyst, and obtained high yields and selectivities. In 2012, Chirik published a modified version of this complex, and was able to expand the substrate scope to primary silanes, which are of industrial interest.[16]

Apart from iron complexes, other forms of iron that were reported to be catalytically active for this reaction are scarce. An iron colloid has been studied in 1962,[70] but no characterization of the particles was provided. To our knowledge, small and well-defined iron nanoparticles have never been studied as alkene hydrosilylation catalysts.

Here we present a new synthesis of very small iron nanoparticles, starting from easily accessible commercial products, and the synthesis of several oxidized or reduced Fe/silica solids from this Fe colloid. We also discuss the catalytic tests of these various forms of Fe NPs with several model reactions.

5.2 Results

5.2.1 Fe colloid

For the synthesis of Fe(0) NPs, plenty of methods have been developed,[209] usually based on the reduction of Fe salts, complexes or oxides, or on the decomposition of iron carbonyls. We decided to use the same methodology as our group used for other metal NPs (nickel,[159] platinum[156] and ruthenium[157]): the decomposition of a metal(0) precursor in presence of an organosilane stabilizer. We choose $Fe_3(CO)_{12}$ as Fe(0) precursor since it is commercially available and non-volatile (thus minimizing the danger caused by the toxicity of Fe carbonyls).

[209] D. L. Huber, *Small* **2005**, 1, 482–501.

$Fe_3(CO)_{12}$ was dissolved in toluene, giving a deep green solution (Figure 5.1, left), and *n*-octylsilane was added. The solution was heated up to 60 °C under 4 bar of H_2. After one night under these conditions, no visible change in the color of the solution was observed. We increased the temperature to 80 °C, and the solution turned orange (Figure 5.1, right) after some hours.

Figure 5.1: Synthesis of the Fe(0) colloidal solution.

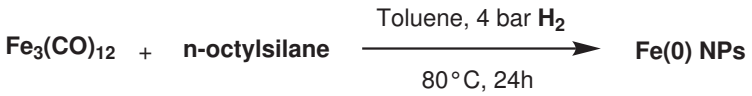
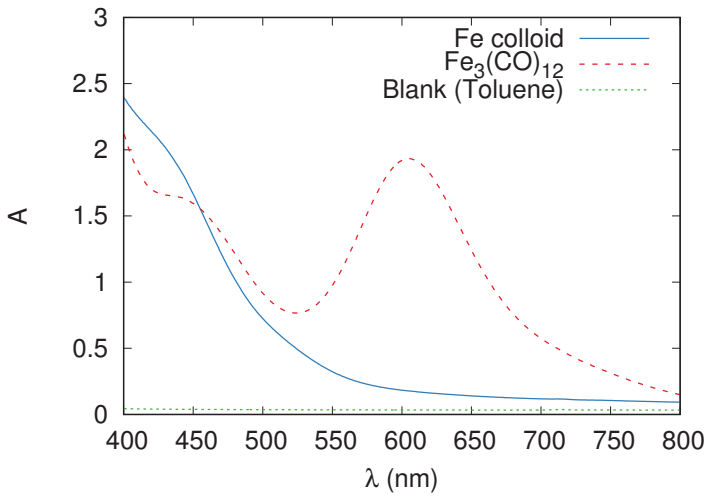


Figure 5.2: Left: $Fe_3(CO)_{12}$ solution in toluene, right: Fe colloidal solution.



The starting solution of $Fe_3(CO)_{12}$ and the final colloid were analyzed by UV-visible spectrophotometry under argon (Figure 5.3). The $Fe_3(CO)_{12}$ showed an absorption band at 605 nm, which was absent in the final colloid, meaning that $Fe_3(CO)_{12}$ had been completely decomposed.

Figure 5.3: UV-visible spectrophotometry of the $Fe_3(CO)_{12}$ precursor and the Fe colloidal solution.



The resulting orange solution was then characterized by STEM. As for Ni NPs, the sample preparation and insertion in the microscope were performed under inert atmosphere, so that the Fe NPs were not oxidized under air. The STEM images showed the presence of small and isolated Fe NPs (Figure 5.4), with an average size of 2.0 nm. The low contrast, due to the low atomic mass of Fe, made the image acquisition difficult and the determination of the average size quite imprecise.

5.2.2 Fe-containing solids

Several Fe-containing solids were prepared from the Fe colloid (Figure 5.5) by incipient wetness impregnation on silica followed by various thermal treat-

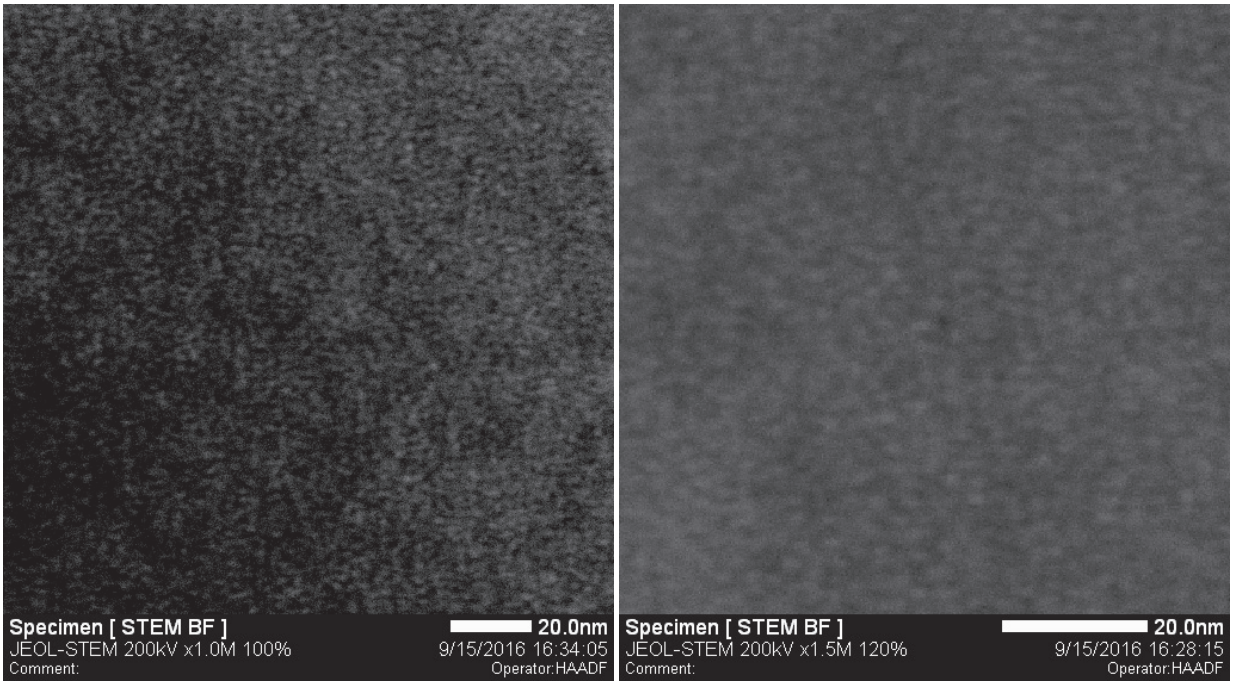


Figure 5.4: STEM of the Fe colloidal solution.

ments, in order to study the catalytic behaviour of Fe in different chemical environments, as was done for Ni NPs in Chapter 4. First, the colloidal solution was impregnated on silica under argon, then dried under vacuum (Figure 5.5, called "RawSolid"), giving a green-brown solid. A second solid, deep brown and called "OxidizedRT", was obtained by dry air oxidation of the "RawSolid" at room temperature. A third solid, orange and called "Oxidized500", was obtained by calcination at 500 °C under dry air flow of the "OxidizedRT" solid. A fourth solid, grey and called "Reduced500", was obtained by reduction of this "Oxidized500" solid under H_2 flow at 500 °C. Finally, a fifth solid, deep grey and called "Reduced500Direct", was obtained by treatment of the "RawSolid" under H_2 at 500 °C (without exposure to air prior to the treatment).

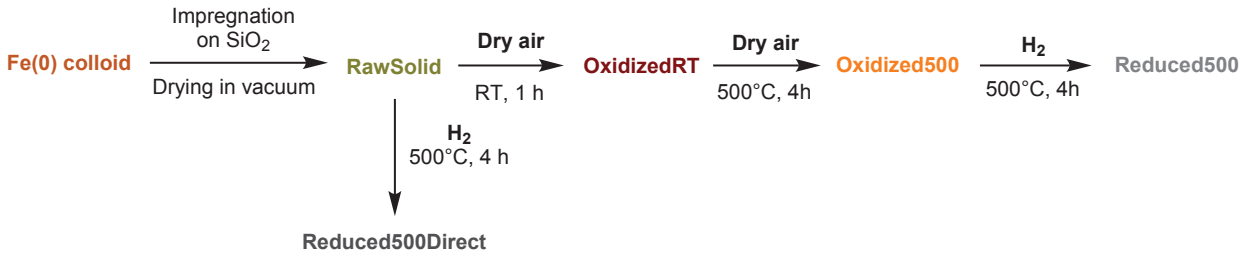


Figure 5.5: Synthesis of Fe-containing solids from the Fe(0) colloid. The text colors are representative of colors of the solids.

Characterization of the Reduced500 solid by TEM (Figure 5.6) and STEM (Figure 5.7) revealed that the particles were mostly small and well-dispersed. Although the contrast was too low to reliably measure a particle size distribution, the particles had diameters around 2.5 nm, with some larger particles of 20 nm to 50 nm, as seen on Figure 5.7 (right).

The Reduced500Direct solid was also characterized by TEM (Figure 5.8), showing Fe NPs with a diameter of mostly 2 nm to 2.5 nm, and no large Fe NPs. However, the contrast was too low to reliably establish a size distribution

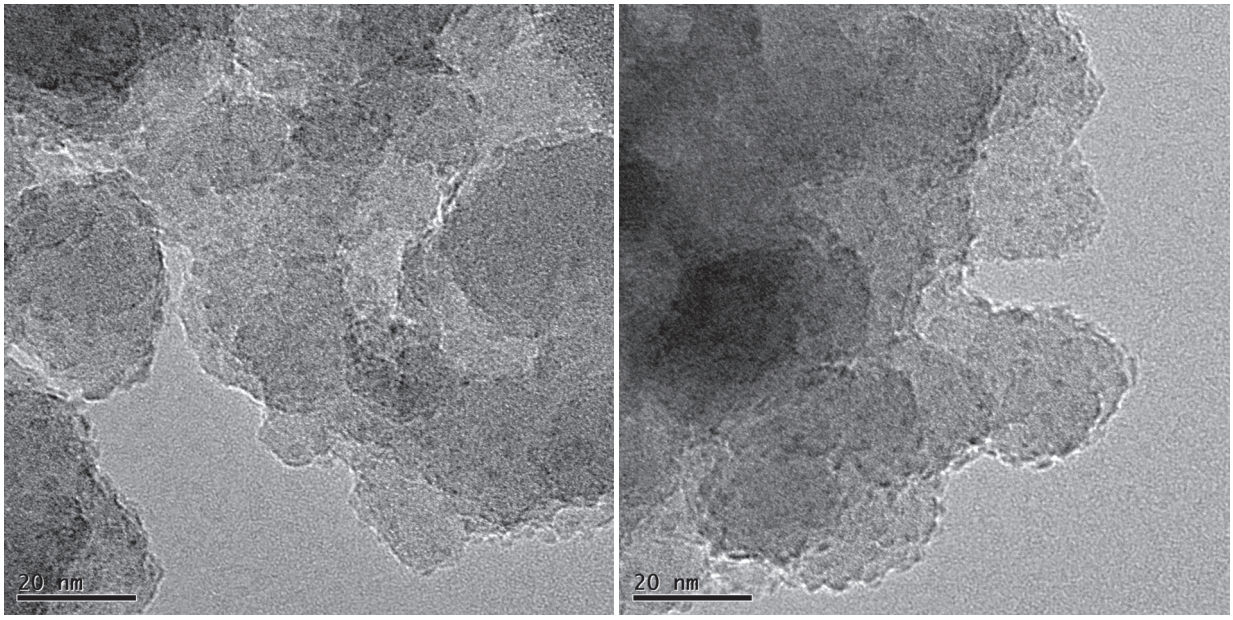


Figure 5.6: TEM of the "Reduced500" solid.

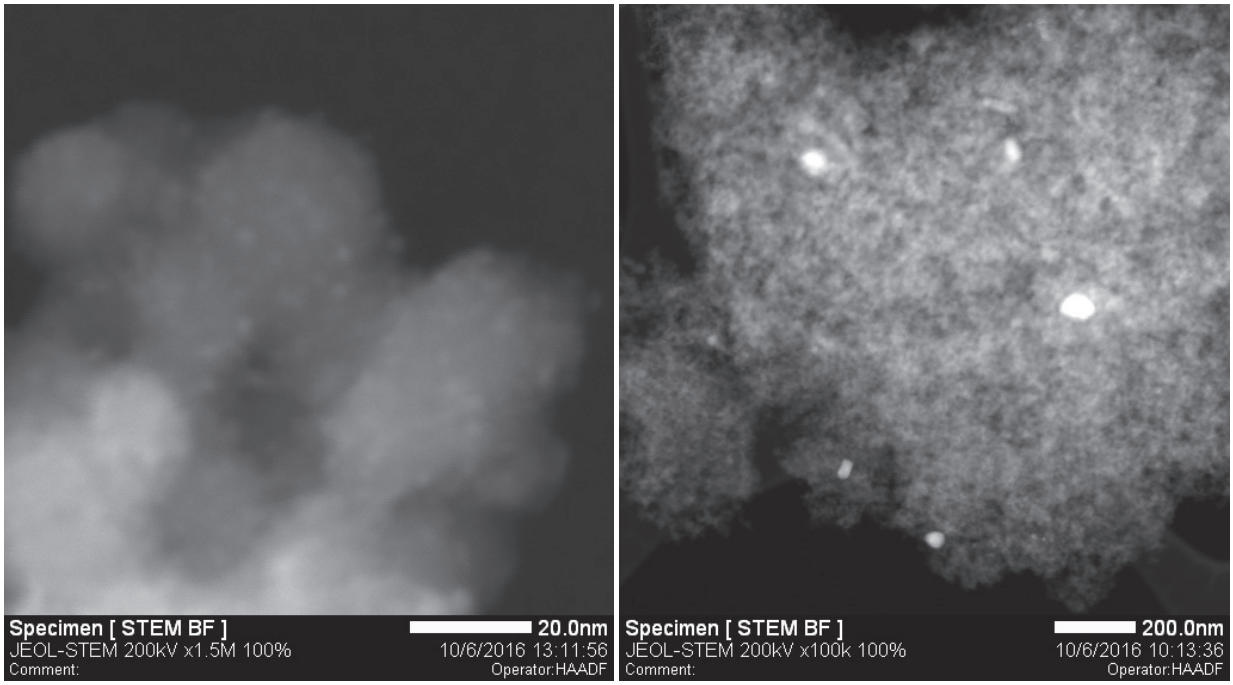


Figure 5.7: STEM of the "Reduced500" solid.

histogram.

Overall, there was no significant difference in the size of Fe NPs between the observed solids, which indicates the absence of sintering during thermal treatments.

The characterization of these Fe NPs-containing solids with a transmission electron microscope having a higher acceleration tension (300 kV) and a spherical aberration correction is currently carried out. Hopefully, this will allow to establish a more precise particle size histogram and to determine the Fe cristallographic phases in order to gather additional structural information.

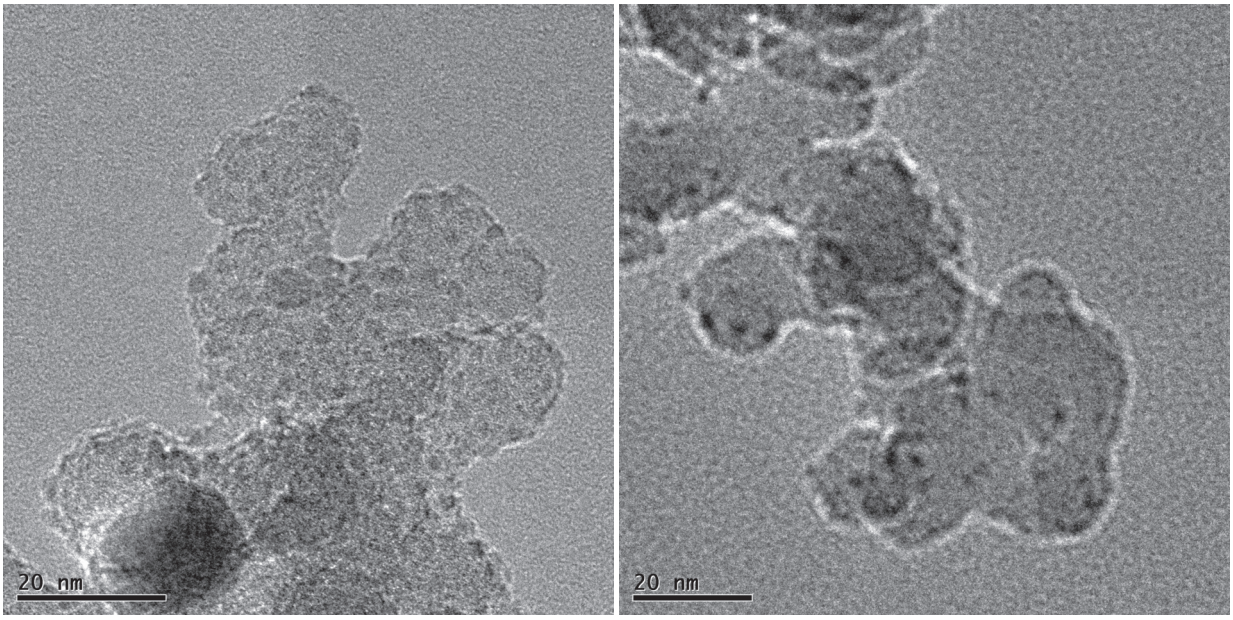


Figure 5.8: TEM of the "Reduced500Direct" solid.

5.2.3 Mössbauer spectroscopy

^{57}Fe Mössbauer spectroscopy was performed at room temperature on the five silica-supported solids (Figure 5.9 and Table 5.1).

		IS (mm/s)	QS (mm/s)	FWHM (mm/s)	Rel. area (%)	Attribution
RawSolid	Fe(c)	−0.05	0.94	0.46	48	Fe(0), superparamagnetic
	Fe(x)	0.19	0.33	0.26	52	Fe silicide
OxidizedRT	Fe(e)	0.33	0.87	0.53	100	Fe(III)
Oxidized500	Fe(e)	0.33	0.87	0.53	62	Fe(III)
	Fe(f)	0.33	1.46	0.44	38	Fe(III)
Reduced500	Fe(c)	−0.05	0.15	0.28	10	Fe(0), superparamagnetic
	Fe(d)	1.02	1.47	0.47	28	Fe(0) surface
	Fe(d)	1.1	1.98	0.52	51	Fe(0) surface
	Fe(d)	0.83	0.87	0.31	11	Fe(0) surface
Reduced500Direct	Fe(c)	−0.03	0.2	0.68	46	Fe(0), superparamagnetic
	Fe(d)	1.24	1.78	0.31	7	Fe(0) surface
	Fe(d)	1.04	1.36	0.33	8	Fe(0) surface
	Fe(d)	0.75	0.80	0.71	39	Fe(0) surface

Table 5.1: IS = isomer shift, QS = quadrupole splitting, FWHM = full width at half maximum. IS is reported relative to α-Fe.

The RawSolid features two contributions. The first, Fe(c), is unambiguously attributed to superparamagnetic Fe(0), that is commonly found with small metallic Fe NPs. The second, Fe(x) has an isomer shift of 0.19 mm/s, which could correspond to an iron silicide.

The OxidizedRT solid features one signal, Fe(e), attributed to Fe(III). This means that even at room temperature, all of the Fe is oxidized to Fe(III).

The Oxidized500 solid is very similar to the OxidizedRT solid, except that another Fe(III) contribution is present, Fe(f), attributed to Fe(III) atoms in a

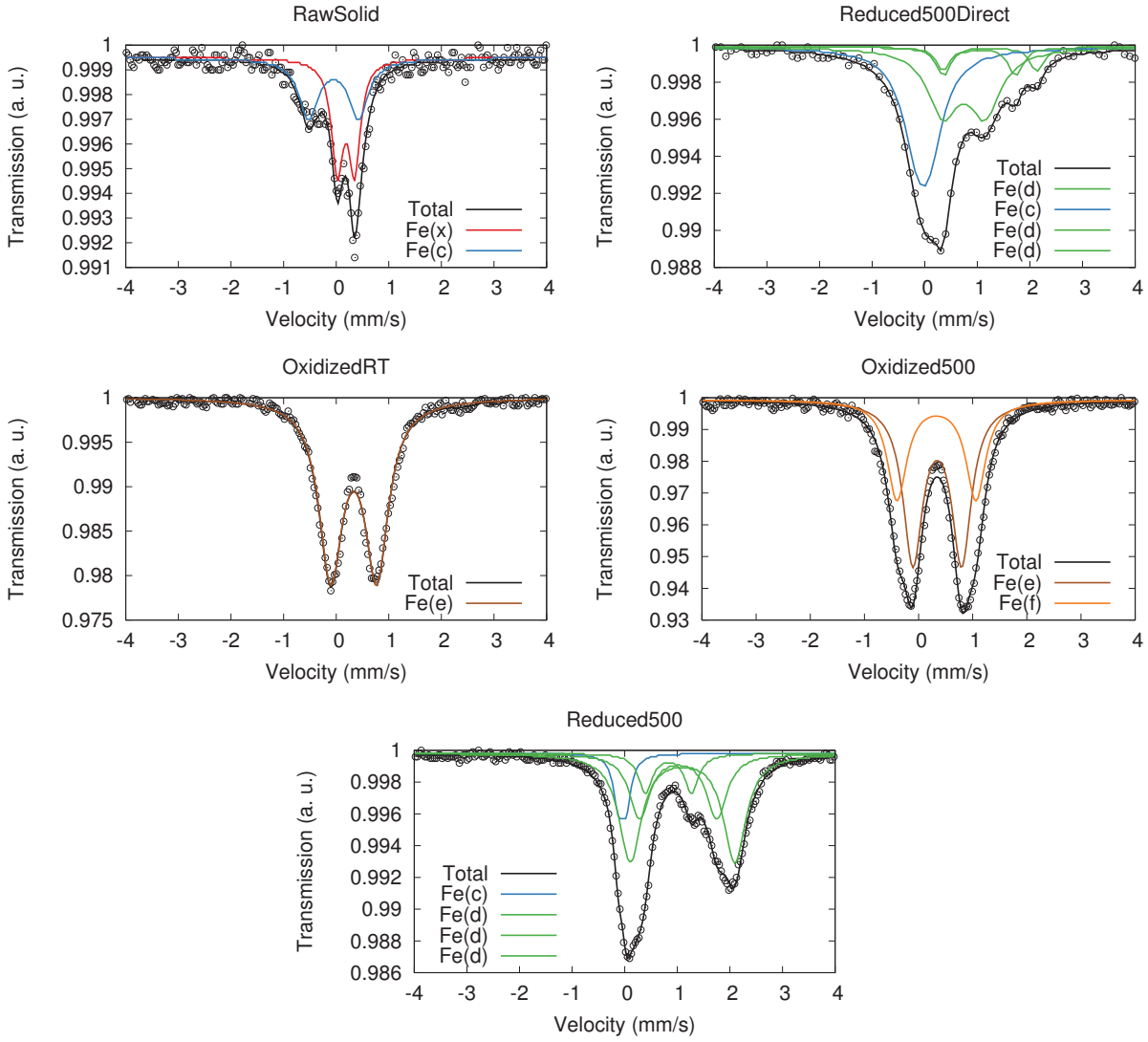


Figure 5.9: Mössbauer spectra.

different environment than Fe(e) atoms. They could for example be atoms at the surface of the NPs, more coordinatively unsaturated than in OxidizedRT, because the stabilizing silane ligands originally present at the surface were removed by the calcination at 500 °C.

The Reduced500 solid features one Fe(c) signal, attributed to superparamagnetic Fe(0), and three Fe(d) signals. These three signals have isomeric shifts that could correspond to high spin Fe(II) centers, or, more likely in our case, to coordinatively unsaturated Fe(0) centers at the surface of the Fe NPs. In 2007, our group used ^{119}Sn Mössbauer spectroscopy to show that surface tin atoms of $PtSn_x/SiO_2$ catalysts gave a signal with a large quadrupole splitting, distinct from the signal of Sn atoms in the bulk $PtSn_x$.[210] This large quadrupole splitting was explained by the "anisotropy of the electron cloud" around the ^{119}Sn nuclei located at the surface of the NPs. Given that our Fe NPs are very small, the metal dispersion is very high, meaning that these surface Fe atoms could be responsible for this important Fe(d) contribution.

The Reduced500Direct has a similar spectrum, with a Fe(c) contribution

[210] J. Candy et al., *Hyperfine Interactions* **2007**, 165, 55–60.

(superparamagnetic Fe(0)) accounting for about half of the Fe atoms and three Fe(d) contributions accounting for the other half of Fe atoms. The attribution of these Fe(d) contributions to surface Fe(0) atoms is even more direct in this case, because the solid has been synthesized from the RawSolid (made of Fe(0)), without any oxidation process in its synthesis. Furthermore, accidental exposure of the sample to air that would have caused its oxidation to Fe(II) can be ruled out. Indeed, during one of our Mössbauer experiment, such an accidental exposure to air has happened, but only one signal corresponding to Fe(III) appeared, meaning that Fe(0) NPs are directly oxidized to Fe(III) NPs when exposed to air. Thus, the H_2 treatment of RawSolid at 500 °C likely causes hydrogenolysis of the stabilizing silane ligands and appearance of coordinatively unsaturated Fe(0) centers that are responsible for the Fe(d) signals. Moreover, the total proportion of Fe(d) signals in Reduced500Direct is 54%, very close to the 52% of Fe(x) (attributed to Fe silicide) in RawSolid, which is coherent with a transformation of the surface Fe atoms.

Mössbauer analysis of the RawSolid and Reduced500 solids at low temperature is planned in order to gain more insight on the Fe phases and confirm our hypothesis on the origin of the Fe(d) contributions.

5.2.4 Tests with MD'M and 1-octene

The reaction of MD'M with 1-octene was used as model catalytic reaction (Figure 5.10). It was conducted in toluene, at 120 °C, with 2 mol% Fe and dodecane as internal standard for gas chromatography analysis.

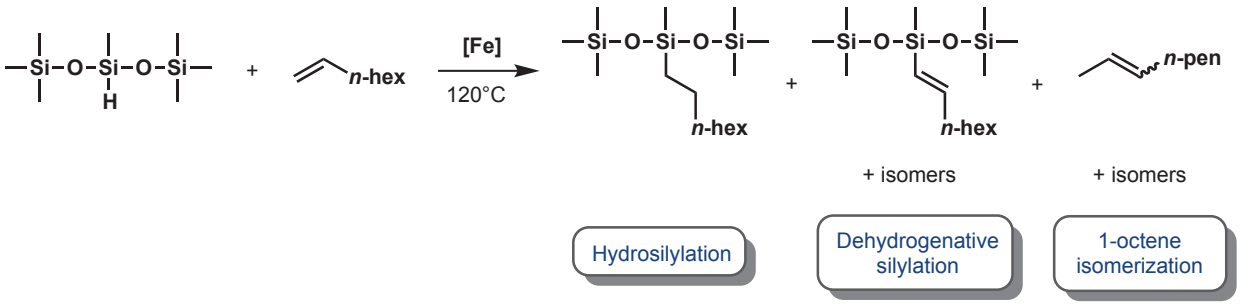


Figure 5.10: Reaction of MD'M with 1-octene.

The RawSolid was first tested as catalyst. Several peaks appeared at retention times similar to that of 1-octene (Figure 5.11). They were identified by GC-MS as being octene isomers. MS fragmentation profiles indicated that 2-octene, 3-octene and 4-octene were present, as *E* and *Z* isomers. At higher retention times, several products were observed (see the zoom in Figure 5.11). GC/MS analysis of the reaction mixture identified the linear product of alkene hydrosilylation (m/z $[M-Me]^+ = 319$ u), accompanied by several products with a mass corresponding to dehydrogenative silylation products (m/z $[M-Me]^+ = 317$ u). These products could be either isomers of position of the C = C bond on the octyl chain or isomers of position of the siloxane on the octyl chain (Figure 5.13). To further characterize these dehydrogenative silylation products we will attempt to separate them by HPLC-MS. If this separation is successful on analytical scale, we will try to apply the same elution conditions on a preparative scale, in order to isolate them in sufficient amounts for NMR analysis.

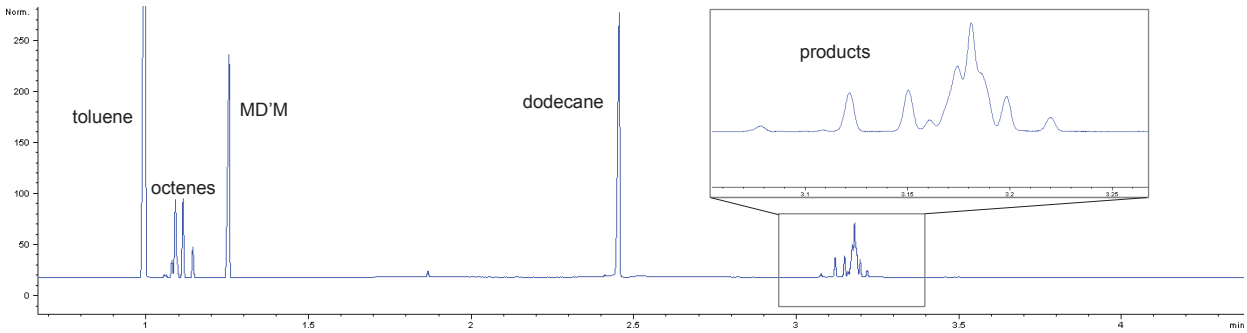


Figure 5.11: Chromatogram of a catalytic test after 24 h.

The yield of hydrosilylation product obtained with RawSolid was quantified by GC-FID to be 26% (Table 5.2, Entry 1), while the yield of dehydrogenative silylation was of 8%. The dehydrogenative silylation reaction is accompanied by either hydrogenation of the alkene or by production of molecular H_2.[98] In our case, no octane was detected by GC-MS, indicating that dehydrogenative silylation was probably accompanied by the production of molecular H_2.

From the kinetic profile of the reaction catalyzed by RawSolid, plotted in Figure 5.14, it is clear that isomerization is much faster than hydrosilylation and dehydrogenative silylation. It can also be observed that octene is consumed by the reactions of hydrosilylation and dehydrogenative silylation, even if it cannot be determined which of the octene isomers is/are consumed.

Entry	Catalyst	Yield HSI	Yield DHSI	Yield Isom
1	RawSolid	26%	8%	69%
2	OxidizedRT	3%	<1%	10%
3	Oxidized500	<1%	<1%	2%
4	Reduced500	<1%	<1%	17%
5	Reduced500Direct	<1%	<1%	97%

Table 5.2: Results of the catalytic tests. HSI: hydrosilylation, DHSI: dehydrogenative silylation, Isom = 1-octene isomerization.

The OxidizedRT solid (Table 5.2, Entry 2) and Oxidized500 solid 500 °C (Entry 3) gave low to null yields, indicating that Fe(0) is necessary as catalyst resting state, and that oxidized forms of Fe are not reduced by the SiH in these reaction conditions.

The Reduced500 solid (Entry 4) did not show hydrosilylation activity. Thus, it seems that the chemical environment of Fe(0) atoms has a crucial influence on catalytic activity for this reaction, as was observed in Chapter 4 for different Ni(0) NPs, which had different selectivities depending on the environment of the Ni(0) centers.

Likewise, the Reduced500Direct solid (Entry 5) showed only isomerization activity, showing a drastic influence of the chemical environment of Fe(0) atoms on activity.

To propose a mechanism that accounts for the production of the hydrosilylation and several dehydrogenative silylation products with the RawSolid, we used a similar reasoning as for nickel catalysts in Chapter 4. In this Chapter, we presented all the ways the alkene could undergo insertion (the Figure 4.16 is inserted again for convenience as Figure 5.15), and the subsequent products

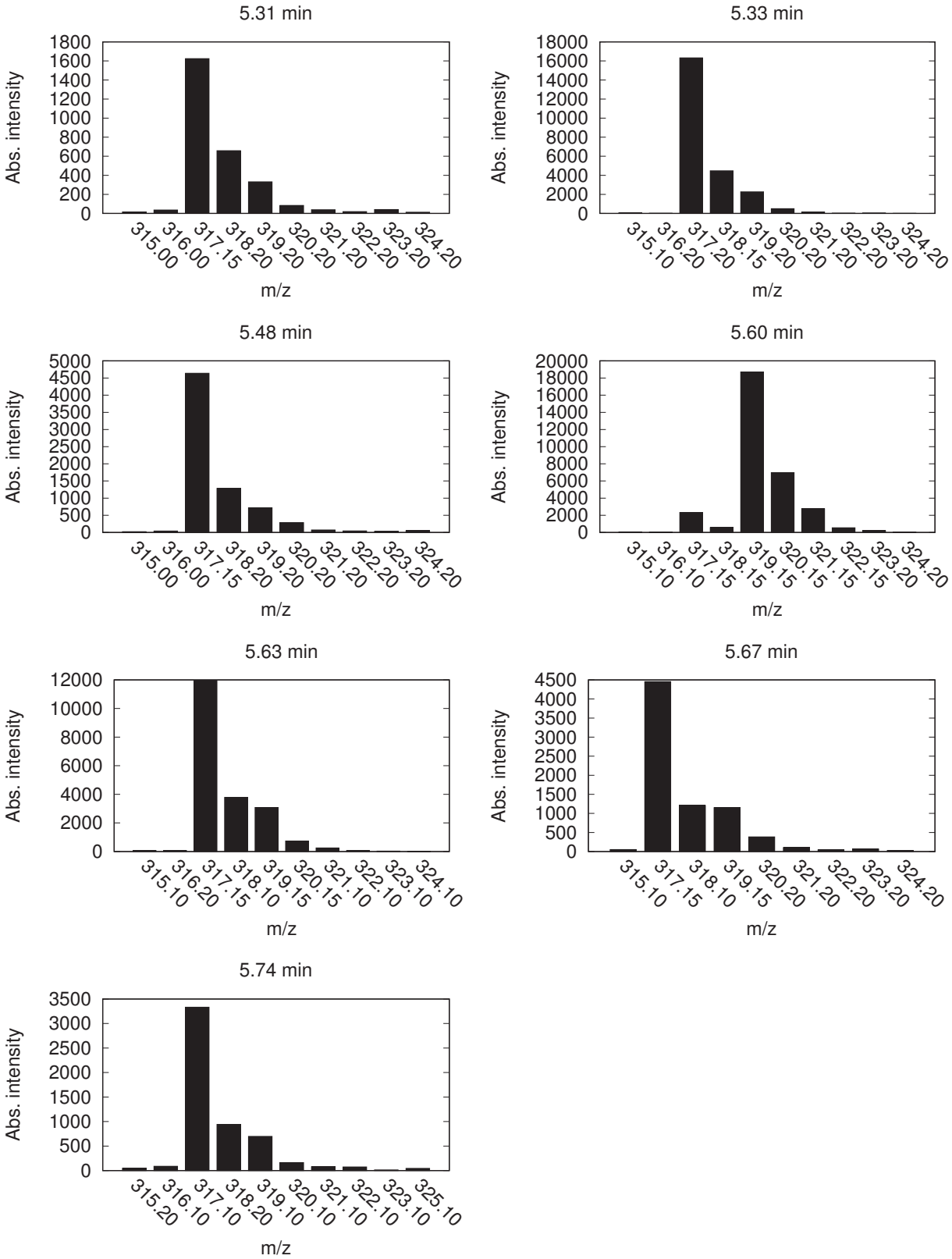


Figure 5.12: GC-MS spectra of the different reaction products with their retention times.

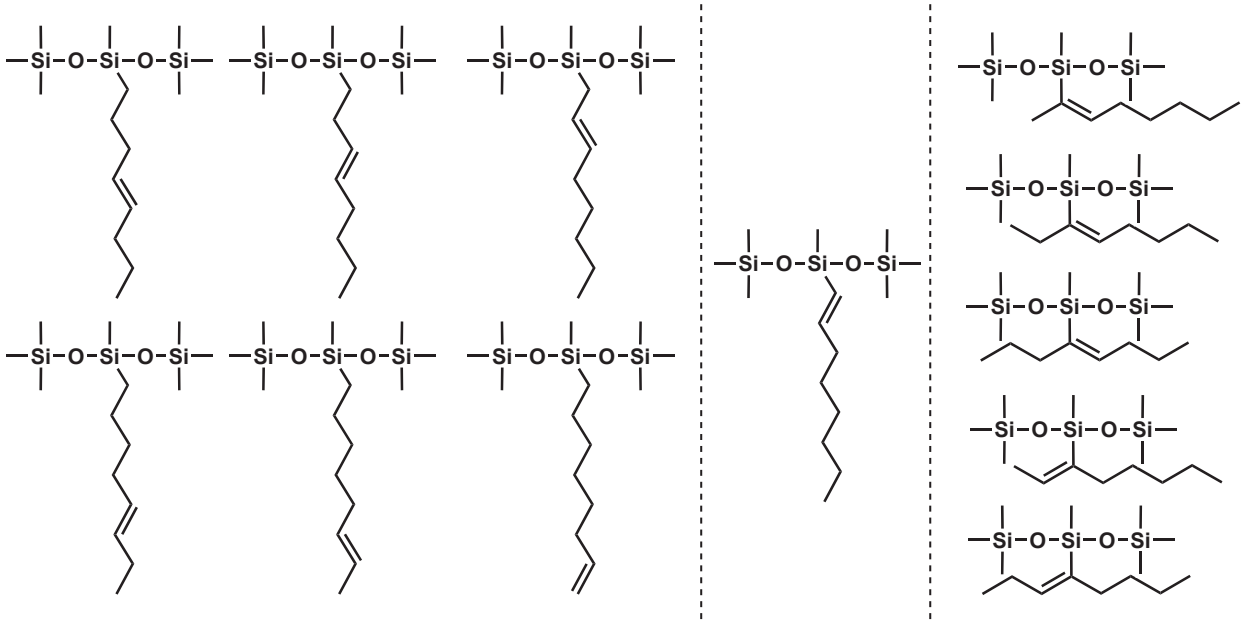


Figure 5.13: Possible products of dehydrogenative silylation. On the left, the isomers differ by the position of the C = C bond on the octyl chain, which is linear. On the right, the isomers differ by the position of the siloxane on the octyl chain.

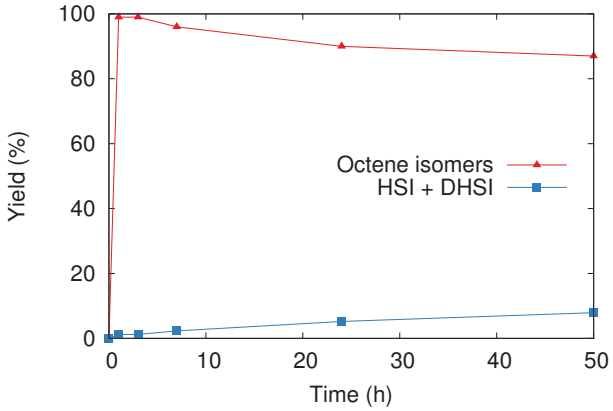


Figure 5.14: Kinetic profile of the reaction of MD'M and 1-octene catalyzed by RawSolid. SiH/1-octene/Fe = 1/1/0.02, 120 °C. HSI = hydrosilylation, DHSI = dehydrogenative silylation. Lines are guide to the eye.

of reductive elimination or β-H elimination.

Given that we obtain the linear hydrosilylation product and that the product of dehydrogenative silylation with the 1,1-disubstituted C = C bond was never reported in the hydrosilylation literature, we can exclude a 1,2-insertion in the Fe – Si bond. Then, the very high rate of alkene isomerization means that a 2,1-insertion in the Fe – H bond is followed by a β-H elimination, also confirmed by the absence of branched hydrosilylation product. Then, given this very high rate of isomerization, we can hypothesize that when the alkene undergoes 1,2-insertion in the Fe – H bond, the β-H elimination is so fast that this path does not lead to hydrosilylation. Thus, to account for the formation of the hydrosilylation and dehydrogenative silylation products, we postulate that the oxidative addition of the Si – H on a Fe(0) site is followed by a 2,1-insertion in the Fe – Si bond, followed by either reductive elimination (giving the hydrosilylation product) or β–H elimination (giving the dehydrosilylation product), as presented in Figure 5.16. However, we cannot fully exclude that

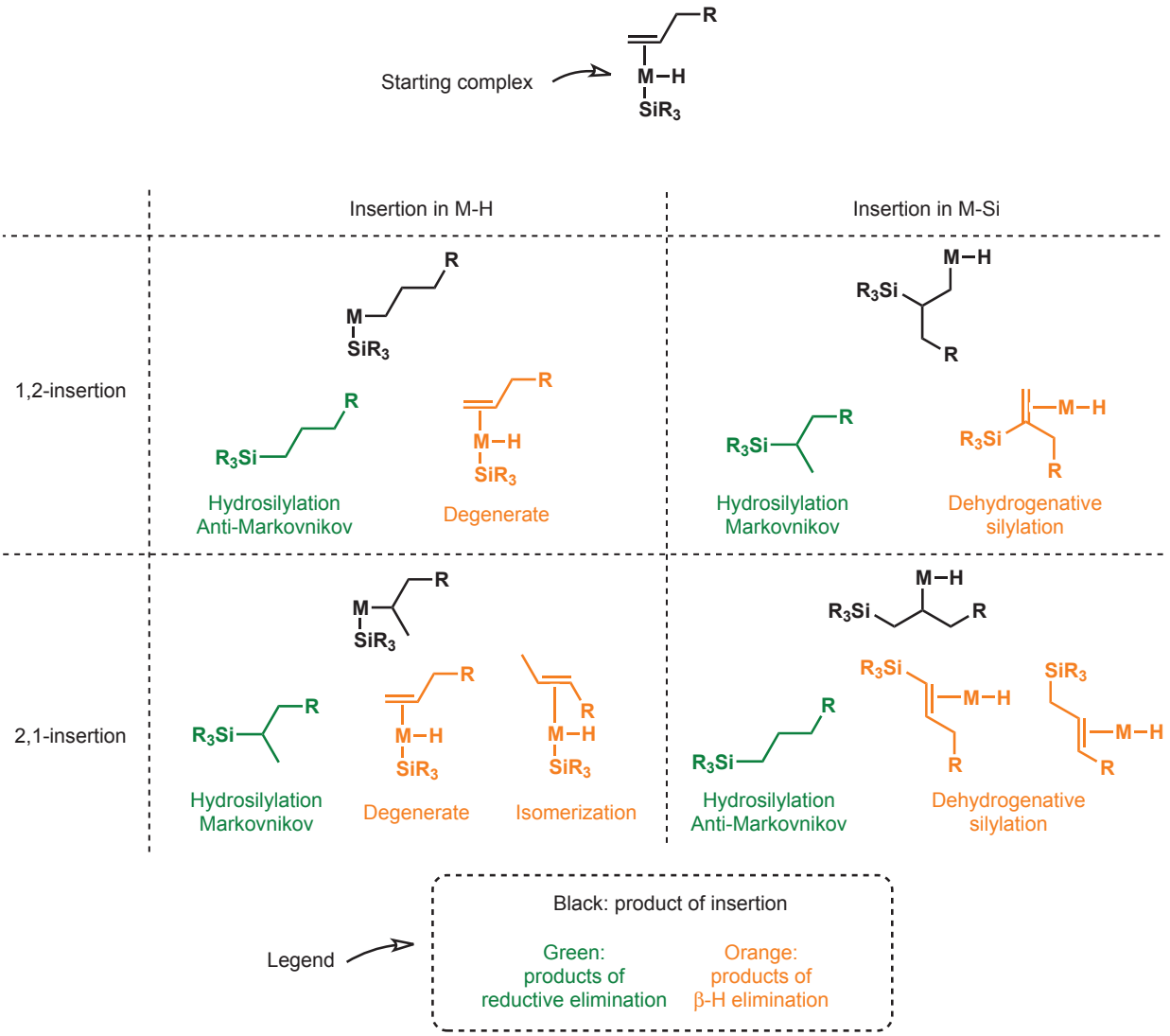


Figure 5.15: Possible alkene insertion modes for a Fe(H)(SiR_3)(alkene) complex, and subsequent products of reductive elimination or β-H elimination.

the hydrosilylation product is produced by 1,2-insertion of 1-octene in the Fe – H bond followed by reductive elimination.

The elucidation of the structure of the dehydrogenative silylation isomers will have implications on the postulated mechanism. If these isomers differ only by the position of the C = C bond on the (linear) octyl chain, it would mean that 1-octene inserts in the Fe – Si bond, followed by β-H elimination, yielding the dehydrogenative silylation product with the C = C bond in α position to the Si atom. The other isomers would then be produced by isomerization of the C = C bond, as happens for 1-octene. At the reverse, if these isomers differ by the position of the siloxane on the octyl chain, it would mean that there is insertion of any of the octene isomers in the Fe – Si bond (which is already suggested by the fact that 1-octene isomerization doesn't stop at 2-octene but also produces 3-octene and 4-octene), followed by β-H elimination.

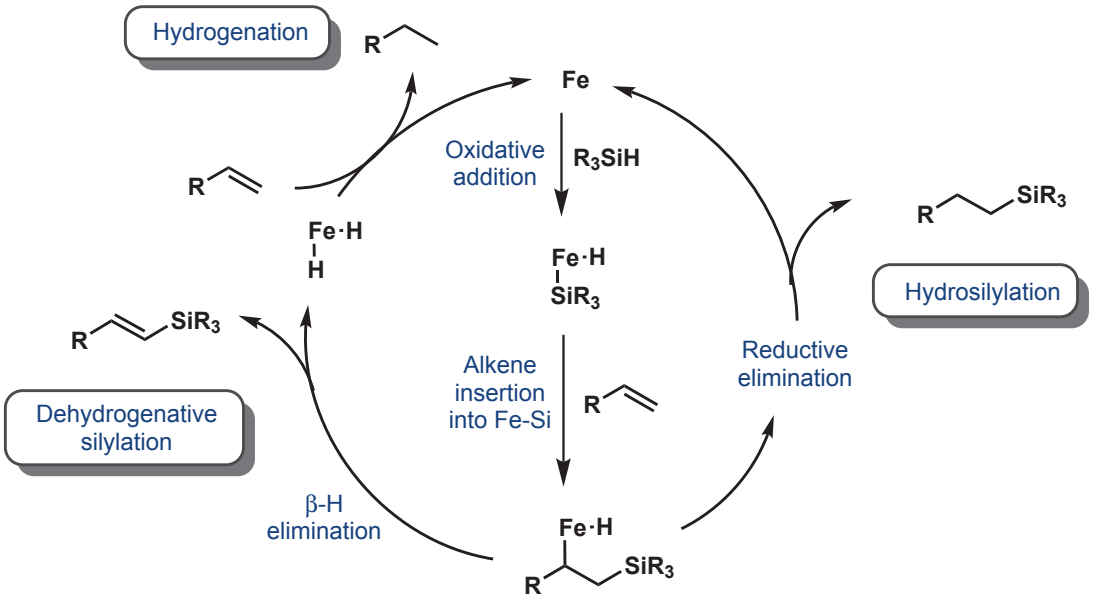


Figure 5.16: Postulated mechanism explaining the formation of both the hydrosilylation and dehydrogenative silylation products.

5.2.5 Other catalytic tests

Given that the Fe colloid was the only one of the tested catalysts to be significantly active in the hydrosilylation of 1-octene by MD'M, we conducted catalytic tests of this Fe colloid with other substrates, still with 2 mol% Fe.

First, in an attempt to avoid alkene isomerization, we performed a reaction with MD'M and a non-isomerizable aliphatic alkene: 3,3-dimethyl-1-butene (Figure 5.17). Unfortunately, after 96 h at 120 °C, no product was detected. This absence of catalytic activity may be due to the high steric hinderance caused by the tert-butyl group of the alkene.

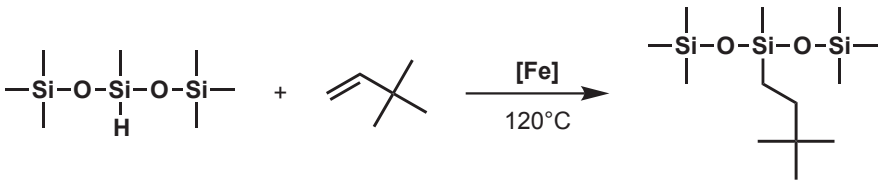


Figure 5.17: Catalytic test with MD'M and 3,3-dimethyl-1-butene.

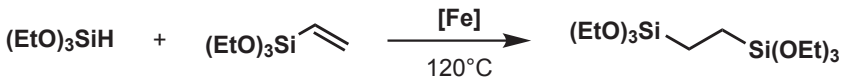


Figure 5.18: Reaction of $(EtO)_3SiH$ with $(EtO)_3SiVi$.

We then tested the colloid on the reaction of $(EtO)_3SiH$ with $(EtO)_3SiVi$ (Figure 5.19). No catalytic activity was observed after 48 h, at the reverse of what was observed with the Ni_3Si_2 colloid and the Ni/SiO_2 solid, which both gave the hydrosilylation product along with side-products (see Chapter 4).

Finally, we tested the colloid on the reaction of $(EtO)_3SiH$ with 1-octene, and we only obtained 1-octene isomerization products (Figure 5.19). This absence of hydrosilylation activity is surprising, when comparing with the

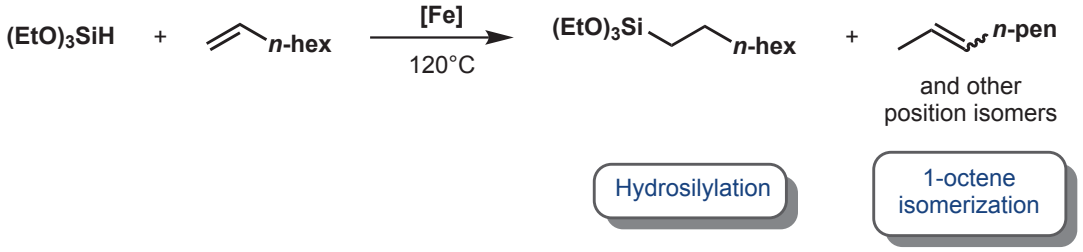


Figure 5.19: Reaction of $(EtO)_3SiH$ with 1-octene.

MD'M + 1-octene which gave hydrosilylation activity. This suggests that this Fe catalyst is especially sensitive to the nature of the SiH reagent.

5.3 Conclusion

In conclusion, we reported a new synthesis of small and well-defined iron nanoparticles starting from the commercially available cluster $Fe_3(CO)_{12}$, and the subsequent synthesis of various silica-supported Fe-containing NPs. TEM and STEM characterization of these Fe NPs showed mostly well-dispersed and small particles, around 2 nm diameter most of the time. Mössbauer spectroscopy characterization are being performed, and preliminary results suggest that the NPs produced by the colloidal synthesis may be iron silicide.

We then tested these Fe NPs on different model catalytic reactions. For the reaction of MD'M with 1-octene, the products of hydrosilylation, dehydrogenative silylation and octene isomerization were detected by GC-MS. Several dehydrogenative silylation products were detected, but were not fully characterized yet. Only one form of Fe(0) NPs, the NPs obtained by the initial colloidal synthesis, were active in hydrosilylation. The other Fe(0) NPs catalyzed only 1-octene isomerization. Since there was no significant difference in the Fe NPs size in these solids, as shown by electron microscopy, the difference of hydrosilylation reactivity can be attributed to a difference of composition of these NPs caused by the thermal treatments. Oxidized Fe NPs had no catalytic activity at all, like we had observed in Chapter 4 for NiO NPs. Surprisingly, for the reaction of triethoxysilane with triethoxyvinylsilane, contrary to what was observed with Ni NPs, no catalytic activity was obtained at all for any of the Fe-containing solids.

Now that we have given the proof of concept that Fe NPs could catalyze alkene hydrosilylation, two tasks are envisioned in order to achieve practically usable Fe NPs catalysts. First, screening other Fe(0)-containing NPs (for example: other silicides,[211–213] carbides[214,215], nitrides[215], borides[216,217], phosphides[218] or alloys with other non-noble metals) to further study the effect of Fe environment and identify interesting candidates for optimization.

Then, a mechanistic study of a selected catalyst could provide valuable answers to questions such as: is it possible to favor hydrosilylation over isomerization and dehydrogenative silylation ? What is the the rate-determining step ? How is it possible to increase the rate of this step? The answers to these questions could allow to rationally design more performant Fe NP-based catalysts.

[211] N. Dahal and V. Chikan, *Chem. Mater.* **2010**, 22, 2892–2897.
[212] J. Guan et al., *J. Mater. Chem. C* **2014**, 2, 5292–5298.
[213] J. M. McEnaney and R. E. Schaak, *Inorg. Chem.* **2015**, 54, 707–709.
[214] Z. Yang et al., *Chem. Sci.* **2016**.
[215] C. Schliehe et al., *Chem. Mater.* **2012**, 24, 2716–2721.
[216] S. Rades et al., *ChemPhysChem* **2011**, 12, 1756–1760.
[217] S. Carenco et al., *Chem. Rev.* **2013**, 113, 7981–8065.
[218] C. Qian et al., *J. Am. Chem. Soc.* **2004**, 126, 1195–1198.

5.4 Experimental

5.4.1 Syntheses

Fe colloid synthesis

Warning: the Fe precursor is toxic, and the reaction forms carbon monoxide, a toxic gas!

In a glass Fisher-Porter reactor, under argon, 277 mg (1.82 mmol Fe) of $Fe_3(CO)_{12}$ were dissolved in 50 mL of toluene, giving a deep green solution. 0.47 mL (350 mg, 2.4 mmol, 1.4 eq) of *n*-octylsilane were added. Argon was evacuated, then the solution was put under 4 bar of hydrogen, then stirred at 80 °C during 24 h. An orange-brown solution containing 33 µmol mL^{-1} of Fe was obtained. It was cooled down to room temperature, the reactor evacuated to eliminate residual hydrogen and the carbon monoxide formed by the decomposition of the Fe precursor, then stored under argon.

Impregnation on silica ("RawSolid")

27.2 mL of Fe colloid were concentrated under reduced pressure until reaching a volume of 1.5 mL. The solution was then used to impregnate (Incipient Wetness Impregnation method) 1 g of fumed silica. The brown-green solid was dried under secondary vaccuum. It contains 5% w/w Fe.

Solid oxidized at room temperature ("OxidizedRT")

The "Rawsolid" was exposed to dry air at room temperature, and turned into a deep brown solid.

Solid oxidized at 500 °C ("Oxidized500")

The "Rawsolid" was calcinated with 40 mL min^{-1} of dry air, with a heating ramp of 2 °C min^{-1} until 500 °C, then maintained at 500 °C during 4 h. An orange solid was obtained.

Solid reduced at 500 °C ("Reduced500")

The "Oxidized500" solid was reduced with 40 mL min^{-1} of hydrogen, with a heating ramp of 2 °C min^{-1} until 500 °C, then maintained at 500 °C during 4 h.

Mössbauer spectroscopy

Absorbers have been prepared under Ar in glove box and protected from air by heat sealed metallized film. The absorber masses (90 mg cm^{-2} to 200 mg cm^{-2}) differ slightly depending on the available materials.

The used spectrometer is operated in transmission geometry at room temperature, using a ^{57}Co(Rd) source with and activity of 900 MBq and a NaI(Tl) detector. Data acquisition was 2-7 days per sample. The spectra are fitted using a combination of lorentzian lines, all the parameters are fitted freely (except when specified).

Note that each iron environment is fitted with a doublet which is characterized by its center (isomer shift), its splitting (quadrupole splitting), its linewith (peak full width at half-height) and its spectral area (relative absorption) that can be considered as the atomic fraction of each iron environment.

Catalytic test

In a Schlenk tube equipped with a magnetic stirrer, under argon, are introduced 5 mmol (1.11 g, 1.27 mL) of heptamethyltrisiloxane (also called MD'M), 5 mmol (0.61 g, 0.85 mL, 1 eq) of 1-octene, 0.5 mL of dodecane (internal standard) and 3 mL of Fe colloid (0.1 mmol Fe, 0.02 eq) or 111 mg of silica-supported catalyst (0.1 mmol Fe, 0.02 eq). The mixture was heated at 120 °C under stirring during 24 h. Samples were regularly taken, filtered, exposed to air and analyzed by gas chromatography.

5.4.2 Gas chromatography

See Appendix C at the end of the manuscript.

5.5 Appendices

5.5.1 Particle size histogram

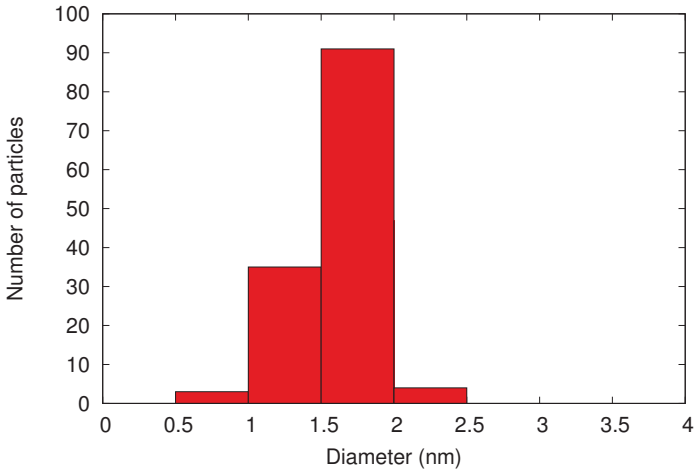


Figure 5.20: Particle size histogram of the Fe colloid, from STEM images.

6

Conclusion

The original goal of this project was to study metallic nanoparticles as catalysts for alkene hydrosilylation.

In the first part of this project, we studied the catalytic performances of Pt NPs in colloidal solution for the industrially relevant hydrosilylation of 1-octene with a PMHS, and we showed that these nanoparticles were as active as Karstedt's complex, the benchmark catalyst for this reaction. Moreover, these results confirmed the conclusion of a recent study of our group that showed that Karstedt's catalyst was rapidly transformed into Pt NPs during the hydrosilylation reaction,[136] and that these NPs were responsible for the majority of the catalytic activity.

In the second part of the project, we studied two strategies for enhancing Pt recovery based on heterogeneization of Pt NPs. We first synthesized catalysts based on Pt NPs immobilized in the walls of a mesostructured silica, SBA-15, following a method developed by our group.[171] We showed that the resulting catalyst was highly active and that very little Pt leached into the reaction medium. We then used two different carbon forms (carbon nanotubes, CNTs, and active carbon, AC) as catalyst support. We did not observe significant differences between these two supports in the catalytic performances of the resulting catalysts. Evidence in favour of a dissolution-redeposition phenomenon was gathered, something that had never been reported before in alkene hydrosilylation. The reduction of the Pt/CNTs and Pt/AC solids by hydrogen was found to influence strongly their induction period, activity and reusability. Even if Pt leaching was not avoided with these catalysts, the redeposition phenomenon allowed to obtained products with reduced Pt content.

In the third part of the project, we have studied three Ni-based catalysts that were previously developed by our group:[159] a Ni_3Si_2 colloid, a NiO colloid and a Ni/SiO_2 solid. The NiO colloid showed no catalytic activity at all, indicating that a Ni(0) precatalyst was necessary. The Ni_3Si_2 colloid and the Ni/SiO_2 solid both showed activity for the reaction of triethoxysilane with vinyltriethoxysilane, with completely different selectivities, showing that controlling the chemical environment of the Ni atoms was one key to achieving high selectivity. For the reaction of heptamethyltrisiloxane with 1-octene, these two catalysts only produced 1-octene isomers. Preliminary mechanistic hypotheses

were formulated to explain the observed reactivities.

Finally, in the fourth part of the project, we have synthesized a new Fe colloid and several Fe-containing solids (with silica support) from this colloid. Preliminary characterization of these solids by Mössbauer spectroscopy have in particular revealed that Fe atoms in the colloid and in the calcined then reduced solid had different chemical environment. These analyses are still underway. The use of these solids in the reaction of 1-octene with MD'M revealed that only the Fe colloid displayed hydrosilylation activity, along with dehydrogenative silylation and 1-octene isomerization. Tests on the reaction between triethoxysilane and triethoxyvinylsilane showed no catalytic activity, contrary to what was observed with Ni NPs.

In an article from 2011 entitled "Managing the scarcity of elements",[219] Nakamura and Sato discussed several strategies to address the concern of rare elements used in chemistry, including reduction, recycling and substitution. The Figure 6.1, which is inspired by this article, puts into perspective these different strategies.

[219] E. Nakamura and K. Sato, *Nat. Mater.* **2011**, 10, 158–161.

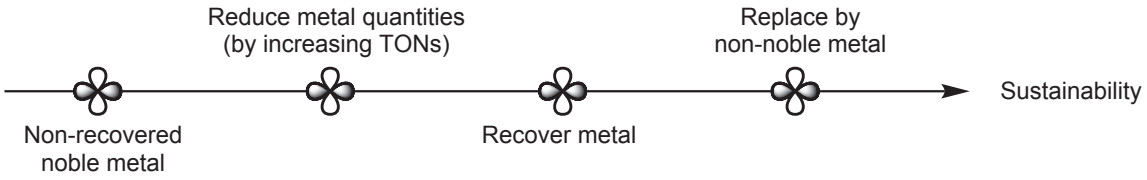


Figure 6.1: The road to sustainability with noble metal catalysts. Inspired from reference [219].

Every strategy drawn in this Figure is covered by a part of our project. The first part, studying platinum colloids, can be classified in the first strategy: "Reduce metal quantities". Even if our work did not properly allow to reach higher TONs than Karstedt's catalyst, it contributed to the better understanding of the interplay between Pt complexes and colloidal species, which seems important in order to design more efficient Pt-based catalysts, since the aggregation of unstabilized Pt particles plays a role in catalyst deactivation. The second part of the project, about heterogeneous Pt catalysts, obviously belongs to the "Recover metal" part. Finally, our work on nickel and iron nanoparticles belongs to the "Replace by non-noble metal" part. Cobalt has not been studied during this project, because iron and nickel were more represented in the literature, but Chirik has recently proven that it was a promising metal for alkene hydrosilylation.[89] Thus, we could benefit from studying cobalt NPs. Overall, our study of metal nanoparticles as catalysts for alkene hydrosilylation has risen a number of interesting questions, has started to answer some of these, and proposes routes to continue the work towards practically usable catalyts.

I wish to conclude this thesis with a personal opinion: the future of alkene hydrosilylation catalysis will certainly be without platinum. The works of Chirik's group have proven that this was possible with tailored complexes of iron, nickel and cobalt with non-innocent ligands. I am certain that there are other possibilities to utilize these non-noble metals for this task, and that the study and development of non-noble metal nanoparticles as catalysts may be one of them.

A

Bibliography analysis

A.1 Platinum

Reviews : [220, 221]

Ref.	Catalyst	Substrates	Conditions	SiH/Pt	Notes
US2721873 (1955)[222]	none	trichlorosilane, butyldichlorosilane, tributylsilane with ethylene, styrene, allyl chloride, pentene, cyclohexene, isoprene,	200–450 °C, high pressures		Mixtures of products obtained, and carbonaceous material. "The presence of added catalysts of the addition type are not essential but the walls of the bomb reaction chamber may itself act sufficiently as a catalyst." One example with UV light, allowing to run the reaction at 90°C.
US2637738A[29]	Pt/C (commercial or prepared by impregnation with H_2PtCl_6 and reduced with hydrogen.	trichlorosilane, triethoxysilane, dichlorosilane, vinylidene fluoride, ethyldichlorosilane with acetylene, ethylene, trichloroethylene, allyl chloride, butadiene	no solvent, 130–160°C	2×10^6 (Ex. 6)	Exotherms observed.
J. Am. Chem. Soc. 1957, 79, 974-979[30]	K_2PtCl_4, Pt-black, $H_2PtCl_6 \cdot 6\,H_2O$, Pt/C and catalysts of other metals	$MeCl_2SiH$, Cl_3SiH with 1-pentene, 2-pentene, cyclohexene and several allyl compounds	in sealed tubes, 100 °C	up to 1.6×10^7	"More careful examination proved that only *n*-pentylsilanes were produced from pentene-2, unlikely though this appeared". (It means probably consecutively isomerization and hydrosilylation.) Allyl compounds and isoprenyl acetate form propylene as side-product (up to 64%). Exotherm up 100 °C observed. $H_2PtCl_6 \cdot 6\,H_2O$ is the most active.
J. Am. Chem. Soc., 1958, 80 (15), pp 4104–4106[32]	$H_2PtCl_6 \cdot 6\,H_2O$	Cl_3SiH with 3-pentene	Reflux, 24 h	2×10^4	*n*-heptylsilanes were produced from pentene-3
J. Org. Chem., 1959, 24 (12), pp 2052–2053[223]	$H_2PtCl_6 \cdot 6\,H_2O$	Cl_3SiH, methylcyclosiloxanes with styrene and α-methylstyrene			Mixture of Markovnikov (about 30% yield) and anti-Markovnikov (about 50% yield).

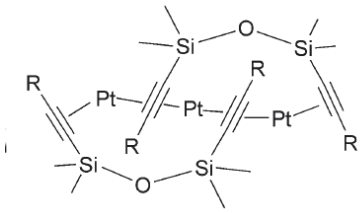
J. Org. Chem. 1964, 29, 2519 10.1021/jo01032a009	H_2PtCl_6 in *i*PrOH	$Ph(CH_2)_nCH=CH_2$, n=0-2 or pentenes with Me_2ClSiH, $MeCl_2SiH$ and Cl_3SiH	100 °C	10^5	Study of the regioselectivity of the reaction with phenylalkenes. Alkene isomerization is observed when using excess of alkene. "... the isomerization of olefins during the addition reaciton is probably not stereoselective but tends towards reaching a thermodynamically determined distribution of isomers.". Showed that isomerization-hydrosilylation sequences can happen. The product ration depends on the nature of the SiH reagent, and by the presence of functional groups on the phenyl group.
U.S. Patent 3,775,452 1973[33]	$Pt_2(DVTMS)_3$ (DVTMS = divinyltetramethylsiloxane), now known as Karstedt's complex				Patents the complex and the method of synthesizing it. In the exemples, silicone crosslinking tests. See [34] for the elucidation of the structure of the complex by XRD.
J. Organomet. Chem. 1983, 251, 39–44[165]	silica-supported poly-*γ*-mercaptopropylsiloxane-platinum complex	triethoxysilane with 1-hexene	rt to 80°C, 2 h to 8 h	500 (x 20 runs)	
J. Am. Chem. Soc., 1987, 109 (12), pp 3586–3595[224]	$Pt(C_2O_4)(PR_3)_2$ on 300 m^2/g silica, activated by UV light. Characterization by carbon, phosphorus and silicon CP-MAS SSNMR, SEM, TEM.	$MeCl_2SiH$, $(EtO)_3SiH$, Et_3SiH with 1-heptene and trans-2-pentene	45 min UV irradiation in olefin/hexane, reaction at 30 °C	1850	Oxygen-sensitive (may be due to the oxygen-sensitivity of the alkylphosphine ligands), no induction period, inhibition by coordinating solvents and excess olefin, not poisoned by Hg. When activated thermally, formation of 2 nm Pt NPs ; this catalyst exhibits an induction period, and is poisoned by Hg. First-order in silane. "An important requirement suggested by the lack of activity in coordinating solvents and the inhibition with excess olefin is generation of a coordinatively unsaturated species before silane oxidatively adds. This differs from the mechanism proposed for conventional hydrosilation catalysts where olefin addition precedes silane oxidative addition."

EP0652222[225]	Pt/C	Methyldichlorosilane with allyl chloride	Continuous flow reactor (stainless steel pipe) in a 100 °C bath. Temperature in the reactor rises to 200 °C.	41000	Di-tert-butyl peroxide or benzoyl peroxide are introduced in the reactor to maintain catalytic activity.
Inorganica Chimica Acta 1997, 264, 125–135[152]	Colloidal silica particles modified with triethoxysilane (giving a 13 nm hydridosilsesquioxane layer), reacted with Pt(0) complexes.	chlorodimethylsilane, triethylsilane, $(TMSO)_2MeSiH$ with allylbenzene	THF, 60°C, 8 h.	2800	If dried, the Pt(0) complexes decompose into nanoparticles. "Triethylsilane did not undergo hydrosilation with allylbenzene. Instead, the double bond migrated, a common problem with platinum catalysts, to give beta-methylstyrene. This reaction did not take place in the absence of the silane"
WO1997047677[226]	Karstedt's catalyst, Pt/TiO_2, "Cal101" (alumina support), "Pt/CECA 2S" (carbon suuport),	$MD_70D'_7M$ with vinylcyclohexene epoxide	90 °C, 5 h	2250	
Chem. Eur. J. 1998, 4, 2008[154]	$Pt(quinone)_2(DVTMS)$, DVTMS = divinyltetramethylsiloxane, with various quinones	triethylsilane, MD'M with triethylvinylsilane	30 °C, in hexane, 5-30 h	1.6×10^5	Aim: synthesize and evaluate Pt(0) complexes. Proved that they are more active and stable than Karstedt's complex, and that the active species is homogeneous. Catalysts performances compared with half-reaction times. Naphtaquinone ligands gave more active complexes than Karstedt's catalyst; attributed to the π-acidity of these ligands. More π-acid ligands than naphtaquinones gave less active complexes, though. Hg poisoning test with Karstedt's catalyst: loss of activity after 40% SiH conversion, meaning it is "largely heterogeneous in action"; with Pt-naphtaquinone complex: no loss of activity, indicating a homogeneous active species.

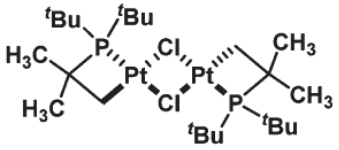
US6100408A[227]	Pt/C (0.1% w/w Pt) (impregnation of active carbon with $PtNO_3$ then reduction under hydrogen).	trimethoxysilane with allyl glycidyl ether	Tubular reactor with recirculation (ie. batchwise operation, 75 min total reaction time, 3 s contact time per circulation, 3 bar) or continuous fixed bed reactor (17 min. contact time), 120°C.	50 000 (batch)	Reaction monitored by GC. Space-time yield 158 mol product/h/g_{cat} for batch tubular reactor and 137 mol product/h/g_{cat}. For tubular batch reactor, catalyst is 0.1% Pt w/w, but for continuous flow reactor, catalyst is 0.02% Pt w/w.
US 6087523 A (2000)[228]	Pt/Al_2O_3 0.5% (purchased from Engelhard Corporation or Johnson Matthey)	methyldichlorosilane with cyclohexene	1 L CSTR, 100–140°C	?	70% conversion max. Very little information.
Chem. Comm. 2000, 19, 1931–1932[229]	diamine-functionnalized polystyrenes platinum complexes	trichlorosilane with 1-octene (2 eq.)	Sealed vials, rt, solventless, 3–8 h.	10 000	Split tests were performed. 6 cycles. Comparison with Speier's catalyst.
EP1070720 (2001)	Pt/Al_2O_3	Methyldichlorosilane with cyclohexene	In a CSTR, 100 °C to 140 °C, 10.8 min contact time		
J. Mol. Catal. A: Chem. 2001, 177, 49–69.[230] See also [231, 232]	Diamine-funcionnalized methacrylate/styrenic resins	Trichlorosilane, methyldichlorosilane with 1-octene	RT, 4 h, solventless	2000	Split tests, comparison of different resins.
Science 2002, 298, 204[43]	Pt-NHC (NHC = N-heterocyclic carbene)	1-octene, vinylcyclohexene epoxide with MD'M and $MD_{80}D'_7M$	In toluene/xylene, 72 °C, 30 ppm		Short communication. Phosphine-Pt complexes are tested, and bring improvements in selectivity, but do not prevent colloid formation. Pt-NHC complexes are stable under air for several months. They are less active than Karstedt, but suppress Pt colloid formation and improve selectivity (reduced amount of alkene isomerization and epoxide opening). Reactivity and selectivity are optimal with the bis-Cy NHC.
Adv. Synth. Catal. 2004, 346, 1429-1434[44]. See also patents [44, 233–237]. See also for direct preparation of Pt-NHC complexes[47].	Pt-NHC(DVTMS) complexes. Symetrical NHC with Me, Cy, tBu, Ad, Mes, (2,6-iPr)Ph.	MD'M with alcohols (free, TBS-protected and THP-protected), epoxides, ketone, ester	In xylene, 72 °C	2×10^4 to 10^6	Continuation of [43]. Anti-Markovnikov selectivity exclusively. 2-octene is unreactive. Example of Tamao-Kumada-Fleming oxidation of a product. Mechanism proposal based on preliminary kinetic studies.

Catalysis Communications 4 (2003) 637–639[166]	vinyltriethoxysilane-modified silica impregnated with chloroplatinic acid	Diphenylsilane, dimethylphenylsilane with vinyldimethylphenylsilane, M^{vi}_2, MMA, allylepoxypropylether, styrene	Solventless, 30 °C monitored by GC.	1500 (x 5 runs)	Almost only beta-addition. Short kinetic study. 5 recycling tests at 90% conversion (but the reaction times are not.
Appl. Organomet. Chem. 2003, 17, 127–134[61]	Pt/C	Chlorosilane with allyl chloride	In benzene, 50–70°C, 1–5 h, 1.1–1.3 eq. trichlorosilane (to compensate for the side-reaction)	1000–20 000	Significant side-reaction : metathesis reaction giving $SiCl_4$ and propene (which can then be hydrosilylated). Short kinetic study.
J. Mol. Catal. A: Chem. 2004, 208, 187–194[167]	"Vinyl-functionalized polysiloxanes having different degree of branching, grafted on silica" impregnated with a toluene solution of Pt complex	Dimethylphenylsilane with 1-hexene	In toluene, 40°C.	2000	50% loss of Pt loading after 8 cycles.
Chem. Comm. 2005, 3856-3858[45]	Pt-NHC with benzimidazoylidene ligands	MD'M with 1-octene	Toluene, 70 °C, 3 h	200	"Second-generation" Pt-NHC complexes. Benzimidazoylidenes "possess a σ-donating ability which is intermediate between that of imidazolylidene and imidazolinylidene carbenes". Is it relevant to compare these benzimidazoylidene carbenes to the less active of their imidazoylidene analogs (ImMe, knowing that ImCy 2-3 times more active[43])?
J. Organomet. Chem. 2005, 690, 6156–6168[46]	Pt-NHC complexes	MD'M with 1-octene	70 °C, *o*-xylene	2×10^4	Investigation of the effects of the NHC structure on the catalytic features of the Pt complex. Characterization of the complexes by XRD, 13C and 195Pt NMR. A large part of the discussion is copied from ref [45].
Dalton Trans., 2005, 74–81[238]	Pt complexes of silicone-modified ligands (nitriles, pyridines).	MM' with MM^{vi}, $M^{vi,OEt}$, isoprene	85°C, 2h, in toluene	1400	

Green Chem., 2005, 7, 283-287[239]	H_2PtCl_6 and Di-μ-Cl(Cl)$_2$(cyclohexene)diplatinum(II)	M'D$_n$M', n = 18, 28, 78 and MD'$_5$D$_4$3M with allyl glycidyl ether and alkenes comprising ethylene oxide and propylene oxide oligomer chains	In ionic liquids (1% w/w of the reaction mixture), 90 °C, 20 ppm Pt	1.2×10^4	Industrial application of ionic liquids as process aid, 20 ppm Pt recyclable 5 times at least "whithout loss of activity" (but no experimental proof). Pt content analysis in the products: generally lower than 1 ppm.
J. Am. Chem. Soc., 2005, 127, 5790-5791[148] See also [149]	Pt nanoparticles	MD'$_{33-35}$M with various alkenes	RT, 32-78 h, benzene	7*1000	Separation of the Pt NPs from the reaction products by centrifugation.
WO2006061138[240]	Pt/nanoscale TiO_2	Me(H)Si(OEt)$_2$ with Me(Vi)Si(OEt)$_2$ (Vi = vinyl)	100 °C, 4 h		
J. Am. Chem. Soc., 2006, 128 (30), pp 9773–9780[241]	$PtCl_2$(COD), $PtCl_2(PPh_3)_2$, Pt-92, $Pt(PPh_3)_4$ dissolved in ionic liquid and treated with H_2	MD$_2$D'$_2$M with 1-decene	90 °C, 1% vol/vol ionic liquid containing Pt catalyst, 1-3 h	1.5×10^6 after 10 cycles	Biphasic. At 5 ppm Pt, mass transfer is limiting.
J. Mol. Catal. 2006, 257, 141–148[242]	Pt/C or Pt/polystyrenes	MD'M, MD'$_n$M with 1-octene, 1-hexadecene	100°C, 1–3 h	?	
Chem. Mater. 2007, 19, 6373–6375[243]	di(ethylene oxide)-functionnalized silica platinum complex	CH2=CH-(CH2)2Br, CH2=CH-(CH2)3Br, CH2=CH-(CH2)9Br, CH2=CH-(CH2)7-COOCH2CH3, CH2=CH-CH2-O-(CH2-CH2-O)2-CH2-CH=CH2	50–80°C, 36h, 1.5–5 equiv. SiH vs. alkene	37 x (5 runs)	Claim to obtain platinum-free product, but no experiment to prove it.
WO2007106427[52]	Pt/modified Al_2O_3 (Al_2O_3 + poly(diallyldimethylammonium chloride) + KCl, impregnated with chloroplatinic acid, reduced with hydrazine). During catalytic tests, AcONa added as cocatalyst	M'$_2$ with ethylene glycol monoallyl ether, trimethylolpropane diallyl ether	80–100°C, solventless, no reaction time mentionned	54 000	IR spectroscopy to monitor the reaction. APHA color measurement. The prepared silicones were tested (after separation from the catalyst by filtration) in coating preparations to monitor color changes over several days.
Catal. Today 2011, 169, 69–74[244]	Pt/PS-DVB (PS = polystyrene, DVB = divinylbenzene) reduced under H_2	Dimethylchlorosilane and methyldichlorosilane with 1-octene	60 °C, 3 h	5000	Comparison with Pt/C catalysts. Pt dispersion is 8% for Pt/PS-DVB vs. 67% for Pt/C (calculated by H_2 chemisorption.

J. Fluorine Chem. 2011, 132, 123–127[245]	pyridine-containing polystyrenes platinum complexes	triethoxysilane with trifluoropropene	60°C, 6h, 1 atm trifluoropropene	3250 (x 4 runs).	
Catalysis Today 2011, 169, 69–74[244]	Pt/PS-DVB (PolyStryrene-DivinylBenzene) Support bought from Aldrich, IWI with chloroform solution of $Pt(acac)_2$, reduction under hydrogen (160°C, 3 h)	trichlorosilane, methyldichlorosilane, dimethylchlorosilane with allyl chloride, 1-octene	Batch : 60°C, 3h. Continuous : 140°C.	5000	Comparison with commercial Pt/C. Elemental analysis of Pt content in catalysts after 5 cycles : 20% loss for both Pt/C and Pt/PS-DVB, even if Pt/C activity decreased while Pt/PS-DVB was stable.
J. Organomet. Chem. 2011, 696, 2918–2927[246]	Platinum(II)-bis-(N-heterocyclic carbene) complexes	MD'M, dimethylphenylsilane with styrene	50 to 140 °C, 10-360 min	200 to 26000	No indications as to how are reused catalysts. Karstedt's complex seems to be more active than their Pt-NHC complexes on reuse.
Catal. Comm. 2011, 12, 1166 [247]	Karstedt's complex with various amounts of Et_2S added *in situ*	Chlorodimethylsilane with tetravinylsilane, trimethylsilyl-4-pentenoate	In DCM, 40 °C	22000	Diethylsulfide increase catalytic activity of Pt centers.
Appl. Organomet. Chem. 2011, 25, 400-405[248]. See also [153, 249]	Carboxylic acid-terminated PEG impregnated with H_2PtCl_6	$(EtO)_3SiH$, $ClMe_2SiH$ with various styrenes and aliphatic alkenes	60 °C to 90 °C, 3 to 8 h	40000-80000	Better β-selectivity than classical Pt complexes.
Catal. Sci. Technol., 2012,2, 220-226	Polymeric monolith prepared by olefin ring-opening metathesis polymerization, impregnated with $PtCl_4$	MD'M and triethoxysilane with 1-alkenes, styrene, norborn-2-ene and norbornadiene	45 °C, batch or continuous	20000-30000	Pt NPs of 7 nm average diameter. In batch and continuous reactor, Pt leaching less than 4 ppm. In batch, "a significant increase in the average Pt-nanoparticle diameter from 7 nm to 12 nm during catalysis was observed by TEM [...], indicating Ostwald ripening during the catalytic process".
ChemCatChem 2012, 4, 1935[250]		MD'M with 1-hexene, $MD^{vi}M$	50 °C to 120 °C, 3-16 h	10^6	Complex characterized by 1H, 13C, 29Si, 195Pt NMR and XRD, MS (ESI) in solution. Catalytic activity slightly higher than Karstedt's complex.
J. Appl. Polym. Sci. 2012, 126, 1580–1584[251]	Pt/Halloysite (aluminosilicate)	M'_2 with phenyltriallylsilane	60°C, 2 h	1100	The reaction product is a resin.

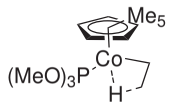
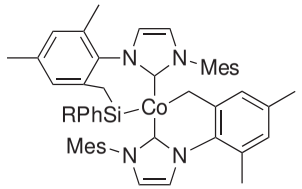
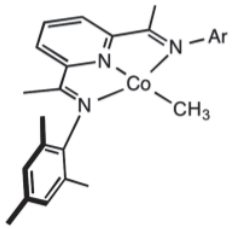
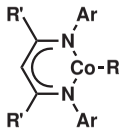
Catal. Sci. Technol., 2012,2, 725-729[252]	PtO_2	MD'M with 1-octene	85°C	50 000	Split tests. There is an induction period, but even at 10 ppm Pt, the PtO_2 is not entirely dissolved. "Unfortunately, it is very difficult to determine the amount of the dissolved platinum species by classical quantitative analysis because of a strong interference with the silicone matrix. Because the induction period is present in every catalytic cycle, we assume that the catalytically active species has to be formed anew in every cycle to perform the hydrosilylation reaction. After decantation, the supernatant are mixed with fresh reactants, and there is a significant catalytic activity, with a much shorter induction period." Recycling experiments were done with 300 ppm Pt, and there is no information about recyclability of the catalyst (and maximum TON) at 10 ppm.
WO2013158272A1[253]	0.2% w/w Pt NPs on a vinyl-modified silica	MD'M, M'D_nM', MD'$_5$M with 1-octene	80–120°C, solventless, 20 ppm Pt	27000 (Ex. 12)	NPs preparation : $Pt(COD)(Me)_2$ + PMHS d+ toluene at 80°C, followed by cross-linking with oxygen flow.
ACS Sust. Chem. Eng. 2013, 1, 249–253[50]	SiliaCat Pt(0) (trade name) : "sol-gel-entrapped Pt nanocatalysts made of ultrasmall Pt nanoparticles (4–6 nm) encapsulated within a methyl-modified ORMOSIL porous matrix" Condensation of MTES in acidic water, concentration of the sol, addition of potassium tetrachloroplatinate and soda to gelify, solid dried and reduced with $NaBH_4$ in THF/water, and dried.	triethoxysilane with 1-octene, 1-decene, 1-octadecene, 4-vinylaniline, 3,3-diethoxyprop-1-ene, styrene, etc.	in toluene, 5–24h 22–60°C	100–200	Pt quantification in reaction media (< 5ppm), catalyst reused twice with a decrease in activity, that can be restored by sonication 1h in DCM.
J. Organomet. Chem. 2013, 744, 113–118[254]	$PtCl_2$ or Karstedt's complex in tunable aryl alkyl ionic liquids	Dimethylphenylsilane with various alkenes	50 °C, air, petroleum ether	1100	Reused 4 times whithout observed loss of activity. No Pt concentration measurements to characterize leaching.

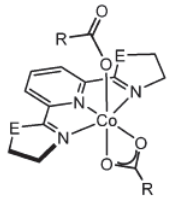
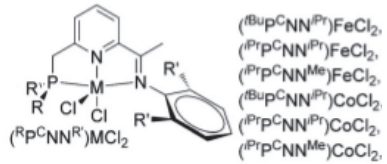
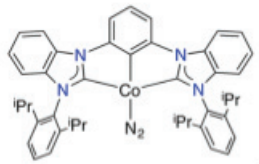
Ind. Eng. Chem. Res. **2014**, 53, 1588-1597 and WO2013066983[53, 255]	"Self-made" Pt/SiO_2 (impregnation of a modified silica with ethanolic solution of H_2PtCl_6 followed by drying) or Pt/alumina or Pt/silica sphere	MD'M, M'D_{45}M', M'D_{15}M', MD_2D'M, MD_{13}D'$_5$M with APEG-350-OMe, eugenol, 1-octene, allylmethoxytriethyleneglycol	In batch reactor or fixed-bed, 110–130°C, solventless	10000–40000	Comparison fixed-bed with/without recirculation with batch reactor. Pt leaching measurement (< 1ppm for heterogeneous catalysts). Product color measurement. No catalyst characterization except elemental analysis.
J. Am. Chem. Soc. 2014, 136, 4857[256]	 activated with 4 eq. MeMgCl	Triethoxysilane with butadiene, myrcene, dimethylbutadiene	50 °C, DCM, 1 h	400	Aim: 1,2-addition on 1,3-dienes (giving 3-butenylsilanes), instead of 1,4-addition (giving 2-butenylsilanes) as generally obtained. Pt(II)/Pt(IV) catalytic cycle is proposed.

A.2 Cobalt

Review : ACS Catal., 2016, 6 (1), pp 290–300[81]

Ref.	Catalyst	Substrates	Conditions	SiH/Co	Notes
J. Am. Chem. Soc., 1967, 89 (7), pp 1640–1647[82]	$Co_2(CO)_8$	triethylsilane, triethoxysilane, phenyldichlorosilane with α-alkenes	Solventless, [Co] = 0.001–0.01 M, rt	1000	"In all three cases the rate of olefin isomerization exceeded that of olefin hydrosilylation", but hydrosilylation continued even when all the 1-olefin had been isomerized. At higher temperatures (60°C), catalyst deactivation, lower yields. Catalyst deactivation less severe in excess of alkene, and when avoiding exotherms.
J. Organomet. Chem. 1970, 21, 207-213[83]	$Co_2(CO)_8$, $RhCl(PPh_3)_3$, $[RhCl(CO)_2]_2$	Me_2ClSiH, phenyldimethylsilane with ethylene, 1-pentene, 2-pentene, acrylonitrile	In benzene, under nitrogen, RT to reflux of benzene.	10	2 eq. alkene. Discussions on the α/β product distribution and alkene isomerization. Silane redistribution observed in some cases.
Inorg. Chem., 1980, 19 (12), pp 3858–3860[65]	$Co_2(CO)_8$ or $Ph_3Co(CO)_4$ or $Et_3SiCo(CO)_4$	Et_3SiH with 1-pentene	Solventless or in octane, under irradiation (355 nm), RT	2000	Pentene isomerization is a major side reaction.

US 5233071 A (1992)[84]	$Co_2(CO)_8$ or $Co_2(CO)_6[P(OMe)_3]_2$	$MD'_{14}M$, M'DM', $PhMeSiH_2$ with (Perfluoro-n-butyl)ethylene	rt to 60°C, 1 h to several days	50–375	
J. Am. Chem. Soc. 1993, 115 (6), pp 2151–2156[85]		Et_3SiH with 1-hexene	20 h, rt, in DCM	50–250	Deuterium labeling study, kinetic study, NMR (identification of an intermediate). Turnover-limiting step : isomerization (series of β-elimination/migratory insertion steps).
Angew. Chem. Int. Ed. 2013, 52, 10845[86]	 R = H, Me, Ph	$PhSiH_3$ with 1-octene	rt, solventless, 5 min to 24 h	100–20 000	Good selectivity for beta-hydrosilylation, some alpha-hydrosilylation as hell as isomerized and hydrogenated alkene. Comparison with $Co_2(CO)_8$.
J. Am. Chem. Soc. 2014, 136, 12108-12118[87]		Ph_2SiH_2, MD'M with 1-octene, cyclohexene	Solventless, rt, 15 min to 24 h	200	Principally dehydrogenative silylation. One example with 45% hydrosilylation, one other with 86%. Dehydrogenative silylation of internal olefins to give terminally functionnalized allylsilanes. Double silylation of olefins (one on each end). Application of the double silylation to cross-linking of PMHS/PDMS copolymers in presence of an alpha-olefin. Deuterium labeling study, stoichiometric experiments, proposition of a mechanism.
J. Am. Chem. Soc., 2015, 137 (41), pp 13244–13247 [88]		$PhSiH_3$, $(EtO)_3SiH$ with 1-hexene and various functionalized alkenes	Solvent-free, RT to 60 °C	50-2000	β-diketiminate ligands are non-innocent. When starting from internal alkenes, the terminal alkylsilanes are obtained (isomerization followed by hydrosilylation of the terminal olefin). Catalyst can be activated in situ.

J. Am. Chem. Soc., 2016, 138 (8), pp 2480–2483[80]	$Fe(OPv)_2$ or $Co(OPv)_2$ with adamantyl isocyanide as cocatalyst	MM', MD'M, M'DnM', MD'nM with styrenes, alphamethylstyrene, norbornene, MviM, MDviM, MviDnMvi, 1-octene, allyl glycidyl ether, allyl benzyl ether	Solvent-free, RT to 80 °C, 3 to 24 h	100 to 1000	Catalytic tests on model molecules, silicone fluids, and silicone cross-linking experiments. Catalysts precursors are air-stable. Hypotheses: oxygenated anion is necessary because of Si affinity for O, which promotes metathesis with SiH to give the hydride, and isocyanide acts as strong π-acceptor ligand.
ACS Catal., 2016, 6 (4), pp 2632–2636[89]	 **(PyBox)Co(2-EH)$_2$**: E = O **(^{TF}APDI)Co(2-EH)$_2$**: E = CH_2	$Me(OEt)_2SiH$, $Me_2(OEt)SiH$, MD'M, MM', Et_3SiH with 1-octene and other functionalized alkenes including allyl glycidyl ether	Solventless, RT, 1 h	100-400	Idea: ligands with smaller imine substituents to accelerate the rate of bimolecular reaction with silane versus unimolecular β-H elimination leading to dehydrogenative silylation.[87] Precatalysts are air-stable, with accessible cobalt carboxylates. Catalyst able to cross-link silicones with as low as 1 ppm Co.
Angew. Chem. Int. Ed. 2016, 55, 6671[90]	 (^{R}P^{C}NN$^{R'}$)MCl_2 (^{tBu}P^{C}NN^{iPr})$FeCl_2$, (^{iPr}P^{C}NN^{iPr})$FeCl_2$, (^{iPr}P^{C}NN^{Me})$FeCl_2$, (^{tBu}P^{C}NN^{iPr})$CoCl_2$, (^{iPr}P^{C}NN^{iPr})$CoCl_2$, (^{iPr}P^{C}NN^{Me})$CoCl_2$,	$PhSiH_3$ with a great variety of alkenes	In THF or solventless, RT to 60 °C 3 to 24 h	50-1250	Iron complex gives anti-Markovnikov, cobalt complex gives Markovnikov product (interesting for the synthesis of secondary alcohols). Radical mechanism is excluded.
ACS Catal., 2016, 6 (6), pp 3589–3593[91]		$PhSiH_3$, Ph_2SiH_2, Et_3SiH, $PhMe_2SiH$, MD'M, $(EtO)_3SiH$ with 1-octene and alkenes containing ketone, ester, aldehyde, ether, epoxide, nitrile and amine functionalities	Benzene, RT, 1-21 h	20	Anti-Markovnikov selectivity. Chalk-Harrod mechanism is proposed.

WO2013043783 (Dow Corning)

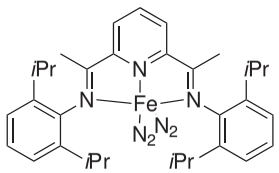
Mechanistic studies

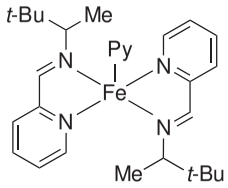
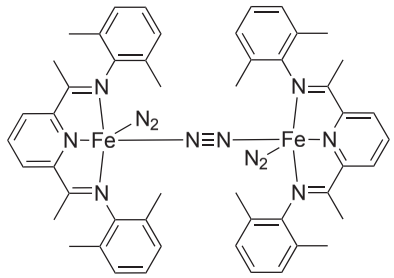
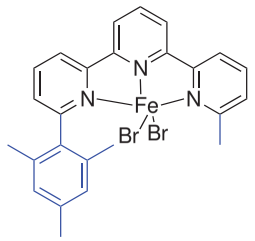
Angew. Chem. Int. Ed. Eng. 1988, 27, 289–291[66]

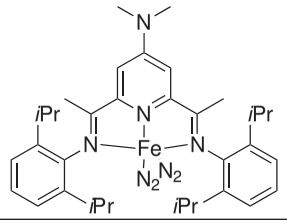
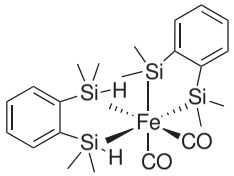
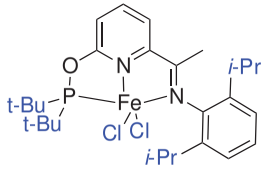
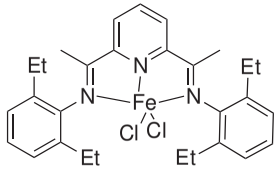
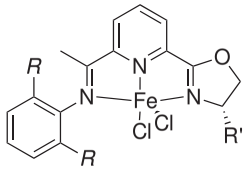
J. Am. Chem. Soc., 1993, 115 (6), pp 2151–2156[85]
J. Am. Chem. Soc., 2009, 131 (8), pp 3007–3015[257]

A.3 Iron

Review : Chem. Cat. Chem. 2015, 7, 190-222[258]

Ref.	Catalyst	Substrates	Conditions	SiH/Co	Notes
Tetrahedron 1962, 17, 61–68[70]	Colloidal Fe[259] (Preparation : decomposition of 3 mL $Fe(CO)_5$ in naphtalene at 220°C) or $Fe(CO)_5$	$MeCl_2SiH$ with propylene	In stainless steel autoclave, 130–140°, 4 h.	100	
J. Organomet. Chem. 1977, 128, 345–358[71]	$Fe(CO)_5$ irradiated with near-UV	Trimethylsilane, triethylsilane with 1-pentene	0–50°C, 12–188 h in sealed tubes (alkene/SiH = 0.1)	3000	Competition hydrosilylation/dehydrogenative silylation. Experiments with $DSiMe_3$, followed by MS analysis of the products. Discussion on a possible mechanism.
J. Am. Chem. Soc. 1981, 103, 975-977[72]. See also J. Organomet. Chem. 1977, 128, 345-358	Photoexcitated $Fe(CO)_5$ and $Fe_3(CO)_{12}$	Et_3SiH with 1-pentene	Neat, rt.	400	
J. Am. Chem. Soc., 1986, 108 (12), pp 3366–3374					
J. Organomet. Chem. 1993, 456, 45–47[73]	$Fe_2(CO)_9$, $Fe_3(CO)_12$	Et_3SiH with styrenes	40–80°C, 6–110 h, in benzene	100	Styrene/SiH = 3. Dehydrogenative silylation is the major reaction by far.
Inorg. Chem. Comm. 2000, 7, 371[74]	$Fe(CO)_5$ irradiated by UV	Et_3SiH with styrene, Me_3Sivi	80°C, 24 h, 1 h UV irradiation, in benzene, 10-fold excess C=C	100	Stoichiometric experiments, discussion of a mechanism proposal.
J. Am. Chem. Soc. **2004**, 126 (42), 13794–13807[75]		$PhSiH_3$, Ph_2SiH_2 with 1-hexene, *E*-2-hexene, styrene, α-methylstyrene, 1,5-hexadiene, limonene	rt, 60–4200 min,	333	Anti-Markovnikov selectivity exclusively. Works also with alkynes. Mechanistic study : stoichiometric experiments, crystallizations, solution NMR (mononuclear and mutlinuclear), isotopic labelling. The complex is also active in alkene hydrogenation. Magnetic susceptibility measurements, UV/visible spectroscopy. No dehydrogenative silylation. When starting from *trans*-2-hexene, 25% of internal silane is obtained.

Organometallics, 2006, 25 (18), pp 4269–4278					
WO2010016416[260]		MM' with 1-hexene, 1-octene, styrene	in toluene, 48 h, 80°	100	
J. Am. Chem. Soc. **2010**, 132 (38), pp 13214–13216[261]	 well-defined well-characterized (XRD, NMR, Mössbauer)	$(EtO)_3SiH$ with dienes	toluene, rt, 6–24 h	20	Mechanisme proposal, kinetic profile. Well-defined complex.
Organometallics **2012**, 31 (13), pp 4886–4893[262] and patent application WO2011006049		Et_3SiH, MD'M, $(EtO)_3SiH$ with 1-octene	solventless, 60°C, 1 h	200	Experimental and theoretical work to determine electronic structure of Fe complexes.
Science **2012**, 335, 6068, 567-570 [16]		Et_3SiH, MD'M, $(EtO)_3SiH$ with 1-octene, allyl polyether, styrene	rt, neat	5 000–25 000	Silicone cross-linking experiments. Experiment with a deuterated silane.
Organometallics **2012**, 31 (10), pp 3825–3828[263]		$PhSiH_3$ with 1-octene	100 °C, 24 h, 2/1 octene/silane	20 000	Max. TON = 1533. Catalyst activated by $NaBHEt_3$.

ACS Catal., 2012, 2 (10), pp 2169–2172[76]		MD'M, Et_3SiH with 1,2,4-trivinylcyclohexane	5–180 min, rt, neat	250	Better selectivity for monohydrosilylation than Pt catalysts (desired product for coupling agents in silica-filled automotive tires). The more sterically hindered ligands gave better selectivities in general.
Dalton Trans. **2013**, 42, 16687-16692[264]	 and isomers (position of H atoms)	$PhLe_2SiH$, Et_3SiH, $(EtO)_3SiH$, M'_2, MD'M with ethylene, 1-octene, cyclopentene	5–16 h, toluene, rt–80°C	10–1000	
J. Am. Chem. Soc. **2013**, 135 (51), pp 19154–19166[78]		$PhSiH_3$, Ph_2SiH_2 with functional alkenes	In toluene, rt 3 h.	100	Catalyst activated by 2 eq. $NaBHEt_3$ (vs. catalyst). Less active than Chirik catalyst, but more tolerant towards FGs such as ketone, amide, ester.
Adv. Synth. Catal. **2014**, 356, 584-590[258]		$PhSiH_3$ with functional alkenes	In THF, rt, 1 h	100	Catalyst activated by 2 eq. EtMgBr (vs. catalyst). Bench-stable precatalyst.
Appl. Catatal. A: General 2014, 486, 230–238[265]	$Fe(CO)_3L$, $[Fe(CO)_3]_2L$, L = diene, triene, tetraene, polyvinyl silicon derivative.	$(MeO)_2MeSiH$ with $(MeO)_2MeSivi$	80°C, 1 h, in toluene	100	Dehydrogenative silylation of fluids, and cross-linking (by hydrosilylation !) of silicones. Stoichiometric reactions, followed by NMR and GC/MS. Mechanism proposal.
Angew. Chem. Int. Ed. **2015**, 54, 4661[79]	 R = Me, *i*-Pr R' = Bn, *i*-Pr, *t*-Bu	Ph_2SiH_2 with 1,1-disubstituted alkenes (great variety)	Neat or in toluene, rt–60°C, 12 h.	20	Asymmetric (up to 94% ee.). Catalyst activated by 3 eq. $NaBHEt_3$ (vs. catalyst).

Organometallics, 2015, 34 (12), pp 2896–2906[266]	$Fe(COT)_2$ or $Fe(pentadienyl)_2$ ("open ferrocenes") + adamantyl isocyanide	MM', Me_2PhSiH, $M'D_{27}M'$ with styrenes	neat, rt–80°C, 3–23 h	33–100	Very little dehydrogenative silylation, only anti-Markovnikov addition : good results for styrenes.
J. Am. Chem. Soc., 2016, 138 (8), pp 2480–2483	$Fe(OPv)_2$ or $Co(OPv)_2$ with adamantyl isocyanide as cocatalyst	MM', MD'M, M'DnM', MD'nM with styrenes, alphamethylstyrene, norbornene, MviM, MDviM, MviDnMvi, 1-octene, allyl glycidyl ether,	Solvent-free, RT to 80 °C, 3 to 24 h	100 to 10 000	Catalytic tests on model molecules, silicone fluids, and silicone cross-linking experiments. Catalysts precursors are air-stable. Hypotheses: oxygenated anion is necessary because of Si affinity for O, which promotes metathesis with SiH to give the hydride, and isocyanide acts as strong π-acceptor ligand.

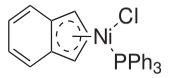
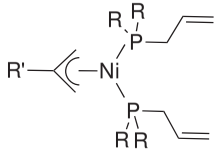
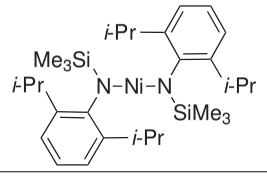
WO2014186513
WO2011006049
WO2014182670
WO2013081794
WO2012071359
WO2012071360 (Momentive)
WO2011006044 (Momentive)
WO2012071358
WO2013090548
WO2013043912 (Dow Corning)
WO2013043783 (Dow Corning)
WO2013043846 (Dow Corning)

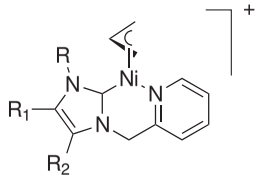
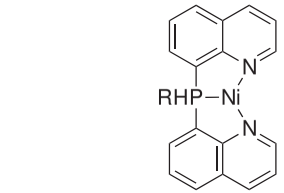
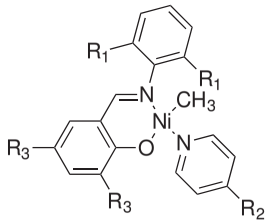
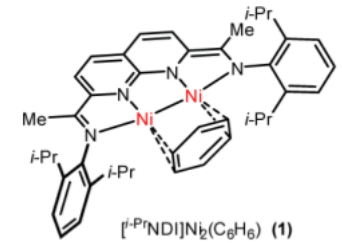
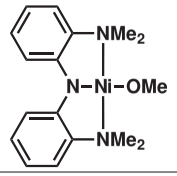
A.4 Nickel

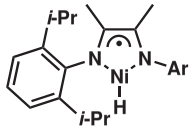
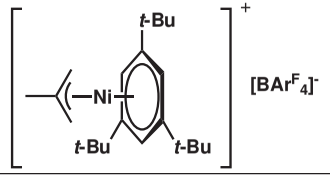
Ref.	Catalyst	Substrates	Conditions	SiH/Ni	Notes
Izvestiya Akademii Nauk SSSR, Seriya Khimicheskaya 1956, 256-257[92]	Raney Ni	$HSiCl_3$ with acrylonitrile	160 °C to 170 °C, 4 h		12% yield, rest is polymer.
Bull. Chem. Soc. Japan, 1956, 29, 326[93]	$NiCl_2$ or $NiCl_2 \cdot$Pyridine or Ni powder-pyridine	trichlorosilane with acrylonitrile	5 h, sealed tube, 160 °C	180	The reaction started between 150 °C to 170 °C. 22% yield.
Tetrahedron 1962, 17, 61[70]	$Fe(CO)_2$, colloidal iron,[259] mixture $NiCl_2$ + $Fe(CO)_2$	$MeCl_2SiH$, triethylsilane with propylene, actylonitrile	stainless steel autoclave, 5h, 130°C, 70 atm	500	First example of dehydrogenative silylation.

Izvestiya Akademii Nauk SSSR, Seriya Khimicheskaya 1963, 761-763[267]	$Ni(CO)_4$	$MeSiCl_2H$, Et_3SiH with acrylonitrile, methacrylonitrile, acrolein	120 °C		Colloidal Ni was ineffective.
J. Chem. Soc. D : Chem. Comm., 1970, 611-611[94]	$Ni(dmpf)Cl_2$ (dmpf = bis[dimethylphosphino]ferrocene)	$MeCl_2SiH$, Cl_3SiH, trimethylsilane with 1-octene	120°C, 20h, sealed tube	2000	Very short paper. First observation of H-Cl exchange in chlorosilanes with Ni catalysts. Monodentate phosphines and amines not effective.
J. Organomet. Chem. 1971, 28, 137–144[95]	NiX_2 with X = Cl, Br, OAc, Acac and L = PPh_3, PBu_3 or NiL_4, L = $(Py)_4$, $P[OPh]_3$ + CuX with X = Cl, Br, I	Cl_3SiH with styrene	Under N_2 in sealed glass ampoules. 150°C, 3–18 h	1500	Square planar vs. tetrahedral complex. Positive effect of the presence of air in one example. Used CuX as reducing agent to reduce Ni(II) species ; in some case important improvement of the yield and of the alpha-selectivity. This effect was specific to Cl_3SiH (didn't work with $(MeO)_3SiH$. Styrene telomerization is a side-reaction.
J. Organomet. Chem. 1973, 50, 297–310[96] Continuation of J. Chem. Soc. D : Chem. Comm., 1970, 611-611	$Ni(dmpf)Cl_2$ (dmpf = bis[dimethylphosphino]ferrocene) and other monodentate and bidentate phosphines	Linear 1- and 2-alkenes, Cyclic alkenes, vinyl monomers with Me_nCl_mSiH	20h, 120°C	1000	Almost no rxn at 90°C, but ok at 120°C. H-Cl exchanges during the hydrosilylation, depending on the alkene. Alkene isomerization observed. Dmpf ligand very electron-donating. Two alkynes tested. The less electron-rich the SiH compds were, the more reactive.
J. Organomet. Chem. 1973, 50, 311–318[97]	$Ni(PPh_3)_2(CH_2{=}CH_2)$ or Ni(1,2-bis(diphenylphosphino)ethane)$(CH_2{=}CH_2)$ or Ni(bis(triphenylphosphine))$(CH_2{=}CH_2)$ and their dichloro Ni(II) analogues	methyldichlorosilane, HCl_2SiH chlorosilane with 1-octene	70–135°C, 20–264 h	?	(Following J. Organomet. Chem. 1973, 50, 297–310) Comparison of Ni(II) complexes with their Ni(0) equivalents : no significant difference in activity, only difference in induction period. Proposed explanation : time needed to reduce Ni(II) into Ni(0) which is the resting state of the catalyst.
J. Organomet. Chem. 1979, 177, 153[268]	Ni atoms obtained by cocondensation of Ni vapor with a toluene or methylcyclohexane solution of the reagents at -196°C.	$(OEt)_3SiH$, $(Me_3SiO)_2MeSiH$, Et_3SiH with Isoprene	0°C	20–100	Other metal atoms work considerably less (Fe, Co) or do not work at all (Cr, V, Ti, Mn). Polymerization was a side-reaction. They concluded from an experiment that the catalytic species was not metallic particles, but it is unclear why.

J. Organomet. Chem. 1991, 418, 61-67[98]	$Ni(acac)_2$ dihydrate or anhydrous	$(EtO)_3SiH$ with $(EtO)_3Sivi$	> 100°C, 1h	330	"During the reaction, it is observed that the nickel precipitates from the reaction mixture, but most products are formed within a few minutes in the reaction occuring above 100°C, so the real catalyst is assumed to be a labile Ni(0) complex with vinylsilane as a ligand." Typically 20% of hydrogenative dimerization, 30% of dehydrogenative silylation, rest being oligomers, hydrosilylation product, hydrogenation product, redistribution products. Mechanism proposal for explaining the formation of all products, but not supported by experiments.
J. Chem. Soc., Chem. Commun., 1991, 1424-1425[199] and EP0306177[] (see also 10.1039/C39910000245 and 10.1021/om00137a035)	"Activated nickel, prepared by lithium or sodium reduction of nickel iodide under sonication in THF"	various alkenes with Me_nCl_mSiH	RT, in THF, 1–2 h	6	20–30 min induction periods observed. Stirring the nickel powder with alkene or silane prior to the reduction lowers the induction period in both cases. No protocol for catalyst synthesis is provided. No catalyst characterization.
J. Organomet. Chem. 1993, 454, 45–50[99]	$Ni(acac)_2$ anhydrous or hexahydrate	trimethoxyvinylsilane, triethoxyvinylsilane, triisopropoxyvinylsilane, methoxydimethylvinylsilane, trimethylvinylsilane, phenyldiethoxyvinylsilane with Triethylsilane, triethoxysilane with	120°C, 2 h	200	A lot of byproducts are present. GC/MS analysis of the products. Discussion about the effect of the substrate substituents on the reaction selectivity.
J. Organomet. Chem. 1994, 484, 147[100] 10.1016/0022-328X(94)87198-1	$Ni(COD)_2$ $Ni(acacF)_2$ $Ni(PPh_3)_2(acac)_2$ $Ni(PCy_3)_2(acac)_2$ $Ni(P[C_6H_4(OMe)_2]_3)_2$	$(EtO)_3SiH$ with $(EtO)_3Sivi$	2h, 120°C, Ar	200	Seems to be no difference in mechanism between Ni(O) and Ni(II) precatalysts. Hydrosilylation 0–20%. Comparison of the effects of the phosphines on product distribution.

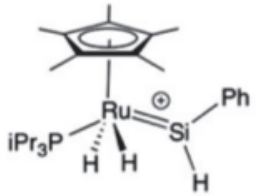
J. Mol. Catal. A 1998, 135, 223-231[101]	$Ni(COD)_2$ and $Ni(acac)_2$	$(EtO)_3SiH$, $(EtO)Me_2SiH$, $(EtO)_2MeSiH$, $PhMe_2SiH$ with styrene	120 °C, 4 h	200	Dehydrogenative silylation mainly. Hydrosilylation and vinylsilane dimerization are also observed.
J. Organomet. Chem. 2000, 597, 175-181[102]	Ni equivalent of Karstedt's catalyst	$PhMe_2SiH$, $(EtO)_3SiH$ with styrene, vinylsilanes and vinylsiloxanes	RT to 120°C	1000	Dehydrosilylation major product (approx. 80%) hydrosilylation minor products (approx. 20%). "contrary to the case when [Ni(acac)2]- and [Ni(cod)2]-based catalysts are used, there is no precipitation of nickel products after completion of the reaction". Mechanism proposal based on stoichiometric reactions.
Can. J. Chem., 2003, 81(11): 1299-1306[103] Organometallics 2005, 24, 149–155[104] Organometallics 2005, 24, 4003–4013[269]	 activated by MAO or $NaBPh_4$	$PhSiH_3$ with styrene	C_6D_6, RT, 3 h - 24 h	50–100	Regioselective for styrene. Trisubstituted silanes unreactive. Comparison of the methylated and cationic precatalysts. Mechanistic study. In situ generated Ni cations react first with $PhSiH_3$ (and not with styrene) to give Ni-H and silylium species, followed by insertion of the alkene into the Ni-H bond to give an alkylnickel species, and reaction with another silane to give the product (how ?).
Dalton Trans., 2007, 3000-3009[270]	 R = Ph, *i*-Pr, R' = H, Me	$PhSiH_3$ with styrene, paramethylstyrene	DCE, 40°C, 5h	100	Only a short part of the study is dedicated to hydrosilylation.
Chem. Commun., 2012, 48, 7146-7148[271]		Ph_2SiH_2 with 1-octene	benzene d6, RT, 2h	50	Only one catalysis example. The paper is more centered on the synthesis and structure of the two-coordinate Ni complex.

Organometallics, 2012, 31 (6), pp 2175-2183[272]		$PhSiH_3$ with 2-, 3-, 4-fluorostyrene	60°C, 2 eq. silane vs. alkene.	100-200	Mixtures of Markovnikov and anti-Markovnikov products.
WO2013/120057[273]	 R = alkyle, aryle, OAryle, Oalkyle, amine	Ph_2SiH_2	benzene-d6, RT, 1–40h	200	Claimed for Fe, Co, Ni, Cu, but examples only with Ni
Catal. Sci. Tech. 2015, 5, 2081-2084[105]		Et_2SiH_2 with 1-octene and various olefins	ACN, RT, 1–24 h	200	Active olefin polymerization catalysts. Substituent redistribution on Si observed. When an excess of alkene was used, no internal alkene (that would be formed by isomerization) was formed. Tertiary silanes were unreactive. 2-octene was succesfully hydrosilylated. Stoichiometric experiments (and NMR) to obtain mechanistic information.
J. Am. Chem. Soc. 2015, 137, 6104[106]	 [$^{i\text{-Pr}}$NDI]Ni$_2$(C_6H_6) **(1)**	Diphenylsilane with styrene, 1-octene (+ dienes, alkynes, carbonyls)	rt, 22 h, C_6D_6	20	Dinuclear silane activation by the Ni-Ni bond supported by a redox-active ligand. First case of activation with a dimetallic bond which stays intact during the catalytic cycle. Trisubstituted silanes are unreactive (the double SiH activation is necessary).
Angew. Chem. Int. Ed. 2015, 54, 14523[38]		Ph_2SiH_2 with a variety of terminal and internal alkenes	In TFH, RT, 6 h	10-100	Internal alkenes can be used in an isomerization/hydrosilylation.

ACS Catal., 2016, 6, pp 4105–4109[107]		MD'M, MM', $(EtO)_3SiH$, $(EtO)_2MeSiH$, $(EtO)Me_2SiH$, $MD_xD'_yM$ with 1-octene and $M^{vi}D_xM^{vi}$	RT or 40 °C, 6 h, solventless	100-1000	"Significant isomerization to internal octene isomers occurred over the course of the experiment but n-octylSi$(OEt)_3$ eventually formed over the course of hours as the sole hydrosilylation product." Deuterium-labeling experiments show that β-H elimination happens faster than C – Si bond formation. Cross-linking experiments were done. DFT calculations to probe the oxidation state of the diimine ligand: Ni(II) with one-electron reduced ligand (the ligand formally stabilizes a Ni(I) species.
Chem. Commun., 2016,52, 6723-6726[108]		n-hexSiH_3, n-octSiH_3, Et_2SiH_2, n-penSiH_2, Et_2SiH_2 with 1-octene, styrene	30 min to 24 h, RT, in DCM	200	The catalysts are not active with tertiary silanes. DFT calculations support a new mechanism.

A.5 Ruthenium

Ref.	Catalyst	Substrates	Conditions	SiH/Ni	Notes
J. Organomet. Chem. 1983, 253, 349[110]	$RuCl_2(PPh_3)_3$ and similar complexes	triethoxysilane with 1-pentene, 2-pentene, 1-hexene, 2-hexene, 1-heptene, 1-octene, 1-dodecene	120°C, 6h, in air, in glass ampoules. Some reactions at 80°, 2 h.	5000	Propose a Chalk-Harrod mechanisme (not clear why). No activity with cyclooctene. Better results under air than under argon.
J. Organomet. Chem. 1984, 3, 335[111]	$Ru_3(CO)_{12}$	trifluoropropene or pentafluorostyrene and tertiary silanes	70–150°C, 3–76 h, stainless steel autoclave.	300	Dehydrogenative silylation often main product.
J. Am. Chem. Soc. 2003, 125 (45), pp 13640–13641[117]	$[Cp^*(iPr_3P)(H)_2$-Ru=Si(H)Ph,$Et_2O]$ $[B(C_6F_5)_4]$	Phenylsilane, hexylsilane with 1-hexene, ethylene, cyclohexene, styrene, methylcyclohexene	3–18 h, 60°, in benzene	20–200	First proposal of the Glaser-Tilley mechanism. Works only with primary silanes.

Organometallics 2006, 25 (19), pp 4504–4513[112]	$RuCl_2(CO)_2(PPh_3)_2$	$Me(Vi)Si(OEt)_2$ with $Me(H)Si(OEt)_2$	100°C, 6 h, solventless.	200	Main part of the article = DFT study, in favor of σ-bond metathesis
J. Organomet. Chem. 2007, 692, 2282[113]	ion pair $[RuCl(MeCN)_5][RuCl_4(MeCN)_2]$	$Me(Vi)Si(OEt)_2$ with $Me(H)Si(OEt)_2$	100°C, 2 h, solventless.	400	Following Organometallics 2006, 25 (19), pp 4504–4513 (very similar paper). DFT study in favor of σ-bond metathesis.
Dalton Trans., 2009, 5894-5901[114]	$RuCl_2$(*p*-cymene)	$Me(Vi)Si(OEt)_2$ with $Me(H)Si(OEt)_2$	100°, 1–2 h	1000	Following Organometallics 2006, 25 (19), pp 4504–4513 and J. Organomet. Chem. 2007, 692, 2282 (very similar papers). DFT study in favor of a hydride Chalk-Harrod (because Ru less coordinatively saturated than in the previous two articles).
J. Organomet. Chem. 2013, 745, 275-283[115]	$RuCl_3$ + 2 I_2	Ethylene with trimethoxysilane	25–90°C, 5–20 h, solventless	50000	When used, 2.2 mol I_2 per mol $RuCl_3$.
J. Organomet. Chem. 2013, 745, 454[116]	$RuCl_3$ + CuCl	Ethylene with trimethoxysilane	30–80 °, 6–16 h, solventless	15000	Following J. Organomet. Chem. 2013, 745, 275-283 (very similar article).
Chem. Sci., 2013, 4, 3882-3887[120]		$PhSiH_3$, $CySiH_3$ with 1-octene, 1-hexene, cyclopentene, cyclohexene, *t*-butylethylene	1 h, 80°C, in C_6D_5Br	100	Catalytic tests + kinetics + dft + crystallography. Counterion of the Ru complex : $CB_{11}H_6Br_6$
WO 2013043787[274]	Screening ligand + Ru salt + activator				Very little information : active/not active, but no quantitative data.
WO 2014133014[275]	$Ru(CO)_n(SiR_3)_2$				Sept 2014, no english translation for the moment.
WO 2014058819[276]	$RuCl_3$ zinc-reduced to (II) + *t*-butylhydroperoxide	methylallyl chloride and trimethoxysilane or methyldimethoxysilane or triethoxysilane	60°C overnight, catalyst solution sparged with 3% O_2 in N_2.	40 000	

A.5.1 Mechanistic studies

J. Am. Chem. Soc., 2004, 126 (42), pp 13564–13565[118]

J. Am. Chem. Soc., 2007, 129 (51), pp 15855–15864[119]
Organometallics, 2012, 31 (14), pp 5049–5057[277]
ACS Catal. 2015, 5, 3189-3195[278]

A.6 Rhodium

Patents[279–286]
- J. Chem. Soc. A. (1968) 787[287]
- J. Chem. Soc. A. (1969) 683[288]
- J. Organometal. Chem., 21 (1970) 207[83]
- J. Organomet. Chem 1975, 87, 203–216
- J. Mol. Catal. 1991, 66, 105-113[122]
- J. Organomet. Chem. 1978, 160, C1-C7[289]
- J. Am. Chem. Soc., 1992, 114 (6), pp 2128–2135[290]
- New J. Chem., 2010,34, 1330-1334[291]
- Dalton Trans., 2012,42, 270-276[292]
- Synlett 2012, 23(20), 2957-2960[293]
- Org. Lett. 2013, 15 (13), pp 3412–3415[121]
- Appl. Organomet. Chem. 2014, 28, 120[294]
- Eur. J. Org. Chem 2014, 27, 5890–5895[295]

A.7 Iridium

Patents[296–307]
- J. Am. Chem. Soc., 2008, 130 (29), pp 9226–9227[308]
- Org. Lett., 2014, 16 (5), pp 1330–1333[123]

B

Chemicals

Chemical	Supplier	Storage	Notes
1-octene (97%)	Alfa Aesar		
3,3-dimethyl-1-butene	Sigma-Aldrich	Under Ar, fridge	
Chloroform-d (isotopic) (99.9%)	Sigma-Aldrich		
Dibenzylideneacetone	Alfa Aesar		
Dodecane	Sigma-Aldrich		
Ethanol (99%)	VWR Chemicals		
$(EtO)_3SiH$	Alfa Aesar	Under Ar, fridge	
$(EtO)_3SiVi$	Alfa Aesar	Under Ar, fridge	
Et_3SiH	Alfa Aesar	Under Ar, fridge	
Et_3SiVi	Alfa Aesar	Under Ar, fridge	
$Fe_3(CO)_{12}$	STREM	Glovebox freezer	
Fumed silica (Aerosil® 200)	Evonik		
HNO_3 (68%)	VWR Chemicals		
$H_2PtCl_6 \cdot 6\,H_2O$ (99.9%)	Alfa Aesar	Glovebox	
H_2SO_4 (95%)			
$Ni(COD)_2$	Strem	Glovebox freezer	
MD'M	Bluestar Silicones		
$MD^{Vi}M$	ABCR	Under Ar, fridge	
$MD'_{50}M$	Bluestar silicones		
MWCNTs Graphistrength® C100	Arkema		
n-octylsilane	ABCR	Under Ar, fridge	
Potassium tetrachloroplatinate	Alfa Aesar		
Tetrahydrofuran	Sigma-Aldrich	Under Ar	Distilled on Na/benzophenone immediately before use
Toluene (99%)	Carlo Erba	Under Ar	Purified in a MBraun SPS-800 system, stored on activated 3 Å molecular sieves

Table B.1: Details about chemicals.

C

Analytical methods

C.1 Elemental analyses

Elemental analyses were performed at the IRCELyon (Lyon, France) or Mikroanalytisches Labor Pascher (Remagen, Germany), or by Solvay (St Fons, France).

C.2 N_2 and H_2 adsorption

Nitrogen and hydrogen adsorption analyses were performed on a Belsorp Max (BEL Japan, Inc.).

C.3 Gazometry

The technique called "gazometry" allows to measure the concentration of SiH functionalities in a mixture. The apparatus used is shown in Figure C.1.

A solution containing 2 g of KOH dissolved in 50 mL of *n*-butanol is prepared and placed in the flask (bottom left). This solution was be used for the analysis of 10 to 20 samples, in general.

A sample (0.1 mL for mixtures rich in SiH, or more for mixtures that contain less SiH) is injected in the flask containing the solution of KOH through a rubber septum. H_2 gas is produced by the reaction SiH + *n*-BuOH → SiO*n*-Bu + H_2.

The volume of H_2 produced is measured by a burette, and using the law of perfect gases:

$$PV = nRT$$

it is possible to calculate the quantity of SiH injected:

$$n_{\mathrm{SiH}} = \frac{PV}{RT}$$

From this quantity, knowing the volume of solution injected, it is possible to calculate the SiH concentration, and thus the SiH conversion.

C.4 Gas chromatography

Gas chromatography was performed on an Agilent 6890 Network Gas Chromatograph equipped with a Macherey-Nagel Optima® 5 column (10 m × 0.1 mm

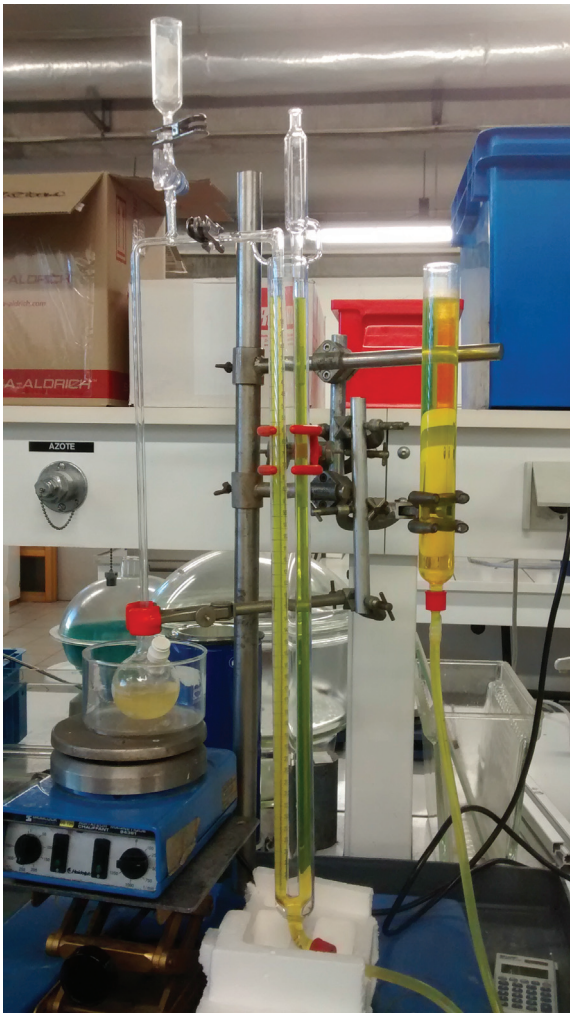


Figure C.1: Gazometry apparatus. On the bottom left, the flask containing the KOH solution, connected to the burette (middle). On the right, a water reservoir allowing to equilibrate the pressure inside the burette with the atmospheric pressure.

× 0.1 µm, 5% phenyl - 95% polydimethylsiloxane) and a flame ionization detector (FID). The injected volume was 1 µL, with a split ratio of 1:5000, in an injection chamber at 250 °C and 0.5 bar. The vector gas was H_2 at 0.4 mL min^{-1} at 1.5 bar, corresponding to 50 cm s^{-1}. The oven temperature was 50 °C during 30 s, then a ramp at 50 °C min^{-1} until 250 °C, then 250 °C during 30 s.

In these conditions, the retention times were as reported in table C.1.

Table C.1: Retention times

Molecule	Retention time (min)
3,3-dimethyl-1-butene	0.41
M'$_2$	0.59
Toluene	0.89
1-octene	0.95
Et_3SiH	0.96
MD'M	1.14
$(EtO)_3SiH$	1.72
$MD^{vi}M$	1.74
Dodecane	2.32
$MD^{oct}M$	3.04

Calibration curves of the analytes were done by injecting mixtures with dif-

ferent analyte/dodecane ratios and plotting the molar quantities ratio ($\frac{A_{\text{analyte}}}{A_{\text{dodecane}}}$) versus the areas ratio ($\frac{n_{\text{analyte}}}{n_{\text{dodecane}}}$).

The response coefficients versus dodecane were as reported in table C.2.

Molecule	Response coefficient versus dodecane
1-octene	0.66
MD'M	0.52
$(EtO)_3SiH$	0.35
$(EtO)_3SiVi$	0.54
$MD^{oct}M$	1.20

Table C.2: Response coefficients versus dodecane

Bibliography

[1] L. Rösch, P. John and R. Reitmeier. "Silicon Compounds, Organic" in: *Ullmann's Encyclopedia of Industrial Chemistry*. Wiley-VCH Verlag GmbH & Co. KGaA, 2000. (see p. 21)

[2] C. Cheng and J. F. Hartwig, *Chem. Rev.* **2015**, 115, 8946–8975. (see pp. 22, 26)

[3] L. H. Sommer, E. W. Pietrusza and F. C. Whitmore, *J. Am. Chem. Soc.* **1947**, 69, 188–188. (see pp. 22, 27, 28)

[4] S. Putzien, O. Nuyken and F. E. Kühn, *Prog. Polym. Sci.* **2010**, 35, 687–713. (see p. 22)

[5] D. Troegel and J. Stohrer, *Coord. Chem. Rev.* **2011**, 255, 1440–1459. (see pp. 22, 33, 63, 75)

[6] M. Pagliaro, R. Ciriminna, V. Pandarus and F. Béland, *Eur. J. Org. Chem.* **2013**, 2013, 6227–6235. (see pp. 22, 33, 75)

[7] Y. Nakajima and S. Shimada, *RSC Adv.* **2015**, 5, 20603–20616. (see p. 22)

[8] B. Marciniec. *Comprehensive handbook on hydrosilylation*. Pergamon Press, 1992. (see p. 22)

[9] B. Marciniec, *Silicon Chemistry* **2002**, 1, 155–175. (see p. 22)

[10] I. Ojima, Z. Li and J. Zhu. "The Chemistry of Organic Silicon Compounds" in: *The Chemistry of Organic Silicon Compounds*. vol. 2 John Wiley & Sons, Ltd, 2003. chap. Recent Advances in the Hydrosilylation and Related Reactions, 1687–1792 (see p. 22)

[11] A. K. Roy. In: A. F. H. Robert West and M. J. Fink, eds. Vol. 55chap. A Review of Recent Progress in Catalyzed Homogeneous Hydrosilation (Hydrosilylation), 1 –59. Academic Press, 2007. (see p. 22)

[12] B. Marciniec. "Hydrosilylation and Related Reactions of Silicon Compounds" in: *Applied Homogeneous Catalysis with Organometallic Compounds*. Wiley-VCH Verlag GmbH, 2008. 487–506 (see p. 22)

[13] B. Marciniec. *Hydrosilylation: A Comprehensive Review on Recent Advances*. silicones: Springer, 2009. (see pp. 22, 25, 29, 52, 53)

[14] Gelest, Inc. *Reactive Silicones: Forging New Polymer Links* 2015 (see p. 22)

[15] H. Moretto, M. Schulze and G. Wagner. "Silicones" in: *Ullmann's Encyclopedia of Industrial Chemistry*. Wiley-VCH Verlag GmbH & Co. KGaA, 2000. (see p. 23)

[16] A. M. Tondreau, C. C. H. Atienza, K. J. Weller, S. A. Nye, K. M. Lewis, J. G. P. Delis and P. J. Chirik, *Science* **2012**, 335, 567–570. (see pp. 23, 39, 119, 150)

[17] Gelest, Inc. *Silane Coupling Agents: Connecting Across Boundaries* 2014 (see p. 24)

[18] Dow Corning *The Basics of Silane Chemistry: A Guide to Silane Solutions* 2009 (see p. 24)

[19] U. Deschler, P. Kleinschmit and P. Panster, *Angew. Chem. Int. Ed.* **1986**, 25, 236–252. (see pp. 24, 25)

[20] H. Engelhardt and P. Orth, *J. Liq. Chrom.* **1987**, 10, 1999–2022. (see p. 25)

[21] R. Farkas, V. Lhiaubet-Vallet, J. Corbera, M. Törincsi, O. Gorchs, C. Trullas, O. Jiménez, M. A. Miranda and L. Novak, *Molecules* **2010**, 15, 6205–6216. (see p. 25)

[22] A. K. Franz and S. O. Wilson, *J. Med. Chem.* **2013**, 56, 388–405. (see p. 26)

[23] K. Tamao, N. Ishida, T. Tanaka and M. Kumada, *Organometallics* **1983**, 2, 1694–1696. (see pp. 26, 43)

[24] I. Fleming, R. Henning and H. Plaut, *J. Chem. Soc., Chem. Comm.* **1984**, 29–31. (see pp. 26, 43)

[25] I. Fleming, A. Barbero and D. Walter, *Chem. Rev.* **1997**, 97, 2063–2192. (see p. 26)

[26] Y. Uozumi and T. Hayashi, *J. Am. Chem. Soc.* **1991**, 113, 9887–9888. (see pp. 26, 52)

[27] N. Ghavtadze, F. S. Melkonyan, A. V. Gulevich, C. Huang and V. Gevorgyan, *Nat. Chem.* **2014**, 6, 122–125. (see pp. 26, 27)

[28] M. A. Larsen, S. H. Cho and J. Hartwig, *J. Am. Chem. Soc.* **2016**, 138, 762–765. (see pp. 26, 27)

[29] G. H. Wagner *Reaction of silanes with aliphatic unsaturated compounds* US2637738 Patent 1953 (see pp. 27, 28, 75, 138)

[30] J. L. Speier, J. A. Webster and G. H. Barnes, *J. Am. Chem. Soc.* **1957**, 79, 974–979. (see pp. 28, 138)

[31] J. C. Saam and J. L. Speier, *J. Am. Chem. Soc.* **1958**, 80, 4104–4106. (see p. 28)

[32] J. L. Speier and D. E. Hook *Process for the production of organo-silicon compounds* 1958 (see pp. 28, 138)

[33] B. D. Karstedt *Platinum complexes of unsaturated siloxanes and platinum containing organopolysiloxanes* U.S. Patent 3,775,452 1973 (see pp. 28, 139)

[34] P. B. Hitchcock, M. F. Lappert and N. J. W. Warhurst, *Angew. Chem. Int. Ed.* **1991**, 30, 438–440. (see pp. 28, 139)

[35] *The Periodic Table's Endangered Elements* [Online; accessed 23-August-2016] 2015 (see pp. 28, 29)

[36] H. Renner, G. Schlamp, I. Kleinwächter, E. Drost, H. M. Lüschow, P. Tews, P. Panster, M. Diehl, J. Lang, T. Kreuzer, A. Knödler, K. A. Starz, K. Dermann, J. Rothaut, R. Drieselmann, C. Peter and R. Schiele. "Platinum Group Metals and Compounds" in: *Ullmann's Encyclopedia of Industrial Chemistry*. Wiley-VCH Verlag GmbH & Co. KGaA, 2000. (see p. 28)

[37] C. Yang, *Energy Policy* **2009**, 37, 1805–1808. (see p. 28)

[38] I. Buslov, J. Becouse, S. Mazza, M. Montandon-Clerc and X. Hu, *Angew. Chem. Int. Ed.* **2015**, 54, 14523–14526. (see pp. 30, 46, 47, 53, 101, 156)

[39] L. N. Lewis, *J. Am. Chem. Soc.* **1990**, 112, 5998–6004. (see pp. 30, 31, 34, 63)

[40] P. Cancouët, S. Pernin, G. Helary and G. Sauvet, *J. Polym. Sci. A: Polym. Chem.* **2000**, 38, 837–845. (see pp. 31, 109)

[41] J. W. Ryan, *J. Am. Chem. Soc.* **1962**, 84, 4730–4734. (see p. 31)

[42] S. C. Berk and S. L. Buchwald, *J. Org. Chem.* **1992**, 57, 3751–3753. (see p. 31)

[43] I. E. Markó, S. Sterin, O. Buisine, G. Mignani, P. Branlard, B. Tinant and J.-P. Declercq, *Science* **2002**, 298, 204–206. (see pp. 32, 63, 141, 142)

[44] I. E. Markó, S. Stérin, O. Buisine, G. Berthon, G. Michaud, B. Tinant and J. Declercq, *Adv. Synth. Catal.* **2004**, 346, 1429–1434. (see pp. 32, 141)

[45] O. Buisine, G. Berthon-Gelloz, J.-F. Briere, S. Sterin, G. Mignani, P. Branlard, B. Tinant, J.-P. Declercq and I. E. Marko, *Chem. Comm.* **2005**, 3856–3858. (see pp. 32, 142)

[46] G. Berthon-Gelloz, O. Buisine, J. Brière, G. Michaud, S. Stérin, G. Mignani, B. Tinant, J. Declercq, D. Chapon and I. E. Markó, *J. Organomet. Chem.* **2005**, 690, 6156–6168. (see pp. 32, 142)

[47] G. Berthon-Gelloz, J.-M. Schumers, F. Lucaccioni, B. Tinant, J. Wouters and I. E. Markó, *Organometallics* **2007**, 26, 5731–5734. (see pp. 32, 141)

[48] G. Berthon-Gelloz and I. E. Markó. "Efficient and Selective Hydrosilylation of Alkenes and Alkynes Catalyzed by Novel N-Heterocyclic Carbene Pt0 Complexes" in: *N-Heterocyclic Carbenes in Synthesis* ed. by S. P. Nolan. Wiley-VCH Verlag GmbH & Co. KGaA, 2006. 119–161 (see pp. 32, 95)

[49] S. Dierick and I. E. Markó. "NHC Platinum(0) Complexes: Unique Catalysts for the Hydrosilylation of Alkenes and Alkynes" in: *N-Heterocyclic Carbenes* ed. by S. P. Nolan. Wiley-VCH Verlag GmbH & Co. KGaA, 2014. 111–150 (see pp. 32, 36, 37)

[50] R. Ciriminna, V. Pandarus, G. Gingras, F. Béland and M. Pagliaro, *ACS Sustain. Chem. Eng.* **2013**, 1, 249–253. (see pp. 33, 76, 145)

[51] S. Hübner, J. G. de Vries and V. Farina, *Adv. Synth. Catal.* **2016**, 358, 3–25. (see p. 33)

[52] S. J. Thomas and W. H. Retsch *Heterogeneous Hydrosilylation Catalysts, Polymers Formed Therewith, and Related Coating Compositions* Patent application WO 2007106427 A3 2007 (see pp. 33, 143)

[53] H. Bai, *Ind. Eng. Chem. Res.* **2014**, 53, 1588–1597. (see pp. 33, 68, 75, 76, 146)

[54] S. J. Meek, C. L. Pitman and A. J. M. Miller, *J. Chem. Ed.* **2016**, 93, 275–286. (see p. 34)

[55] L. N. Lewis and N. Lewis, *J. Am. Chem. Soc.* **1986**, 108, 7228–7231. (see pp. 34, 56, 63, 101)

[56] J. Stein, L. N. Lewis, Y. Gao and R. A. Scott, *J. Am. Chem. Soc.* **1999**, 121, 3693–3703. (see pp. 34, 63, 68)

[57] A. K. Roy and R. B. Taylor, *J. Am. Chem. Soc.* **2002**, 124, 9510–9524. (see pp. 35, 36, 63)

[58] A. J. Chalk and J. F. Harrod, *J. Am. Chem. Soc.* **1965**, 87, 16–21. (see p. 35)

[59] W. Caseri and P. S. Pregosin, *J. Organomet. Chem.* **1988**, 356, 259–269. (see pp. 35–37)

[60] T. K. Meister, K. Riener, P. Gigler, J. Stohrer, W. A. Herrmann and F. E. Kühn, *ACS Catal.* **2016**, 1274–1284. (see pp. 36, 37, 72)

[61] B. Marciniec, H. Maciejewski, W. Duczmal, R. Fiedorow and D. Kitynski, *Appl. Organomet. Chem.* **2003**, 17, 127–134. (see pp. 37, 142)

[62] Y. Wu, L. W. Chung and X. Zhang. "Hydrosilylation Reactions Discovered in the Last Decade: Combined Experimental and Computational Studies on the New Mechanisms" in: *Computational Modeling for Homogeneous and Enzymatic Catalysis* ed. by K. Morokuma and D. G. Musaev. Wiley-VCH Verlag GmbH & Co. KGaA, 2008. 285–316 (see p. 37)

[63] S. Sakaki, N. Mizoe and M. Sugimoto, *Organometallics* **1998**, 17, 2510–2523. (see p. 37)

[64] S. Sakaki, N. Mizoe, M. Sugimoto and Y. Musashi, *Coord. Chem. Rev.* **1999**, 190–192, 933–960. (see p. 37)

[65] C. L. Reichel and M. S. Wrighton, *Inorg. Chem.* **1980**, 19, 3858–3860. (see pp. 38, 41, 146)

[66] F. Seitz and M. S. Wrighton, *Angew. Chem. Int. Ed. Eng.* **1988**, 27, 289–291. (see pp. 38, 41, 148)

[67] F. Faglioni, M. Blanco, W. A. Goddard and D. Saunders, *J. Phys. Chem. B* **2002**, 106, 1714–1721. (see p. 37)

[68] G. Giorgi, F. D. Angelis, N. Re and A. Sgamellotti, *J. Mol. Struct.: THEOCHEM* **2003**, 623, 277–288. (see p. 38)

[69] C. A. Tsipis, A. C. Tsipis and C. E. Kefalidis. "Exploring the Catalytic Cycle of the Hydrosilylation of Alkenes Catalyzed by Hydrido-Bridged Diplatinum Complexes Using Electronic Structure Calculation Methods" in: *Fundamental World of Quantum Chemistry* ed. by E. J. Brändas and E. S. Kryachko. Dordrecht: Springer Netherlands, 2004. 619–643 (see p. 38)

[70] A. Nesmeyanov, R. Freidlina, E. Chukovskaya, R. Petrova and A. Belyavsky, *Tetrahedron* **1962**, 17, 61–68. (see pp. 38, 101, 119, 149, 152)

[71] M. A. Schroeder and M. S. Wrighton, *J. Organomet. Chem.* **1977**, 128, 345–358. (see pp. 38, 119, 149)

[72] J. C. Mitchener and M. S. Wrighton, *J. Am. Chem. Soc.* **1981**, 103, 975–977. (see pp. 38, 119, 149)

[73] F. Kakiuchi, Y. Tanaka, N. Chatani and S. Murai, *J. Organomet. Chem.* **1993**, 456, 45–47. (see pp. 38, 119, 149)

[74] B. Marciniec and M. Majchrzak, *Inorg. Chem. Comm.* **2000**, 3, 371–375. (see pp. 38, 119, 149)

[75] S. C. Bart, E. Lobkovsky and P. J. Chirik, *J. Am. Chem. Soc.* **2004**, 126, 13794–13807. (see pp. 39, 149)

[76] C. C. Hojilla Atienza, A. M. Tondreau, K. J. Weller, K. M. Lewis, R. W. Cruse, S. A. Nye, J. L. Boyer, J. G. P. Delis and P. J. Chirik, *ACS Catal.* **2012**, 2, 2169–2172. (see pp. 40, 151)

[77] *Sustainability Research: Silicone Production | Sustainability at Princeton* [Online; accessed 21-June-2016] 2016 (see p. 40)

[78] D. Peng, Y. Zhang, X. Du, L. Zhang, X. Leng, M. D. Walter and Z. Huang, *J. Am. Chem. Soc.* **2013**, 135, 19154–19166. (see pp. 40, 151)

[79] J. Chen, B. Cheng, M. Cao and Z. Lu, *Angew. Chem. Int. Ed.* **2015**, 54, 4661–4664. (see pp. 40, 151)

[80] D. Noda, A. Tahara, Y. Sunada and H. Nagashima, *J. Am. Chem. Soc.* **2016**, 138, 2480–2483. (see pp. 40, 41, 148)

[81] J. Sun and L. Deng, *ACS Catal.* **2016**, 6, 290–300. (see pp. 41, 146)

[82] A. J. Chalk and J. F. Harrod, *J. Am. Chem. Soc.* **1967**, 89, 1640–1647. (see pp. 41, 146)

[83] A. J. Chalk, *J. Organomet. Chem.* **1970**, 21, 207–213. (see pp. 41, 146, 160)

[84] L. Wilczek *Hydrosilation of fluorinated olefins with cobalt catalysts* Patent US 5233071 A 1993 (see pp. 41, 147)

[85] M. Brookhart and B. E. Grant, *J. Am. Chem. Soc.* **1993**, 115, 2151–2156. (see pp. 41, 42, 147, 149)

[86] Z. Mo, Y. Liu and L. Deng, *Angew. Chem. Int. Ed.* **2013**, 52, 10845–10849. (see pp. 41, 42, 147)

[87] C. C. H. Atienza, T. Diao, K. J. Weller, S. A. Nye, K. M. Lewis, J. G. P. Delis, J. L. Boyer, A. K. Roy and P. J. Chirik, *J. Am. Chem. Soc.* **2014**, 136, 12108–12118. (see pp. 41–43, 147, 148)

[88] C. Chen, M. B. Hecht, A. Kavara, W. W. Brennessel, B. Q. Mercado, D. J. Weix and P. L. Holland, *J. Am. Chem. Soc.* **2015**, 137, 13244–13247. (see pp. 42, 44, 53, 147)

[89] C. H. Schuster, T. Diao, I. Pappas and P. J. Chirik, *ACS Catal.* **2016**, 6, 2632–2636. (see pp. 42, 44, 136, 148)

[90] X. Du, Y. Zhang, D. Peng and Z. Huang, *Angew. Chem. Int. Ed.* **2016**, 55, 6671–6675. (see pp. 43, 44, 148)

[91] A. D. Ibrahim, S. W. Entsminger, L. Zhu and A. R. Fout, *ACS Catal.* **2016**, 6, 3589–3593. (see pp. 43, 45, 148)

[92] A. D. Petrov, V. F. Mironov, V. M. Vdovin and S. I. Sadykh-Zade, *Izvestiya Akademii Nauk SSSR, Seriya Khimicheskaya* **1956**, 256–257. (see pp. 45, 101, 152)

[93] S. Nozakura and S. Konotsune, *Bull. Chem. Soc. Jpn.* **1956**, 29, 326–331. (see pp. 45, 152)

[94] M. Kumada, Y. Kiso and M. Umeno, *J. Chem. Soc. D: Chem. Comm.* **1970**, 611. (see pp. 45, 101, 153)

[95] E. Bennett and P. Orenski, *J. Organomet. Chem.* **1971**, 28, 137–144. (see pp. 45, 153)

[96] Y. Kiso, M. Kumada, K. Tamao and M. Umeno, *J. Organomet. Chem.* **1973**, 50, 297–310. (see pp. 45, 108, 153)

[97] Y. Kiso, M. Kumada, K. Maeda, K. Sumitani and K. Tamao, *J. Organomet. Chem.* **1973**, 50, 311–318. (see pp. 45, 153)

[98] B. Marciniec, H. Maciejewski and J. Mirecki, *J. Organomet. Chem.* **1991**, 418, 61–67. (see pp. 45, 104, 105, 126, 154)

[99] B. Marciniec and H. Maciejewski, *J. Organomet. Chem.* **1993**, 454, 45–50. (see pp. 45, 105, 154)

[100] B. Marciniec, H. Maciejewski and U. Rosenthal, *J. Organomet. Chem.* **1994**, 484, 147–151. (see pp. 45, 105, 154)

[101] B. Marciniec, H. Maciejewski and I. Kownacki, *J. Mol. Catal. A: Chemical* **1998**, 135, 223–231. (see pp. 45, 155)

[102] H. Maciejewski, B. Marciniec and I. Kownacki, *J. Organomet. Chem.* **2000**, 597, 175–181. (see pp. 45, 155)

[103] F. Fontaine, R. Nguyen and D. Zargarian, *Can. J. Chem.* **2003**, 81, 1299–1306. (see pp. 45, 101, 155)

[104] Y. Chen, C. Sui-Seng, S. Boucher, and D. Zargarian, *Organometallics* **2005**, 24, 149–155. (see pp. 45, 155)

[105] V. Srinivas, Y. Nakajima, W. Ando, K. Sato and S. Shimada, *Catal. Sci. Tech.* **2015**, 5, 2081–2084. (see pp. 46, 101, 156)

[106] T. J. Steiman and C. Uyeda, *J. Am. Chem. Soc.* **2015**, 137, 6104–6110. (see pp. 46, 156)

[107] I. Pappas, S. Treacy and P. J. Chirik, *ACS Catal.* **2016**, 4105–4109. (see pp. 47, 48, 101, 108, 157)

[108] J. Mathew, Y. Nakajima, Y. Choe, Y. Urabe, W. Ando, K. Sato and S. Shimada, *Chem. Comm.* **2016**, 52, 6723–6726. (see pp. 48, 157)

[109] I. Buslov, F. Song and X. Hu, *Angew. Chem. Int. Ed.* **2016**, 55, 12295–12299. (see pp. 48, 49, 101)

[110] B. Marciniec and J. Guliński, *J. Organomet. Chem.* **1983**, 253, 349–362. (see pp. 49, 157)

[111] I. Ojima, T. Fuchikami and M. Yatabe, *J. Organomet. Chem.* **1984**, 260, 335–346. (see pp. 49, 157)

[112] T. Tuttle, D. Wang, W. Thiel, J. Köhler, M. Hofmann and J. Weis, *Organometallics* **2006**, 25, 4504–4513. (see pp. 49, 158)

[113] T. Tuttle, D. Wang, W. Thiel, J. Köhler, M. Hofmann and J. Weis, *J. Organomet. Chem.* **2007**, 692, 2282–2290. (see pp. 49, 158)

[114] T. Tuttle, D. Wang, W. Thiel, J. Köhler, M. Hofmann and J. Weis, *Dalton Trans.* **2009**, 5894–5901. (see pp. 49, 158)

[115] L. Liu, X. Li, H. Dong and C. Wu, *J. Organomet. Chem.* **2013**, 745–746, 275–283. (see pp. 49, 158)

[116] L. Liu, X. Li, H. Dong and C. Wu, *J. Organomet. Chem.* **2013**, 745–746, 454–459. (see pp. 49, 158)

[117] P. B. Glaser and T. D. Tilley, *J. Am. Chem. Soc.* **2003**, 125, 13640–13641. (see pp. 49, 157)

[118] C. Beddie and M. B. Hall, *J. Am. Chem. Soc.* **2004**, 126, 13564–13565. (see pp. 49, 158)

[119] M. A. Rankin, D. F. MacLean, G. Schatte, R. McDonald and M. Stradiotto, *J. Am. Chem. Soc.* **2007**, 129, 15855–15864. (see pp. 50, 159)

[120] M. E. Fasulo, M. C. Lipke and T. D. Tilley, *Chem. Sci.* **2013**, 4, 3882–3887. (see pp. 50, 158)

[121] Y. Hua, H. H. Nguyen, W. R. Scaggs and J. Jeon, *Org. Lett.* **2013**, 15, 3412–3415. (see pp. 51, 160)

[122] L. N. Lewis, R. J. Uriarte and N. Lewis, *J. Mol. Catal.* **1991**, 66, 105–113. (see pp. 51, 63, 160)

[123] J. A. Muchnij, F. B. Kwaramba and R. J. Rahaim, *Org. Lett.* **2014**, 16, 1330–1333. (see pp. 51, 160)

[124] S. E. Gibson and M. Rudd, *Adv. Synth. Catal.* **2007**, 349, 781–795. (see p. 52)

[125] T. Takahashi, M. Hasegawa, N. Suzuki, M. Saburi, C. J. Rousset, P. E. Fanwick and E. Negishi, *J. Am. Chem. Soc.* **1991**, 113, 8564–8566. (see p. 52)

[126] S. Sakaki, T. Takayama, M. Sumimoto and M. Sugimoto, *J. Am. Chem. Soc.* **2004**, 126, 3332–3348. (see p. 52)

[127] S. Harder, *Chem. Rev.* **2010**, 110, 3852–3876. (see p. 52)

[128] F. Buch, J. Brettar and S. Harder, *Angew. Chem. Int. Ed.* **2006**, 45, 2741–2745. (see pp. 52, 53)

[129] P. Fu, L. Brard, Y. Li and T. J. Marks, *J. Am. Chem. Soc.* **1995**, 117, 7157–7168. (see p. 53)

[130] M. H. Holthausen, M. Mehta and D. W. Stephan, *Angew. Chem. Int. Ed.* **2014**, 53, 6538–6541. (see p. 53)

[131] G. A. Molander and P. J. Nichols, *J. Am. Chem. Soc.* **1995**, 117, 4415–4416. (see p. 54)

[132] M. Oestreich, *Angew. Chem. Int. Ed.* **2016**, 55, 494–499. (see p. 54)

[133] A. Simonneau and M. Oestreich, *Angew. Chem. Int. Ed.* **2013**, 52, 11905–11907. (see p. 54)

[134] A. Simonneau and M. Oestreich, *Nat. Chem.* **2015**, 7, 816–822. (see p. 54)

[135] A. Roucoux, J. Schulz and H. Patin, *Chem. Rev.* **2002**, 102, 3757–3778. (see pp. 54, 55, 68, 101)

[136] V. Meille, M.-L. Zanota, F. D. Cruz-Boisson, C. Chamignon and S. Marrot, *Silicon* **2014**, 6, 247–255. (see pp. 55, 68, 135)

[137] C. Thieuleux, R. Sayah, M.-L. Zanota, V. Meille, R. Viver and S. Marrot *Hydrosilylation method* WO Patent App. PCT/EP2013/077,581 2014 (see pp. 55, 75, 80)

[138] A. T. Bell, *Science* **2003**, 299, 1688–1691. (see p. 55)

[139] D. Astruc, F. Lu and J. R. Aranzaes, *Angew. Chem. Int. Ed.* **2005**, 44, 7852–7872. (see p. 55)

[140] D. Astruc, ed. *Nanoparticles and Catalysis*. Wiley-VCH, 2008. (see p. 55)

[141] C. Jia and F. Schüth, *Phys. Chem. Chem. Phys.* **2011**, 13, 2457–2487. (see pp. 55, 68, 101)

[142] V. Iablokov, Y. Xiang, A. Meffre, P. Fazzini, B. Chaudret and N. Kruse, *ACS Catal.* **2016**, 6, 2496–2500. (see p. 56)

[143] L. N. Lewis, *Chem. Rev.* **1993**, 93, 2693–2730. (see p. 56)

[144] C. Burda, X. Chen, R. Narayanan and M. A. El-Sayed, *Chem. Rev.* **2005**, 105, 1025–1102. (see p. 56)

[145] K. Lee, M. Kim and H. Kim, *J. Mater. Chem.* **2010**, 20, 3791–3798. (see p. 56)

[146] K. Zhou and Y. Li, *Angew. Chem. Int. Ed.* **2012**, 51, 602–613. (see p. 56)

[147] S. Roy and M. A. Pericàs, *Org. Biomol. Chem.* **2009**, 7, 2669–2677. (see p. 56)

[148] B. P. S. Chauhan and J. S. Rathore, *J. Am. Chem. Soc.* **2005**, 127, 5790–5791. (see pp. 56, 63, 64, 143)

[149] B. P. S. Chauhan and B. Balagam, *Macromolecules* **2006**, 39, 2010–2012. (see pp. 56, 143)

[150] P. A. Cox. *The Elements: Their Origin, Abundance, and Distribution*. Oxford University Press, 1989. (see p. 59)

[151] R. H. Crabtree, *Chem. Rev.* **2012**, 112, 1536–1554. (see pp. 63, 90, 97)

[152] M. A. Brook, H. A. Ketelson, F. J. LaRonde and R. Pelton, *Inorg. Chim. Acta* **1997**, 264, 125–135. (see pp. 63, 64, 140)

[153] Y. Bai, S. Zhang, Y. Deng, J. Peng, J. Li, Y. Hu, X. Li and G. Lai, *J. Colloid Interface Sci.* **2013**, 394, 428–433. (see pp. 63, 64, 144)

[154] P. Steffanut, J. A. Osborn, A. DeCian and J. Fisher, *Chem. Eur. J.* **1998**, 4, 2008–2017. (see pp. 63, 68, 140)

[155] L. N. Lewis and R. J. Uriarte, *Organometallics* **1990**, 9, 621–625. (see pp. 63, 101)

[156] M. Boualleg, J.-M. Basset, J.-P. Candy, P. Delichere, K. Pelzer, L. Veyre and C. Thieuleux, *Chem. Mater.* **2009**, 21, 775–777. (see pp. 64, 70, 76, 119)

[157] K. Pelzer, B. Laleu, F. Lefebvre, K. Philippot, B. Chaudret, J. P. Candy and J. M. Basset, *Chem. Mater.* **2004**, 16, 4937–4941. (see pp. 64, 119)

[158] M. Boualleg, K. Guillois, B. Istria, L. Burel, L. Veyre, J.-M. Basset, C. Thieuleux and V. Caps, *Chem. Comm.* **2010**, 46, 5361–5363. (see p. 64)

[159] D. Baudouin, K. C. Szeto, P. Laurent, A. De Mallmann, B. Fenet, L. Veyre, U. Rodemerck, C. Copéret and C. Thieuleux, *J. Am. Chem. Soc.* **2012**, 134, 20624–20627. (see pp. 64, 101, 103, 115, 119, 135)

[160] K. Moseley and P. M. Maitlis, *J. Chem. Soc. D: Chem. Comm.* **1971**, 982–983. (see p. 69)

[161] J. Anderson. *Structure of Metallic Catalysts*. Academic Press, 1975. 296 (see p. 72)

[162] L. N. Lewis and N. Lewis, *Chem. Mater.* **1989**, 1, 106–114. (see p. 73)

[163] T. Kobayashi, F. A. Perras, T. W. Goh, T. L. Metz, W. Huang and M. Pruski, *J. Phys. Chem. Lett.* **2016**, 7, 2322–2327. (see p. 73)

[164] *<232> Elemental impurities—limits, Pharmacopeial Forum 36 (Jan–Feb. 2010)* (see p. 75)

[165] L. Wang and Y. Jiang, *J. Organomet. Chem.* **1983**, 251, 39–44. (see pp. 75, 139)

[166] Q. J. Miao, Z. Fang and G. P. Cai, *Catal. Comm.* **2003**, 4, 637–639. (see pp. 75, 142)

[167] Z. M. Michalska, L. Rogalski, K. Rózga-Wijas, J. Chojnowski, W. Fortuniak and M. Ścibiorek, *J. Mol. Catal. A: Chem.* **2004**, 208, 187–194. (see pp. 75, 142)

[168] R. Bandari and M. R. Buchmeiser, *Catal. Sci. Tech.* **2012**, 2, 220–226. (see p. 76)

[169] D. Zhao, Y. Wan and W. Zhou. *Ordered Mesoporous Materials*. John Wiley & Sons, 2012. (see p. 76)

[170] J. Tang, X. Zhou, D. Zhao, G. Q. Lu, J. Zou and C. Yu, *J. Am. Chem. Soc.* **2007**, 129, 9044–9048. (see p. 76)

[171] M. Boualleg, S. Norsic, D. Baudouin, R. Sayah, E. Quadrelli, J.-M. Basset, J.-P. Candy, P. Delichere, K. Pelzer, L. Veyre and C. Thieuleux, *J. Catal.* **2011**, 284, 184–193. (see pp. 76, 77, 135)

[172] L. Djakovitch, H. Heise and K. Köhler, *J. Organomet. Chem.* **1999**, 584, 16–26. (see p. 79)

[173] R. G. Heidenreich, J. G. E. Krauter, J. Pietsch and K. Köhler, *J. Mol. Catal. A: Chem.* **2002**, 182–183, 499–509. (see p. 79)

[174] S. Iijima, *Nature* **1991**, 354, 56–58. (see p. 81)

[175] S. Iijima and T. Ichihashi, *Nature* **1993**, 363, 603–605. (see p. 81)

[176] D. S. Bethune, C. H. Klang, M. S. de Vries, G. Gorman, R. Savoy, J. Vazquez and R. Beyers, *Nature* **1993**, 363, 605–607. (see p. 81)

[177] S. Bordere, J. Corpart, N. E. Bounia, P. Gaillard, N. Passade-Boupat, P. Piccione and D. Plée, *Industrial Production and Applications of Carbon Nanotubes - Technical document by Arkema* **2007**. (see p. 81)

[178] J. M. Schnorr and T. M. Swager, *Chem. Mater.* **2011**, 23, 646–657. (see p. 81)

[179] Q. Zhang, J. Huang, W. Qian, Y. Zhang and F. Wei, *Small* **2013**, 9, 1237–1265. (see p. 81)

[180] F. Rodríguez-reinoso, *Carbon* **1998**, 36, 159–175. (see p. 81)

[181] P. Serp, M. Corrias and P. Kalck, *Appl. Catal. A: General* **2003**, 253, 337–358. (see pp. 82, 83)

[182] H. Vu, F. Gonçalves, R. Philippe, E. Lamouroux, M. Corrias, Y. Kihn, D. Plee, P. Kalck and P. Serp, *J. Catal.* **2006**, 240, 18–22. (see p. 82)

[183] P. Serp and E. Castillejos, *ChemCatChem* **2010**, 2, 41–47. (see pp. 82, 87)

[184] K. Gong, F. Du, Z. Xia, M. Durstock and L. Dai, *Science* **2009**, 323, 760–764. (see p. 82)

[185] D. S. Su, S. Perathoner and G. Centi, *Chem. Rev.* **2013**, 113, 5782–5816. (see p. 82)

[186] A. Muneendra Prasad, C. Santhosh and A. Nirmala Grace, *Appl. Nanosci.* **2012**, 2, 457–466. (see p. 82)

[187] S. Takenaka, H. Miyamoto, Y. Utsunomiya, H. Matsune and M. Kishida, *J. Phys. Chem. C* **2014**, 118, 774–783. (see p. 82)

[188] Y.-F. Dai, F.-Y. Li and B. Xiao, *Organic Chemistry: An Indian Journal* **2005**, 1, (see p. 82)

[189] Z. Jian-bo, S. U. N. Yu-an, L. I. U. Ying-fan, C. Chang-fu, X. I. E. Bing and Z. Xian-jun, *China Surfactant Detergent & Cosmetics* **2010**, 40, 427–431. (see p. 83)

[190] F. Simescu-Lazar, T. Chaieb, S. Pallier, L. Veyre, R. Philippe and V. Meille, *Appl. Catal. A: General* **2015**, 508, 45–51. (see pp. 84, 85, 88)

[191] D. Tasis, N. Tagmatarchis, A. Bianco and M. Prato, *Chem. Rev.* **2006**, 106, 1105–1136. (see p. 84)

[192] M. R. Axet, O. Dechy-Cabaret, J. Durand, M. Gouygou and P. Serp, *Coord. Chem. Rev.* **2016**, 308, Part 2, 236–345. (see p. 85)

[193] A. Solhy, B. F. Machado, J. Beausoleil, Y. Kihn, F. Gonçalves, M. F. R. Pereira, J. J. M. Orfao, J. L. Figueiredo, J. L. Faria and P. Serp, *Carbon* **2008**, 46, 1194–1207. (see p. 85)

[194] F. Zhao, B. M. Bhanage, M. Shirai and M. Arai, *Chem. Eur. J.* **2000**, 6, 843–848. (see p. 90)

[195] B. H. Lipshutz, S. Tasler, W. Chrisman, B. Spliethoff and B. Tesche, *J. Org. Chem.* **2003**, 68, 1177–1189. (see p. 90)

[196] D. Astruc, *Inorg. Chem.* **2007**, 46, 1884–1894. (see p. 90)

[197] K. Köhler, R. G. Heidenreich, S. S. Soomro and S. S. Pröckl, *Adv. Synth. Catal.* **2008**, 350, 2930–2936. (see p. 90)

[198] M. Gruttadauria, F. Giacalone and R. Noto, *Green Chem.* **2013**, 15, 2608–2618. (see p. 90)

[199] P. Boudjouk, B. Han, J. R. Jacobsen and B. J. Hauck, *J. Chem. Soc., Chem. Comm.* **1991**, 1424–1425. (see pp. 101, 154)

[200] T. Hinotsu, B. Jeyadevan, C. N. Chinnasamy, K. Shinoda and K. Tohji, *J. Appl. Phys.* **2004**, 95, 7477–7479. (see p. 101)

[201] Y. Hou and S. Gao, *J. Mater. Chem.* **2003**, 13, 1510–1512. (see p. 101)

[202] Y. Chen, D. Peng, D. Lin and X. Luo, **2007**, 18, 505703. (see p. 101)

[203] S. Carenco, C. Boissière, L. Nicole, C. Sanchez, P. Le Floch and N. Mézailles, *Chem. Mater.* **2010**, 22, 1340–1349. (see p. 101)

[204] J. Park, E. Kang, S. U. Son, H. M. Park, M. K. Lee, J. Kim, K. W. Kim, H. Noh, J. Park, C. J. Bae, J. Park and T. Hyeon, *Adv. Mater.* **2005**, 17, 429–434. (see p. 101)

[205] M. Holz, X. Mao, D. Seiferling and A. Sacco, *J. Chem. Phys.* **1996**, 104, 669–679. (see p. 103)

[206] K. A. Brown-Wensley, *Organometallics* **1987**, 6, 1590–1591. (see p. 107)

[207] P. Sabatier. *La Catalyse en chimie organique*. ed. by C. Béranger (Paris ; Liège) 1913. (see p. 113)

[208] M. Raney *Method of producing finely-divided nickel* 1927 (see p. 113)

[209] D. L. Huber, *Small* **2005**, 1, 482–501. (see p. 119)

[210] J. Candy, E. Roisin, J. Basset, D. Uzio, S. Morin, L. Fischer, J. Olivier-Fourcade and J. Jumas, *Hyperfine Interactions* **2007**, 165, 55–60. (see p. 124)

[211] N. Dahal and V. Chikan, *Chem. Mater.* **2010**, 22, 2892–2897. (see p. 131)

[212] J. Guan, X. Chen, K. Yang, A. Rykov, J. Wang and C. Liang, *J. Mater. Chem. C* **2014**, 2, 5292–5298. (see p. 131)

[213] J. M. McEnaney and R. E. Schaak, *Inorg. Chem.* **2015**, 54, 707–709. (see p. 131)

[214] Z. Yang, T. Zhao, X. Huang, X. Chu, T. Tang, Y. Ju, Q. Wang, Y. Hou and S. Gao, *Chem. Sci.* **2016**. (see p. 131)

[215] C. Schliehe, J. Yuan, S. Glatzel, K. Siemensmeyer, K. Kiefer and C. Giordano, *Chem. Mater.* **2012**, 24, 2716–2721. (see p. 131)

[216] S. Rades, A. Kornowski, H. Weller and B. Albert, *ChemPhysChem* **2011**, 12, 1756–1760. (see p. 131)

[217] S. Carenco, D. Portehault, C. Boissière, N. Mézailles and C. Sanchez, *Chem. Rev.* **2013**, 113, 7981–8065. (see p. 131)

[218] C. Qian, F. Kim, L. Ma, F. Tsui, P. Yang and J. Liu, *J. Am. Chem. Soc.* **2004**, 126, 1195–1198. (see p. 131)

[219] E. Nakamura and K. Sato, *Nat. Mater.* **2011**, 10, 158–161. (see p. 136)

[220] L. N. Lewis, J. Stein, Y. Gao, R. E. Colborn and G. Hutchins, *Platinum Metals Review* **1997**. (see p. 138)

[221] A. J. Holwell, *Platinum Metals Review* **2008**, 52, 243–246. (see p. 138)

[222] L. Spialter, M. C. A and M. Schoffman *Reaction of silanes with unsaturated aliphatic compounds* Patent US 2721873 A 1955 (see p. 138)

[223] J. Ryan and J. Speier, *J. Org. Chem.* **1959**, 24, 2052–2053. (see p. 138)

[224] A. L. Prignano and W. C. Trogler, *J. Am. Chem. Soc.* **1987**, 109, 3586–3595. (see p. 139)

[225] H. M. Bank *Method for maintaining catalytic activity during a hydrosilylation reaction.* 1995 (see p. 140)

[226] S. Breunig and G. Mignani, *Patent* **1997**, WO1997047677, (see p. 140)

[227] S. D. Bade, J. D. Monkiewicz and U. D. Schoen *Process for preparing 3-Glycidyloxypropyltrialkoxysilanes* Patent US 6100408 A 2003 (see p. 141)

[228] H. M. Bank, P. C. Dinh and M. Tzou *Platinum catalyst for hydrosilations* Patent US 6087523 A 2000 (see p. 141)

[229] R. Drake, R. Dunn, D. C. Sherrington and S. J. Thomson, *Chem. Comm.* **2000**, 1931–1932. (see p. 141)

[230] R. Drake, R. Dunn, D. Sherrington and S. Thomson, *J. Mol. Catal. A: Chem.* **2001**, 177, 49–69. (see p. 141)

[231] R Drake, R Dunn, D. C. Sherrington and S. J. Thomson, *Comb. Chem. & high throughput screening* **2002**, 5, 201–209. (see p. 141)

[232] R. Drake, D. C. Sherrington and S. J. Thomson, *React. Funct. Polym.* **2004**, 60, 65–75. (see p. 141)

[233] S. Stérin *Method for preparing silicone oils by hydrosilylation of synthons containing at least a hydrocarbon cycle wherein is included an oxygen atom in the presence of a catalytic metal complex* 2002 (see p. 141)

[234] *Silicone composition which can be crosslinked into an elastomer by hydrosilylation in the presence of carbene-based metal catalysts, and catalysts of this type* 2002 (see p. 141)

[235] C. George, D. Blanc-Magnard, A. Pouchelon and S. Sterin *Silicone composition crosslinkable into elastomer by hydrosilylation, in the presence of carbene-based metal catalysts, and catalysts* 2003 (see p. 141)

[236] O. Buisine, I. Marko and S. Sterin *Method for Preparing Metallic Carbene-Based Catalysts for Hydrosilylation of Unsaturated Compounds and Resulting Catalysts* 2006 (see p. 141)

[237] G. L. Larson, B. C. Arkles and R. A. Cameron *Fixed-Bed Hydrosilylation Catalyst Complexes and Related Methods* 2013 (see p. 141)

[238] M. Amako, J. Schinkel, L. Freiburger and M. A. Brook, *Dalton Trans.* **2005**, 74–81. (see p. 142)

[239] B. Weyershausen, K. Hell and U. Hesse, *Green Chem.* **2005**, 7, 283–287. (see p. 143)

[240] M. Hofmann and H. J. Eberle, *WO Patent* **2006**, WO2006061138, (see p. 143)

[241] T. J. Geldbach, D. Zhao, N. C. Castillo, G. Laurenczy, B. Weyershausen and P. J. Dyson, *J. Am. Chem. Soc.* **2006**, 128, 9773–9780. (see p. 143)

[242] H. Maciejewski, A. Wawrzynczak, M. Dutkiewicz and R. Fiedorow, *J. Mol. Catal. A: Chem.* **2006**, 257, 141–148. (see p. 143)

[243] J. Alauzun, A. Mehdi, C. Reyé and R. Corriu, *Chem. Mater.* **2007**, 19, 6373–6375. (see p. 143)

[244] A. Wawrzynczak, M. Dutkiewicz, J. Gulinski, H. Maciejewski, B. Marciniec and R. Fiedorow, *Catal. Today* **2011**, 169, 69–74. (see pp. 143, 144)

[245] Y. Bai, J. Peng, Y. Hu, J. Li and G. Lai, *J. Fluorine Chem.* **2011**, 132, 123–127. (see p. 144)

[246] M. A. Taige, S. Ahrens and T. Strassner, *J. Organomet. Chem.* **2011**, 696, 2918–2927. (see p. 144)

[247] C. M. Downing and H. H. Kung, *Catal. Comm.* **2011**, 12, 1166–1169. (see p. 144)

[248] Y. Bai, J. Peng, J. Li and G. Lai, *Appl. Organomet. Chem.* **2011**, 25, 400–405. (see p. 144)

[249] Y. Bai, J. Peng, H. Yang, J. Li, G. Lai and X. Li, *Chin. J. Chem. Eng.* **2012**, 20, 246–253. (see p. 144)

[250] B. Marciniec, K. Posała, I. Kownacki, M. Kubicki and R. Taylor, *ChemCatChem* **2012**, 4, 1935–1937. (see p. 144)

[251] D. Zhang, W. Huo, J. Wang, T. Li, X. Cheng, J. Li and A. Zhang, *J. Appl. Polym. Sci.* **2012**, 126, 1580–1584. (see p. 144)

[252] S. Putzien, E. Louis, O. Nuyken and F. E. Kühn, *Catal. Sci. Tech.* **2012**, 2, 725–729. (see p. 145)

[253] S. Komati, V. Khare, K. Lewis, A. Sakar, A. Srikanth and A. Roy *High Activity Catalyst for Hydrosilylation Reactions and Methods of Making the Same* Patent application US 20150051357 A1 patent, 2013 (see p. 145)

[254] T. Schulz and T. Strassner, *J. Organomet. Chem.* **2013**, 744, 113–118. (see p. 145)

[255] H. Bai, K. Bobbitt and M. Powell *Process of Manufacturing Organosilicon Products with Improved Quality Using Heterogeneous Precious Metal Catalysts* Patent application WO 2013066983 A1 2013 (see p. 146)

[256] S. E. Parker, J. Börgel and T. Ritter, *J. Am. Chem. Soc.* **2014**, 136, 4857–4860. (see p. 146)

[257] V. Gandon, N. Agenet, K. P. C. Vollhardt, M. Malacria and C. Aubert, *J. Am. Chem. Soc.* **2009**, 131, 3007–3015. (see p. 149)

[258] M. D. Greenhalgh, D. J. Frank and S. P. Thomas, *Adv. Synth. Catal.* **2014**, 356, 584–590. (see pp. 149, 151)

[259] C. J. Sims and E. W. J. Mardles, *Trans. Faraday Soc.* **1926**, 22, 363–371. (see pp. 149, 152)

[260] H. Nakazawa, M. Itazaki, K. Tanaka and A. Itagaki *Catalyst for hydrosilylation reaction, and process for producing organic silicon compound using the catalyst* Patent application WO 2010016416 A1 2010 (see p. 150)

[261] J. Y. Wu, B. N. Stanzl and T. Ritter, *J. Am. Chem. Soc.* **2010**, 132, 13214–13216. (see p. 150)

[262] A. M. Tondreau, C. C. H. Atienza, J. M. Darmon, C. Milsmann, H. M. Hoyt, K. J. Weller, S. A. Nye, K. M. Lewis, J. Boyer, J. G. P. Delis, E. Lobkovsky and P. J. Chirik, *Organometallics* **2012**, 31, 4886–4893. (see p. 150)

[263] K. Kamata, A. Suzuki, Y. Nakai and H. Nakazawa, *Organometallics* **2012**, 31, 3825–3828. (see p. 150)

[264] Y. Sunada, H. Tsutsumi, K. Shigeta, R. Yoshida, T. Hashimoto and H. Nagashima, *Dalton Trans.* **2013**, 42, 16687–16692. (see p. 151)

[265] B. Marciniec, A. Kownacka, I. Kownacki and R. Taylor, *Appl. Catal. A: General* **2014**, 486, 230–238. (see p. 151)

[266] Y. Sunada, D. Noda, H. Soejima, H. Tsutsumi and H. Nagashima, *Organometallics* **2015**, 34, 2896–2906. (see p. 152)

[267] ,*Izvestiya Akademii Nauk SSSR, Seriya Khimicheskaya* **1963**, 761–763. (see p. 153)

[268] A. Cornish, M. Lappert, J. Macquitty and R. Maskell, *J. Organomet. Chem.* **1979**, 177, 153–161. (see p. 153)

[269] D. Gareau, C. Sui-Seng, L. F. Groux, F. Brisse and D. Zargarian, *Organometallics* **2005**, 24, 4003–4013. (see p. 155)

[270] I. Hyder, M. Jiménez-Tenorio, M. C. Puerta and P. Valerga, *Dalton Trans.* **2007**, 3000–3009. (see p. 155)

[271] M. I. Lipschutz and T. D. Tilley, *Chem. Comm.* **2012**, 48, 7146–7148. (see p. 155)

[272] L. Benitez Junquera, M. C. Puerta and P. Valerga, *Organometallics* **2012**, 31, 2175–2183. (see p. 156)

[273] T. D. TILLEY and J. Yang *First row metal-based catalysts for hydosilylation* Patent application WO2013120057A1 2013 (see p. 156)

[274] K. Brandstadt, S. Cook, B. T. Nguyen, A. Surgenor, R. Taylor, M. Tzou, A. Dash and M. Olsen *Ruthenium containing hydrosilylation catalysts and compositions containing the catalysts* Patent application WO 2013043787 A2 2014 (see p. 158)

[275] H. Nagashima, Y. Sunada, H. Tsutsumi, T. Hashimoto and K. Sakuta *Mononuclear ruthenium complex and organic synthesis reaction using same* Patent application WO 2014133014 A1 2014 (see p. 158)

[276] K. M. Lewis, J. S. Rathore, A. Trotto and G. D'agostino *Hydrosilylation synthesis of haloalkylorganosilanes using peroxide promoters* Patent application WO 2014058819 A1 2014 (see p. 158)

[277] M. E. Fasulo and T. D. Tilley, *Organometallics* **2012**, 31, 5049–5057. (see p. 159)

[278] A. Bokka, Y. Hua, A. S. Berlin and J. Jeon, *ACS Catal.* **2015**, 5, 3189–3195. (see p. 159)

[279] P. Jenkner, A. Frings, M. Horn, J. Monkiewicz and B. Standke *N-[omega-(methyl),omega-(silyl)]alkyl-N-organocarboxamide, their oligomers and polycondensates, process for their preparation and their use* 2001 (see p. 160)

[280] S. Sakaki, M. Sumimoto, M. Fukuhara, M. Sugimoto, H. Fujimoto and S. Matsuzaki, *Organometallics* **2002**, 21, 3788–3802. (see p. 160)

[281] A. Fehn and J. Weidinger *Use of rhodium-catalyzed siloxane elastomers for the fabrication of baking molds* 2006 (see p. 160)

[282] A. Fehn, J. Weidinger and A. Duernberger *Cross-Linking Silicone Elastomers, Method for the Production Thereof, and Use of the Cross-Linkable Masses* 2006 (see p. 160)

[283] I. Chorvath, J. Degroot, M. Dipino, R. Drake, D. Lawson, S. Robson, D. Shawl and L. Tonge *Silicone Elastomers for High Temperature Performance* 2008 (see p. 160)

[284] K. Uehara and T. Kubota *Preparation of 1-(alkoxysilyl) ethyl-1,1,3,3-tetramethyldisiloxane* 2008 (see p. 160)

[285] D. D. Farris, C. J. Rinard and M. D. Leatherman *Selective Hydrosilylation Method with Alcohol or Epoxide Reactant and Product* 2009 (see p. 160)

[286] L. Rapson *Preparation of Silicone Rubber Elastomers* 2008 (see p. 160)

[287] F. de Charentenay, J. A. Osborn and G. Wilkinson, *J. Chem. Soc. A* **1968**, 787–790. (see p. 160)

[288] R. N. Haszeldine, R. V. Parish and D. J. Parry, *J. Chem. Soc. A* **1969**, 683–690. (see p. 160)

[289] H. Watanabe, M. Aoki, N. Sakurai, K.-i. Watanabe and Y. Nagai, *J. Organomet. Chem.* **1978**, 160, C1–C7. (see p. 160)

[290] S. H. Bergens, P. Noheda, J. Whelan and B. Bosnich, *Journal of the American Chemical Society* **1992**, 114, 2128–2135. (see p. 160)

[291] J. Li, J. Peng, G. Zhang, Y. Bai, G. Lai and X. Li, *New J. Chem.* **2010**, 34, 1330–1334. (see p. 160)

[292] B. J. Truscott, A. M. Z. Slawin and S. P. Nolan, *Dalton Trans.* **2012**, 42, 270–276. (see p. 160)

[293] T. Naito, T. Yoneda, J.-i. Ito and H. Nishiyama, *Synlett* **2012**, 23, 2957–2960. (see p. 160)

[294] M. Xue, J. Li, J. Peng, Y. Bai, G. Zhang, W. Xiao and G. Lai, *Appl. Organomet. Chem.* **2014**, 28, 120–126. (see p. 160)

[295] Y. Hua, H. H. Nguyen, G. Trog, A. S. Berlin and J. Jeon, *Eur. J. Org. Chem.* **2014**, 2014, 5890–5895. (see p. 160)

[296] A. Bauer, O. Schaefer, M. Kriegbaum, L. Brader, B. Pachaly and V. Frey *Process for preparing organosilanes* 2003 (see p. 160)

[297] A. Bauer and O. Schaefer *Iridium-Catalyzed Production Method for Organosilicon Compounds* 2008 (see p. 160)

[298] F. Baumann and M. Hoffmann *Preparation of organosilane compounds, useful as e.g. coupling agents, comprises reacting silane compounds with alkene and/or alkyne in the presence of iridium compound and cocatalyst (inorganic/metalorganic/o rganic oxidation agents)* 2006 (see p. 160)

[299] F. Baumann *Kontinuierliche Herstellung von Organosilanen in Gegenwart von Iridium-Katalysatoren und Cokatalysatoren* 2007 (see p. 160)

[300] J. Droese, H. Geisler, W. Hiersche, K. Klein, W. Knott, A. Mehrwald and D. Windbiel *Process and apparatus for continous hydrosilylation reactions* 2004 (see p. 160)

[301] G. Geisberger, F. Baumann and A. Daniels *Process for continuous hydrosilylation* 2006 (see p. 160)

[302] N. Guennouni and J. Galland *Method of Preparing Halogenoalkyldialkylchlorosilane* 2004 (see p. 160)

[303] T. Kornek, A. Bauer and D. Senden *Continuous production of (cyclo)alkylsilanes, used e.g. as adhesion promoter or crosslinker, by hydrosilylation of (cyclo)alkene uses bis(chloro-iridium-diene) compound as catalyst and free diene as cocatalyst* 2003 (see p. 160)

[304] F. Kropfgans, A. Frings, M. Horn, H. Koetzsch, J. Monkiewicz, C. Seiler, H. Srebny and B. Standke *Process for the preparation of 3-halogeno- or -pseudohalogeno-alkylsilane esters, respectively* 2001 (see p. 160)

[305] K. Ramdani, B. Vogin and N. Guennouni *Method of Preparing Organo Dialkylalkoxysilane* 2007 (see p. 160)

[306] K. Ramdani *Method for Preparing an Omega-Haloalkyl Dialkylhalosilane* 2009 (see p. 160)

[307] Y. Tonomura, T. Kubota and M. Endo *Preparation of halopropyldimethylchlorosilanes* 2006 (see p. 160)

[308] E. Calimano and T. D. Tilley, *J. Am. Chem. Soc.* **2008**, 130, 9226–9227. (see p. 160)